Isolation and Characterisation of CML and Normal Quiescent Haemopoietic Stem Cells

Susan M Graham BSc

Submission for the Degree of Doctor of Philosophy

in

The Faculty of Medicine
Division of Cancer Sciences and
Molecular Pathology

at the

University of Glasgow

June 2005

Abstract

Haemopoietic stem cells (HSC) in vivo are generally accepted to be quiescent, entering cell cycle relatively infrequently. However, their capacity for self-renewal and multilineage differentiation renders them a formidable target when transformation occurs. Chronic myeloid leukaemia (CML), characterised by the presence of the BCR-ABL fusion gene, arises in a pluripotent HSC and also features a population of quiescent stem cells. Recent data on the effectiveness of a targeted therapy for CML, STI571 (STI), designed to inhibit the tyrosine kinase activity of the oncoprotein, has cast doubt on the success and durability of clinical responses to this treatment. The work contained in this thesis was aimed at isolation of quiescent stem cells from both normal and CML samples and characterisation of the properties of these rare populations, the response of CML stem cells to STI treatment in vitro was also examined; and finally a microarray study was undertaken in an effort to elucidate the gene expression profiles of both normal and CML quiescent cells compared to their cycling counterparts.

To isolate these specific cell populations, enrichment of the stem cell fraction was achieved by selection methods based on the stem cell marker CD34. Positive or negative CD34 selection yielded up to 99% pure $CD34^+$ cell populations. A fluorescent activated cell-sorting (FACS) strategy was developed to allow isolation of quiescent and cycling stem cells. Using Hoechst (HST) and Pyronin Y (Py) to stain the DNA and RNA respectively and gating on the viable, Propidium $Iodide^-$ $(PI)^-$, $CD34^+$ population, it was possible to isolate viable stem cells in G0, G1 and S/G2/M phases of the cell cycle.

Success of the sorting strategy was demonstrated by PCR analysis of differential cell cycle gene expression in the sorted populations. Further development of FACS methodology allowed the division history and stem cell status, as defined by CD34 expression, to be monitored under a range of conditions. By staining cells with a non-toxic permanent cytoplasmic dye, carboxyfluorescein diacetate succinimidyl ester (CFSE), combined with a sorting strategy to enhance division peaks, high resolution tracking of cell division was possible. Growth factor independence was established for CML stem cells and was used to identify leukaemic stem cell proliferation, as normal cells failed to divide under these conditions.

Using this experimental strategy, it was shown that a number of CML stem cells were able to survive exposure to concentrations of STI in excess of those achievable in vivo, and that the surviving cells were undivided or quiescent. A range of sensitivities to STI between patient samples was shown, however in all cases a population of viable, undivided stem cells was observed. In addition, STI was also shown to exhibit antiproliferative activity causing the number of quiescent cells to increase following treatment in vitro. It is possible that these observations may contribute to the lack of disease eradication in vivo by STI, which is rare with most patients harbouring detectable BCR-ABL transcripts, despite significant clinical responses.

In an effort to further characterise quiescent stem cells, the HST/Py FACS strategy was used to isolate quiescent and cycling stem cell populations from both normal and CML samples, which were then processed for microarray studies. The analysis of these very specific stem cell populations has yielded a significant amount of new data.

Firstly, the results have shown a differential gene expression profile between normal G0 and cycling cells that fully validates the sorting strategy. Significant up-regulation of known cell cycle genes was observed between normal G0 and cycling cells. In contrast, CML G0 cells exhibited aberrant expression of a number of cell cycle genes in the G0 fraction, representing a gene profile closer to that of cycling cells. The most significant differential gene expression was in a set of chemokine genes, which were up-regulated in both normal and CML G0 cells compared to cycling cells. This has not been previously reported and represents a novel finding. Additional data analysis is ongoing and may, in time, yield therapeutic targets for CML disease eradication.

In summary, isolation of specific CML stem cell populations has enabled the identification of a quiescent population of cells that are able to escape the effects of a targeted therapy in vitro. These results may have significant clinical importance as mechanisms of disease persistence, already observed in vivo, are elucidated. Furthermore, identification of gene differences between quiescent and cycling cells has validated the FACS strategy for isolation of these rare quiescent stem cell populations. In addition, data analysis has identified unique differences in gene expression of a set of chemokine genes, up-regulated in quiescent cells,

from both normal and CML populations. These data will have significant importance in our understanding of quiescent HSC behaviour.

Table of Contents

List of Tables

List of Figures

List of accompanying material

Relevant Publications

Holyoake TL, Jiang X, Jorgensen HG, **Graham SM**, Alcorn MJ, Laird C, Eaves AC, Eaves CJ.
Primitive quiescent leukemic cells from patients with chronic myeloid leukaemia spontaneously initiate factor-independent growth in vitro in association with up-regulation of expression of interleukin-3.
Blood, 2001, 97(3): 720-728

Graham SM, Jorgensen HG, Allan E, Pearson C, Richmond L, Holyoake TL.
Primitive, quiescent, Philadelphia-positive stem cells from patients with chronic myeloid leukaemia are insensitive to STI571 in vitro.
Blood, 2002, 99(1): 319-325

Jorgensen HG, Allan EK, **Graham SM**, Godden JL, Richmond L, Elliot MA, Mountford JC, Eaves CJ, Holyoake TL.
Lonafarnib reduces the resistance of primitive quiescent CML cells to imatinib mesylate in vitro.
Leukemia, 2005, May 12 [Epub ahead of print]

Drummond MW, Hoare SF, Monaghan A, **Graham SM**, Alcorn MJ, Keith WN, Holyoake TL.
Deregulated expression of the major telomerase components in leukaemic stem cells.
Leukaemia, 2005, 19(3): 381-389.

Appendix 1

Gene lists produced by IGA analysis of microarray data

Appendix 2

Affymetrix raw data.

Acknowledgements

The list of people who deserve my gratitude and thanks is lengthy, and I am eternally grateful to all of them.

Firstly, I cannot thank my supervisors Professors Gerry Graham and Tessa Holyoake enough for their immeasurable support and guidance throughout this journey. I also extend my gratitude to my advisor Dr Paul Harrison for his advice and helpful discussions. I must also thank my colleagues in ATMU and in Gerry's group at the University for always being on hand to help. Special thanks goes to Dr Kenny Douglas for his infinite patience and tolerance whilst instructing me in the art of molecular biology and for the cups of coffee and encouragement when needed– Kenny you are a star. I am also indebted to the members of haemato-oncology for their help and support over the years especially Dr Michael Alcorn, Dr Fiona Reid, Dr Jan Baird, Mrs Linda Richmond and Mrs Elizabeth Farrell. I am especially grateful to Mr Charlie Pearson for teaching me all I know about FACS and for providing endless moral support during sorting experiments – this work would not have been possible without your help. I would also like to thank Mrs Elaine Allan for assistance with FISH, Dr Keith Vass for help with bioinformatics, Dr Heather Jorgensen for BCR-ABL PCR, Mrs Christine Lang for sequencing and Dr Giorgia Riboldi-Tunnicliffe and Dr Pawel Herzyk for microarray processing and analysis.

I also extend my sincere thanks to Judith Harriman for expert help in computing. Finally, my infinite thanks and appreciation goes to my husband Stewart and children, Lauren and Rory, you have been fantastic.

I am also indebted to the Leukaemia Research Fund, Chief Scientist Office, Sylvia Aitkin Trust and GRI Endowment Fund for supporting this research.

Declaration

I declare that all the work presented in this thesis was performed by me personally unless acknowledged otherwise.

Dedication

This thesis is dedicated to my father, Francis Hawthorne, a constant source of inspiration.

Abbreviations

A	Adenine
ABCG2	ATP binding cassette subfamily member 2
ALDH	Aldehyde dehydrogenase
ALL	Acute lymphocytic leukaemia
AlloSCT	Allogeneic stem cell transplant
AML	Acute myeloid leukaemia
AP	Accelerated phase
ATP	Adenine tri-phosphate
BC	Blast crisis
BCR	Breakpoint-cluster region
BCR-ABL	The BCR-ABL fusion gene
bcr-abl	bcr-abl protein
BFUe	Burst forming unit erythroid
BM	Bone Marrow
BP	Blastic phase CML
CAFC	Cobblestone area forming cell
CCR	Complete cytogenetic response
CDK	Cyclin dependant kinase
cDNA	Complementary DNA
CFC	Colony forming cell
CFSE	Carboxy fluorescein succinimidyl ester
CLP	Common lymphoid progenitor
CML	Chronic myeloid leukaemia
CMP	Common myeloid progenitor
CP	Chronic phase CML
CV	Co-efficient of variation
C	Cytosine
DMSO	Di-methyl sulphoxide
DMF	Dimethylformamide
DNA	Deoxyribonucleic acid
DPBS	Dulbecco's phosphate buffered saline without calcium and magnesium
EST	Expressed sequence tag
FACS	Fluorescence –assisted cell sorting
FCS	Foetal calf serum
FDR	False discovery rate
FISH	Fluorescence *in situ* hybridisation
FITC	Fluorescein isothiocyanate
FL1	Fluorescence channel 1
FLT3L	Fms-like tyrosine kinase 3 ligand
FSC	Forward scatter
FTI	Farnesyl transferase inhibitor
G	Guanine
G0	Gap-phase 0 (of cell cycle)
G1	Gap-phase 1 (of cell cycle)
G2	Gap-phase 2 (of cell cycle)
GAPDH	Glyceraldehyde-3-phosphate dehydrogenase
GCSF	Granulocyte colony stimulating factor
GM-CSF	Granulocyte-macrophage colony stimulating factor
HSC	Haemopoietic stem cell
HST	Hoechst 33342
iGA	Iterative group analysis

IL3	Interleukin 3
IL6	Interleukin 6
INF	Interferon
LB Broth	Luria-Bertani broth
LDL	Low density lipoprotein
Lin^-	Lineage negative
LTC-IC	Long-tem culture initiating cell
LTRC	Long-term repopulating cell
MCM5	Mini chromosome maintenance protein 5
M-phase	Mitotic phase of the cell cycle
MACS	Magnetic cell sorting and separation
MIN	Minutes
MMOL	Milimolar
ML	Millilitre
MLL	Mixed lineage leukaemia
MNC	Mononuclear cell
mRNA	Messenger RNA
ng	Nanogram
PB	Peripheral blood
PBSC	Peripheral blood stem cell
PBS	Phosphate buffered saline
PCNA	Proliferating cell nuclear antigen
PCR	Polymerase chain reaction
PE	Phycoerythrin
Pgp	P glycoprotein
Ph	Philadelphia chromosome
PI	Propidium iodide
Py	Pyronin Y
Q-RT-PCR	Real time RT-PCR
rHu-GCSF	Recombinant human granulocyte colony stimulating factor
RMA	Robust mutichip average
RNA	Ribonucleic acid
RP	Rank products
RT	Room temperature
RT-PCR	Reverse transcriptase polymerase chain reaction
SCF	Stem cell factor
SD	Standard deviation
SDF-1	Stromal derived factor 1
SE	Standard error
Sec	Seconds
SEM	Standard error of the mean
SHWFG	Sir Henry Wellcome Functional Genomics
SNBTS	Scottish Blood Transfusion Service
S-phase	Synthesis phase (DNA) of cell cycle
SSC	Side scatter
STI571	Signal transduction inhibitor 571
STRC	Short-term repopulating cell
T	Thymine
WBC	White blood cell
µl	microlitre
µM	micromolar
UV	Ultra violet

Chapter 1 Introduction

1.1 The Normal Haemopoietic System.

The integrity and functional capacity of the immuno-haemopoietic system is maintained throughout the lifetime of an animal by a pool of pluripotent stem cells residing in the bone marrow. These cells have the capacity to both self renew and to differentiate into all haemopoietic cell types, preserving the stem cell pool and sustaining a functioning haemopoietic system. In order to achieve this a hierarchical structure exists, which results in progressive lineage commitment of haemopoietic stem and progenitor cells with successive division in response to demand for mature functional cell types. Simply to maintain the status quo the haemopoietic system has to produce around $2x10^{11}$ erythrocytes and 10^{10} white blood cells each day. Terminally differentiated cells are generally unable to divide further and are continuously replaced by the differentiation and proliferation of more primitive progenitors.

By definition all stem cells, regardless of their origin, must possess the intrinsic properties of self-renewal, differentiation and proliferation. HSC are rare (~1 in 10^5 total bone marrow cells), relatively quiescent, and are defined as those cells whose replicative potential is capable of restoring haemopoiesis after marrow ablation, therefore possessing the capacity to generate every cell of the immuno-haemopoietic system. Clearly this means that the proliferative potential of these cells is immense and must be tightly controlled to prevent excessive numbers of cells accumulating in the circulation. The control of the HSC compartment is closely associated with the bone marrow microenvironment, where the cells are influenced by regulatory factors and adhesive interactions.

1.1.1 Organisation of the Stem Cell Compartment

HSCs are closely associated with the bone marrow where stromal cells interact with stem cells and transmit signals that influence their behaviour. Two types of HSC have been identified; long-term repopulating cells (LTRC) and short-term repopulating cells (STRC). STRC's are capable of reconstituting myeloid and/or lymphoid haemopoiesis for a short period of time, around 4 months in mice (Morrison SJ, Weissman IL. 1994; Morrison SJ, Wandycz AM et al. 1997). In

contrast LTRC are capable of rescuing an ablated host for the lifetime of the animal and of producing cells that can reconstitute a secondary host (Harrison DE and Zhong RK. 1992; Morrison SJ and Weissman IL 1994). The initial reconstitution by STRC is thought to be a necessary prerequisite to long-term engraftment (Szilvassy SJ, Humphries RK et al. 1990)

Stem cells give rise to an array of terminally differentiated cells via a pool of committed progenitors. The primary function of the progenitor population is to vastly increase the numbers of differentiated cells, thereby reducing the requirement for extensive proliferation of primitive stem cells, minimising the chance of a mutation being perpetuated in a cell with self-renewal capacity (Abkowitz JL, Catlin SN et al. 2002; Gordon MY, Lewis JL et al. 2002). As HSC divide and move toward lineage commitment their self-renewal capacity is lost. Their immediate progeny, although multiipotent, have limited self-renewal potential and comprise common myeloid precursors (CMP) and common lymphoid precursors (CLP). CMP in turn give rise to committed myeloid progenitors including erythrocyte/megakaryocytes and granulocyte/macrophages. CLP give rise to B and T lymphocytes and NK cells (Akashi K, Traver D et al. 2000; Hao QL, Zhu J et al. 2001). However, the boundaries may not be as clear-cut as first thought, as an early T-cell progenitor (ETP) which retained some myeloid potential has been identified in the Thymus. This is distinct from the CLP in the bone marrow, which has no myeloid potential (Allman D, Sambandam A et al. 2003). In addition a bi-potential B-cell/macrophage progenitor has been described as being present in small numbers in adult murine bone marrow that has the capacity to develop into both lineages under the correct conditions (Montecino-Rodriguez E, Leathers H et al. 2001). A diagrammatic representation of haemopoietic cell development is shown in figure 1.1.

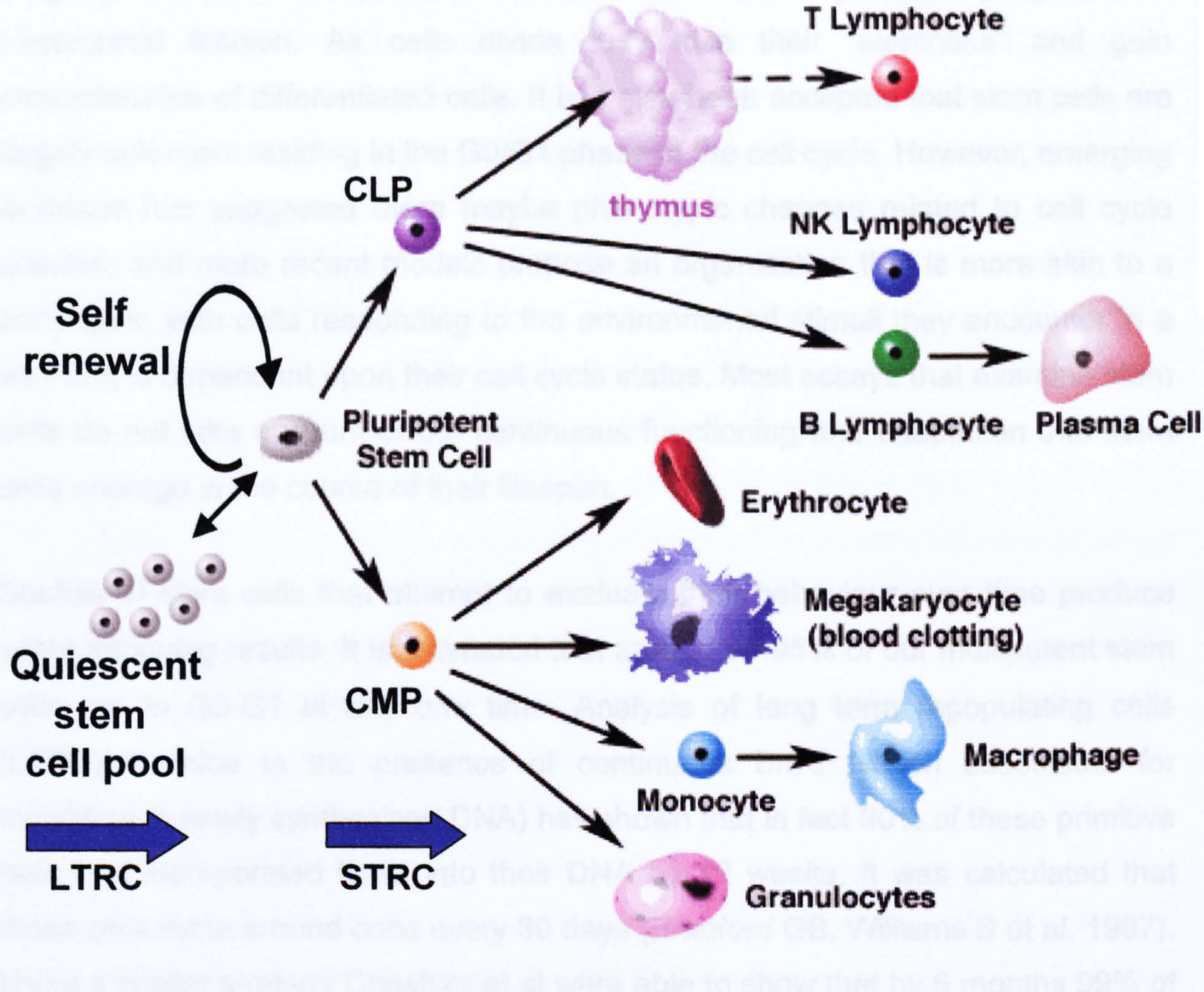

Figure 1-1 A diagrammatic representation of the haemopoietic cell hierarchy.

The classic model of haemopoiesis is a stochastic one, where stem cells produce progenitors that in turn produce differentiated functionally mature progeny in a hierarchical fashion. As cells divide they lose their "stemness" and gain characteristics of differentiated cells. It has also been accepted that stem cells are largely quiescent residing in the G0/G1 phase of the cell cycle. However, emerging evidence has suggested there maybe phenotypic changes related to cell cycle position, and more recent models propose an organisation that is more akin to a continuum, with cells responding to the environmental stimuli they encounter in a way that is dependent upon their cell cycle status. Most assays that examine stem cells do not take account of the continuous functioning and adaptation that stem cells undergo in the course of their lifespan.

Studies of stem cells that attempt to evaluate their behaviour over time produce some intriguing results. It is estimated that around 90-95% of our multipotent stem cells are in G0-G1 at any one time. Analysis of long term repopulating cells (LTRC) in mice in the presence of continuous BrdU (which substitutes for thymidine in newly synthesised DNA) has shown that in fact 90% of these primitive cells had incorporated BrdU into their DNA by 12 weeks. It was calculated that these cells cycle around once every 30 days (Bradford GB, Williams B et al. 1997). Using a similar strategy Cheshier et al were able to show that by 6 months 99% of LTRC had entered cell cycle and calculated that approximately 8% of stem cells enter cell cycle daily (Cheshier SH, Morrison SJ et al. 1999). However stem cell kinetics in the murine system may not be mirrored for human stem cells, and clearly similar experiments in human subjects are not feasible. An interesting set of experiments using non-human primates (with similar transplantation kinetics to humans) showed that primitive stem cells do enter cell cycle although at a much slower rate than those of rodent stem cells (Mahmud N, Devine SM et al. 2001). Quiescent cells are not inert; whilst they may not be transiting the cell cycle they are transcriptionally active including DNA repair. Synthesis of newly repaired fragments of DNA will also incorporate BrdU, albeit at a much lower level than replicated DNA, and this should be excluded from measurements of incorporation due to proliferation (Pang L, Reddy PV et al. 2003).

1.1.2 Haemopoietic Stem Cell and Progenitor Assays

All haemopoietic stem and progenitor assays generally determine two factors; differentiation potential and proliferation. This necessitated that each assay was

specific for the cell population being measured. Clonogenic assays have been designed to identify the progeny of each progenitor and usually take the form of cells seeded in semi-solid medium containing growth factors specific for the population of interest. The read out from these assays is no longer than 3 weeks; therefore they are only capable of measuring progenitor and not stem cell function.

Clonogenic assays detect more mature progenitors and are normally specific for a particular lineage depending on the growth factors included. The cells used to establish these assays in semi-solid medium may be un-manipulated bone marrow, peripheral blood mononuclear cells or cells generated from assays of more primitive stem cells such as LTC-IC, discussed in more detail below. CFU-GM, CFU-G, CFU-M, and BFU-e are commonly used to demonstrate the potential to differentiate down a particular pathway and colonies containing multiple cell types are generally regarded as indicative of multipotency. It is accepted that combinations of growth factors are needed to induce stem cell differentiation (some of which can only act in synergy) and this in turn produces a variety of cell types in clonogenic assays.

The first haemopoietic stem cell assay was the CFU-S assay described by Till and McCulloch (Till JE and McCulloch EA. 1961). This assay measured in vivo stem cell proliferation and differentiation based on the observation that transplanted stem cells form colonies on the spleen of a lethally irradiated host within two weeks of transplantation, and that the number of colonies is directly proportional to the number of input cells. The cells contained in these visible colonies have the capacity to form colonies in a secondary transplant demonstrating self-renewal capability. The CFU-S colonies visible at day 8 contain mostly differentiated cells with day 12 colonies containing more multilineage cells, which is a reflection of the differentiation status of the initiating cells. However, both of these belong to the STRC class of stem cells; accordingly, the terminology pre-CFU-S has been used to refer to LTRCs.

To detect more primitive cells in vitro, cultures that include a supportive stroma are required. To proliferate in culture LTRC need to have stromal contact that mimics the bone marrow microenvironment. The first stromal assay was developed by Dexter (Dexter TM, Allen TD et al. 1977) using mouse whole bone marrow that was able to generate mature progeny for several months. Ploemacher and Brons further refined the assay by seeding cells onto preformed stromal layers that had

been irradiated to prevent proliferation of indigenous cells (Ploemacher RE and Brons NC. 1988). This technique allowed the development of the cobblestone area forming cell assay (CAFC) in which the cells that form a distinctive cobblestone pattern underneath the stromal layer, were subsequently shown to demonstrate a maturity which correlated inversely with time, as tested in secondary colony forming assays. Day 28 CAFC was shown to be proportional to the expected frequency of marrow repopulating cells and day 7 CAFC to be equivalent to D-12 CFU-S (Ploemacher RE, Van Der Sluijs JP et al. 1989). The sequence of events in CAFC, which apparently mirrored in vivo stem cell development, led to this assay being utilised for the measurement of drug and radiation sensitivity of various stem cell populations (Down JD and Ploemacher RE. 1993)

Another similar assay is the long-term culture initiating cell (LTC-IC) assay but this assay has a different end-point. Cells are seeded onto established irradiated stromal layers and colony forming assays carried out at 5 weeks using the non-adherent cells from the cultures. It has been reported for human cells that the CAFC and LTC-IC assays may give conflicting results in terms of primitive cell numbers. This may be explained on the basis of differences in the stromal cells used. Whilst these assays give an indication of the proliferative capacity of stem cells it must be borne in mind that they give no indication of the in vivo homing capability which is crucial for HSC reconstitution.

The only reliable measure of true stem cell potential is still the in vivo repopulation assay, a xenograft model which allows human transplanted cells to analysed. This model utilises cells transplanted into a diabetic mouse with severe combined immunodeficiency disease (NOD/SCID) mice. These mice were produced by crossing SCID (T and B cell defects) and NOD mice (partially deficient in NK cells, antigen presentation and macrophage function). Interestingly there was no requirement to supplement these mice with human cytokines if >500 cells were transplanted (Bonnet D, Bhatia M et al. 1999). Either the mouse bone marrow stroma produced the required cytokines or the transplanted cells were able to secrete them.

First described by Kamel-Reid and Dick in 1988, this xenograft model has been extensively used to demonstrate homing, proliferation, differentiation and self-renewal of human stem cells, and has opened the way for more rational investigations of human haemopoietic stem cell behaviour (Kamel-Reid S and Dick

JE. 1988). Some mouse strains have been further modified to produce human cytokines improving the environment for transplanted human cells. This model though one of the most useful is not without limitation. For example, there is a bias in the transplanted mice toward B cell development with T cell production being less favoured. Engraftment can only be monitored for a short time period (around 6 months lifespan), which is limiting for a model of long-term human engraftment. Other xenograft models have been established, most notably in sheep by Zanjani et al, however immune rejection necessitated that human HSC be introduced into the developing foetus to induce immune tolerance (Zanjani ED, Flake AW et al. 1994). This model has allowed transplanted human HSC to be monitored over several years, and in addition, no radiation or conditioning of the host environment was required, minimising disruptive effects on the stem cell niche. However, there are a number of disadvantages in large animal models including expense, handling, and long term read out.

1.1.3 Identification of Haemopoietic Stem Cells

Due to the relative accessibility of haemopoietic stem cells they are probably the most extensively studied of all adult stem cell populations. The remarkable similarity between mouse and human haemopoietic systems has allowed much of the investigative work aimed at defining markers, to be done in the mouse and subsequently confirmed for human stem cells. However, the markers used to identify stem cells differ between the two, with in vivo repopulating capacity being the ultimate verification of stem cell status.

1.1.3.1 Stem Cell Markers

There is no single marker for haemopoietic stem cells; a combination of surface markers and lack of lineage specific markers expressed on more mature progeny is commonly used to isolate stem cell populations. These populations have been shown to contain cells with the ability to rescue an ablated host, therefore by inference they must contain multipotent stem cells. Table 1.1 lists the markers used most commonly for isolation of both mouse and human cells. Fluorescently tagged monoclonal antibodies to these surface antigens allow cells to be identified by FACS and the relative stem cell numbers to be calculated. Using FACS sorting, stem cells can be isolated from whole blood or bone marrow though, given their rarity, for practical reasons a prior enrichment step is usually included.

Human	Mouse
CD34$^+$ c-kit$^+$ Thy-1^{lo}	Sca-1$^+$ cKit$^+$ Thy-1^{lo}
Negative for:-	
CD10 CD14 CD15 CD16 CD19 CD20	B220 CD3,4,8 Mac-1 Gr-1 Ter 116

Table 1-1 Table of surface markers used for identification of human and mouse haemopoietic stem cells.

The most common surface markers used to isolate mouse HSC are Lin$^-$ Sca-1$^+$ Thy-1^{lo} cKIT$^+$. (Spangrude GJ, Heimfeld S et al. 1988) The addition of IL-7Rα as a marker has allowed the discrimination of CMP and CLP populations. The IL-7Rα$^+$ fraction contains almost all of the common lymphoid progenitors giving rise to T, B and NK cells, whereas the common myeloid progenitor is found almost exclusively in the IL-7Rα$^-$ fraction of the Lin$^-$ Sca-1$^+$ Thy-1^{lo} population (Kondo M, Weissman IL et al. 1997; Akashi K, Traver D et al. 2000). Murine cells also express CD34, however experiments using transgenic mice engineered using P1-based artificial chromosomes (PAC-transgenics allow human gene and protein expression in mouse cells) have shown that CD34 is expressed differently in mice than in human stem cells. CD34 is only expressed on human repopulating cells whereas murine CMP and CLP express both human and murine CD34. It has been further revealed that elements regulating the gene expression of CD34 are very different in human and mouse haemopoietic stem cells (Akashi K, Traver D et al. 2000; Okuno Y, Huettner CS et al. 2002; Okuno Y,).

Undoubtedly the most important human stem cell marker is CD34, a transmembrane glycoprotein expressed on the surface of haemopoeitic stem and progenitor cells, which was first discovered in a myeloblastic leukaemia cell line (Civin CI, Strauss CL et al. 1984). The exact function of the CD34 molecule on

stem cells is as yet undefined; roles in differentiation and cytoadhesion have recently been suggested (Krause DS, Kapadia SU et al. 1997; Hidalgo A, Weiss LA et al. 2002). Although it's precise role in haemopoiesis is still under investigation, it's importance in selection and purification of HSC for both experimental purposes and for human transplantation is indisputable.

CD34 is expressed on ~1-4% of normal bone marrow nucleated cells and on <0.1% of the nucleated peripheral blood cells under homeostatic conditions. This small fraction of the total white blood cells contains almost all of the cells with in vivo repopulating capacity as well as the LTC-IC and CFC, but does not include terminally differentiating cells (Saeland S, Duvert V et al. 1992), (Civin CI, Strauss CL et al. 1990). Following depletion of cells expressing lineage markers (Lin^-) the $CD34^+$ cell population is still extremely heterogeneous, and in an effort to identify a more primitive stem cell population, CD34 has been used in combination with other surface markers e.g. CD38, which is expressed on $CD34^+$ cells as they become more mature. $CD34^+CD38^-$ cells have the capacity to rescue immunodeficient mice following transplantation, whereas the more mature $CD34^+CD38^+$ cells can only confer short-term reconstitution and have no secondary repopulation potential (Hogan CJ, Shpall EJ et al. 2002).

There is now a considerable body of evidence to suggest that $CD34^-$ stem cells exist in both humans and mice that also have repopulation capacity (Osawa M, Hanada K et al. 1996; Bhatia M, Bonnet D et al. 1998). Sato et al documented that murine CD34 expression is inducible both in vitro and in vivo and that it is a reversible process (Sato T, Laver JH et al. 1999), (Dao MA, Arevalo J et al. 2003). Recently it has been demonstrated that the same is true of human CD34 expression and that $CD34^-Lin^-$ cells have marrow-engrafting capacity. Furthermore tertiary transplants confirmed that long-term engraftment potential was demonstrable for both $CD34^+$ and $CD34^-$ cells (Zanjani ED, Almeida-Porada G et al. 2003). These observations suggest either that expression of the CD34 antigen is not necessary for stem cell function or that phenotypically different cells can have similar functional capacity.

Recent published work by Dooley et al has shown that in vitro modulation of the CD34 antigen takes place and that it is associated with proliferation status. These experiments illustrated that $CD34^-$ cells can regain CD34 expression and that their proliferative capacity is similar to $CD34^+$ cells. This modulation was not associated

with differentiation. In addition, if $CD34^+$ cells remained undivided i.e. quiescent in culture for more than 2 days, they lost CD34 expression, which was reinstated when these cells started to proliferate. All of these findings illustrate that the Lin^- $CD34^+$ population is intrinsically heterogeneous with respect to CD34 expression, but still retains repopulation activity in this primitive subset that can be used clinically for transplantation (Dooley DC, Oppenlander BK et al. 2004).

Other possible markers for primitive stem cells include CD133, which is expressed on a subset of $CD34^+$ cells. These cells include the repopulating cells and primitive progenitors excluding erythroid progenitors. However CD133 is also expressed on $CD34^-$ human cord blood HSC (Yin AH, Miraglia S et al. 1997; Gallacher L, Murdoch B et al. 2000). It is unclear whether CD133 provides any advantage over CD34 as a stem cell selection marker. Another recently identified marker for human HSC is the vascular growth factor receptor 2 (KDR). It has been reported that KDR^+ cells are Lin^- $CD34^+CD38^-$ and are highly enriched for SRC (SCID repopulating cell) potential, with lineage committed stem cells being $CD34^+KDR^-$ (Ziegler BL, Valtieri M et al 1999). More recently, Danet et al have identified $C1qR_P$ (the human homologue of the mouse stem cells antigen AA4) which is expressed on both $CD34^+$ and on $CD34^-$ stem cells from human cord blood and bone marrow as a positive marker of BM repopulating cells (Danet GH, Luongo JL et al. 2002). Interestingly, these experiments also showed that $C1qR_P$ cells have the capacity to develop into human hepatocytes in NOD/SCID mice, indicative of stem cell plasticity discussed in more detail below.

1.1.3.2 Alternative Ways to Identify HSC

In 1996 Goodell et al identified a new population of mouse stem cells by staining with Hoechst 33342 and viewing the dual wavelength UV emission on a FACS plot. These cells were designated side population cells due to their position on this plot. These cells were subsequently shown to be Lin^-CD34^- and to contain repopulation potential. The SP position of these cells depended on their ability to efflux dyes like Rhodamine or Hoechst (Goodell MA, Brose K et al. 1996) The efflux of drugs and dyes such as these has since been attributed to the activity of P-glycoprotein; an ATP-binding cassette (ABC) transporter expressed on the cell surface. When the activity of this transporter pump is inhibited by verapamil the numbers of SP cells decrease. However P-gp knockout mice contain SP cells indicating that other ABC transporters may contribute to the SP phenotype.

Human SP cells were also shown to be $Lin^{-}CD34^{-}$ and highly enriched for LTC-IC activity and to express CD34 following stromal cell culture (Goodell MA, Rosenzweig M et al. 1997).

An additional method to purify HSC, which also relies on a functional characteristic, involves the activity of the cytosolic enzyme aldehyde dehydrogenase (ALDH). Responsible for oxidising aldehydes to carboxylic acids, ALDH is found in high concentration in the cytoplasm of HSC rendering them resistant to the effects of alkylating agents such as cyclophosphamide. The introduction of a fluorescent substrate for ALDH allowed the identification of cells with high levels of enzyme to be distinguished and sorted from the rest of the HSC population (Storms RW, Trujillo AP et al. 1999). These cells were found to be enriched for repopulating cells when introduced into NOD/SCID mice (Hess DA, Meyerrose TE et al. 2004). Given that there appears to be some debate regarding the surface phenotype of HSC, perhaps isolation methods that rely on biological function rather than surface markers may prove to be more reliable.

1.1.4 Self Renewal of HSC

In clinical terms, understanding the control of stem cell self-renewal has been the ultimate goal for ex vivo stem cell expansion. If stem cells could be induced to self renew in culture, the implications for transplantation would be enormous. By definition a stem cell is one that can both renew itself and differentiate into multiple lineages. In addition, when a malignancy occurs in a self-renewing stem cell it can perpetuate the disease limiting the chances of a cure. Factors that control self-renewal are still largely unknown, however the recent availability of technology to identify gene expression profiles in purified stem cell populations has shed light on possible candidates. To date, genes implicated in self-renewal include transcription factors, genes involved in chromosomal rearrangements, cell cycle inhibitors and signalling pathways. It is not surprising that many of the genes involved in stem cell self-renewal identified so far have their origins in developmental biology. For an embryo to survive, the early cells must divide and retain their stem cell characteristics before differentiating into the cells of various organs in due course.

1.1.4.1 HOX genes.

HOX genes are highly conserved transcription factors involved in embryogenesis. HOXB4 was first shown 10 years ago to cause the selective expansion of primitive progenitors when over expressed in HSC and to confer an enhanced repopulation advantage over non-transduced cells assessed after several months. Despite the expansion of primitive HSC in these repopulation experiments the HSC pool size did not exceed that of non-transduced HSC suggesting that overexpression of HOXB4 did not influence the regulation of pool size (Sauvageau G, Thorsteinsdottir U et al. 1995).

Further experiments with HOXB4 HSC expanded ex vivo and marked with GFP (green fluorescent protein) have shown that the expanded cells were functional and able to reconstitute long term haemopoiesis when transplanted. Furthermore there was greater expansion in primitive HSC compared to more mature cell types. Using a stromal cell line engineered to produce HOXB4, Amsellem et al showed that human LTC-IC and SCID repopulating cells were expanded in vitro by >20- and 2.5-fold respectively (compared to input numbers) and that this expansion was accompanied by increased repopulating ability in vivo (Amsellem S, Pflumio F et al. 2003). Thus it would appear that primitive human stem cells could be expanded in vitro in response to HOXB4 and still retain their stem cell phenotype.

Other published work has shown a similar role for HOXC4, where over expression in human $CD34^+$ cells induces in vitro expansion of both primitive and committed progenitors (Daga A, Podesta M et al. 2000). HOXC4 is a paralog of HOXB4 and the similar results obtained with over expression experiments suggest overlapping roles for paralogs in the maintenance of the primitive status of HSC. On the other hand, more recent studies have shown that HOXB4 deficient mice only have a minor proliferation deficiency and sustain comparatively normal haemopoiesis (Brun AC, Bjornsson JM et al. 2004). In vitro, the cells from these mice show reduced proliferation of primitive cells, which is also observed following transplantation. Further analysis revealed that the lack of HOXB4 also appeared to influence the expression of other HOX genes as well as some genes associated with cell cycle. It was also noted that these HOXB4 deficient mice had reduced cellularity in both the bone marrow and spleen, suggesting that although other HOX genes compensate for the loss of B4 they do so at a sub optimal level. There is a close association with the development of leukaemia and many of the HOX

genes, however HOXA4 (a paralog of HOXB4) does not appear to be associated with the disease. If HOXA4 plays a central role in stem cell self-renewal, this would suggest that augmentation of self-renewal alone is not, in itself, able to cause leukaemia.

1.1.4.2 Polycomb-group Genes

Recent studies have highlighted another candidate involved in haemopoietic stem cell self-renewal, the polycomb-group (PcG) gene Bmi-1. PcG genes play a vital role in embryogenesis, cell cycle regulation and lymphopoiesis. They are responsible for maintenance of gene silencing and in so doing confer the cell's functional identity. Their involvement in malignant transformation has created a great deal of interest and subsequent investigation. PcG proteins form complexes containing histone deacetylase and methylase activity and are involved in the modification of chromatin structure and histone tails (reviewed in (Orlando V 2003).

Park et al have demonstrated that adult mouse and human HSC express the proto-oncogene Bmi-1 and that bone marrow transplanted from Bmi-1$^{-/-}$ mice was able to initiate temporary haemopoiesis only. In addition, there was no evidence of self-renewal of adult HSC and gene expression analysis showed that a range of stem cell associated genes was altered in the bone marrow of these mice (Park IK, Qian D et al. 2003). Lessard et al showed that Bmi-1 has a role in the regulation of proliferative capacity in both normal and leukaemic stem cells and that endogenous Bmi-1 can rescue cells from apoptosis, growth arrest and differentiation (Lessard J and Sauvageau G 2003). A further study by Iwama et al has confirmed that increased expression of Bmi-1 promotes HSC self-renewal. By transducing HSC with GFP or Bmi-1, culturing single cells and separating the daughter cells by micromanipulation, the authors were able to show that forced expression of Bmi-1 promoted symmetrical cell division. Each of the daughter cells was shown to exhibit similar proliferation potential in colony assays, and the probability of symmetrical cell division was significantly higher in the Bmi-1 transduced cells than in the controls (Iwama A, Oguro H et al. 2004). The additional finding that Bmi-1 can extend the lifespan of mammary epithelial cells by up regulating the telomerase RT gene (hTERT) could have further implications for HSC self-renewal and malignant transformation (Dimri GP, Martinez JL et al. 2002).

1.1.4.3 Notch Genes

Notch receptors are critical to HSC regulation where they are involved in stem cell fate decision i.e. whether a cell self-renews or differentiates. They are also involved in specification of T or B lymphocyte development from the common lymphoid progenitor cell (Pui JC, Allman D et al. 1999). Notch receptor gene knockouts are embryonic or perinatally lethal, demonstrating the importance of these genes in development (Xue Y, Gao X et al. 1999), (Jiang R, Lan Y et al. 1998), (Hrabe de Angelis M, McIntyre J 2nd et al. 1997). There are 4 Notch receptors that have partially overlapping functions and share homology in structure and in ligand binding. The ligands for Notch receptors are the transmembrane proteins Jagged 1, Jagged 2 and Delta. Following binding the intracellular portion is cleaved and translocates to the nucleus where it acts as a transcriptional activator.

Varnum-Finney et al have demonstrated, using a retroviral vector, that constitutive expression of the intracellular domain of Notch leads to the generation of immortalised cell lines from cytokine dependant haemopoietic cells. These cells are capable of in vivo repopulation of both myeloid and lymphoid lineages (Varnum-Finney B, Xu L et al. 2000). In a series of experiments using the Notch ligand Delta 1 immobilised on tissue culture plates in combination with defined cytokines, Varnum-Finney et al demonstrated a 4-5 log increase in the number of cells capable of short-term lympho/myeloid repopulation in NOD/SCID mice after 28 days in culture. The significant increases in progenitor cells observed in this study are in contrast to other published work where only modest increases in primitive cells have been observed using Delta 1 as a soluble factor. The considerable expansion seen here is attributed to the immobilised presentation of the ligand in combination with the cytokine cocktail (Varnum-Finney B, Brashem-Stein C et al. 2003). These results confirm a role for Notch in self-renewal of HSC and progenitors.

More recent studies have identified Notch signalling as indispensable for the maintenance of undifferentiated stem cells but not for their survival or cell cycle initiation. In transgenic Notch reporter mice, Notch signalling was identified in HSC in vivo, and was down regulated as differentiation progressed. In addition when Notch signalling was inhibited differentiation was hastened. Furthermore Wnt (see

below) alone was unable to maintain undifferentiated HSC when Notch signalling was absent (Duncan AW, Rattis FM et al. 2005).

1.1.4.4 Wnt Genes

Wnt-mediated signalling is implicated in a number of processes in both vertebrate and invertebrate development. Wnt proteins have been shown to regulate segment polarity in Drosophila and axis specification in Xenopus as well as limb, somite and axis configuration in mice. More recently, Wnt signalling pathways have been implicated in HSC self-renewal and proliferation.

There are 19 Wnt genes that encode lipid-modified signalling proteins that serve as ligands for the Frizzled family of receptors or the lipoprotein receptor-related protein (LRP). In the absence of Wnt signalling, β-catenin is retained in the cytoplasm where it becomes associated with a destruction complex containing APC, Axin and GSK-3β. In the presence of Wnt signalling, GSK-3β is inhibited by Dishevelled and is unable to phosphorylate β-catenin, which results in its stabilization and accumulation in the cytosol. β-catenin then translocates to the nucleus where it forms a complex with the lymphoid-enhancer-binding factor (LEF)/T-cell factor (TCF) family of transcription factors, which in turn allows induction of specific target genes (Reya T 2003), (Ikeda S, Kishida S et al. 1998; Kishida S, Yamamoto H et al. 1998).

Murdoch et al have demonstrated that injection of Wnt5A into mice transplanted with human cord blood haemopoietic cells increased the level of reconstitution and output of primitive haemopoietic cells in vivo. Reya et al provided further evidence of Wnt induced expansion of HSC, where active β-catenin (normally produced as a consequence of Wnt signalling) was constitutively over expressed in retrovirally-transduced stem cells resulting in the proliferation of HSC populations in the absence of differentiation. It was estimated that β-catenin caused an 8-80-fold increase in HSC number after just 1 week in culture. Conversely, engineered expression of soluble Frizzled receptor (which inhibits Wnt signalling), or intracellular expression of Axin (involved in β-catenin degradation) caused a reduction in the proliferation and survival of primitive HSC in vitro. Interestingly, these experiments also revealed that Wnt activation produced an increase in expression of HOXB4 and Notch 1, previously associated with HSC self renewal. (Reya T, Duncan AW et al. 2003).

1.1.4.5 p21 and p27

Stem cells are comparatively quiescent, entering cell cycle relatively infrequently compared to progenitor cells, whose expansion is rapid and extensive. Cyclin dependant kinases (CDK) and inhibitors (CDKI) control cell cycle progression, with the CDKIs serving as checkpoints limiting progression through the different cell cycle phases. There are two families of CKIs; the CIP/KIP family which includes $p21^{Cip/Waf}$ (p21), $p27^{Kip}$ (p27), and $p57^{Kip2}$, and the INK4 family including $p16^{Ink4}$, $p15^{Ink4b}$, $p18^{Ink4c}$ and $p19^{Ink4d}$. The two families are distinguished by the CDKs they inhibit; the INK4 members act on CDK4 and CDK6 and the CIP/KIP family acts on a number of CDKs but particularly on CDK2. p27 is distinct from p21 in its C terminus and is not a target for p53. Most CDKIs are regulated at the post-transcriptional level, however p27 is also subject to post-translational regulation.

It has been shown that the bone marrow of $p21^{-/-}$ mice contain increased numbers of HSC and show increased HSC cell cycling, however exhaustion of stem cells was observed under conditions of stress. (Cheng T, Rodrigues N et al. 2000). p27 was shown to have a similar effect, however this was observed in a more mature progenitor population. Recent studies by Yuan et al have demonstrated that deletion of $p18^{Ink4c}$ results in vastly improved engraftment of murine stem cells, largely due to an increase in self-renewal divisions (Yuan Y, Shen H et al. 2004). These observations suggest that different CDKIs have diverse effects depending on cell context and activation status.

1.1.4.6 Others

Maintenance of telomeres is critical to self-renewal. Telomeres are guanine-rich repeat sequences at the ends of chromosomes that act to preserve genomic stability. In the absence of telomerase (an RNA/protein complex that extends telomeres) DNA is not fully replicated and as a result progressive shortening of the chromosome ends occurs. Progressive telomere shortening leads to replicative senescence and ultimately to cell death. A feature of many malignant cells is the up-regulation of telomerase, and thus escape from senescence and preservation of division potential. Telomerase is expressed in HSC with self-renewal capacity and declines as cells become more differentiated (Morrison SJ, Prowse KR et al. 1996). Despite the intrinsic telomerase activity in HSC, their telomeres continue to shorten with division in vivo. Accelerated shortening of telomeres in transplanted

HSC compared with donor HSC is observed initially, however the differences reach a level that does not change after around a year post-transplant (Brummendorf TH, Rufer N et al. 2001). Serial transplants in mice are limited to ~4 rounds suggesting that HSC cannot self-renew indefinitely, however stresses on transplanted cells in terms of homing and establishment of cell interactions within the bone marrow niche may influence their long term stability (Harrison DE and Astle CM. 1982).

Yet another candidate implicated in stem cell regulation has its origins in embryogenesis; the Hedgehog (Hh) family of proteins is involved in the organisation and specification of early mesoderm and embryonic tissues. The group comprises Sonic Hedgehog (Shh), Indian Hedgehog (Ihh) and Desert Hedgehog (Dhh), and two transmembrane receptors Patched (Ptc) and Smoothened (Smo), with Ptc being the primary receptor. When Hh binds Smo the subsequent signalling events modulate expression of genes such as Wnt (described above) and the bone morphogenic protein (BMP)-4 specific inhibitor Noggin. BMP-4 is a member of the transforming growth factor (TGF-β) superfamily and has been shown to enhance stem cell survival at high concentration (Bhatia M, Bonnet D et al. 1999). Shh, Ptc and Smo gene expression has been identified in primitive HSC. Bhardwaj et al have shown that addition of anti-Hh inhibited the cytokine-induced proliferation of HSC; in contrast treatment with Shh induced expansion of primitive human HSC in transplanted mice. In addition Noggin was able to inhibit the mitogenic effect of Shh showing that Shh acts through BMP-4 (Bhardwaj G, Murdoch B et al. 2001).

1.1.5 The Stem Cell Niche

Central to the behaviour of stem cells are the environmental influences to which they are subject. The bone marrow stroma consists of a variety of cell types including endothelial cells, fibroblasts and osteoblasts as well as extra cellular matrix (ECM) components, which include collagen, fibronectin, laminin and proteoglycans. The cell-cell interactions between these and HSC are mediated through a variety of specific molecular targets within this niche, which act to control stem cell behaviour. The ECM can bind growth factors produced by stromal cells creating distinct "pockets" that accumulate HSC. The ECM can also bind to glycoproteins expressed on HSC. Stromal cells are known to secrete or present in bound form a variety of cytokines important for HSC survival and proliferation.

These include IL-1, -6, -11 and certain colony stimulating factors e.g. stem cell factor (SCF), flt3 ligand (FL), tumour necrosis factor α (TNFα) and TGFβ (Sensebe L, Deschaseaux M et al. 1997).

Adhesive interactions also play a critical role in HSC regulation by the BM microenvironment. Numerous receptors on HSC are involved in adhesion to stroma, including very late antigen-4 (VLA-4) and VLA-5 receptors for fibronectin, CD44, the receptor for hyaluroinc acid (a component of the ECM), and a number of stromal cell surface receptors such as intracellular adhesion molecule (ICAM) and vascular adhesion molecule (VCAM), a ligand for VLA-4. In fact, blocking VCAM with monoclonal antibody in vivo leads to an increase in circulating HSC, suggesting that these cells are unable to efficiently adhere to molecules within the BM stroma (Kikuta T, Shimazaki C et al. 2000). Studies of BM $CD34^+$ cells cultured with and without stroma, fixed stromal layers or integrin binding FN fragments showed increased preservation of LTC-IC and ELTC-IC with or without associated cell division in the presence of stroma or FN fragments (Bhatia R, Williams AD et al. 2002), reinforcing the significance of stromal interaction with stem cell behaviour.

More recently two groups have identified a population of osteoblasts in the BM that appear to influence HSC behaviour. In the study by Calvi et al, mice were genetically altered to produce active parathyroid hormone PTH/PTHrP receptors (PPRs) controlled by an osteoblast specific promoter. They were able to show that not only was there an increase in the number of osteoblasts in response to PPR but this was accompanied by a 2-fold increase in HSC (but not progenitor cells), and that the effect could be reproduced in normal mice by injection of PTH. Significantly these changes were also associated with increased production of the Notch ligand, Jagged 1 by osteoblasts and increased Notch activation in vivo, that could be negated by specific inhibition of Notch (Calvi LM, Adams GB et al. 2003). Using a different approach Zhang et al demonstrated that mutant mice with an increased endosteal bone surface and reduced BM cavity also show around a 2-fold increase in HSC. In addition, they also show that long-term HSC are preferentially attached to the N-cadherin$^+$ osteoblasts. N-cadherin forms a complex in tissue cell junctions and also forms active signalling complexes with β-catenin, recently shown to play a role in HSC self-renewal (Zhang J, Niu C et al. 2003).

These studies provide conclusive evidence for the involvement of osteoblasts in HSC regulation and recent data has suggested that angiopoietin-1 (Ang-1, expressed on osteoblasts) mediated signalling through its receptor Tie2 (expressed on HSC) plays a role in HSC quiescence and protection from apoptosis (Arai F, Hirao A et al. 2004).

1.1.5.1 Stem Cell Homing and Mobilisation

As detailed in the previous section, stem cells have an intimate relationship with the BM microenvironment and with specific cell types. Tracking transplanted stem cells stained with CFSE (a permanent non-specific stain) demonstrated that more primitive cells selectively migrated to the endosteal region whereas more mature cells lodged in the central bone marrow region and that this migration occurred rapidly within 5-15 hours post-transplant. Non-ablated hosts were used in this study to eliminate the possible influence of a damaged stromal environment (Nilsson SK, Johnston HM et al. 2001).

Central to the success of BM and peripheral blood stem cell (PBSC) transplantation is the ability of stem cells to locate and colonise the host stem cell niche. These processes are likely to be regulated by a combination of adhesive and chemokine receptor-ligand interactions. Adhesive interactions play a central role in homing and in particular VLA-4 (discussed in detail previously) has been shown to be a crucial factor. Preincubation with anti-VLA-4 antibody decreased the engraftment of human $CD34^+$ cells in the BM of fetal sheep, with a corresponding increase in human cells in the peripheral blood (Zanjani ED, Flake AW et al. 1999). Also key to the homing process is the chemoattractant interaction between stromal-derived factor-1 (SDF-1 also known as CXCL12) and its receptor CXCR4 expressed on stem cells. SDF or CXCR4 knockouts have multiple lethal defects including impaired haemopoiesis (Nagasawa T, Hirota S et al. 1996; Ma Q, Jones D et al. 1998). However $CXCR4^{-/-}$ fetal liver cells are capable of engraftment in the BM of wild type mice albeit with defects in retention of B-lymphoid and granulocytic lineage precursors in the BM (Ma Q, Jones D et al. 1999). These results suggest SDF-1/CXCR4 interactions can act in combination with other mediators of homing and engraftment. Nonetheless SDF-1 has been shown to be a potent chemoattractant for human stem cells in vitro and addition of antibody to CXCR4 abolished these effects (Jo DY, Rafii S et al. 2000). Lack of engraftment in vivo by treatment with anti-CXCR4 and successful engraftment of $CD34^+$ cells induced to

express CXCR4 illustrate the importance of this receptor-ligand interaction in HSC reconstitution (Peled A, Petit I et al. 1999).

One of the most important aspects of stem cell transplantation is the movement of repopulating cells out of the BM niche and into the circulation termed mobilisation. Stem cell mobilisation can be stimulated by administration of cytotoxic drugs such as cyclophosphamide, hydroxyurea or 5-fluorouracil and by certain cytokines including G-CSF, GM-CSF, IL-11, IL-3, IL-8 Flt3L etc or by a combination of both cytotoxic drugs and cytokines. By far the most commonly used regimen utilises G-CSF. Although the kinetics of mobilisation are relatively slow (peak at 5-6 days), the benefits include minimal toxicity and relative ease of administration (IV injection, dose based on weight). Not surprisingly, many of the factors involved in BM homing also play a part in mobilisation. For example, in mice treated with cyclophosphamide/G-CSF, expression of VLA-2 and VLA-4 is reduced on mobilised peripheral blood HSC. Also, treatment with anti-VLA-4 antibodies induces mobilisation of CFC and long-term repopulating cells (Craddock CF, Nakamoto B et al. 1997).

More recent data have described the cleavage of the N-teminus of CXCR4 on HSC in the BM and on those mobilised into the circulation in response to GCSF. This leads to a reduction in the chemoattractant interactions of CXCR4 and SDF-1, which was further shown to involve a decrease in SDF-1 concentration in the BM, accompanied by an increase in proteases able to cleave SDF-1 (Levesque JP, Hendy J et al. 2003). Petit et al have further shown G-CSF stimulated mobilisation by reducing SDF-1 in the BM, and that the gradual reduction was due to degradation by neutrophil elastase. Reduction in SDF-1 was associated with increased mobilisation, which was reduced by inhibition of neutrophil elastase. (Petit I, Szyper-Kravitz M et al. 2002). A recent report from Broxmeyer et al has demonstrated that in vivo (mouse and human), treatment with a CXCR4 antagonist can produce mobilisation of HSC and can act in synergy with G-CSF to increase stem cell mobilisation. They also showed that the mobilised cells were primitive HSC able to repopulate a secondary host (Broxmeyer HE, Orschell CM et al. 2005).

One of the notable aspects of cytokine-induced mobilisation is that most of the circulating HSC are quiescent (in G0 or G1 phases of the cell cycle), however it was not known if quiescent cells were preferentially released into the circulation or

if the cells had divided prior to release (Ponchio L, Conneally E et al. 1995; Donahue RE, Kirby MR et al. 1996; Uchida N, He D et al. 1997). In an interesting study by Wright et al, mice were treated with cyclophosphamide/G-CSF and BrdU (which is incorporated into dividing cells) and assessed for the presence of divided and undivided stem cells. The results indicated that almost all of the LT-HSC had entered cell cycle prior to release from the BM and that cells enter the blood in the post mitotic M phase of the cell cycle (Wright DE, Cheshier SH et al. 2001). It is known that the proportion of cycling cells in the BM is greater than in mobilised peripheral blood, which could be explained by these findings.

1.1.6 Stem Cell Plasticity

No discussion on stem cells would be complete without some mention of plasticity or the apparent ability of stem cells to develop alternative fates. The demonstration of fate switching in B-lineage cells from Pax-5-deficient mice to different haemopoietic cell types has indicated that plasticity may be a genuine feature (Rolink AG, Nutt SL et al. 1999). Kondo et al have also demonstrated that the fate of common lymphoid progenitors could be redirected to the myeloid lineage by stimulation through IL-2 receptor, suggesting that the fate of individual cells can be influenced by cytokine stimulation (Kondo M, Scherer DC et al. 2000). A body of evidence existed that HSC could switch to a non-haemopoietic fate, particularly at the site of injury for example to muscle or heart or following transplantation. However, more recent studies have cast doubt on the interpretation of these results. Studies using parabiotic mice (surgically joined to develop a common circulatory system) and GFP^+/GFP^- cells showed that haemopoietic but not non-haemopoietic chimerism existed suggesting that "transdifferentiation" was rare if at all possible (Wagers AJ, Sherwood RI et al. 2002), reviewed in (Wagers AJ and IL. 2004). It has also been noted that cell fusion may have been misinterpreted as plasticity when high levels of cell fusion were found in liver cells following HSC transplantation in mice (Vassilopoulos G, Wang PR et al. 2003).

1.2 Chronic Myeloid Leukaemia

Chronic myeloid leukaemia (CML) is a stem cell disease originating in a pluripotent haemopoietic cell that acquires a defined chromosomal abnormality. CML was first identified clinically in the mid 1800s when three physicians independently

described patients with massive splenomegaly and lethal leukocytosis not associated with documented conditions (Virchow R 1845; Bennett JH 1845; Craigie D 1845). A major breakthrough was the pioneering discovery of the Philadelphia chromosome (Ph) by Nowell and Hungerford in 1960. They noticed that in all CML samples there was an abnormally small chromosome 22 not observed in other leukaemias (Nowell PC and Hungerford DA 1960). This was the first chromosomal abnormality to be linked to a human cancer. It took a further 13 years to elucidate that the Ph chromosome was the result of a translocation between the long arms of chromosomes 9 and 22 (Rowley JD 1973). In 1984 Groffen et al showed that the translocation event involved the ABL proto-oncogene on chromosome 9 and a new "break point cluster" gene (BCR) on chromosome 22 (Groffen J, Stephenson JR et al. 1984). It was confirmed some time later that in fact the translocation was reciprocal also producing ABL-BCR (Melo JV, Gordon DE et al. 1993).

1.2.1 Clinical Features of CML

CML accounts for ~15-20% of all leukaemias with an incidence of 1 in 100,000 of the general population. It can occur at any age, however incidence increases with age and the median age at diagnosis is around 60. There are no predisposing factors to the development of CML, though survivors of the atomic bombs in Japan showed an increased incidence 4-10yrs following radiation exposures from explosions. It has also been suggested that the proximity of BCR and ABL genes in haemopoietic cells during interphase is related to cell cycle and differentiation, with a closer than predicted position observed for BCR and ABL in more primitive cells. This could facilitate the opportunity for chromosome rearrangement in some cells which may be enhanced by their cell cycle position (Neves H, Ramos C et al. 1999).

There are typically 3 distinct phases of disease: chronic phase (CP), which lasts ~4-6 years, accelerated phase (AP), which lasts up to 1 year and blast crisis (BC), which lasts around 3-6 months. CP is characterised by the accumulation of excessive numbers of mature and functional blood cells produced from a transformed pluripotent stem cell (Fialkow PJ, Jacobson RJ et al. 1977). There is a marked expansion of myeloid lineage cells at the expense of erythroid cells. AP lasts upto 1yr and is characterised by an increase in more primitive cells proportional to mature cells. Disease progression is inevitable and results in a fatal

BC, which resembles an acute leukaemia, and may happen suddenly without an intervening AP. An accumulation of more immature cell types and increased resistance to therapy in BC leads to mortality in ~3-6 months (Thijsen S, Schuurhuis G et al. 1999). Around 30% of these acute leukaemias are acute lymphoblastic leukaemia (ALL) and the rest are acute myeloid leukaemia (AML) or acute undifferentiated leukaemia (AUL). As yet the mechanism of progression from CP to BC is undefined but additional genetic events have been associated with development of BC. These include trisomy 8, loss of p53 function, alterations in the retinoblastoma gene, p16 gene rearrangements, amplification of the c-Myc gene and alterations in RAS signalling (Ahuja HG, Jat PS et al. 1991; Feinstein E, Cimino G et al. 1991; Sill H, Goldman JM et al. 1995; Jennings BA and Mills KI. 1998; Voss J, Posern G et al. 2000).

1.2.1.1 Treatment Options

Historically the main aim of treatment for CML was to reduce the excessive numbers of circulating white blood cells. This was achieved using various cytotoxic drugs, which prolonged life for ~3-5yrs following diagnosis of CP. Treatment with α-interferon (IFN) prolonged survival by a further 12 months compared to cytotoxic drug treatment and in a small percentage of cases (6-20%) induced a complete cytogenetic remission (Silver RT, Woolf SH et al. 1999). However, BCR-ABL transcripts could still be detected in patients in cytogenetic remission using sensitive RT-PCR techniques. IFN is also relatively toxic and can result in severe side effects, in addition some patients either cannot tolerate the drug or their leukaemia does not respond to it. The only curative therapy for CML is an allogeneic BM transplant. However, many patients are outwith the transplant age limit of <55yrs. In addition, only around one third of patients have a suitable donor. In effect this means that the majority of patients have chemotherapy as their only treatment option. The quest to find more effective drugs lead to the development of targeted therapy for CML in the form of STI571 (or Glivec), which will be discussed in more detail later. Figure 1.2 shows time lines of therapeutic and scientific landmarks for CML relevant to the following discussion.

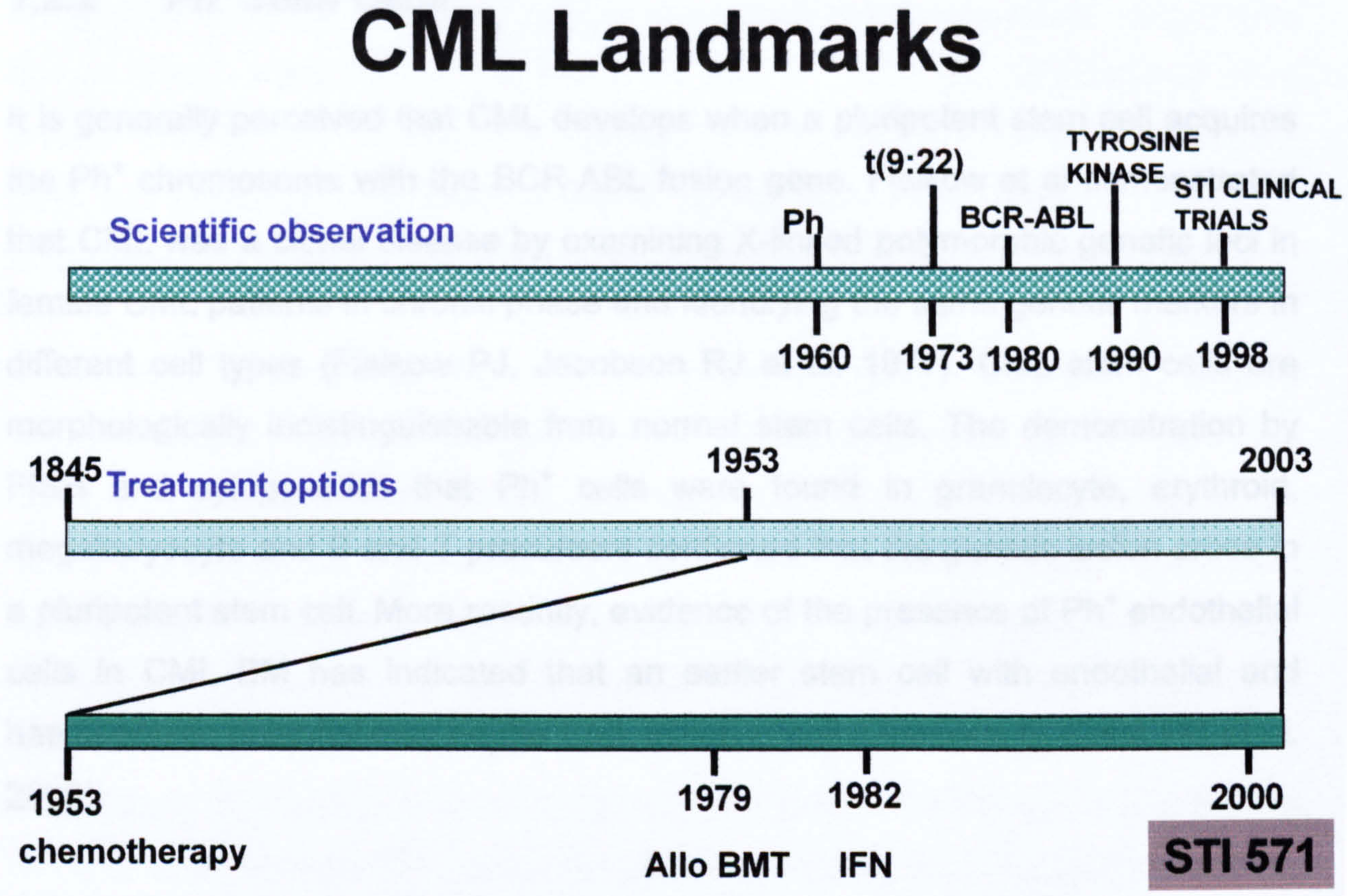

Figure 1-2 Time lines of scientific observation and treatment options for CML.

1.2.2 *Ph⁺ Stem Cells*

It is generally perceived that CML develops when a pluripotent stem cell acquires the Ph⁺ chromosome with the BCR-ABL fusion gene. Fialkow et al demonstrated that CML was a clonal disease by examining X-linked polymorphic genetic loci in female CML patients in chronic phase and identifying the same genetic markers in different cell types (Fialkow PJ, Jacobson RJ et al. 1977). CML stem cells are morphologically indistinguishable from normal stem cells. The demonstration by FISH and cytogenetics that Ph⁺ cells were found in granulocyte, erythroid, megakaryocyte and B and T precursors confirmed that the genetic lesion arose in a pluripotent stem cell. More recently, evidence of the presence of Ph⁺ endothelial cells in CML BM has indicated that an earlier stem cell with endothelial and haemopoietic potential may be the CML initiating cell (Gunsilius E, Duba HC et al. 2000).

CML progenitors are able to generate LTC-IC similar to normal stem cells; experiments culturing CML BM showed that normal haemopoietic progenitors coexisted alongside their leukaemic counterparts. Interestingly, on further long-term culture, the leukaemic progenitors rapidly disappeared whereas the normal progenitors could be detected for 2-3 months (Coulombel L, Kalousek DK et al. 1983). A similar observation was made by Udomsakdi et al using CML peripheral blood or BM. This study also showed that the number of LTC-IC in CML BM was significantly decreased compared to normal BM, and that CML LTC-IC in the peripheral blood were significantly increased to >10 times that of normal (Udomsakdi C, Eaves CJ et al. 1992). These data suggest that CML progenitors have limited capacity for self-renewal, and exhibit an increased tendency towards maturation. This may seem at odds with the idea of CML as a stem cell disease with uncontrolled proliferation. However, emerging evidence is of a complex series of interactions, with the suggestion that bcr-abl may exert effects on cell behaviour that vary with maturation, cell cycle and microenvironment. It has been demonstrated previously, that whereas normal and CML mature cells have similar responses and proliferation patterns to cytokines, more primitive progenitors display altered responses (Reviewed in (Clarkson B and Strife A 1993; Clarkson B, Strife A et al. 2003). Strife et al have also demonstrated that primitive CML cells display an increased sensitivity to single cytokines and that this may allow accelerated maturation, and thereby facilitate an accumulation of committed

progenitors. In support of this theory Buckle et al have shown that CML primitive progenitors comprise a lower proportion of the stem cell compartment compared to normal primitive progenitors and that there was an increased proportion of more mature cells in CML (Buckle AM, Mottram R et al. 2000). Ultimately, leukaemic stem and progenitor cells replace normal haemopoeisis and disease progression is associated with an accumulation of more primitive CML cells in the circulation.

It has been documented that CML stem and progenitor cells display altered adhesive interactions with BM stroma, and this could account for the increased number of progenitor cells in the circulation (Verfaillie CM, McCarthy JB et al. 1992). CML cells, like normal cells, express integrins, however CML cells exhibit significantly decreased adhesion to fibronectin (Verfaillie, McCarthy et al. 1992). Recent work by this group has demonstrated that binding of integrins in normal cells causes up regulation of the proliferation inhibitor $p27^{kip}$, preventing cell cycle entry (Jiang Y, Prosper F et al. 2000). Further studies by the same group have revealed that although CML cells bind integrins, binding does not inhibit cell cycle progression. They also found that in contrast to normal cells, $p27^{kip}$ is found mostly in the cytoplasm where it is unable to bind CDK2 and inhibit proliferation (Jiang Y, Zhao RC et al. 2000). In addition Bhatia et al have recently demonstrated that β1 integrin-fibronectin interaction preserved normal primitive progenitors by decreasing proliferation, and enhanced preservation of dividing primitive progenitors, possibly by preventing differentiation. In contrast, CML cells showed abnormal β1 integrin-mediated adhesion and impaired signalling following contact with FN or stroma (Bhatia R, Williams AD et al. 2002). It has also been demonstrated that the effects of impaired integrin function are bcr-abl associated since they can be reversed by inhibition of bcr-abl or induced in normal cells by expression of the BCR-ABL gene (Bhatia R and Verfaillie CM 1998; Zhao R, Fan E et al. 1999). Other studies have shown that both BM and PB CML $CD34^+$ cells display lower migration responses to SDF-1 compared with normal $CD34^+$ cells and that this was not a result of receptor (CXCR4) down-regulation (Durig J, Rosenthal C et al. 2000). More recently, it has been shown that CML $CD34^+CXCR4^+$ cells show lower migratory responses to SDF-1 than normal $CD34^+CXCR4^+$ cells from the same patient (Peled A, Hardan I et al. 2002). These data indicate that altered adhesive interactions almost certainly play a role in mobilisation of CML progenitors into the circulation and possibly affect retention of leukaemic stem and progenitor cells in the BM.

1.2.2.1 Stem Cell Kinetics

The molecular basis for the proliferative advantage of CML cells is not fully clarified. There is continuing debate regarding the importance of apoptosis in the CML phenotype. Some studies have shown that CML cells have an innate resistance to apoptosis and suggest that could account for the expansion of the leukaemic clone (Bedi A, Zehnbauer B et al. 1994). Conversely, in studies using serum deprivation, X-rays or glucocorticoids to induce apoptosis, Amos et al found no difference in survival of normal and CML myeloid progenitors or in more mature colony-forming cells (Amos TAS, Lewis JL et al. 1995). A more recent study has shown that non-dividing CML progenitor cells are more resistant to drug induced apoptosis, which may have implications for treatment (see discussion chapter 7) (Holtz MS, Forman SJ et al. 2005).

Differences in cell cycle position between normal and CML $CD34^+$ cells have been observed. Traycoff et al have demonstrated that there are fewer BM CML stem cells in the G0/G1 cell cycle phases compared to normal $CD34^+$ cells. They also observed that upon stimulation with cytokines, CML cells exit G0/G1 more rapidly, suggesting CML cells exhibit greater cell cycle activation. Furthermore, in the absence of cytokine stimulation, CML cells were able to enter cell cycle, unlike normal stem cells (Traycoff CM, Halstead B et al. 1998). Experiments using exposure to tritiated thymidine have shown that a higher proportion of CML LTC-IC and CFC are in S-phase of the cell cycle, with most being killed following exposure. In the case of normal LTC-IC, only around 5% were killed in this suicide assay, indicating that normal LTC-IC are largely quiescent (Ponchio L and Eaves CJ 1995). In a further study by Bhatia et al using staining techniques to evaluate division history, these authors show that most CML LTC-IC were generated from $CD34^+$ cells that had previously undergone division, whereas normal LTC-IC originated from undivided stem cells (Bhatia R, Munthe HA et al. 2000). It has been demonstrated that, unexpectedly, a population of quiescent CML stem cells exists in CP. Holyoake et al have isolated G0 and G1/S/G2/M cells from CML patients by FACS and shown that, when transplanted into NOD/SCID mice that are also β-microglobulin$^-$, some quiescent CML cells can exit G0 and effect engraftment (Holyoake T, Jiang X et al. 1999). The finding that a quiescent stem cell population existed in CML has raised the question of how to target therapy, when historically, cytotoxic drug treatment was aimed at eliminating the cycling

population. This very important issue will be addressed in the experimental and discussion chapters as a central theme in this work.

1.2.3 The Molecular Biology of CML

The majority of CML cases are associated with the presence of the Ph chromosome, the result of the reciprocal translocation between chromosomes 9 and 22. The molecular consequence of this translocation is to place the ABL gene in close proximity to the BCR gene, creating the BCR-ABL fusion gene. The properties of the individual genes and the fusion gene are discussed below.

1.2.3.1 c-ABL

The ABL gene on chromosome 9 is the human homologue of a gene formerly recognized in a murine oncogenic virus, the Ableson murine leukaemia virus (A-MuLV). The ABL gene family encodes highly conserved intracellular non-receptor tyrosine kinases with similar features to the SRC family of kinases (Laneuville P 1995). c-ABL is universally expressed with 2 isoforms, 1a and 1b, which result from alternative splicing of the first exon. Several functional domains on c-ABL have been identified including 3 SRC homology domains (SH1-SH3), positioned near the NH_2 terminus. The SH1 domain contains the tyrosine kinase function whereas the other two SH domains are involved in interactions with other proteins. Nuclear localisation signals, actin-binding and DNA-binding motifs are located closer to the COOH end. Until recently the mechanism of c-abl control of was speculated to involve a cellular inhibitor. However, a series of experiments by Pluk et al have demonstrated that in fact c-abl is controlled by autoinhibition and the elements involved in control are absent in bcr-abl. By testing the kinase activity of mutant forms of the protein, they identified 80 residues at the N-terminal that bind intramolecularly and are critical for regulation of c-abl. These residues are encoded by the first exon of ABL, which is always absent in fusion proteins formed with BCR (Pluk H, Dorey K et al. 2002).

The function of c-ABL is not completely understood but conservation and expression in different species suggest developmental importance. In addition, ABL knockouts display a number of developmental abnormalities such as abnormal eyes, runtedness, and defective spermatogenesis (Schwartzberg PL, Stall AM et al. 1991). c-abl protein is located in both the cytoplasm, where it co-

localises with F-actin, and in the nucleus, where it is bound to chromatin. abl proteins associated with transformation are exclusively cytoplasmic where they are bound to F-actin. Roles for c-abl in cell cycle regulation, integrin signalling and stress response have been suggested. (Reviewed in (Van Etten RA. 1999).

1.2.3.2 BCR

The BCR gene on chromosome 22 has 23 exons and produces a 160kd protein, which is also ubiquitously expressed. It contains several structural motifs including GTPase activity for Rac, a small GTPase of the Ras superfamily. BCR can also be phosphorylated on several tyrosine residues, particularly 177, which binds the adaptor molecule Grb-2, involved in the Ras pathway. The function of BCR as yet remains undetermined, and given that BCR knockout mice are viable, argues for at least a degree of redundancy in function (Voncken JW, van Schaick H et al. 1995). Interestingly, recent data has suggested a possible role for bcr in the regulation of c-abl. Work by Ling et al has shown that BCR overexpression inhibits cytoplasmic c-abl and that sequestration of bcr releases c-abl from the complex with bcr, which in turn, leads to oncogenic transformation as a result of c-abl activation (Ling X, Ma G et al. 2003). These data indicate that autoinhibition of c-abl as described above may not be the only mechanism of c-abl regulation.

1.2.3.3 BCR-ABL

The breakpoint on the ABL gene can occur over a relatively large area (>300bp) of the 5' end, most commonly between exons 1a and 1b, although breakpoints either side of these exons have been observed (Melo J 1996). The mRNA product invariably lacks exon 1a even if the breakpoint is anterior of this exon, probably as a result of mRNA splicing. In contrast, the breakpoints in BCR occur over a large variable region of >5kb, which spans exons 12-16 and is described as the major breakpoint cluster region or M-bcr. Alternative splicing within this region, generates two fusion transcripts containing either b2a2 or b3a2 junctions. Both mRNAs produce a 210kd oncoprotein commonly labelled $p210^{BCR-ABL}$. As well as the M-bcr there are two other breakpoint regions named m-BCR (minor breakpoint cluster region) and μ-BCR. Breakpoints in these regions produce p190 and p230 oncogenic bcr-abl proteins respectively. p190 is associated with Ph^+ ALL (acute lymphocytic leukaemia) and only rarely with CML, and p230 with rare Ph^+ chronic neutrophilic leukaemia. Breakpoints in other regions associated with ALL and CML

have been identified in rare cases. For the classic b2a2 and b3a2 junctions in CML there appears to be no correlation between breakpoint and prognosis or time to disease progression (de Braekeleer M 1987; Rozman C, Urbano-Ispizua A et al. 1995). Figure 1.3 details the position of the breakpoints and the resultant fusion products.

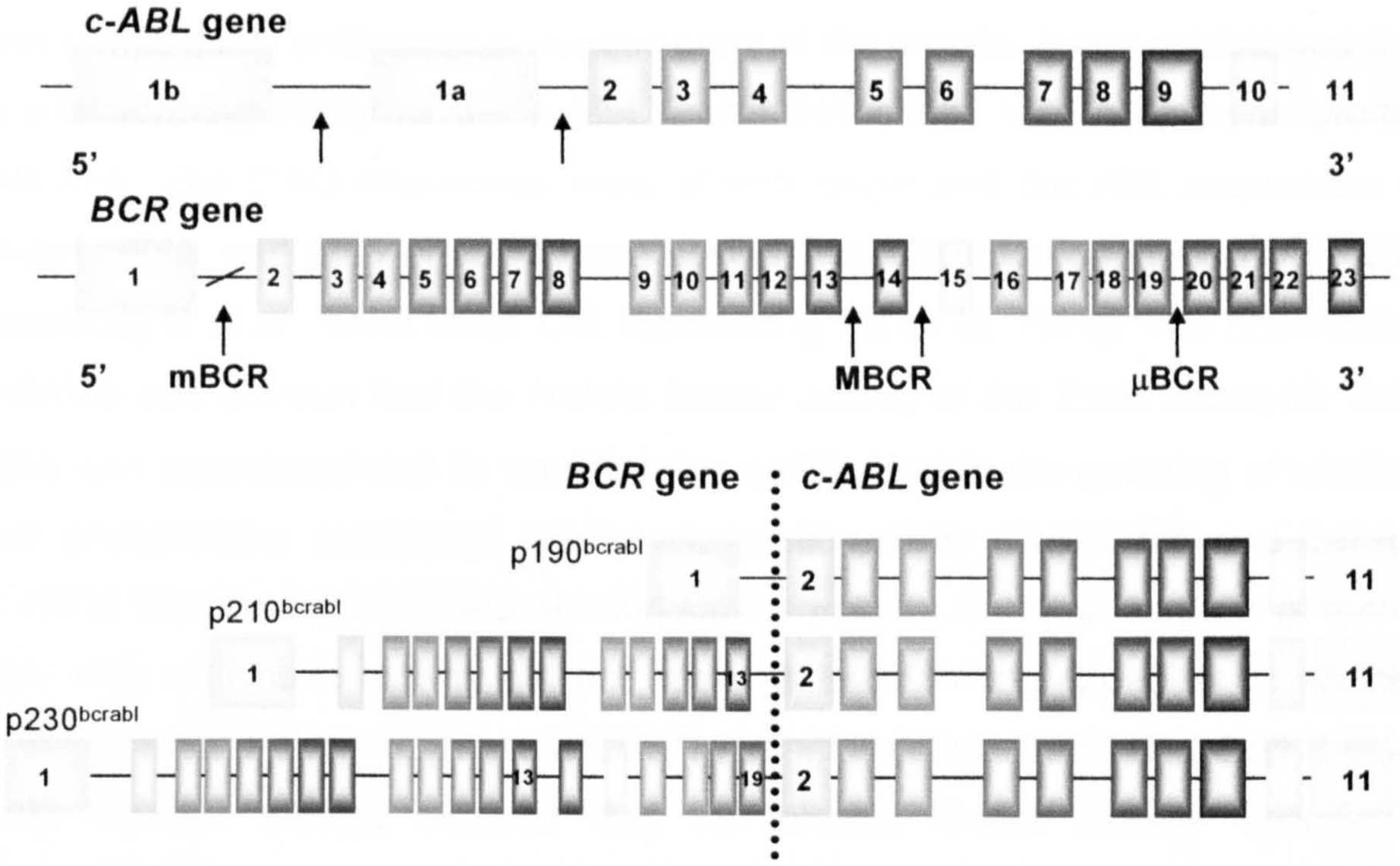

Figure 1-3 BCR and ABL breakpoints and fusion products.

The presence of the BCR-ABL transcript is not in itself sufficient to cause disease. Using sensitive RT-PCR, BCR-ABL mRNA transcripts were detected in a very small number of white blood cells in healthy individuals. Many of the transcripts were found to encode non-functional proteins, however transcripts encoding functional bcr-abl protein were identified (Bose S, Deininger M et al. 1998). The potential to develop CML disease may depend on the cell type in which the translocation arises and/or the microenvironmental stimuli encountered by the cell. It is possible some cells that acquire the translocation are eliminated by the immune system, or that these cells have limited division/differentiation potential, and are therefore are unable to sustain disease.

1.2.3.4 Oncogenic Activity of BCR-ABL

Following the identification of the Ph chromosome and its translocation partners, investigations into the mechanism of transformation gained momentum. The association between ABL and transformation had previously been established by studies of the Ableson leukaemia virus (A-MuLV), which had been shown to cause transformation of NIH 3T3 cells and lymphoid cells in vitro (Rosenberg N, Baltimore D et al. 1975; Scher CD and Siegler R 1975). In a series of elegant experiments using antibodies to various parts of the protein, it was established that the transforming ability of the A-MuLV was associated with a chimeric protein GAG-ABL. The GAG sequences were of viral origin and the ABL sequences of cellular origin, and both proteins were associated with transformation (Witte ON, Rosenberg N et al. 1979; Witte ON, Rosenberg NE et al. 1979). The observation by Collett and Erikson that the protein kinase activity of the Rous Sarcoma Virus (RSV) was associated with its transforming ability, lead to the question of whether other oncoproteins possessed similar enzymatic activity (Collett MS and Erikson RL 1978).The finding that GAG-abl had kinase activity, and that variants of the A-MuLV with no kinase activity did not possess transforming capability, confirmed the importance of this enzymatic activity in transformation (Witte ON, Goff S et al. 1980). Further studies showed that the protein kinase activity specifically phosphorylated tyrosine residues, and subsequently, that abnormal tyrosine kinase activity was associated with a number of malignancies (Hunter T and Sefton BM 1980).

The demonstration that the ABL gene mapped to chromosome 9 and that it was involved in the translocation that generated the Ph chromosome, lead to the identification of abl as part of the protein product of BCR-ABL (Bartram CR, De Klein A et al. 1983). These findings were confirmed in cell lines expressing BCR-ABL and in cell lysates of primary CML cells (Konopka JB, Watanabe SM et al. 1985). Antisera generated from Gag-Abl studies, discussed previously, was used to show that $p210^{BCR-ABL}$ had comparable tyrosine kinase activity to Gag-Abl and that a mutation in the protein that inactivated the kinase activity impaired its transforming ability. These observations confirmed the necessity of the abl tyrosine kinase in malignant transformation (Konopka JB, Watanabe SM et al. 1984; Pendergast AM, Gishizky ML et al. 1993).

One of the most significant differences between c-abl and bcr-abl proteins is their location within the cell. bcr-abl is found exclusively in the cytoplasm despite it containing three nuclear localization signals (NLS) and a nuclear export sequence (NES) (McWhirter JR and Wang JY 1993; Wen ST, Jackson PK et al. 1996). In contrast c-abl shuttles between the nucleus and cytoplasm, and exerts a proapoptotic effect in its nuclear form (Taagepera S, McDonald D et al. 1998). It has been documented that bcr-abl exerts an antiapoptotic effect (discussed more fully below) and elegant experiments by Vigneri and Wang have shown that this can be reversed to a proapoptotic effect. Inhibiting the tyrosine kinase activity of bcr-abl with STI (see below) caused bcr-abl to enter the nucleus and the addition of Leptomycin B (blocks nuclear export) trapped it there. Removal of STI and subsequent reactivation of the bcr-abl tyrosine kinase then induced an apoptotic cell death (Vigneri P and Wang JY. 2001).

1.2.3.5 Model Systems To Study BCR-ABL Effects

Daley et al demonstrated that BCR-ABL was the genetic element responsible for CML by infecting murine BM with retrovirus encoding $p210^{BCR-ABL}$ and using these cells to transplant irradiated animals. The result was a range of malignancies including a myeloproliferative syndrome that closely resembled CP CML. The leukaemic cells were shown to express viral BCR-ABL and it was possible to transplant the disease into secondary recipients, confiming the target cell for leukaemic transformation was a HSC (Daley GQ, Van Etten RA et al. 1990). Attempts to develop a BCR-ABL transgenic model of CML have proved extremely difficult largely due to embryonic lethality (Heisterkamp N, Jenster G et al. 1991). Some of these problems were partially overcome using conditional promoters such as tetracycline (Huettner CS, Zhang P et al. 2000). A further problem was that these mice seldom developed myeloid leukaemia and acute lymphoid leukaemias were much more common, which did not resemble CML-like disease (Heisterkamp N, Jenster G et al. 1990). A new transgenic model has been developed recently using targeted BCR-ABL expression in murine stem and progenitor cells, which produces a biphasic disease in mice, with many of the characteristics of human CML (Koschmieder S, Gottgens B et al. 2005). However this model has yet to be fully tested in other experimental systems. Recent advances in transduction and transplantation efficiency have been able to generate more robust murine models of CML disease, however death in experimental animals from complications not associated with the human disease, continues to be a problem (Pear WS, Miller

JP et al. 1998; Zhang X and Ren R 1998). Models like these still represent important tools for studying BCR-ABL induced leukaemogenesis.

Established cell lines offer greater flexibility in terms of time frame and convenience but it is difficult to faithfully represent a chronic disease that progresses to an acute disease in vitro. Many studies employ BCR-ABL-positive cell lines such as K562, produced in 1975 by Lozzio and Lozzio from blast crisis CML (Lozzio CB and Lozzio 1975). Whilst a useful model, it does not mirror CP CML, possessing multiple copies of BCR-ABL and being derived from the more acute BC phase. In addition, cells that have undergone multiple passages in culture are likely to have acquired other mutations. This may affect their responses to different conditions; therefore caution is warranted when extrapolating data to in vivo CML. Furthermore, many studies employ BCR-ABL inducible on/off or overexpression systems to compare cell behaviour. However, it must be appreciated that in CML where BCR-ABL is constitutively activated this may not represent a true picture, i.e. the cellular effect of suddenly turning on BCR-ABL may be very different to one of long-term continuous exposure.

Studies using primary cells from CML patients and comparable material from normal individuals are likely to yield the most relevant information. One of the most difficult factors is the inherent patient-to-patient variability observed in CP CML, which can result in less robust statistics. The selection of defined cell populations such as $CD34^+$ cells may help to reduce some of the variability. As discussed earlier, the contribution of co-existing normal cells in CML has to be eliminated from experimental data to ensure comparison of the relevant cell populations.

1.2.3.6 BCR-ABL Interactions

The documented cellular processes and pathways influenced by bcr-abl are continuously increasing. A comprehensive review of all of the candidates is out with the scope of this discussion, however some of the most interesting, at least from a clinical standpoint, are worthy of mention. (Reviewed in (Melo JV and Deininger MW. 2004). The functional domains/motifs on the bcr-abl oncoprotein facilitate interactions with a number of other cellular proteins. Interactions with mitogens, cytoskeletal components, anti-apoptotic proteins, cell cycle proteins, cytokines and adaptor proteins have been reported.

The interaction of bcr-abl with members of the RAS pathway has been documented. Protein-protein interactions combine bcr-abl with members of the RAS-MAPkinase signalling complex including Grb2, SHC and Crkl (Puil L, Liu J et al. 1994; Goga A, McLaughlin J et al. 1995; Senechal K, Halpern J et al. 1996). It has been shown that bcr-abl, through autophosphorylation of tyrosine 177 in the bcr component, stabilizes RAS in its active conformation, leading to constitutive activation. In contrast, inactivation of RAS by inhibitors significantly suppresses the cellular transformation by bcr-abl (Peters DG, Hoover RR et al. 2001). To become activated, RAS proteins undergo posttranslational modification, the first of which is farnesylation of their C-terminus catalysed by farnesyl transferases. Studies using farnesyl transferase inhibitors (FTI) have shown that bcr-abl induced leukaemogenesis can be inhibited by FTIs, and these compounds have now reached clinical trial (Reichert A, Heisterkamp N et al. 2001). Indications are that activation of the RAS pathway is critical to bcr-abl induced leukaemogenesis.

The JAK/STAT pathway involves three families of genes, JAK (Janus tyrosine kinases), STAT (signal transducers and activators of transcription) and SOCS (suppressor of cytokine signalling). The JAK/STAT pathway is involved in transduction of signals from cytokine receptors to the nucleus, where stimulation of JAKs produces STAT transcription factor activity. In bcr-abl transformed cell lines a demonstrable activation of STAT5 and to a lesser extent STATs 1 and 3 have been observed (Ilaria RL Jr and Van Etten R 1996). It has also been demonstrated that STAT 5 induces the expression of the antiapoptotic protein Bcl-xl and through this mechanism may promote survival of malignant cells (Horita M, Andreu EJ et al. 2000). CML patient cells and bcr-abl$^+$ cells exhibit similar biological characteristics to IL-3 stimulated cells or those with engineered IL-3 overexpression. It has been further demonstrated in CML CD34$^+$ cells that increased STAT5 phosphorylation is a consequence of bcr-abl induced IL-3 stimulation and that IL-3 is in fact produced through an autocrine mechanism in BCR-ABL$^+$ cells (Jiang X, Lopez A et al. 1999).

PI3 kinase activity has been shown to be a requirement for transformation of bcr-abl expressing cells (Skorski T, Bellacosa A et al. 1997). bcr-abl complexes with PI3K and adaptor molecules which activate PI3K, and requires the intact SH2 domain on bcr-abl. This in turn activates the downstream effector Akt kinase in bcr-abl-positive cells. A kinase deficient Akt mutant was unable to effect transformation of murine cells in vitro and suppressed leukaemia in SCID mice

(Skorski T, Bellacosa A et al. 1997). However, more recent data has suggested there may be a degree of redundancy in both the STAT5 and Ras signalling pathways in bcr-abl transformed cells (Hoover RR, Gerlach MJ et al. 2001). Although as mentioned previously RAS inhibitors can suppress transformation by bcr-abl, it is clear from the apparently conflicting evidence that bcr-abl and its associated tyrosine kinase activity exert a myriad of effects on downstream pathways that have a range of consequences for cell behaviour. The model systems and cell populations used in various studies may yield different results, and this must be considered when comparing data. BCR-ABL expression has been shown to influence different pathways depending on a variety of factors including cell type, cell cycle status, maturation status and cell context.

1.2.4 The Development of an Inhibitor of BCR-ABL

It had been demonstrated that it was possible to design a Tyrosine Phosphorylation Inhibitor (tyrphostin) with specificity for a particular tyrosine kinase (Yaish P, Gazit A et al. 1988). AG490 was the first synthetic tyrosine kinase inhibitor to reduce leukaemic cell proliferation in vitro and in vivo with no effect on normal cells (Meydan N, Grunberger T et al. 1996). Scientists at Ciba-Geigy (now Novartis) began high throughput screening of a range of small molecule inhibitors and identified a platelet derived growth factor receptor inhibitor (PDGF-R), CGP 53716. Unexpectedly this compound was also shown to inhibit Gag-abl tyrosine kinase activity. Following some minor modifications to its structure CGP57148B (STI1571) was generated and shown to selectively inhibit the tyrosine kinases of PDGF-R, KIT, ABL, and ARG (Reviewed in (Traxler P, Bold G et al. 2001).

1.2.4.1 Development of STI571/Glivec

STI571 (STI now known as Glivec or Imatinib Mesylate) is a small molecule inhibitor that competes for the ATP binding site of the tyrosine kinase of bcr-abl, rendering it unable to phosphorylate downstream targets. However, more recent data have suggested that direct competition for the ATP binding site may not be the exact mode of action. Elucidation of the crystal structure of the abl catalytic domain and comparison of the binding of STI and another closely associated molecule (PD17355), has shown that STI only occupies part of the binding pocket of abl and may act by stabilising bcr-abl in its inactive conformation such that it is

unable to bind ATP (Nagar B, Bornmann WG et al. 2002). (See 1.2.4.3 on STI resistance).

In vitro, STI was shown to be effective at micromolar concentrations. A number of bcr-abl$^+$ cell lines were tested and an IC_{50} (50% inhibitory concentration) in the range 0.1 - 0.5μM was established for inhibition of kinase activity. Similar IC_{50} values were calculated for the inhibition of proliferation of bcr-abl$^+$ cells with little effect on bcr-abl$^-$ cells. Cells isolated from CML patients also showed selective inhibition of progenitor colony formation, and proliferation in liquid culture. Eradication of human BCR-ABL$^+$ cells injected into nude mice confirmed the efficacy of STI in vivo (Le Coutre P, Mologni L et al. 1999). In addition, normal haemopoiesis was shown to be relatively unaffected at concentrations of up to 1μM STI (Druker BJ, Tamura S et al. 1996; Deininger MW, Goldman JM et al. 1997). These promising results prompted the commencement of clinical trials in the USA.

1.2.4.2 Clinical Studies with STI571

STI reached the clinic in 1998 and was the first drug specifically targeted to counteract the effects of a cellular oncoprotein. Initially only patients who had failed interferon-α (IFN) in CP were approved for the trial. The toxicity was comparatively low level and the drug was well tolerated. In this first trial 53 out of 54 patients achieved a complete haematological response (CHR) at doses of 300mg and, at this level or above, 31% of patients achieved a cytogenetic response, which was complete in 13% of cases. Pharmacokinetic data revealed that at 300mg/day, the level in the plasma was equivalent to 1μM, shown to be effective in the in vitro studies. On the basis of these results the study was expanded to include patients in BC phase of the disease. However, most of these patients relapsed within a few months of therapy indicating that the drug was much less effective in BC. Phase II and III trials followed, including patients at diagnosis, at all stages of disease and with combinations of conventional drugs versus STI. Overall the STI treated patients showed improved survival and, due to its lack of toxicity, better quality of life (Kantarjian HM, O'Brien S et al. 2003). Although these results lead to confidence that an effective treatment for CML at least in CP had been found, there were certain observations that were cause for concern. One of the most significant was that in patients who achieved a completed cytogenetic response, detectable BCR-ABL transcripts were shown in samples analysed by

sensitive RT-PCR, indicating that molecular remissions were rare (Hughes TP, Kaeda J et al. 2003). It has also been shown, in work included in this thesis, that quiescent BCR-ABL$^+$ stem cells are resistant to the effects of STI in vitro and have the potential to cause relapse (Graham SM, Jorgensen HG et al. 2002). These observations have increased doubts over the durability of responses to STI therapy.

1.2.4.3 Resistance to STI

The less favourable responses of CML patients in AP and BC to STI therapy, together with the existence of low level BCR-ABL transcripts in treated patients in CP, prompted investigations into the possible mechanisms of resistance. It is clear from the clinical data that resistance may be acquired i.e. patients respond initially and then fail therapy, or resistance may be inherent i.e. little or no response is observed. The mechanism of resistance may be associated with disease status and progression, and may be different for both.

As early as 1997, Deininger et al had found that small numbers of Ph$^+$ colonies could be grown in the presence of 1μM STI (Deininger MW, Goldman JM et al. 1997). Le Coutre et al demonstrated that a BCR-ABL$^+$ cell line, LAMA84, could be induced to develop resistance to STI by culturing cells with increasing concentrations of STI over a period of time. They also showed that resistant cells contained a higher level of bcr-abl expression and phosphorylation, and that this was associated with gene amplification (Le Coutre P, Tassi E et al. 2000). The observation that removal of STI from cultures could restore sensitivity to the drug in cell lines, indicated that two populations of cells coexisted i.e. a sensitive and an insensitive one each prevailing under the correct conditions (Tipping AJ, Mahon FX et al. 2001). These results raise the possibility that patients who have become resistant may regain sensitivity by brief withdrawal of the drug. It is not clear what implications these observations may have in the therapeutic context.

Drug resistance is most commonly associated with reactivation of bcr-abl signal transduction and recent data have indicated that the most frequent mechanisms of resistance to STI are point mutations in the kinase domain of bcr-abl or gene amplification at the transcript or genomic level (Gorre ME, Mohammed M et al. 2001). Mutations in the kinase domain may interfere with STI binding or may change the conformation of the protein such that drug binding is reduced.

Investigations have shown that there is a range of sensitivities to STI associated with particular mutations (Corbin AS, Buchdunger E et al. 2002). Recent work by Bhatia's group has shown that kinase mutations can be detected in $CD34^+$ stem cells from patients in CCR on STI therapy, raising the possibility that therapy itself may lead to a selective advantage for the mutant clone and subsequent relapse (Chu S, Xu H et al. 2005). The finding that point mutations could be found in patients prior to STI therapy argues for a pre-existing mutant clone that gains prevalence as its sensitive neighbours are eliminated (Shah NP, Nicoll JM et al. 2002).

Other possible mechanisms for resistance to STI therapy include overexpression of the MDR1 gene, which encodes the P-glycoprotein pump, and was shown to inhibit the entry of STI into K562/DOX cells (resistant to doxirubicin by MDR1 expression). Retroviral transfection of BCR-ABL^+ cells with MDR1 reduced their sensitivity to STI, which could be restored by inhibition of Pgp with verapamil (Mahon FX, Belloc F et al. 2003). Using C^{14}-radiolabelled STI it has been shown recently that both uptake (by hOCT1) and efflux (by MDR1) are active transport processes that can be inhibited by verapamil. Both transporters were expressed in primary CML cells and in cell lines. This observation may mean that resistance is a result of disparity in expression between the two transporters (Thomas J, Wang L et al. 2004). Another recent report has documented the first cellular effect of Pgp modulation in the treatment of a Ph^+ ALL patient with STI (Illmer T, Schaich M et al. 2004). In contrast, other studies have shown overexpression of MDR1 in BCR-ABL^+ K562 cells did not protect them from the effects of STI (Ferrao PT, Frost MJ et al. 2003). The importance of MDR1 in clinical resistance to STI has yet to be established.

To try to overcome the problems of STI resistance other approaches in the treatment of CML include, dose escalation of STI, other bcr-abl inhibitors, combinations of other cytotoxic drugs and STI and inhibitors of downstream targets of bcr-abl. Undoubtedly, STI has had a major impact on both the clinical management of CML and on the laboratory investigations into this fascinating disease. Whether resistance to STI is a feature that has to be overcome with additional therapy or whether there are (quiescent) cells that are genuinely able to evade therapy, will be elucidated in time to come.

1.3 Microarrays

Recent technological advances together with the success of the Human Genome Project have given researchers the tools to investigate gene expression on a genomic scale. The data generated from numerous studies have changed the focus of research in many areas, not least cancer. A complete review of the technology is outwith the scope of this discussion, which will focus on the areas most relevant to this study.

1.3.1 Types of Arrays

The most common formats for microarrays are cDNA arrays and oligonucleotide arrays:

1.cDNA arrays use gene sequences, which are normally PCR products derived from cDNAs that are robotically spotted onto either glass slides or nylon membranes. Labelled single stranded cDNA is produced from RNA samples using reverse transcriptase and hybridised to the array, in a typically competitive reaction. The two samples to be compared are labelled with different dyes, most commonly Cy3 and Cy5, and the arrays are then scanned at two different wavelengths to detect the relative transcript levels for each sample. The main advantages of this type of array are, a) they can be generated in house, b) they can be customised to suit samples and investigation, and c) they are relatively inexpensive. However, the main disadvantages are that managing large cDNA libraries is an onerous task and even the best labs are prone to errors. The reproducibility in array manufacture is variable and the format is limited to a smaller density of spots, largely due to limitations in the robotics. A further drawback of this type of array is the possible failure to detect closely related genes if there is a large degree of sequence homology.

2. Oligonucleotide arrays such as Affymetrix GeneChip® arrays are the gold standard in array technology and are made by synthesising oligonucleotides on the chip by a process known as photolithography. There are 11-16 probe pairs or sets for each gene and hybridisation is non-competitive. A pair consists of a perfectly matched sequence of 25 oligos and partner containing a single mismatch base at position 13. Biotin tagged RNA produced by in vitro transcription is applied to the chips and the signals obtained from the perfect match and mismatch probes

compared. The use of multiple short sequences allows splice variants and sequences of up to 90% homology to be identified. The probe mismatch strategy helps to minimise non-specific and background signals. In addition, Affymetrix chips contain a number of probe sets with known expression levels, which serve as internal controls for signal and background normalisation. This method of manufacture means that at least 12,000 genes can be represented per chip and the sample can be recovered following the first hybridisation and applied to another chip. There are a number of disadvantages of this system, 1) it requires specialist equipment and expertise to operate it, 2) it is very expensive especially if multiple samples are to be included, and 3) the expense of custom chips makes this impractical for even small experiments.

3. Recently, oligonucleotide arrays using 60-mer sequences (or longer) have become available. This format offers an increased level of sensitivity over the early oligonucleotide arrays together with the option of custom gene sets at a reasonable cost. One of the main advantages is that these arrays do not require expensive equipment to process the slides and, due to advances in spotting technology, now offer a high level of reproducibility. Comparisons of oligonucleotide and Affymetrix array formats have shown good correlation of expression values for comparable samples (Barczak A, Rodriguez MW et al. 2003).

Samples for application to microarrays can be from any source providing there are enough cells from which to extract intact RNA. Often clinical samples especially from solid tumours or biopsies yield very small amounts of material. It is possible to amplify the RNA prior to application to the arrays. Linear amplification is based on reverse transcription with primers containing a bacteriophage RNA polymerase promoter sequence and cDNA is amplified by in vitro reverse transcription using the appropriate bacteriophage RNA polymerase (Baugh LR, Hill AA et al. 2001). The results are reproducible and allow as little as 1-50ng of total RNA to be used as starting material, equivalent to 100-5000 cells. Recent data has validated this amplification protocol for small amounts of starting material, showing that similar differential gene expression profiles were generated from both amplified and non-amplified RNA (Patel OV, Suchyta SP et al. 2005).

1.3.2 Data Analysis

Microarray experiments by their nature generate vast amounts of data. The task of analysing this data to produce meaningful results is complex and time consuming, requiring input from specialist bioinformatians. Initially the image data from the array scans has to be normalised to subtract background noise and non-specific signals. In the case of Affymetrix Genechips the controls are internal to the chips giving more robust data. The next level of analysis is aimed at identifying relevant changes in gene expression, usually comparing one sample with a control sample. Specialist array programs are employed at this stage to deal with complexity and quantity of data. One such program is GeneSpring® (Silicon Genetics, USA) and was the one used for the initial analysis in this work. Normalised data from the array chips are imported into the program, which allows the data to be manipulated in various ways. The first step is typically to look at the fold change either up or down between samples. This gives an indication of the number of genes that are changed between experimental groups. Utilising the numerous analysis tools in the program allows generation of gene lists with defined parameters i.e. fold change set at 2, 3, etc or overlapping genes in data sets using Venn diagrams. Further data analysis to determine statistical significance is required to confirm results. Clustering analysis identifies gene groups that are changed between samples and more sophisticated analysis can generate a genetic "fingerprint" for a particular condition or disease, which could be used to predict outcome or identify suitable treatment (Reviewed in (King HC and Sinha AA. 2001).

1.3.3 Confirmation of Microarray Results

Due to the way in which large amounts of data are generated in microarray experiments, confirmation by independent analysis is required. Separate samples other than the ones used for the arrays increases the validation of results. Normally another experimental platform is used to corroborate array data. This is commonly quantitative real time PCR such as Taq-man (Applied Biosciences) or Light Cycler (Roche), which can measure relative expression levels in matched samples. Ultimately, the most relevant biological validation is variation in cellular protein levels, although for technical reasons this may not always be possible. It must be appreciated that although microarrays are a powerful tool they only give a

snapshot of the transcription levels in a cell in that time frame. Moreover, they do not discriminate post-translational or post-transcriptional modifications, which may be just as relevant to the cell's biological state.

1.3.4 Microarrays and Stem Cell Biology

Microarrays have been used in a number of studies in an effort to unlock the genetic program of stem cells. However, numerous investigations have failed to yield consistent gene sets. This is perhaps not surprising given the variations in studies between cell populations, selection methods, array formats, and bioinformatics. A vast amount of data has been generated, however much of it is not directly comparable due to the variations listed above. The ability to examine the gene expression profile of HSC has led to a variety of microarray studies in the search for a "molecular signature" that could be used to define these rare cells, and thus separate them from the general population. Phillips et al have reported a microarray study of murine HSC, which identified gene differences between primitive and more differentiated stem cells. The analysis recognised thousands of known and unknown genes as differentially expressed between the cell types, which were used to construct a stem cell database (Phillips RL, Ernst RE et al. 2000). The results illustrate the problems inherent in these types of experiments i.e. vast amounts of data are generated and it is difficult to identify the most important gene expression differences. Even in studies where similar methodology has been used, microarray results can generate different gene sets. This was illustrated recently when two independent groups used gene profiling to try to identify a molecular signature of "stemness". Both groups examined the expression profile of mouse embryonic, neural and haemopoietic stem cells, and produced a list of genes associated with a common stem cell profile. However, analysis of both data sets by an independent group revealed that there was very little overlap in the gene sets identified, in fact only 6 genes were common to both gene sets. These data emphasise the importance of strictly defined cell populations and caution in interpretation of analysis (Ivanova NB, Dimos JT et al. 2002; Ramalho-Santos M, Yoon S et al. 2002; Evsikov AV and D. 2003).

The problems highlighted can be minimised to some degree by using very defined cell populations, such as sorted cells, although this inevitably means small amounts of starting material. Other microarray studies have confirmed the importance of recognised gene differences and subsequently, increased the

significance of these observations. In a recent report, Steidl et al compared the expression profiles of BM and circulating $CD34^+$ cells and confirmed the increased cycling status of BM $CD34^+$ cells compared with G-CSF mobilised PB $CD34^+$ cells (Steidl U, Kronenwett R et al. 2002). It is clear that this technology has facilitated our understanding of some important pathways and interactions, and has become an important tool in stem cell research.

1.3.5 Clinical Impact of Microarrays

One of the first applications of successful gene profiling, in the context of leukaemia, was used to distinguish acute lymphoblastic leukaemia (ALL) and acute myeloblastic leukaemia (AML). Although the two diseases were distinguishable through the application of various specialist criteria, there was no single test that was sufficient to separate them. Treatment for each disease is markedly different and critical to success. Although both diseases will respond to the corresponding treatment regime, lower cure rates and unnecessary toxicities are observed. Golub et al used the two diseases as a test case to measure the success of a gene profiling strategy for disease classification. They were able to define a class predictor (50 genes) for the AML/ALL distinction and further determined that it could have been automatically discovered without prior knowledge of the biology (Golub TR, Slonim DK et al. 1999).

More recently, gene profiling identified a newly classified leukaemia distinct from ALL or AML. A subset of human leukaemia with a particularly poor prognosis was known to possess a chromosomal translocation involving the mixed-lineage leukaemia gene (MLL). The morphology of the disease is lymphoblastic leading to its classification as ALL. However, unlike classic childhood ALL, relapses post chemotherapy were common and the cells exhibited distinct immunophenotypic differences from ALL, including lack of early lymphocyte antigen and the tendency to express myeloid antigens. The gene expression profiles showed that ALLs with the MLL rearrangement displayed a uniform and distinct pattern distinguishing them from conventional ALL and AML (Armstrong SA, Staunton JE et al. 2002).

There are many more studies that have successfully employed microarray technology to clinical advantage. The possibility of routine diagnosis by gene profiling is a little way off, however there is no doubt that this technology represents a major step forward in clinical investigation and in targeted therapy.

1.4 Aims

Quiescent HSC remain relatively uncharacterised. The existence of quiescent leukaemic stem cells in CML and their potential for disease persistence, presented an attractive target for investigation. The initial experiments were aimed at developing the methodology to select these rare stem cells from the rest of the HSC population. A FACS sorting strategy was developed to isolate pure populations of quiescent and cycling stem cells from both normal individuals and CML patients.

Further FACS sorting methodology was utilised to investigate the differences between normal and CML HSC in vitro in the presence and absence of growth factors. Additional experiments were aimed at examining the effects of a specifically targeted therapy, STI571, on CML stem cells in vitro. Finally, FACS sorting methodology was used to isolate populations of normal and CML HSC in different phases of the cell cycle, in an effort to identify the transcriptional profile of normal and CML quiescent and cycling cells by microarrays .

Chapter 2 Materials and Methods

2.1 Materials

2.1.1 Tissue Culture Supplies

Baxter Healthcare Northampton, UK	Gammagard human i.v. immune globulin Sterile water Isolex stem cell selection kit
Becton Dickinson Plymouth, UK	Hypodermic needles Luer lock syringes Falcon tubes
Bibby–Sterilin Staffordshire, UK	Suspension culture dishes 35mm
Chugai Pharma, London UK	rHU G-CSF
Costar, Cambridge, MA, USA	Cell scrapers
Corning, Bucks, UK	24 well tissue culture plates
Gibco BRL, Paisley, UK	2-mercaptoethanol
Millipore, Watford, UK	Millex-OR single use filter (0.2µm)
Nalge Nunc International, Roskilde, Denmark	50ml Tissue culture flasks Cryotubes
Novartis, Surrey, UK	STI571
Roche Products Ltd Welwyn Garden City, UK	Recombinant human Dnase (Pulmozyme®)
Scottish Blood Transfusion Service, Glasgow, UK	20% Human serum albumin (HSA) 4% Human serum albumin (ALBA) Human immunoglobulin (Ig)
Sigma Aldrich, Dorset, UK	Acetic acid Ammonium chloride Dimethyl sulphoxide Dulbecco's phosphate buffered saline (w/o Ca^{2+} and Mg^{2+}) (PBS) Foetal calf serum (FCS) Glutamine Low density lipoprotein Iscove's modified Dulbecco's medium (IMDM) Methanol Penicillin/streptomycin Potassium chloride Tri-sodium citrate

	Trypan blue solution (0.4%) Isopropyl alcohol Poly-L-lysine
Stem Cell Technologies, British Columbia, Canada	BIT (serum substitute) rHU FLT3L rHU IL-3 rHU IL-6 rHU Stem cell factor (SCF) Methocult Stem cell mix + erythropoeitin Progenitor enrichment cocktail Biotinylated anti-CD15 StemSep columns
Sterilin Ltd Hounslow, UK	90mm petri dishes 30mm triple vent dishes 15ml centrifuge tubes PES filter system (0.2µm) 50ml centrifuge tubes 5ml sterile disposable pipettes 10ml sterile disposable pipettes 25ml sterile disposable pipettes
Tayside Pharmaceuticals, Dundee, UK	Magnesium chloride
Vysis-Abbott, Maidenhead, UK	FISH Dual fusion probe (bcr/abl)

2.1.2 FACS Reagents

Becton Dickinson, Oxford UK	Human anti-CD34 FITC antibody Human anti-CD34 PE antibody Human anti-CD38 PE antibody IgG FITC isotype control IgG PE isotype control Mid range FL1 rainbow alignment particles Calibrite FITC/PE beads FACS flow FACS safe FACS rinse
Cambridge Biosciences, London, UK	CFSE UV alignment beads Hoechst 33342
Sigma Aldrich, Dorset, UK	Propidium iodide Pyronin Y

2.1.3 Molecular Biology Reagents

Abgene, Surrey, UK	ReddyMix PCR Master Mix 50µl reaction tubes
Ambion, Texas, USA	DNA-free Kit
Beatson Laboratory Stock, Glasgow, UK	DH5α E.Coli
Invitrogen, Paisley, UK	Superscript II kit TRIzol reagent TOPO TA kit
MWG, London, UK	PCR Primers
Qiagen, West Sussex, UK	QIAquick PCR Purification Kit QIAquick Nucleotide Removal Kit QIAquick Gel Extraction Kit QIAprep Miniprep Kit Rneasy Mini Kit
Sigma Aldrich, Poole, UK	Ampicillin Chloroform Dimethyl formamide (DMF) Isopropyl alcohol Trizol reagent X-gal Ethidium bromide Hyperladder IV (100-1000bp)

2.1.4 Primers for RT-PCR

Actin: forward: TCC ATC ATG AAG TGT GAC GT

reverse: TAC TCC TGC TTG CTG ATC CAC

CD34: forward: CTG CTA CCA CGG AGA CTT CTA CAC AAG G

reverse: ATG GCA CTC GGA GCA GAA GAT GAT

MCM5: forward: GCA GAG GCG CTT CAA GGA GTT CC

reverse: ATG TTG GTG AGG GTG TTG CGC CAG

PCNA: forward: TCA ACG AGG CCT GCT GGG ATA TTA G

reverse: TGG CTG AGA TCT CGG CAT ATA CGT G

ABL: forward: TTCAGCGGCCAGTAGCATCTGACTT

reverse: GGTACCAGGGTGTTTCTCCAGACTG

BCR-ABL: forward: CAGGGTGCACAGCCGCAACGGCAA

reverse: GTCCAGCGAGAAGGTTTTCCTTGGA

2.2 Media and Solutions

2.2.1 Tissue Culture Media

2.2.1.1 Serum Free Media

77.8ml IMDM
20ml BIT (serum substitute)
1ml L-Glutamine (200mM)
1ml Penicillin (5000u)/Streptomycin (5mg/ml)
200µl 2-Mercaptoethanol (200mM stock)
40µg/ml Low density Lipoprotein

2.2.1.2 Growth Factor Cocktail for Serum Free Media

IL-3 20ng/ml
IL-6 20ng/ml
h-SCF 100ng/ml
FLT-3L 100ng/ml

G-CSF 20ng/ml

2.2.1.3 IMDM 2% FCS

98ml Iscove's modified Dulbecco's medium
2ml Foetal calf serum

2.2.2 Tissue Culture Solutions

2.2.2.1 PBS 2% FCS (PBS/2%)

98ml Dulbecco's modified phosphate buffered saline w/o Ca^{2+} and Mg^{2+}
2ml Foetal Calf Serum

2.2.2.2 PBS 20% FCS (PBS/20%)

80ml Dulbecco's modified phosphate buffered saline w/o Ca^{2+} and Mg^{2+}
20ml Foetal Calf Serum

2.2.2.3 PBS+

327ml Dulbecco's modified phosphate buffered saline w/o Ca^{2+} and Mg^{2+}
0.5ml magnesium chloride
2.5ml Pulmozyme®

2.2.2.4 PBS++

500ml Dulbecco's modified phosphate buffered saline w/o Ca^{2+} and Mg^{2+}
75ml Tri-sodium citrate
25ml Human serum albumin
1ml Magnesium chloride
5ml Pulmozyme®

2.2.2.5 ALBA 20% DMSO

80ml Human serum albumin
20ml dimethylsulphoxide

2.2.3 Molecular Biology Solutions

2.2.3.1 TAE Buffer

40mM Tris-acetate
1mM EDTA

Reagents were dissolved in distilled water and pH adjusted to 8.3 with glacial acetic acid

2.2.4 Bacterial Culture Reagents

2.2.4.1 SOC Medium

2% (w/v) bactotryptone
0.5% (w/v) yeast extract
10mM NaCl
2.5mM KCl
20mM $MgCl_2$
20mM $MgSO_4$
20mM glucose

2.2.4.2 Luria-Bertani (LB) Broth and Agar Plates

1g tryptone
15g yeast extract
10g $NaCl_2$
950ml deionised water
15g Agar (FOR PLATES)

All the ingredients, except the agar were added, and the pH adjusted to 7 using NaOH. The final volume was increased to 1 litre and the solution autoclaved before use. To make bacterial culture plates, agar was added at 15g/l to the LB

broth and autoclaved, before the addition of 50µg/ml ampicillin. Approximately 10ml of the solution was poured into 90mm petri dishes to solidify.

2.2.4.3 X-Gal Stock Solution 40 mg/ml

400mg x-gal
10ml dimethylformamide

X-gal was dissolved in dimethylformamide and stored as a stock solution at –20^{0}C protected from light. Before addition to the agar plates, the plates were warmed to 37^{0}C and 40µl of the stock solution added to each plate and spread evenly with a sterile spreader. The plates were dried for 15 minutes and protected from light, for use within 24 hours after the addition of x-gal.

2.3 Methods

2.3.1 General Cell Culture

2.3.1.1 Cell Counts

Cell counts were performed on a Beckman Coulter T660 analyser, which required 120µl of sample. For counting small cell numbers or for cell viability counts, a haemocytometer counting chamber was used.

2.3.1.2 Cryopreservation of Cells

Sorted or selected cells were stored frozen in liquid nitrogen where appropriate for further use. For cryopreservation, a cell suspension was made not exceeding 1x10^7 cells/ml in appropriate medium to which was added an equal volume of ALBA + 20% DMSO, to give a final concentration of 10% DMSO. The cryotubes were placed in a freezing container (Mr Frosty) that included isopropyl alcohol and placed in a –80^{0}C freezer overnight. This allowed a controlled reduction in temperature of approximately 1^{0}C/minute, before placing into long-term liquid

nitrogen storage. For some $CD34^+$ selected CML and normal samples used, this was performed by either Dr Michael Alcorn or Mrs Linda Richmond.

2.3.1.3 Recovery of Frozen Samples

To recover the maximum number of viable cells from cryopreservation it was necessary to exercise extreme care when thawing patient samples, particularly CML samples. On removal from liquid nitrogen, the vials were immediately thawed in a 37^0 C water bath until all of the ice crystals had disappeared. The cells were transferred to a sterile 15ml centrifuge tube on ice and 10ml of ALBA was added drop-wise over a 15-20 minute period. The tubes were centrifuged at 400g for 10 minutes. The cells were washed twice by adding 10ml of PBS/2% and centrifuging as before. After discarding the final wash supernatant, the cells were resuspended in appropriate medium, counted and assessed for viability.

2.3.1.4 Assessment of Viability

Routinely viability was determined using the trypan blue exclusion method. The cell suspension was diluted to an appropriate number and trypan blue solution added at a ratio of 1:4 trypan blue to cells. The cell suspension was placed in a haemocytometer counting chamber and at least 200 cells were counted under a light microscope at 40x magnification. The blue stained cells were scored as dead and the unstained cells as live. The percentage of viable cells was calculated by dividing the number of viable cells by the total cell count x100.

2.3.1.5 Red cell Lysis by Ammonium Chloride

For most experimental purposes it was necessary remove red cell contamination from leukapheresis products. This was achieved by lysis of the red cells with ammonium chloride solution 0.083%w/v in distilled water, added at a 1:10 cell suspension to NH_4Cl and incubated in a 37^0C water bath for 10 minutes. The cells were recovered by centrifugation at 400g for 10 minutes followed by a further wash in PBS/2%. If red cell lysis was incomplete the above procedure was repeated.

2.3.1.6 Removal of Red Cells by Density Gradient Centrifugation

An alternative method for effectively removing red cells from samples used lymphoprep, a density gradient medium. The cell samples were diluted in PBS2% to give a working cell concentration of less than $5x10^7$/ml. 6-10mls of cell suspension was carefully layered over 4ml of lymphoprep avoiding mixing the two phases. The tubes were centrifuged at 800g for 20 minutes during which the red cells moved through the lymphoprep to the bottom of the tube and the mononuclear cells remained at the interface. Following recovery from the interface, the cells were washed twice in PBS2%.

2.3.1.7 Removal of Platelets

When using leukapheresis products it was necessary to remove contaminating platelets before commencing cell separation. This was done by centrifuging the sample in 50ml tubes at 200g for 10 minutes and stopping the rotor without the brake activated. The supernatant was removed by aspiration and the above step repeated with the addition of PBS++ (section 2.2.2.4) to each tube. The supernatant was discarded and the cell pellet resuspended in appropriate medium.

2.3.1.8 Committed Progenitor Assay

As a measure of functionality, cells were cultured in semi-solid medium in the presence of stimulatory cytokines in CFU-GM/CFU-BFUE assays. Methocult, a commercial ready- made methylcelluose, was supplemented with stem cell mix + erythropoietin (custom cocktail from Stem Cell Technologies). 2.3ml of supplemented methocult was aliquoted into falcon tubes and stored at -20^0C until required. After thawing the tubes, the cell suspension was added in a final volume of 0.2ml in IMDM/2%FCS to each tube and shaken vigorously to mix. 1ml of the suspension was placed in each of two 35mm suspension culture dishes. The dishes were placed in a 90mm petri dish together with a dish of sterile water to prevent drying, and incubated for 12 days at 37^0C in a humidified incubator in 5% CO_2. The plates were counted on day 12 and GM colonies scored as having >40 cells, and each erythroid burst scored as a single colony. Duplicate dishes for each of the cultures were scored and the counts averaged.

2.3.2 Stem Cell Selection

2.3.2.1 Primary Human Cells

All CML cell samples used were leukapheresis products from patients who were undergoing this procedure as part of their clinical management to reduce peripheral white cell counts. Normal cells were obtained from allogeneic donors mobilised with rhG-CSF collected by leukapheresis. Informed consent was obtained from all patients and donors prior to the procedure, and only material surplus to clinical requirement was available for research purposes. All consents were in accordance with ethical approval from the Local Research Ethics Committee.

2.3.2.2 Negative Stem Cell Selection

Stem cells are a relatively rare proportion of mobilised peripheral blood products and therefore need to be selected from the whole population. This can be done in two ways, either by labelling and selecting the population of interest i.e. positive selection (see below) or by removing most of the other cells leaving the stem cell fraction i.e. negative selection. The resultant product for each type of selection is intrinsically different although both contain stem cells. For some applications such as microarrays it was essential that the samples to be compared had been selected in the same way.

Putative stem cells were selected from CML patient samples, using Stem-Sep negative selection according to the manufacturer's instructions. All dilutions and column washes were done in PBS++. Briefly, the cell suspension at a concentration of 2–8 $x10^7$cells/ml in PBS++ (after removal of red cells) was incubated with an antibody cocktail containing CD2, CD3, CD14, CD16, CD19, CD24, CD56, CD66b and Glycophorin A for 15 minutes at room temperature (RT) on a roller mixer. Then 60µl of magnetic colloid/ml of cells was added for a further 15 minutes at RT on a roller mixer. The number of columns required was dependent on the total cell number. The maximum number of cells was $1x10^8$–$1.5x10^9$ per column. Four columns could be run simultaneously and the whole run was repeated if all of the cells could not be accommodated in a single run. Columns were primed with PBS only and washed with PBS++ before being slotted into the magnet prior to addition of the cell suspension. The eluted cells were

collected in three column volumes of PBS++ and centrifuged at 400g for 10 minutes, before resuspension, counting and FACS (detailed in chapter 3). The selected cell numbers were adjusted to ~1x10^7/ml for cryopreservation in ALBA +10%DMSO.

2.3.2.3 Positive Stem Cell Selection

For CD34-positive selections, the cells were labelled with an anti-CD34 antibody, which was subsequently bound to a magnetic bead and used to isolate the $CD34^+$ cells with a magnetic column. For this procedure, stem cells were enriched using the Isolex® kit and Isolex™ 50 automated system. This was essentially a clinical processing kit scaled down for smaller cell numbers and which used a smaller processing machine, the Isolex 50 (procedure detailed in chapter 3). Briefly, following removal of the platelets as described, the cells were resuspended in 30ml PBS++ to a concentration of 1-5x10^7/ml and 5ml human immunoglobulin (Hu Ig) added for 15 minutes at RT with mixing. Anti-CD34 antibody (0.5µg/µl) was added at 1µl/1x10^6 cells and incubated at RT with mixing, for 30 minutes. The cells were loaded onto the column and the automated procedure for washing and release of target cells was followed using the Isolex 50 apparatus. The cells were collected at the end according to the instructions and FACS analysis performed to establish the purity and recovery of the $CD34^+$ cells. Some of the samples used in the CFSE experiments (chapter 5) were processed by Dr Michael Alcorn or Mrs Linda Richmond.

2.3.3 FACS and Cell Sorting

2.3.3.1 FACS Sorter Alignment and Set-up

The machine used was a Becton Dickinson FACS Vantage incorporating an enterprise argon laser for excitation at 488nm and using a beam splitter to give excitation at 340nm in the ultra violet range. The laser required to be aligned before each use. If the UV was to be used it had to be aligned separately. The optical alignment was done using mid-range FL1 Rainbow beads for the primary laser and UV beads for ultra violet beam. The integrity of the alignment was checked using histogram plots with markers indicating the CV (coefficient of variation) values for each parameter. The percentage CV range for forward scatter and FL1 was 2–4%, and for UV in FL4 was 1–3% on linear scales. The

parameters for sorting were defined by choosing the sort mode. There were 4 options with varying purities and counter accuracies depending on the desired cell population. The differences in sort modes defined how the machine dealt with aborted events and were operator controlled. The gating strategies used for sorting defined cell populations are detailed in the relevant results chapters. Once the gating was set the sample differential was adjusted to allow a total event rate of 3000/sec, which was the maximum this particular sorter could deal whilst maintaining acceptable cell recoveries. The most critical parameter for sort purity was the drop delay setting, which was adjusted according to the parameters described in the manual, and constantly monitored throughout the experiment. Following laser alignment, activation of the drop drive caused the stream containing the cells to be broken into droplets and depending on the settings, the drops were charged positively or negatively and sorted left or right into the collection tubes containing PBS/2%. Digital counters allowed the number of threshold, left, right and aborted events to be monitored. The proportion of cells in each parameter gave constant indication of the sorting process and allowed inspection of the sorting procedure.

2.3.3.2 Antibody Staining

All antibodies were titrated to determine the appropriate concentration for use. The concentrations used were the minimum amount of antibody that gave reliable staining and good separation of cell populations. As well as reducing the cost, lower intensity of antibody facilitated compensation in multi-parameter FACS experiments. For standard antibody staining a reaction mix of 200µl PBS 2%, cells and antibody was used. Controls consisted of the same reaction volume with matched isotype and fluorescent label. i.e. if anti CD34-FITC antibody was used and it was an IgG1 antibody the control tube contained IgG1-FITC. Isotype controls were included for all antibody staining.

2.3.3.3 CFSE Staining

The cells to be stained were recovered from liquid nitrogen as described. After resuspension in PBS2%, $2x10^6$ cells were removed for unstained controls. The remainder of the cells were incubated in 1µM CFSE for exactly 10 minutes at 37^0C. 10x volume of ice cold PBS 20% was added to stop the reaction and the cells centrifuged at 400g for 10 minutes. The supernatant was removed and the

cells washed in PBS2%. The stained cells and the unstained control cells were then cultured overnight in serum free medium with or without the addition of a five growth factor cocktail as described to allow excess dye to leach out. The cells were incubated overnight on 90mm sterile non tissue culture treated petri dishes or in suspension flasks at a concentration of $2x10^7$/ml. The following day the cells were recovered from the flasks or plates using a cell scaper, and washed in PBS2%. After removal of a sample of cells for FACS controls, the remaining cells were stained with anti-CD34-PE antibody and incubated at RT for 15 minutes before being washed twice in PBS2%. The second wash contained PI at a concentration of 1µg/ml in all tubes. These cells were now ready for CFSE sort 1 as described below.

2.3.3.4 FACS For CFSE Experiments

The unstained/isotype control cells were run first to check the position of the negative population, and if necessary the detectors were adjusted to place the negatives in the first log decade. The viable gate was set around the PI^- population. Following gating on the viable cells, the $CD34^+$ stained cells were identified and a further gate set around this population. The cells stained with CFSE/CD34/PI were then run and the compensation adjusted to give the same percentage of $CD34^+$ events as for the $CFSE^-/CD34^+/PI^-$ sample. Considerable levels of compensation were required as the CFSE stain was very bright and the spectral overlap into other channels was significant. For CFSE sort 1, the object was to obtain a homogenously stained cell population, which would allow the resolution of the peaks of cell division after 3 further days in culture. Two narrow markers of 19-21 channels, with 5 channels between, were set on the $CFSE^{max}/CD34^+/PI^-$ cell population and sorted left and right. The two populations of sorted cells were kept separate for all further experiments. During sorting all cells were kept on ice and in the dark. All the left-sorted cells were pooled and similarly all the right-sorted cells pooled for counting and subsequent culture.

Following a further three days in culture under various conditions, (as described in the relevant results chapters), the cells were sorted again (sort 2), into divided and undivided populations. Gates were set around the viable (PI^-) cells that were $CD34^+$ (PE^{Bright}). To set gates for divided and undivided cells, the position of the undivided peak was identified using the same cells (left- or right-sorted) cultured in the presence of 100ng/ml colcemid. Markers were set on a histogram plot to sort

the undivided population to the left and all of the divided cells to the right. To preserve cell viability and maximum fluorescence in stained cells during lengthy sorting experiments, all cells were kept on ice in the dark.

2.3.3.5 Hoechst and Pyronin Staining

In order to identify the G0, G1 and S/G2/M phases of the cell cycle, DNA was stained with Hoechst 33342 (HST) and RNA was stained with Pyronin Y (Py). Hoechst was used at a final concentration of 10µM and the cells incubated in a 37^{0}C water bath for 90 minutes. Without washing, Pyronin Y was added at a final concentration of 0.5µg/ml for 45 minutes. Anti-CD34-FITC was then added 1:25v/v again without washing for 15 minutes at RT. The cells were then washed in PBS 2% containing the same concentration of HST and Py. A further wash in the same buffer was done with the inclusion of PI at a final concentration of 1µg/ml. At each stage cells were removed for FACS controls. For antibody stains, a matched isotype control was run prior to the positive samples to verify the position of the negative population..

2.3.3.6 FACS For Hoechst and Pyronin.

FACS was carried out using the BD FACS vantage equipped with UV laser. The position of the positively stained cells was verified using a combination of unstained, single and multiple stained controls. The positively stained cells were gated as follows: PI^- / $CD43^+$/ HST^{lo}/Py^{lo} (G0) and PI^- /$CD34^+$ /HST^{bright} / Py^{bright} (G1/S/G2/M). The gating is shown in detail in chapter 3.

2.3.3.7 FISH on sorted cells

Approximately $1x10^3$ sorted cells were placed in 0.2ml tubes in 50µl of PBS/2% and centrifuged at 4000rpm in a microfuge for 5 minutes. The supernatant was removed by aspiration, without disturbing the pellet. The cell pellet was resuspended in 50µl of pre-warmed hypotonic solution containing 0.075M potassium hydroxide. Aliquots of 20µl were placed in wells of a poly-L-lysine coated slide and incubated for 20 minutes at RT before the hypotonic solution was removed. The cells were fixed by the addition of 20µl freshly prepared methanol:acetic acid (3:1) to each well and incubated at RT for 5 minutes. This fixation step was repeated before air-drying the slide overnight. The slides were

stored at –20^{0}C wrapped in parafilm until FISH was performed using the bcr/abl Dual Fusion probe according to the manufacturers instructions. Interphase nuclei were evaluated using a Leitz fluorescence microscope with a triple-band pass filter for DAPI, Spectrum Orange and Spectrum Green. All FISH slides were processed and read by Mrs Elaine Allan.

2.3.4 Molecular Biology

2.3.4.1 Primer Design

Relevant primers were designed using Oligo/Exe program. First the gene coding sequence was identified by a Pubmed nucleotide search, and the sequence used to search for appropriate primers of between 20 and 25 base pairs (bp) with similar melting temperatures and no internal loops or palindromes. The forward primer was typically around 50bp into the coding sequence and the reverse primer was around 300bp downstream. All primers were diluted to a10µM stock and used at final concentration of 0.2µM.

2.3.4.2 Generation of Total RNA

Cell samples were spun down to a pellet and most of the supernatant removed by aspiration. Up to 1ml of TRIzol® was added depending on the number of cells. After vortexing the samples were frozen at –80^{0}C until required. The RNA extraction was as per the Trizol protocol, briefly the samples were thawed at room temperature and 0.2ml of chloroform added per 1ml of Trizol and shaken for 15 seconds. The volumes of reagents were adjusted if the volume of Trizol was less than 1ml. The samples were centrifuged at 10,000rpm in a microfuge for 15 minutes at 2-8^{0}C. The colourless upper aqueous phase (containing the RNA) was transferred to a fresh tube and 0.5ml isopropanol/ml (of original Trizol volume) was added for 10 minutes at RT and centrifuged at 10,000 rpm, 2-8^{0}C for 10 minutes. The supernatant was removed and discarded. The pellet was washed in 1ml of 75%(v/v) ethanol per ml of Trizol in original preparation, by vortexing thoroughly and spinning at 5000rpm for 5 minutes at 2-8^{0}C. After discarding the supernatant the pellet was air dried briefly and resuspended in RNA-free water. The pellets were incubated at 55-60^{0}C for 10 minutes to ensure total dissolution.

2.3.4.3 First Strand Synthesis

Following the protocol for the superscript kit II, briefly, for each sample a mix was prepared which included 5.5µl RNA, 0.5µl oligo DT, 3µl random hexamers, 1µl DNTP and incubated at 65 ^{o}C for 5 minutes before being transferred to ice for 1 minute. A reaction mix containing 2µl of 10x RT buffer, 4µl of 25mM $MgCl_2$, 2µl of 0.1M DTT, 1µl RNAse Out was added to each sample tube and incubated at 42^{0}C for 2 minutes. 1µl of Superscript II RT enzyme or DPC water (–RT control) was added to each tube and incubated at 42^{0}C for 50 minutes, then at 70^{0}C for 15 minutes. The tubes were transferred to ice and 1µl of RnaseH was added to each sample for 20 minutes at 37^{0}C. All reagents were supplied with the kit.

2.3.4.4 Removal of DNA from RNA Samples

Contaminating genomic DNA was removed from RNA samples using the DNA-free kit from Ambion, briefly 0.1 volume of 10x DNase buffer 1 and 1µl of DNase (2 units) were added to a maximum of 100µl of RNA. The samples were then incubated for 20 minutes at 37^{0}C. After resuspension, 0.1 volume of DNase inactivation reagent was added and mixed thoroughly. Following 2 minutes at RT, the samples were spun at 15,000rpm in a microfuge for 1 minute. The supernatant containing the RNA was removed to a clean tube. The resultant DNA contamination was typically <0.1%.

2.3.4.5 PCR

Using the Reddymix tubes from Abgene, 1µl of each primer at 10µM was added to the 50µl tube together with 5µl of cDNA. Control tubes included H_2O and minus RT samples. The PCR machine was set up to go through 35 cycles with each cycle consisting of 92^{0}C for 2 minutes, 58^{0}C for 30 seconds and 72^{0}C for 1 minute. When 35 cycles were completed the tubes were heated to 72^{0}C for 10 minutes before being cooled to 4^{0}C until removed from the machine.

2.3.4.6 Analysis of PCR Products

The PCR products were run on electrophoresis gels that allowed visualization of the bands. Briefly, a 2% agarose gel was made using 2g of agarose powder in 100ml of TAE buffer which was melted in a microwave for 2 minutes at full power.

To this 1.2µl of ethidium bromide stock was added at 10mg/ml and mixed. The gel was then poured into a cast containing a comb to create sample wells. This was done in a cold (4^0C) room and left to set for approximately 15 minutes. The sample comb was then removed and the gel placed in the gel tank containing 1x TAE buffer before the samples were loaded. 15-20µl of PCR product was loaded into each well. Hyperladder IV (100-1000bp) was included as a reference. Gels were run ~ 150mV constant voltage. The gels were viewed on a UV transilluminator and photographed.

2.3.4.7 Extraction of Gel Bands

Whilst viewing on a transilluminator, bands were cut from the gel using a scalpel, minimising the amount of agarose extracted with each band. The DNA was then extracted using the Qiagen QIAquick gel extraction kit (which contained all reagents) and protocol. Briefly, the gel slices were placed in Eppendorf tubes and weighed. 3x volume of buffer QG was added and the tubes placed in a 50^0C water bath for 10 minutes to melt the agarose. After adding one gel volume of isopropanol, the samples were applied to QIAquick spin columns and centrifuged for 1 minute in a microfuge at full speed. The eluate was discarded and the columns washed with 750µl of buffer PE. The DNA was eluted in 50µl of distilled water.

2.3.4.8 Cloning of DNA Fragments with TOPO TA®

The PCR products were ligated into pCR® 2.1-TOPO® using the TOPO®TA kit from Invitrogen. According to the manufacturer's instructions 0.5-4µl of PCR product was added to 1µl of salt solution and 1µl of TOPO® and the reaction mix made up to 6µl with sterile water. The tube was mixed gently and incubated at RT for 5 minutes. The reaction was placed on ice for between 5 and 30 minutes. 2µl of this mix was added to 1 vial of One Shot chemically competent DH5α E.coli, which were then heat-shocked at 42^0C for 30 seconds and immediately transferred to ice. 250µL of SOC medium at RT was added to each tube and incubated at 37^0C for 1 hour in a shaker at 200rpm. LB agar plates were prepared by adding 1.5% agar to prepared LB medium and autoclaving before pouring into 90mm petri dishes. When the agar had cooled and solidified, 40µl of x-gal at a concentration of 40mg/ml in dimethylformamide (DMF) was added to the surface of each plate, spread with a sterile spreader and dried for 15 minutes.

2.3.4.9 Growth of Plasmids

Following incubation at 37^{0}C, 10-50µl from each transformation was spread evenly on an LB agar plate prepared (as detailed 2.2.4.2) and incubated overnight at 37^{0}C. White colonies containing insert were picked from the plate and cultured overnight at 37^{0}C in LB medium containing 50µg / ml ampicillin.

2.3.4.10 Isolation of Plasmid DNA

DNA was isolated from plasmid preparations using the QIAPprep miniprep kit which is based on the alkaline lysis of bacterial cells, adsorption of DNA onto silica in the presence of high salt, followed by elution in low salt buffer. Only DNA is adsorbed on to the membrane all RNA, cellular protein and metabolites are found in the flow through. Briefly, the bacterial cells were pelleted and the supernatant removed by aspiration before the addition of 250µl of buffer P1 (containing RNase A). The solution was transferred to Eppendorf tubes and 250µl of buffer P2 added with gentle mixing. 350µl of buffer N3 was added and the tubes mixed by inversion. The tubes were centrifuged for 10 minutes at 15000rpm in a microfuge. The supernatants were applied to QIAprep spin columns in a 2ml collection tube and centrifuged for 30-60 seconds and the flow through discarded. The columns were washed by adding 750µl of buffer PE and centrifuging for 30-60 seconds and discarding the flow through. The columns were centrifuged for a further 1minute to remove residual wash buffer. The DNA was eluted by the addition of 50µl of distilled water, letting it stand for 1 minute and centrifuging for 1 minute at 15000rpm.

2.3.4.11 Verification of DNA Sequence

The amount of DNA from each extracted band was measured using a spectrophotometer. A known amount was processed through the ABI sequencer by Mrs Christine Lang and the results recorded. The sequences were compared with the gene coding sequences and the primer:gene specificity verified.

2.3.4.12 Sample Preparation For Microarrays

Cells positively selected for CD34 were recovered from liquid nitrogen as described and sorted for G0 and dividing (G1/S/G2/M) cells according to the

protocol described for HST and Py. Cells sorted on the same parameter were pooled following sorting, centrifuged and placed in Eppendorf tubes, where most of the PBS2% was removed by aspiration. Trizol was added and the volume adjusted depending on the number of sorted cells. The amount of Trizol added was: 1ml per 10^6-10^7 cells, 0.5ml per 10^5-10^6 cells and 0.2ml per 10^4-10^5 cells. The tubes were vortexed and placed immediately in the –80^{0}C freezer until all of the samples had been acquired. Generation of total RNA was as described and it was crucial for the microarray study that all samples were processed at the same time to reduce the possibility of disparity in preparation.

2.3.5 Statistics

Statistical analysis was performed by either the student's *t*-test or the wilcoxon-signed rank test.

Chapter 3 Results 1 - Identification and Isolation of Stem Cells in Different Phases of the Cell Cycle

3.1 Introduction

Chronic myeloid leukaemia is a stem cell disease, which is characterised by excessive numbers of circulating intermediate progenitors and mature granulocytes (Eaves CJ and Eaves AC 1987). Stem cells are intrinsically resistant to damage by either cytotoxic drugs or radiation, and diseases that originate in a stem cell are difficult to eradicate. CML has three distinct phases of progression, an initial chronic phase, during which large numbers of relatively mature granulocytes exist with a typical time scale of 4-6 years (see figure 3.1), is followed by the onset of accelerated phase, which can last up to 1 year, and culminates in blast crisis, where the numbers of immature white cells increase proportionately to mature cell types (Sawyers CL 1999). At this stage the disease becomes much more resistant to therapy and almost certainly involves further acquired mutations. Patient mortality is 100% within 3-6 months of onset of blast crisis if untreated (Spiers ASD 1977).

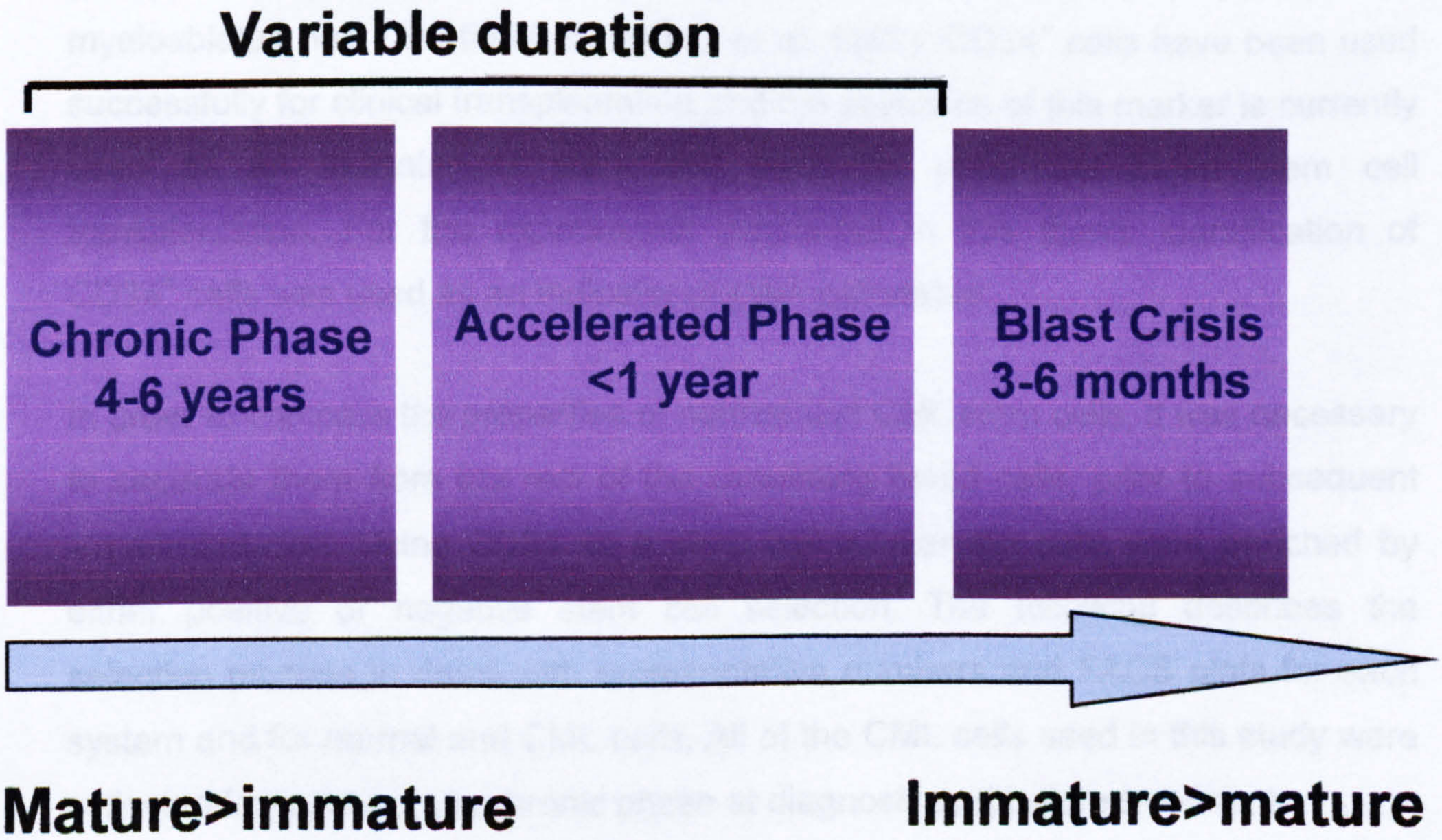

Figure 3-1 **A schematic diagram of the progression of CML disease.**

If an appropriate therapy could be found for the treatment of CML in chronic phase, progression to fatal blast crisis could be arrested. Since chronic phase offers the best opportunity for successful therapy, the work described in this thesis focuses exclusively on this stage of the disease. In an effort to identify possible targets, which could be exploited for therapeutic purposes, some of the properties of normal and CML stem cells in vitro have been investigated.

Normal stem cells are known to be largely quiescent, residing in the G0 phase of the cell cycle, where they can be recruited into division in response to appropriate stimuli (Bradford GB, Williams B et al. 1997),(Ponchio L, Conneally E et al. 1995). This has been demonstrated by introducing quiescent cells into NOD/SCID mice, where some cells can exit G0 and repopulate the haemopoietic system of the mouse. It was an unexpected finding that alongside the actively cycling malignant population in the chronic phase of CML, there also coexisted a quiescent stem cell fraction. These cells were primitive, expressing the stem cell marker CD34 and were part of the leukaemic clone, as verified by FISH (fluorescence in-situ hybridisation) and RT-PCR (Holyoake T, Jiang X et al. 1999). It has been established that cells expressing CD34, but lacking lineage markers, are primitive and able to generate progeny of different phenotypes. However, there is also some evidence that an earlier stem cell exits which does not express CD34 or lineage markers and is able to repopulate the haemopoietic system of a myeloablated host (Bhatia M, Bonnet D et al. 1997). $CD34^+$ cells have been used successfully for clinical transplantation and the presence of this marker is currently used as an indicator of stem cell dose for peripheral blood stem cell transplantation. For the experiments presented in this thesis identification of $CD34^+$ cells was used as an indicator of stem cell status.

In order to compare the properties of normal and CML stem cells, it was necessary to separate them from the rest of the circulating blood cells, prior to subsequent experimentation. Using CD34 as a stem cell marker the cells were enriched by either positive or negative stem cell selection. The following describes the selection process in detail with representative numbers and FACS plots for each system and for normal and CML cells. All of the CML cells used in this study were collected from patients in chronic phase at diagnosis and before treatment.

3.2 Stem Cell Selection

Stem cells represent a very rare fraction of the circulating progenitors, around 0.1%, and in order to study these cells, it was necessary to significantly enrich the stem cell fraction, before FACS sorting specific cell sub-populations. This was achieved by either positive or negative stem cell selection. The starting cell population was collected from CML patients during leukapheresis, which is primarily performed to reduce excessive numbers of circulating white blood cells, or to store autologous material for future treatment. The procedure was performed using a dedicated leukapheresis machine, which allows red blood cells and plasma to be returned to the patient, after removal of a large number of the white cells. Leukapheresis products that are surplus to clinical requirement can be used for research with appropriate patient consent. Within the CML patient group, there was a large variation in the starting $CD34^+$ percentage from 0.3-50%, the median being approximately 3%, characteristic of a stem cell disease (Richmond LJ, Alcorn MJ et al. 2002).

For normal stem cell collections, donors receive G-CSF (granulocyte stimulating factor) for 4-6 days before collection to boost the number of circulating progenitors. There can be large differences in the effectiveness of G-CSF mobilisation, leading to differences in both the percentage of $CD34^+$ cells in the starting fraction, from 0.3-1.7%, and in total white cell numbers harvested. The dose required by the patient for a stem cell transplant at this institution was calculated as $6x10^6$ $CD34^+$ cells/kg and, with consent, a proportion of the remainder could be used for research purposes. The leukapheresis machine settings were operator controlled and the purity of the stem cell collections obtained, influenced by the settings. For this reason, and because of differences in effectiveness of mobilisation, there could be a significant variation in the starting $CD34^+$ number, and subsequent recovery of stem cells following selection.

The stem cell populations derived from positive or negative selections are intrinsically different. There is some evidence that a more primitive cell than a CD34 expressing cell exists within the stem cell compartment that can in turn generate $CD34^+$ cells (Goodell MA, Rosenzweig M et al. 1997). A negative selection would retain these cells since they would also lack lineage markers. A positive selection would exclude these cells since it only targets cells expressing

the CD34 marker. The method of choice was dependant on the final experiments to be performed. Throughout the studies presented in this thesis, it was necessary to freeze cells following stem cell enrichment. Both types of selection involved a considerable time input and further cell sorting required at least 12 hours, including staining and cell culture post-sort.

3.2.1 Positive stem cell selection

In a positive selection, the cells of interest are removed from the rest of the population by labelling with antibody, magnetic beads and selecting using a magnetic column. For the positive selections described here the Isolex® 50 system was used. This was a commercial method used for clinical stem cell selections, which was scaled down using a smaller magnetic column for research samples, as the number of total cells/column was critical to cell recovery and purity.

The cells were labelled with a mouse anti-human monoclonal antibody against the CD34 antigen, and further labelled with a sheep anti-mouse antibody bound to a magnetic bead. The cells were then passed through a magnetic column such that the unlabelled cells were eluted first before a stem cell releasing agent was added in order to detach the bound cells. The releasing agent contained a nano-peptide (PR34®) with a similar sequence to the CD34 antigen, which competed for binding of the active site, and due to the excess of nano-peptide, the antigen-bound cells were released from the magnetic column.

3.2.2 Example of a CML and a Normal Positive Cell Selection

A diagram of the labelling and selection procedure is shown in figure 3.2. Stem cells were released with the CD34 antigen intact and available for further labelling. The selected cells were assessed by flow cytometry for CD34 purity and plots of the pre-column and post-column samples for both normal and CML are shown in figure 3.3.

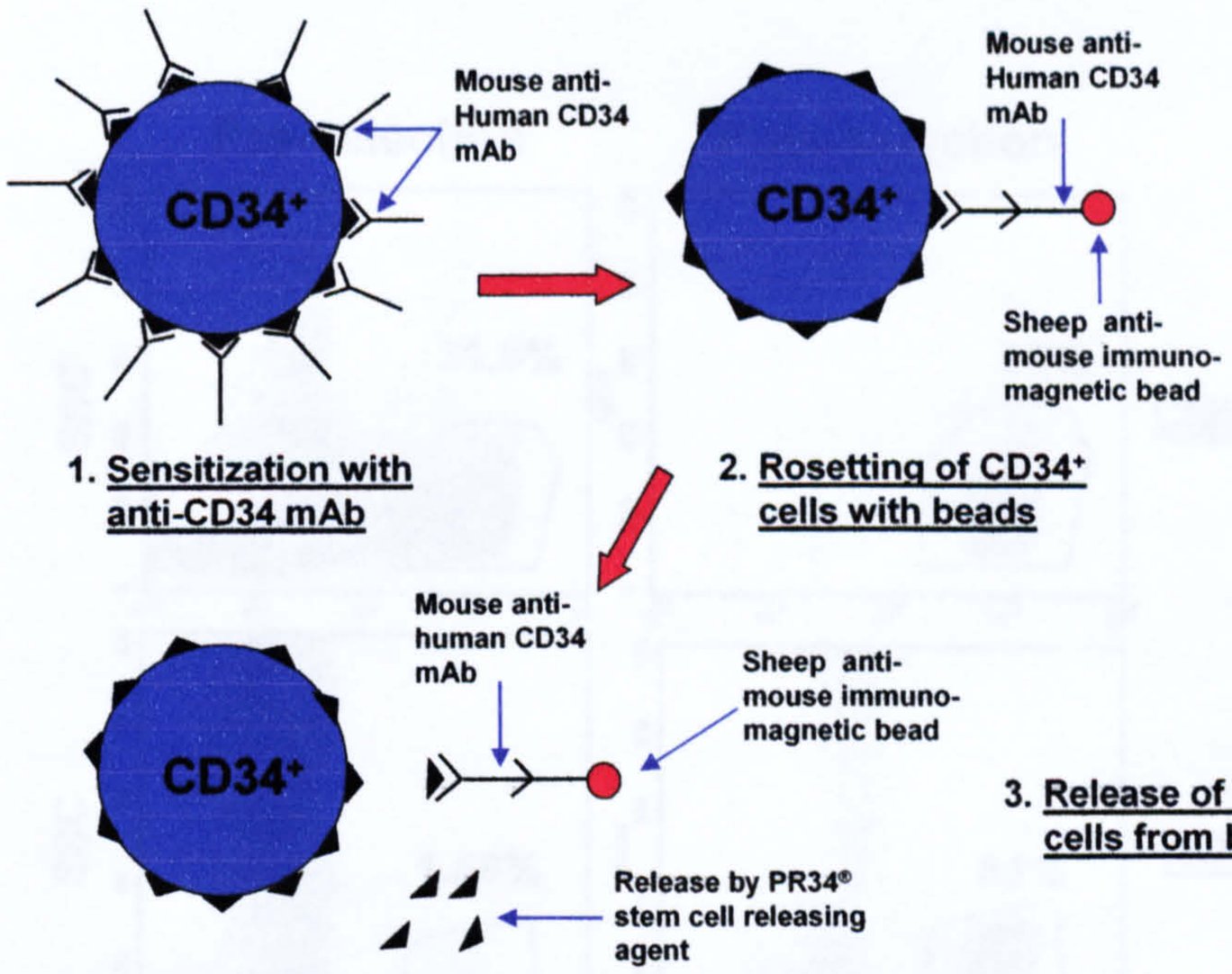

Figure 3-2 Isolex CD34 stem cell selection method.
Cells are labelled and selected as described in the text.

Using side scatter (SSC) to discriminate cells on the basis of their granularity (lower granularity indicates less differentiation) and including a marker for CD34, the more primitive cells can be identified. Figure 3.3 shows that the proportion of CD34 positive cells has increased in the CML sample from 31.8-98%, and in the normal sample from 1.59-83%. The cells were ≥99% viable post selection for both normal and CML examples and these were representative for most selections. The final percentage of CD34 positive cells obtained using this method varied between 53-98% for both CML and normal, with recoveries ranging from 36-71% in normal samples and 69-98% for CML samples. The quality of the starting population both in terms of total cell number and percentage of CD34+ cells influenced the efficiency of the selection.

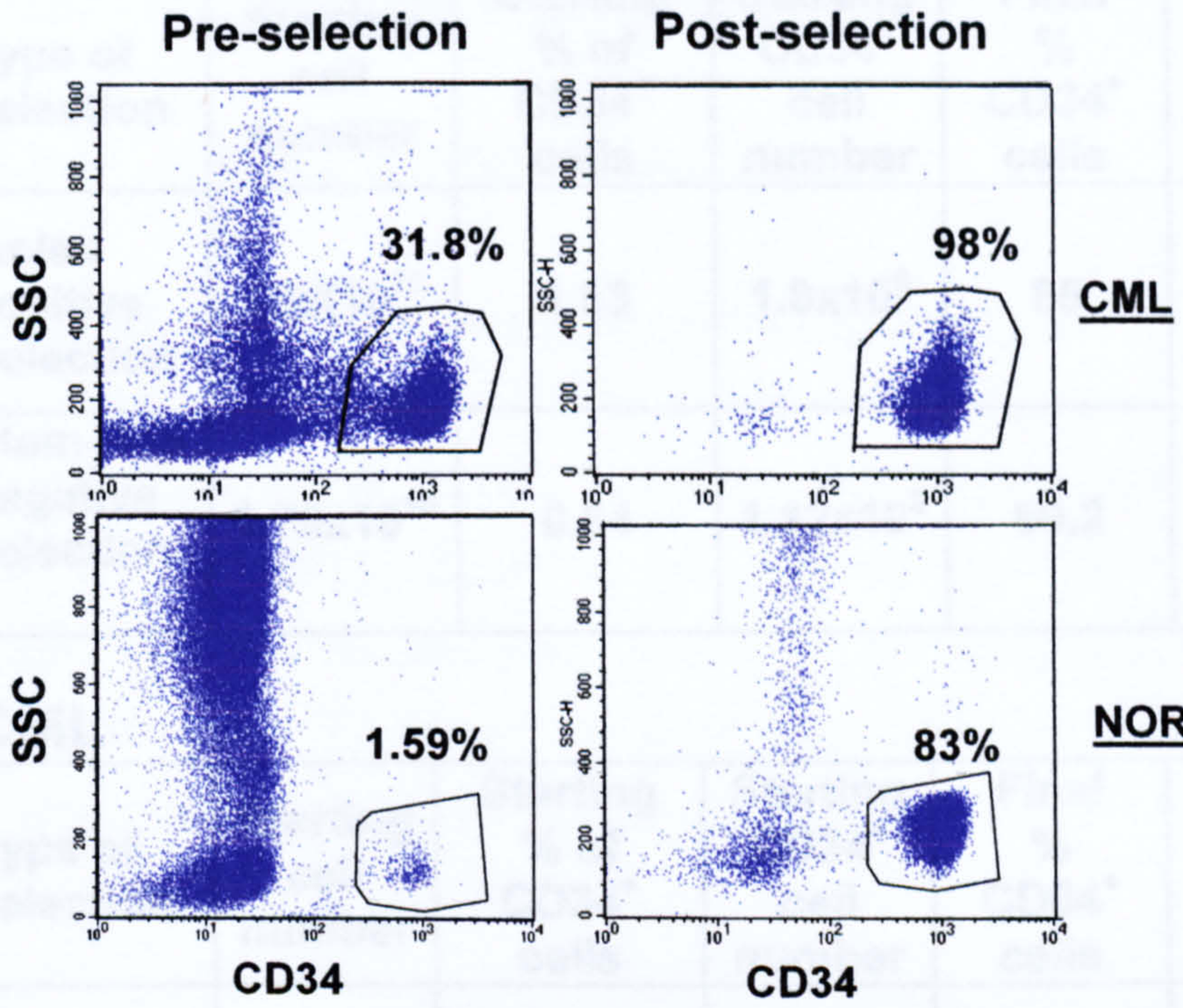

Figure 3-3 FACS plots of normal and CML positive stem cell selections.

The plots show CD34 versus SSC, the gated populations shown are low in SSC and high in CD34 expression. The regions indicate the percentage of $CD34^+$ cells pre- and post-selection for both normal and CML samples.

The plots in figure 3.3 illustrate there is little qualitative difference in post-selection samples between normal and CML. The number of $CD34^+$ cells recovered and the final purity of the sample (as shown in table 3.1) were dependent on the starting cell population and not on the disease status of the patient.

NORMAL

Type of selection	Starting cell number	Starting % of $CD34^+$ cells	Starting $CD34^+$ cell number	Final % $CD34^+$ cells	% Rec of $CD34^+$ cells	Total $CD34^+$ cells recovered
Isolex positive Selection	$1.2X10^{10}$	1.53	$1.8x10^8$	85	62	$1.12x10^8$
Stem-Sep negative selection	$1.75x10^{10}$	0.64	$1.12x10^8$	60.2	82	$9.2x10^7$

CML

Type of selection	Starting cell number	Starting % of $CD34^+$ cells	Starting $CD34^+$ cell number	Final % $CD34^+$ cells	% Rec of $CD34^+$ cells	Total $CD34^+$ cells recovered
Isolex positive Selection	$7.3x10^9$	4.72	$3.4x10^8$	94	53	$1.84x10^8$
Stem-Sep negative selection	$4.5x10^9$	5.6	$2.5x10^8$	77.5	47	$1.17x10^8$

Table 3-1 Table of selection numbers for normal and CML representative examples.

The numbers are shown for both Isolex positive and StemSep negative selections described in the text.

Table 3.1 shows an example of the cell numbers obtained from positive stem cell selections for normal and CML representative samples. The total cell starting number in the normal example was $1.2x10^{10}$ and the total number of CD34 positive cells available was $1.8x10^8$, based on the CD34 starting percentage of 1.53%. The selection produced a cell population which was 85% $CD34^+$ and 62% of the available CD34 cells were recovered from the column giving a total of $1.12x10^8$ cells, which were then frozen in liquid nitrogen in aliquots of $20x10^6$/vial. In the CML example, the stem cell selection produced an increase in $CD34^+$ percentage of 4.72 to 94% with a recovery of 53% of the available $CD34^+$ cells, (which were a total of $3.44x10^8$) giving a final number of $1.84x10^8$ selected stem cells, which were frozen in liquid nitrogen at $20x10^6$/vial. As the selection system used was a unique scaled down clinical system there were no published numbers using this method, however the recoveries and enrichments were within the limits

published for the full clinical system, using the same antibody cocktail and methodology but a different magnetic column (Farley TJ, Ahmed T et al. 1997).

3.2.3 Negative Stem Cell Selection

In negative stem cell selections, cells expressing lineage markers were labelled with a panel of mouse anti-human antibodies including CD2, CD3, CD14, CD16, CD19, CD24, CD56, CD66b, and glycophorin A, then further labelled with a sheep anti-mouse antibody bound to magnetic colloid. The unbound stem cells were eluted from the column separating them from the bound cells, which remained attached. Table 3.2 shows the antibodies contained in the progenitor enrichment cocktail and their relevant target cells.

Antibody	Target cell
CD2	T cells, NK cells
CD3	T cells,
CD14	Monocyte/macrophage
CD15 (CML)	Granulocytes/basophils
CD16	NK cells, granulocytes
CD19	B cells
CD24	B cells
CD56	NK cells,
CD66b	Granulocytes
Glycophorin A	Erythroid cells

Table 3-2 Table of antibodies in the StemSep progenitor enrichment cocktail.

A schematic outline of the selection procedure is shown in figure 3.4. The method was modified when CML cells were processed by the addition of biotinylated anti-CD15 to the cells before the addition of the other antibodies described and anti-biotin included with the magnetic colloid. This step facilitated the removal of the excessive number of granulocytes characteristic of this stage of CML disease. The cells were then passed through a magnetic column where the unlabelled cells were eluted and the labelled lineage$^+$ cells remained attached to the column. The CD34$^+$ purity and recovery of the selected cells was assessed by flow cytometry, in the same way as the positively selected cells i.e. by calculating the percentage of CD34 strongly positive cells that were also low in side scatter before and after selection.

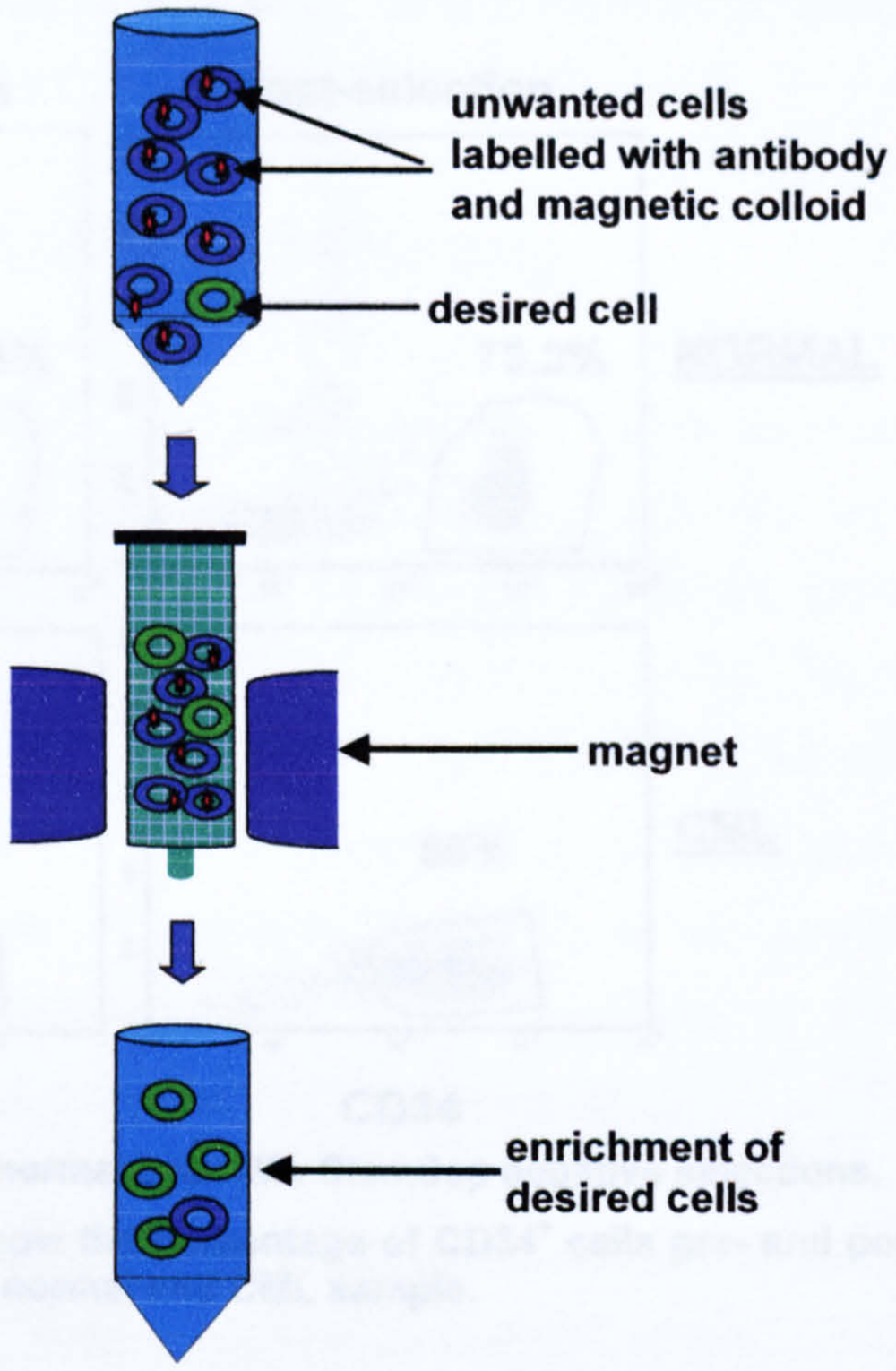

Figure 3-4 Diagrammatic representation of StemSep negative selection.

3.2.4 Example of a Normal and a CML Negative Selection

In the normal example shown in figure 3.5 the number of CD34 positive cells has increased from 1.23 to 76.2% and in the CML sample the percentage of CD34 positive cells has increased from 5.9 to 86%. Since this population also contains cells that do not express lineage markers or CD34 it would not be expected that the percentage of $CD34^+$ cells would be as high as in the positive selection. In practice, negative selections produced a lower percentage of $CD34^+$ cells, typically from 40-88%, compared to 53-98% for positive selections. The FACS plots in figure 3.5 show that, as in the case of the positively selected cells, there was little difference between the normal and CML samples in terms of stem cell purity. The addition of anti-CD15 in the CML sample maximised the purity of the $CD34^+$ cells in the selected fraction by removing the large excess of granulocytes typical of CML in chronic phase.

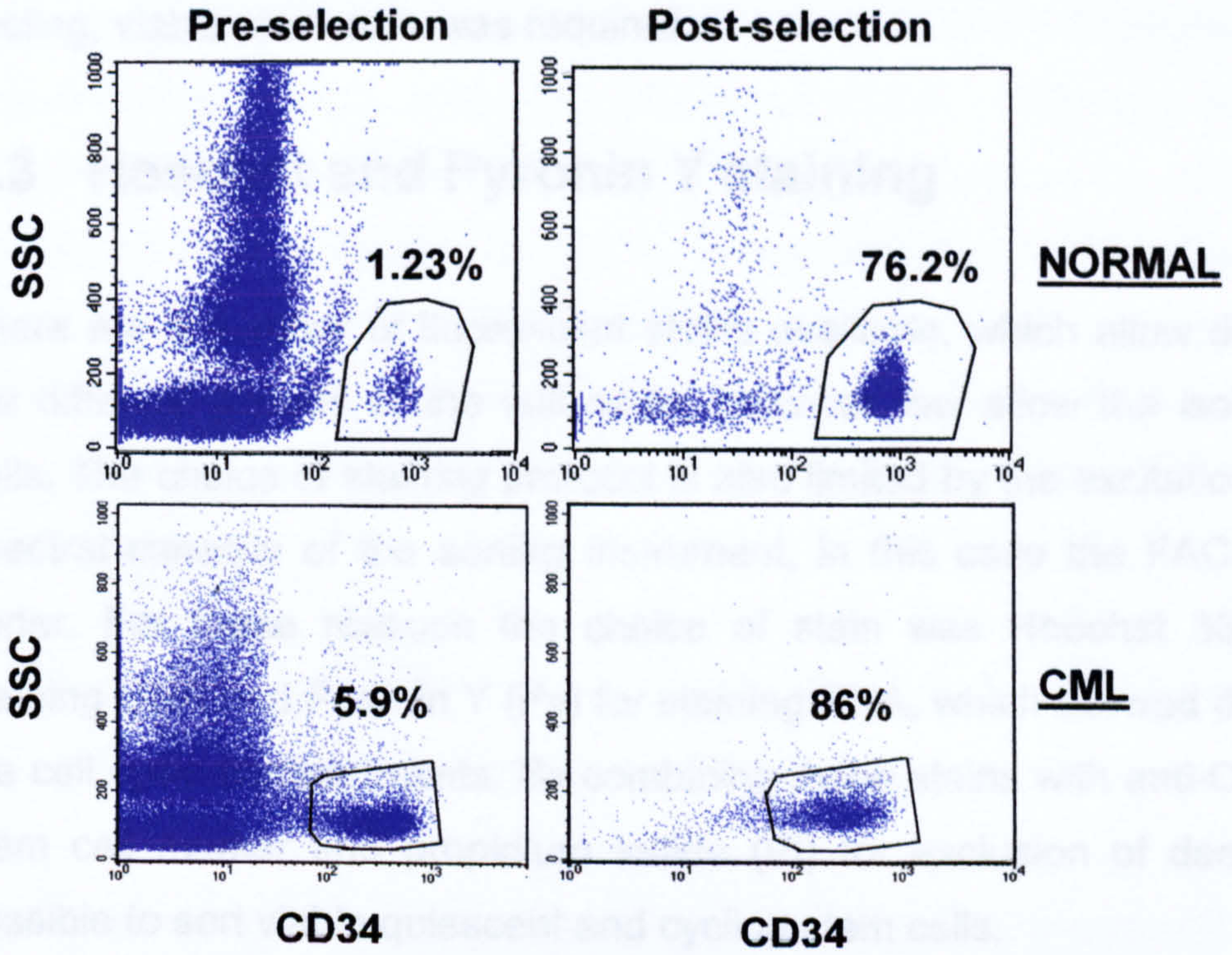

Figure 3-5 FACS plots of normal and CML StemSep negative selections.

The regions show the percentage of $CD34^+$ cells pre- and post-selection for a representative normal and CML sample.

In the negatively selected normal example in table 3.1, a starting cell number of $1.75x10^{10}$, with a starting CD34 percentage of 0.64, giving $1.12x10^8$ available CD34 cells, yielded $9.2x10^7$ $CD34^+$ cells. The yield from the column was 82%. In the CML example, from $2.5x10^8$ available $CD34^+$ cells, $1.17x10^8$ were recovered, indicating a recovery of 47%. Comparing these examples of positive and negative selection for normal cells, the negatively selected example has a better recovery of stem cells 82% compared to 62% in the positive selection. However in the CML examples, there was little difference in recovery between positive and negative selection 53-47%. A possible explanation for the CML examples was that all of the stem cells were not labelled in the positive selection, or that they were not completely released from the column. Due to the nature of the processing in both situations involving multiple wash steps, antibody labelling, columns and sample-to-sample variation, there were differences in the final recovered cell numbers. Also, there were insufficient amounts of any sample to enable direct comparison of selection methods with the same sample. For all of the samples, the recoveries and yields were within the limits suggested by the manufacturers. The rationale for doing the stem cell selections was to enrich for primitive progenitors to facilitate isolation of rare quiescent stem cells. Given that CML is a disease that originates in a pluripotent stem cell and that normal stem cells are largely quiescent, the overall aim was to compare the characteristics of normal and CML stem cells, in

relation to their cell cycle position. To do this, a method of isolating quiescent and cycling, viable stem cells was required.

3.3 Hoechst and Pyronin Y staining

There are a number of fluorescent stains available, which allow discrimination of the different phases of the cell cycle, however few allow the isolation of viable cells. The choice of staining protocol is also limited by the excitation and emission spectral capacity of the sorting instrument, in this case the FACS Vantage cell sorter. For these reasons the choice of stain was Hoechst 33342 (HST) for staining DNA and Pyronin Y (Py) for staining RNA, which allowed discrimination of the cell cycle compartments. By combining these stains with anti-CD34-FITC as a stem cell marker and propidium iodide (PI) for exclusion of dead cells, it was possible to sort viable quiescent and cycling stem cells.

HST is a DNA selective, UV excited, blue fluorescent bisbenzimidazole dye originally synthesized by Loewe (Loewe H and Urbanietz J 1974) as an anti-protozoal drug for Hoechst and was first used in flow cytometry in 1974 by Latt (Latt SA 1974). HST dyes bind to sequences of three A-T base pairs in DNA, binding to the minor groove of the DNA helix, rather than by intercalation. Their affinity for DNA is sufficiently strong that they will displace bound molecules of intercalating dyes (Loontiens FG, Regenfuss P et al. 1990). Binding of dyes like HST has been shown to exhibit a certain level of toxicity (Durand RE and Olive PL 1982), which is relative to cell type. For this reason it was necessary to confirm that the staining process did not adversely affect the viability or functional capacity of the cells.

Py is a homologue of acridine orange (A0) which has been used for the assessment of cell cycle for a number of years. Py diffuses into the cell and allows staining of RNA whilst permitting the cells to remain viable, unlike AO, which requires fixing and permeabilisation of the cells. Py binds to RNA with a preference for G-C rich regions and although DNA staining by Py has been documented in some cases, it is not likely to confuse DNA/RNA based sorting using this protocol as pre-incubation with the HST stain blocks access of Py to binding sites on DNA (Ladd AC, Pyatt R et al. 1997).

Due to the variability of DNA and RNA staining it was necessary to determine the concentration of the combined stains, which would allow discrimination of the cell populations by FACS, whilst preserving cell viability. This was done by staining cells with different concentrations of each stain and measuring, staining efficiency, viability and colony forming capability. The availability of stem cell enriched patient samples was very limited, however it was important to use representative examples of experimental cells, to ensure comparable results. The number of cells required to set up the initial experiments limited the replicates to one normal and one CML.

3.3.1 Comparison of Colony Forming Capacity Following Hoechst and Pyronin Y Staining

Plating cells in a clonogenic assay gives a measure of the colony forming capacity, which in turn gives an indication of functionality. The objective was to determine if the combination of stains required to produce good FACS profiles had a deleterious effect on the capacity of the cells to divide and form colonies. The cells used were $CD34^+$ selected cells, either CML or normal, recovered from frozen and incubated overnight in a 5 growth factor cocktail containing IL-3, IL-6, FLT3L, hSCF and G-CSF to allow recovery from frozen. If the cells were used immediately following recovery from cryopreservation, cells dying as a result of thawing could interfere with the data relating to toxicity of the dyes. By incubating overnight in a growth factor rich cocktail, recovery of viable cells was maximised. The following day the cells were removed from petri dishes or flasks, washed in PBS/2% and stained with HST at concentrations of 0 to 10μM alone or in combination with Py at concentrations of 0 to 1μg/ml. Similar concentrations of these dyes in combination had been used previously, though it was necessary to establish optimal concentrations of both dyes using our FACS sorter. This allowed assessment of the minimum laser power setting required to produce acceptable FACS profiles, as it has been previously reported that increased laser power could be lethal to some cells (Shapiro HM 1981).

The clonogenic assay input cell counts were adjusted for viability and for the percentage of CD34 positive cells so that the same number of viable stem cells was used to initiate each culture. $1x10^4$ viable CD34 positive cells were plated in duplicate in methylcellulose containing a cocktail of cytokines designed to

stimulate both myeloid and erythroid colony growth. The GM colonies (1 colony= >40 cells) and BFU-e (single bursts) were counted after incubation at 37^{0}C in a humidified incubator for 12 days. Counts were an average of two plates. The results are shown in table 3.3.

NORMAL

Hoechst	Pyronin Y	% Viable	GM	BFUe	TOTAL
0	0	38.6	158	407	565
5	0.5	40.7	89	335	424
5	1	43.3	43	79	122
10	0.5	43.6	62	382	450
10	1	40.8	56	160	216
10	0	38.5	49	404	453
0	0.5	45.3	211	348	559

CML

Hoechst	Pyronin Y	% Viable	GM	BFUe	TOTAL
0	0	35.9	190	339	529
5	0.5	40.1	106	177	283
5	1	42.8	108	337	445
10	0.5	39.5	56	512	568
10	1	35.8	58	283	341
10	0	39.1	105	351	456
0	0.5	42.8	190	287	477

Table 3-3 Table of colony counts for normal and CML cells stained with various concentrations of HST and Py.

The cells were stained with the dyes as indicated in the table and plated in colony assays as described in the text. The colonies were counted at day 12 and GM scored as >40 cells and BFU-e as single bursts. The cell viabilities were assessed by PI exclusion by FACS following staining, and before plating in colony assays.

Table 3.3 shows the percentage of total viable cells together with the GM, BFU-e and total colony counts (GM + BFU-e) for unstained and combinations of dyes at various concentrations. Results for both a normal and CML sample are shown. The total cell viabilities were determined by FACS following incubation of the cells with PI after staining with HST and Py as indicated in table 3.3. All combinations of stains were run on the FACS sorter to establish the success of the staining procedure. This indicated that the HST stain was the least consistent especially at low concentrations. Increasing the incubation time with HST from 45to 90 minutes before the addition of Py, improved the reliability of staining.

The results in table 3.3 indicate that compared to unstained cells, for both normal and CML, the staining had some effect on the total colony count. For normal cells, in most cases, the number of CFU-GM was reduced except in the Py only culture

where the number of CFU-GM colonies exceeded the control. The largest reduction in total colony count was seen in the 5μM HST/1μg/ml Py combination in the normal sample, where the total colony count was reduced from 565 to 122. The 10μM HST/1μg/ml Py would have been expected to show a greater reduction in colonies but only reduced the counts from 565 to 216. For CML cells, the large reduction in total colony count, identified in the normal sample with 5μM HST/1μg/ml Py, was not observed, however there was a similar level of reduction in CFU-GM numbers from 190 to 108. Although there was a reduction in overall colony count, it was only from 529 to 445, most of which was attributed to the reduction in CFU-GM.

Comparing the colony counts for the single stains, the numbers indicate that HST appears to affect the CFU-GM count preferentially. AT 10μM, HST alone reduces the CFU-GM count from 158 to 49 for the normal, and from 190 to 105 for the CML, whereas the BFU-e count remains at the same level. In contrast, Py appears to exert a greater effect on the BFU-e count. At 0.5μg/ml the BFU-e count was reduced in the normal from 407 to 348 and in the CML from 339 to 287, while the GM count remained the same for the CML, and increased in the normal from 158 to 211. This phenomenon is worthy of further investigation but was outwith the scope of this project.

The results in table 3.3 also demonstrate that in the normal sample, increasing the Py concentration to 1μg/ml in combination with either 5 or 10μM HST reduced the total number of colony counts to a level below any of the other combinations that used 0 or 5μg/m Py. In the CML example, the 5μmHST/ 0.5μg/ml Py combination appears to have a reduced overall count compared to both unstained and other combinations. This may be experimental error and these results represent one example of each combination, as availability of material limited replication of these experiments. The total population viability appears to be higher in the stained samples than in the unstained control. The lack of replicates in these experiments due to limitations in sample availability meant it was not possible to achieve statistical significance. However, the data gave an indication of the toxicity of the dyes and enabled examination of the FACS profiles.

Following inspection of the FACS profiles of stained cells, the combination of 10μM HST/0.5μg/ml Py gave the most acceptable and reliable staining using our sorter set-up. Having demonstrated that this combination did not appreciably affect

the viability and clonogenicity, at least in terms of the total colony counts, this was the combination used in all subsequent experiments. In addition, similar concentrations of these dyes have been used previously to isolate stem cells, which retain full functional capacity, as demonstrated by their ability to reconstitute immuno-deficient mice (Holyoake T, Jiang X et al. 1999).

Figure 3.6 shows an example of the FACS profile obtained using this combination of dyes. By manipulating the amplitude of the detectors it was possible to increase the level of the detector on the y-axis (Py) to identify cells with the lowest Py staining, which were also HST^{lo}, as those being in G0. Figure 3.6 shows the corresponding profile obtained on the histogram plot of HST (FL4). This demonstrates the cell cycle distribution, with most of the cells in the 2n population, which includes G0 and G1 The 4n population are cells which have reached the end of the cell cycle and are about to divide into two cells and either become quiescent by going back into G0, or continue to divide by moving into G1. The two daughter cells may have different fates depending on the environmental stimuli they receive.

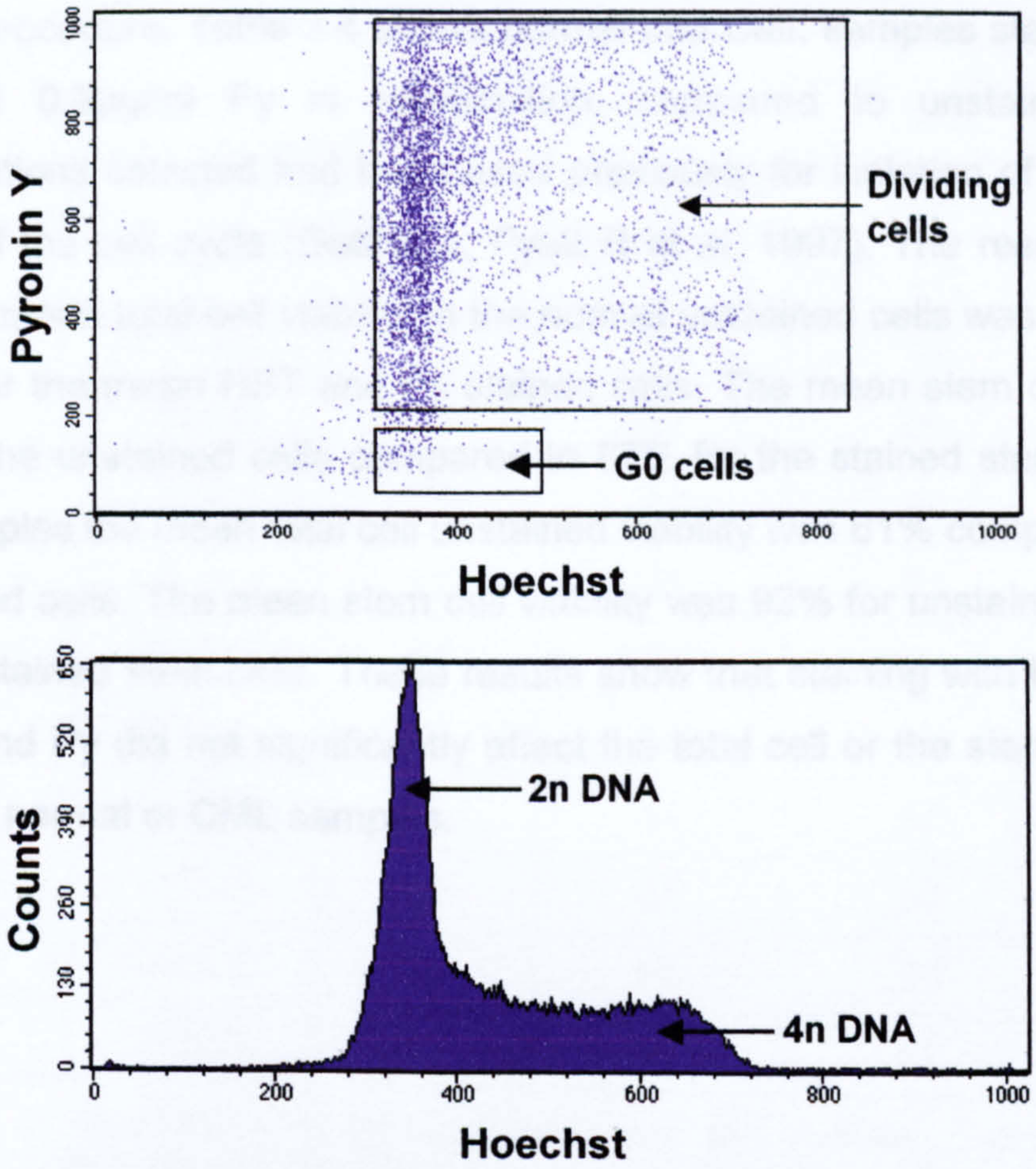

Figure 3-6 FACS profiles of Hoechst and Pyronin Y staining.

The dot plot shows CD34$^+$ selected cells from a normal sample stained with 10μM HST and 0.5μg/ml Py. The cells have been gated on the viable PI$^-$ population. The histogram plot shows the HST profile for the same cells identifying the 2n and 4n populations.

Overall, the combination of 10μM HST and 0.5μg/ml Py gave the most reliable cell staining by FACS and maintained acceptable levels of cell viability. Various staining strategies were employed to increase the reliability of the Hoechst stain, which could be inconsistent. Increasing the HST incubation time from 45 to 90 minutes before the addition of Py resulted in almost 100% reliable profiles for HST.

3.3.2 Comparison of Total Cell and Stem Cell Viability Following Hoechst and Pyronin Y Staining

Since the availability of material precluded doing toxicity analysis on multiple samples, the viabilities of the total and stem cell populations were recorded for each subsequent experiment. This allowed the monitoring of the effects of staining with HST and Py on a larger sample group. Comparing a number of samples both normal and CML cells stained with 10μM HST and 0.5μg/ml Py, indicated that

neither the total cell, nor the stem cell viability was significantly affected by the staining procedure. Table 3.4 shows normal and CML samples stained with 10μM HST and 0.5μg/ml Py in combination, compared to unstained cells. The concentrations selected had been used previously for isolation of cells in various phases of the cell cycle (Gothot A, Pyatt R et al. 1997). The results in table 3.4 show the mean total cell viability in the normal unstained cells was 46% compared to 47% for the mean HST and Py stained cells. The mean stem cell viability was 82% for the unstained cells compared to 87% for the stained stem cells. For the CML samples the mean total cell unstained viability was 61% compared to 62% for the stained cells. The mean stem cell viability was 92% for unstained compared to 94% for stained stem cells. These results show that staining with this combination of HST and Py did not significantly affect the total cell or the stem cell viability in either the normal or CML samples.

		% Viable of Total		% Viable of CD34$^+$	
		Unst	HST/Py	Unst	HST/Py
1	Normal 1	48	44	83	78
2	Normal 2	46	49	82	95
3	Normal 3	44	48	81	89
	MEAN	46	47	82	87
4	CML 1	74	72	91	93
5	CML 2	63	69	94	95
6	CML 3	58	57	77	83
7	CML 4	44	51	96	99
8	CML 5	48	41	99	99
9	CML 6	56	67	90	91
10	CML 7	81	78	97	98
	MEAN	61	62	92	94

Table 3-4 Comparison of total cell and stem cell viabilities following staining with Hoechst and Pyronin Y.

Following recovery from cryopreservation and an overnight incubation in media with 5 growth factors, the cells were stained with 10μM HST and 0.5μg,ml Py. The total cell and stem cell viabilities were assessed by FACS following additional staining with anti-CD34-FITC and PI.

For both CML and normal samples, the unstained stem cell viability (77-99%) was considerably higher than the unstained total cell viability (44-81%), suggesting that stem cells were less susceptible to damage by cryopreservation.

It had been documented previously that exposing cells to increasing laser power rendered them non-viable. Historically, during the development of staining protocols, exposure to laser power of 100mV was common. This was not a problem until researchers wanted to obtain viable sorted cells for further experimentation. Studies revealed that acceptable FACS profiles could be obtained using much lower settings and that cells could survive sorting on this basis (Shapiro HM 1981). For the experiments in this thesis, the laser power level for excitation of Hoechst was set at the minimum of 30mV using UV beads and verified with stained cells.

3.3.3 Sorting Using Hoechst and Pyronin Y

To obtain populations of viable stem cells in different phases of the cell cycle it was necessary to use the HST and Py fluorescent stains described, which allowed discrimination of cell populations whilst maintaining viability, functional capacity and proliferative potential. Cells in the G0 phase of the cell cycle were HST^{lo}/Py^{lo}, cells in the G1 phase were HST^{lo}/Py^{+} and those in the S/G2/M phase were HST^{bright}/Py^{+}. By combining these two stains with a stem cell marker (CD34) and PI as a viable marker, it was possible to obtain pure populations of viable stem cells in three phases of the cell cycle. However, the sorter was only capable of collecting two populations of cells simultaneously, which meant the third population was resigned to waste. For this reason most sorts were set up to collect two parameters only, G0 and dividing. Figure 3.7 shows the gating strategy used to sort the different fractions of the cell cycle. The HST and Py plot was gated on the viable, $CD34^{+}$ cells.

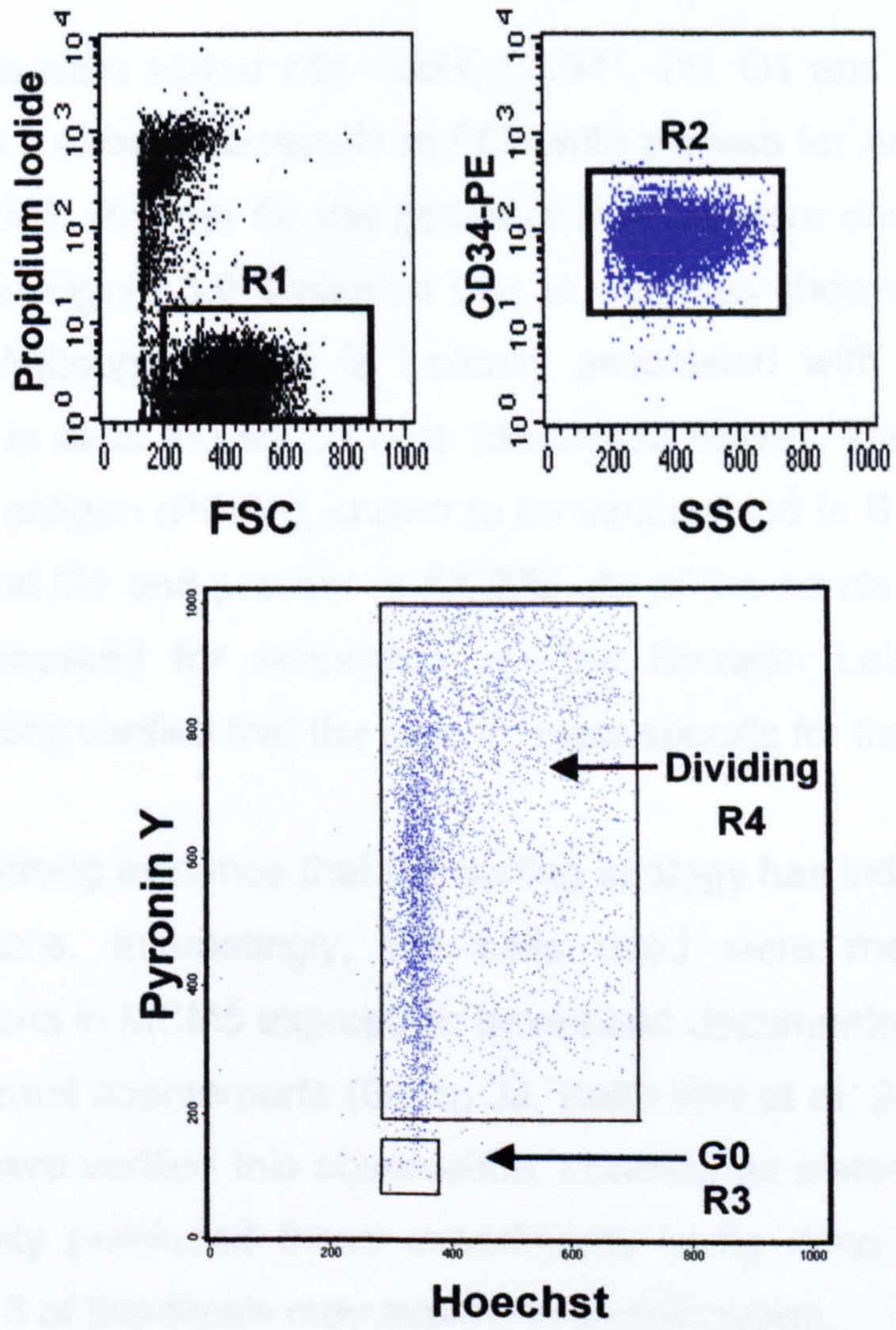

Figure 3-7 FACS gating strategy for isolation of viable quiescent and cycling stem cells.

Following overnight incubation in growth factor supplemented media, the cells were stained with HST, Py, CD34 and PI. A viable gate was set around the PI^- cells (R1) and a further gate set around the $CD34^+$ cells (R2). This combination of gates was used to set further gates on the G0 (R3) and cycling cells (R4).

3.3.4 Assessment of Success of Cell Cycle Stage Sub-Selection

It was not feasible to re-run sorted cells on the FACS to assess sort purity as the cells were collected in sheath fluid and would have effluxed the HST and Py dyes. Since the purity of the sort was operator controlled, it was necessary to verify the correct cell populations had been sorted. This was achieved by analysing the gene expression of sorted cells by PCR for genes specific to cell cycle position. For this experiment an additional gate was used to isolate the G1 population. It was not possible to commit any more than one CML sample to processing for PCR for

verification of sort purity, as cell numbers were prohibitive. Nor was it possible to repeat the PCR with a normal sample as these were in very limited supply.

The cells were sorted into viable, $CD34^+$, G0, G1 and S/G2/M fractions for PCR. Figure 3.8 shows the results of PCR with primers for Actin (control), CD34, PCNA and MCM5. Primers for the genes of interest were designed as described in the methods. Figure 3.9 illustrates that all samples showed a band for actin and for CD34. Although MCM5 is typically associated with proliferating cells, it was present in all of the sorted cells (discussed below). The band for proliferating cell nuclear antigen (PCNA), known to be synthesised in S phase, was clearly absent in G0 and G1 and present in S/G2/M. All of the bands were excised from the gel and processed for sequencing at the Beatson Laboratories. The results of sequencing verified that the primers were specific for the genes indicated.

This is strong evidence that the sorting strategy has indeed separated the relevant populations. Interestingly, the cells used were malignant (CML) cells and aberrations in MCM5 expression have been documented in cancer cells compared their normal counterparts (Going JJ, Keith WN et al. 2002). PCR on normal cells would have verified this observation, however as stated previously limited sample availability precluded these experiments being done. The results presented in chapter 6 of this thesis may explain this observation.

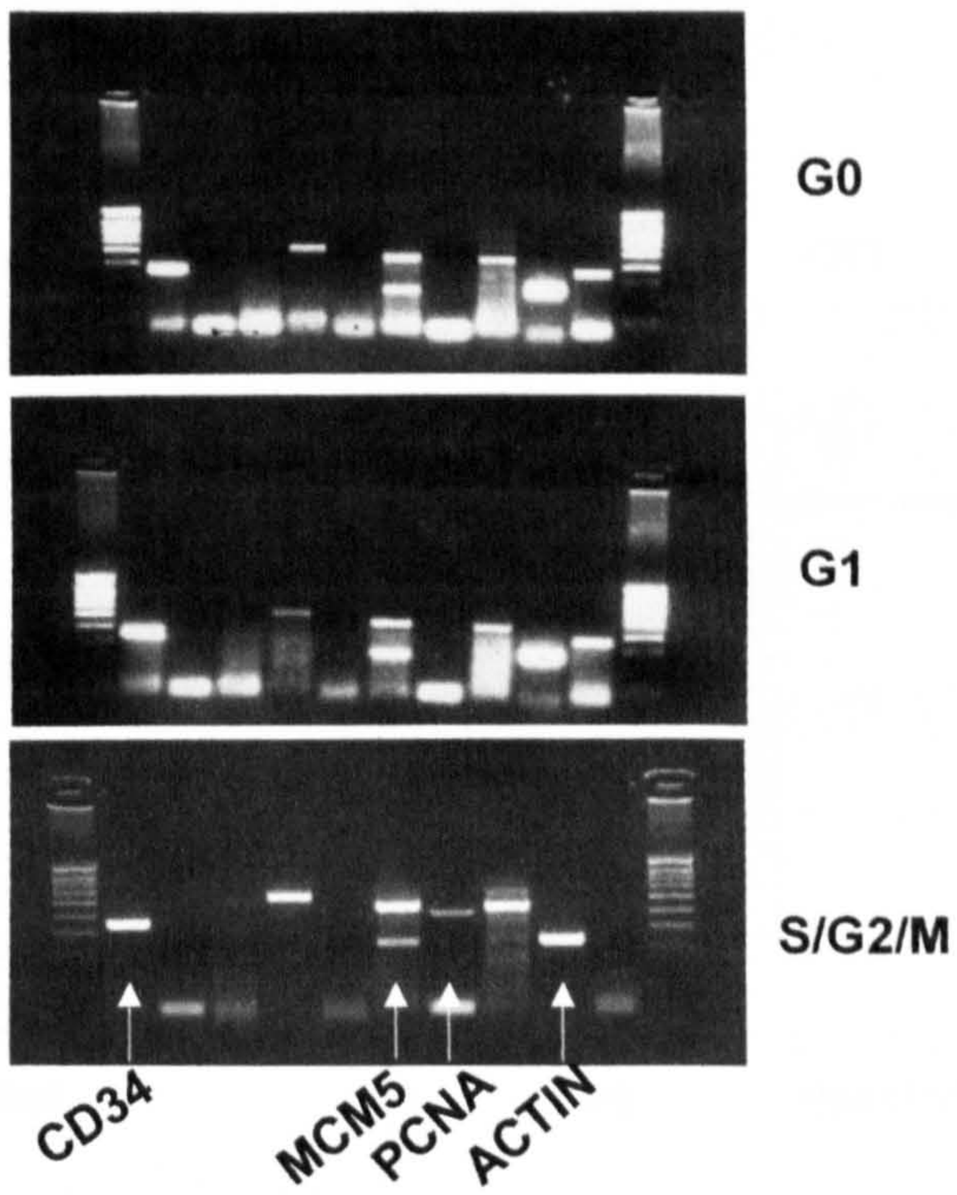

Figure 3-8 PCR of sorted cells.

The cells were sorted into G0, G1, and S/G2/M phases of the cell cycle as described in the text. PCR was performed with primers specific for the genes indicated.

3.3.5 Comparison of Relative Percentage of Cells in Different Cell Cycle Positions for Normal and CML Stem cells

It was noted during the course of staining and sorting for quiescent cells, that there were differences in the proportion of cells in the G0 and G1 phases of cell cycle between normal and CML samples. In particular the number of G0 cells sorted for the CML samples was always lower than for normal samples.

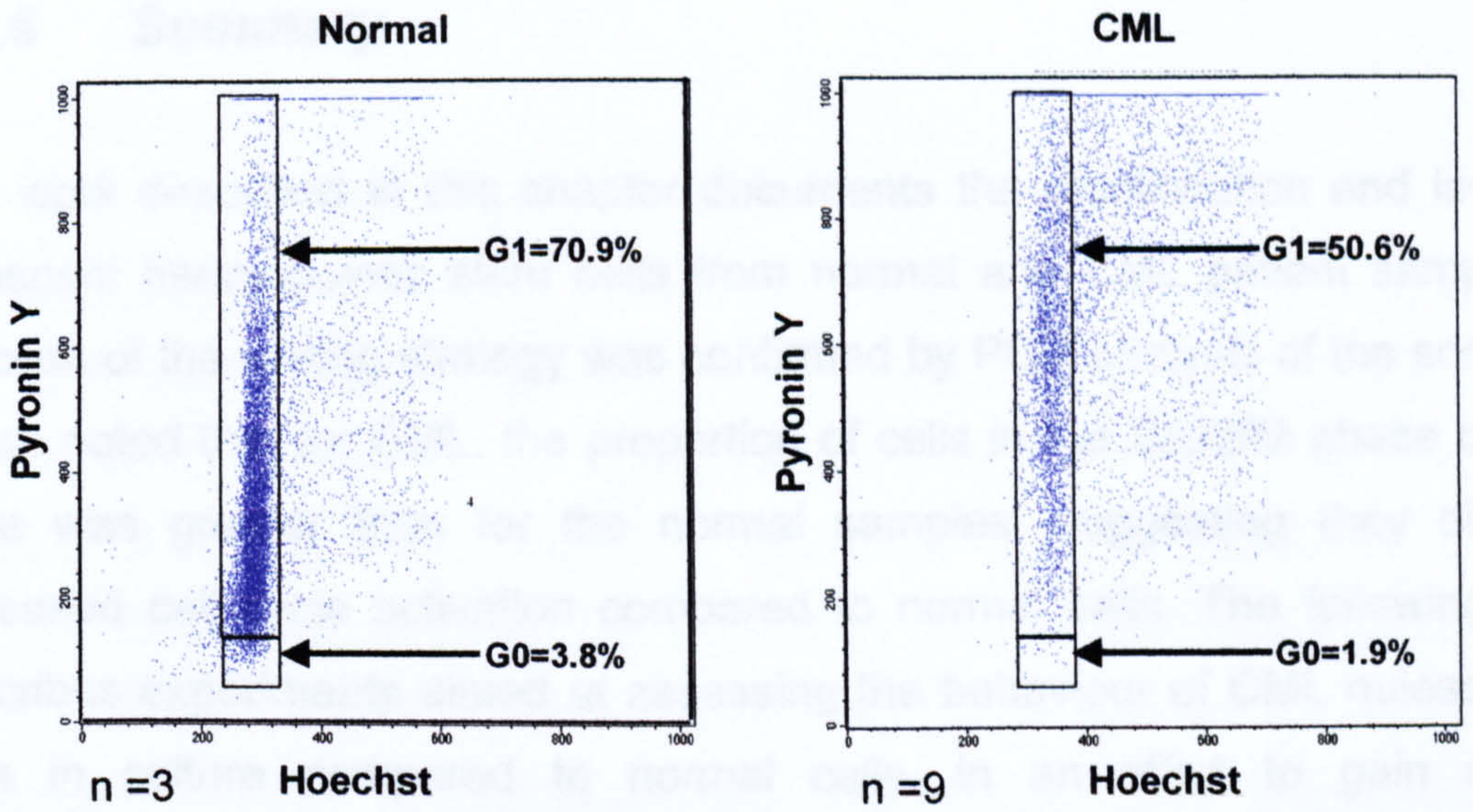

Figure 3-9 FACS plots showing the proportion of cells in G0 and G1 for normal and CML.

The plots are gated on the viable $CD34^+$ cells as described in the text. The percentages are the mean for all samples, n=3 for the normals and n=9 for the CML samples.

A number of normal and CML samples were compared to investigate this observation. Following an overnight incubation in a 5 growth factor cocktail, to enable recovery from cryopreservation, the cells were removed from plates or flasks and washed in PBS2% before staining with HST and Py as described previously. Gates were set around the viable $CD34^+$ cells and the percentage of cells in G0 and G1 compared. The numbers represent the mean of 9 CML samples and 3 normal samples. The number of quiescent cells i.e. those in G0 was significantly lower in the CML sample than in the normal sample, 1.9% compared to 3.8% ($p=0.04$). The difference in the percentage of cells in the G1 gate, 70% in the normal compared to 50% in CML, was also significant ($p=0.04$). These observations suggest that CML cells exhibit greater cell cycle activation than normal cells, or that the CML cells are 'primed' to go into division. The observation that a greater proportion of CML cells were in the G1 phase of the cell cycle compared to normal does not necessarily mean that they were cycling at a greater rate. These data give no information on the time taken to complete the cell cycle, merely that there are fewer CML cells in G0 and G1 compared to normal. Other studies have also documented that for CML $CD34^+$ cells, a greater number are in the S/G2/M phase of the cell cycle compared with normal $CD34^+$ peripheral blood stem cells. In addition, others have shown that CML cells do not cycle at a

faster rate than normal cells, and that this does not explain the increase in cell numbers observed for CML in chronic phase (Buckle AM, Mottram R et al. 2000).

3.3.6 Summary

The work described in this chapter documents the identification and isolation of quiescent haemopoietic stem cells from normal and CML patient samples. The success of the sorting strategy was confirmed by PCR analysis of the sorted cells. It was noted that for CML, the proportion of cells in the S/G2/M phase of the cell cycle was greater than for the normal samples, suggesting they display an increased cell cycle activation compared to normal cells. The following chapter describes experiments aimed at assessing the behaviour of CML quiescent stem cells in culture compared to normal cells, in an effort to gain a clearer understanding of the properties of CML stem cells.

Chapter 4 Results 2 – Comparison of Normal and CML Stem Cell Division Characteristics In-Vitro

4.1 Introduction

Previous work by Buckle et al (Buckle AM, Mottram R et al. 2000) has shown that CML cells do not divide at a greater rate than normal cells. In contrast, Kramer et al (Kramer A, Loffler H et al. 2001) have shown that CML $CD34^+$ cells display greater cell cycle activation than their normal counterparts with many more cells in S/G2/M. It remained a possibility that differences in the pattern of cell division within the stem cell population could shed some light on the abnormal cell behaviour exhibited by malignant cells. Having previously identified quiescent stem cells in both normal and CML samples, the aim of the work presented in this chapter was to further characterise the dynamics of the cell population by tracking the pattern of cell division in normal and CML stem cells under different conditions. It was also proposed that this approach could be used to monitor the division history of the cells in conjunction with their viability and stem cell status using CD34 expression as a stem cell marker.

4.2 CFSE for High Resolution Tracking of Cell Division

In order to follow the pattern of cell division in culture, it was necessary to devise a strategy that would allow discrimination of the number of cell divisions together with stem cell status in each division. Monitoring viability of the cells as they progressed through each division was necessary in order to obtain information on the proliferative status of the culture. A method of specifically tracking cell division in lymphocytes was developed by Lyons et al in 1994 (Lyons AB and Parish CR 1994) using the fluorescent stain CFSE (carboxyfluorescein diacetate succinimidyl ester). CFSE is a non-polar molecule that passively enters cells where it is converted to a reactive dye by non-specific esterases. The amine-reactive coupling of CFSE to cellular proteins results in stable long-term intracellular retention. Thus, when the cell divides each daughter cell will have exactly half of the fluorescence of the parent cell. The effect is permanent, fluorescent, intracellular staining that can be used to track cell division over a period of time. Li et al (Li X, Dancausse H et al. 2003) have shown, using mixtures of stained

human and unstained rat cells in co-culture, that no dye leaks from stained cells and the fluorescence intensity of the undivided cells remains constant. These observations confirm the integrity of this technique for identification of undivided cells. Previous protocols have used a 5μM concentration of CFSE, which was highly fluorescent, allowing the cells to be monitored over a period of time. The disadvantage of such a high concentration of CFSE is that it makes compensation with other fluorescent dyes very difficult, and as monitoring of stem cell status and viability were an integral part of this study certain modifications to the protocol were necessary. Reducing the concentration of CFSE to 1μM gave adequate cell staining but allowed FACS compensation with other dyes, for example CD34-PE. As the cells of particular interest in this study were the undivided ones i.e. the most brightly CFSE stained, it was important that compensation could be achieved at the highest concentration of CFSE. When utilised with a sorting strategy to enhance resolution (described in detail in 4.4), the peaks of cell division could be clearly distinguished. By combining CFSE with cell surface markers such as CD34, this strategy could yield data unobtainable in any other way. It should be emphasised that the undivided cells identified by CFSE staining are not necessarily quiescent as recognised by HST and Py staining in the previous chapter, since their cell cycle position cannot be identified using this labelling technique.

4.3 The Effect of CFSE Staining on Cell Viability

Although higher concentrations of CFSE than the one proposed had been used previously with no deleterious effect on cell viability (Li X, Dancausse H et al. 2003), it was essential to establish that, in this system, cell viability was not adversely affected by the staining protocol. To this end stem cell enriched samples, from either normal donors or CML patients, were recovered from frozen and stained with 1μM CFSE for 10minutes, before washing in PBS/2% and incubating in culture medium containing a 5 growth factor cocktail as described in the methods. Following an overnight incubation, to allow excess stain to leach out, cells were recovered from petri dishes and further stained with PI as an indicator of viability. The total cell viability was measured by gating on the PI^- population. If the samples used in the experiments were >94% (94-98.6%) $CD34^+$, it was not normally a requirement to set a $CD34^+$ gate for the first sort, as all of the $CD34^+$ cells were within the viable gate following overnight incubation. The cells which

failed to recover from cryopreservation, tended to be the $CD34^-$ cells. An example of the staining and gating strategy is shown in figure 4.1. The FACS plots show the viable PI^- cells in (A) gated in R1, which were further gated on the $CD34^+$ cells in R2 shown in (B). The histogram in (C) illustrates both the unstained and $CFSE^+$ cells gated on R1 and R2, thus $PI^-/CD34^+$. The histogram plot in (C) also shows the markers L (left) and R (right), representing the left and right sorting gates used in CFSE sort 1.

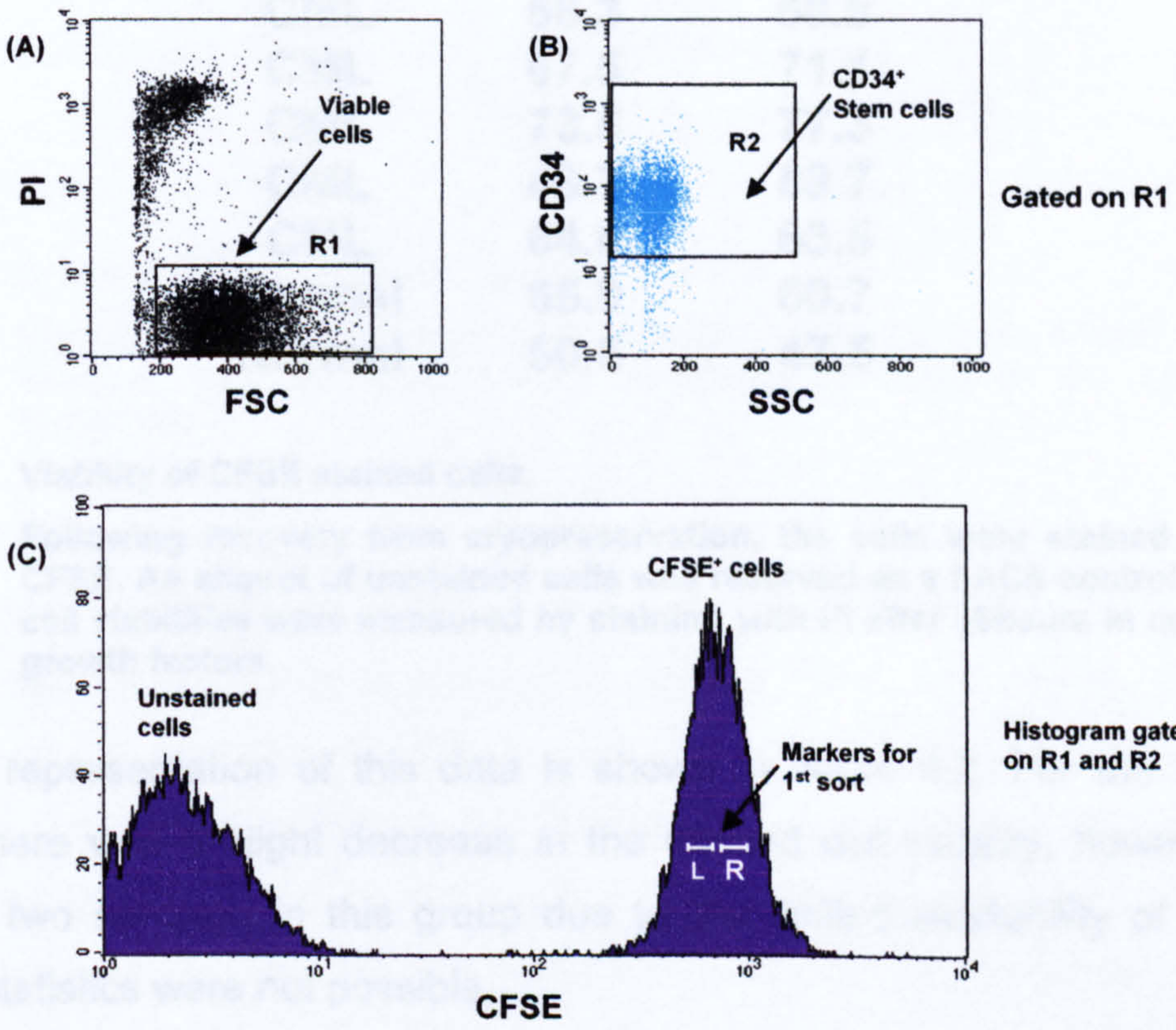

Figure 4-1 FACS gating strategy for first CFSE sort.

FACS plots showing the gating strategy used in the first CFSE sort. The viable PI^- cells are shown in R1 (A). The $CD34^+$ cells, which are already gated on the viable cell population, are contained in R2 (B). The histogram plots shown in (C) indicate the position of the unstained control cells and the CFSE positively stained cells. The markers labelled L (left) and R (right) show the sorting gates used to obtain $CFSE^+$ homogenously stained cell populations. If the percentage of $CD34^+$ cells was less than 95%, a combination of both R1 and R2 were used.

The stained and unstained populations shown on the histogram plot were gated on the viable (PI^-) cells. Table 4.1 shows the total cell viabilities from both normal and CML cells stained with CFSE, following an overnight incubation in 5 growth factor medium. Comparing 10 unstained and stained CML samples there was very little difference between them, with 7 out of 10 showing a slight increase following CFSE staining. The differences in viability were not statistically significant ($p=0.3$).

The small differences in the stained cells were most likely due to the washing steps following staining, which removed some of the dead cells.

	Unstained %Viable	CFSE %Viable
CML	54.5	59.4
CML	59.5	53.4
CML	75.6	75.4
CML	62.2	65.9
CML	58.8	63.6
CML	58.3	58.8
CML	67.5	71.1
CML	73.5	77.3
CML	48.7	52.7
CML	64.6	63.5
Normal	65.9	60.7
Normal	50.6	47.5

Table 4-1 Viability of CFSE stained cells.

Following recovery from cryopreservation, the cells were stained with 1µM CFSE. An aliquot of unstained cells was reserved as a FACS control. The total cell viabilities were measured by staining with PI after 16hours in culture with growth factors.

A graphic representation of this data is shown in figure 4.2. For the 2 normal samples there was a slight decrease in the stained cell viability, however there were only two samples in this group due to the limited availability of material, therefore statistics were not possible.

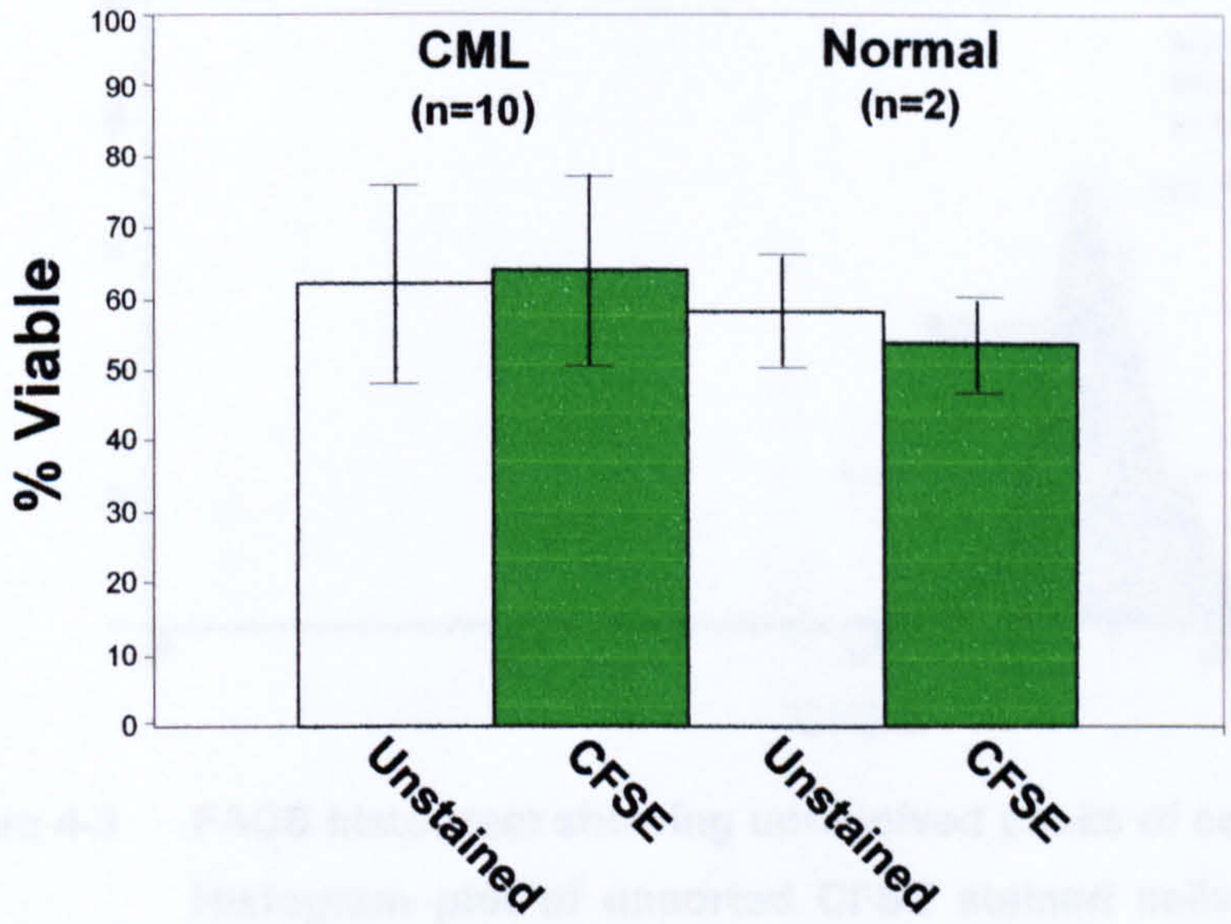

Figure 4-2 Graph of CFSE viabilities for normal and CML.

Viabilities of CFSE stained and unstained cells, for both normal and CML samples. The percentages were calculated by FACS on the basis of PI exclusion.

If the cells were placed in culture at this stage and allowed to proliferate cell divisions could be identified, but due to overlap of the CFSE peaks shown in figure 4.3, it was difficult to determine where one division began and ended. This made calculation of the numbers of cells in each division unfeasible, and it was not possible to set sorting gates on cell peaks in this instance. It was therefore necessary to develop a sorting strategy to enhance the resolution of the peaks of cell division, allowing more data to be obtained from these experiments.

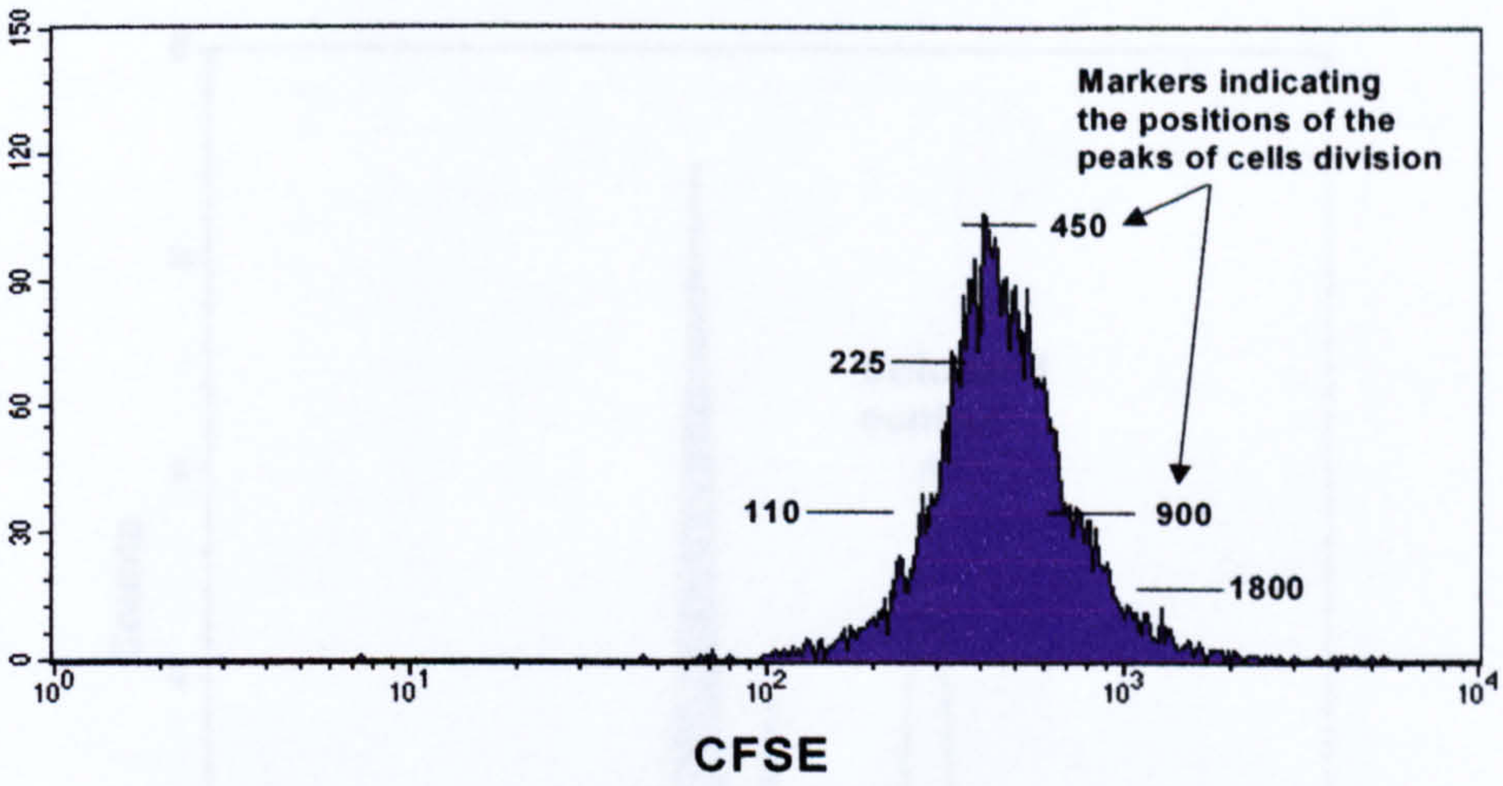

Figure 4-3 FACS histogram showing unresolved peaks of cell division.

Histogram plot of unsorted CFSE stained cells after 3 days in culture with growth factors. The histogram is gated on the viable $CD34^+$ cells with markers showing the position of the peaks and their values. Each peak has exactly half the fluorescence of the previous peak, however lack of resolution makes identification of the exact position of each peak difficult.

4.4 Identification of the Undivided Cells

As the main focus of the experiments contained in this work was the quiescent, undivided cells, it was important to be able to accurately identify the position of the undivided cell peak. Since the number of undivided cells could be so small that the first peak of division could be misinterpreted as undivided cells, accurate measurement was crucial. In order to precisely position the undivided peak it was essential to use the same cell population as the experimental one i.e. one left-sorted and one right-sorted (sort 1), to ensure the level of fluorescence was equivalent. A small number (typically $5x10^4$) of the left and right-sorted cells were incubated in the presence of 0.4µg/ml colcemid, a known inhibitor of cell cycle progression (Taylor E 1965). Figure 4.4 shows a representative example of CFSE sorted normal cells cultured for 3 days and gated on the viable $CD34^+$ cells This histogram plot illustrates the resolved peaks of cell division obtained following the first CFSE sort. The peaks of cell division are overlaid with the colcemid control from the same cell population. This clearly demonstrates the position of the undivided cells and allows a further markers to be set. Colcemid controls were included for each cell population (left and right-sorted) for every experiment.

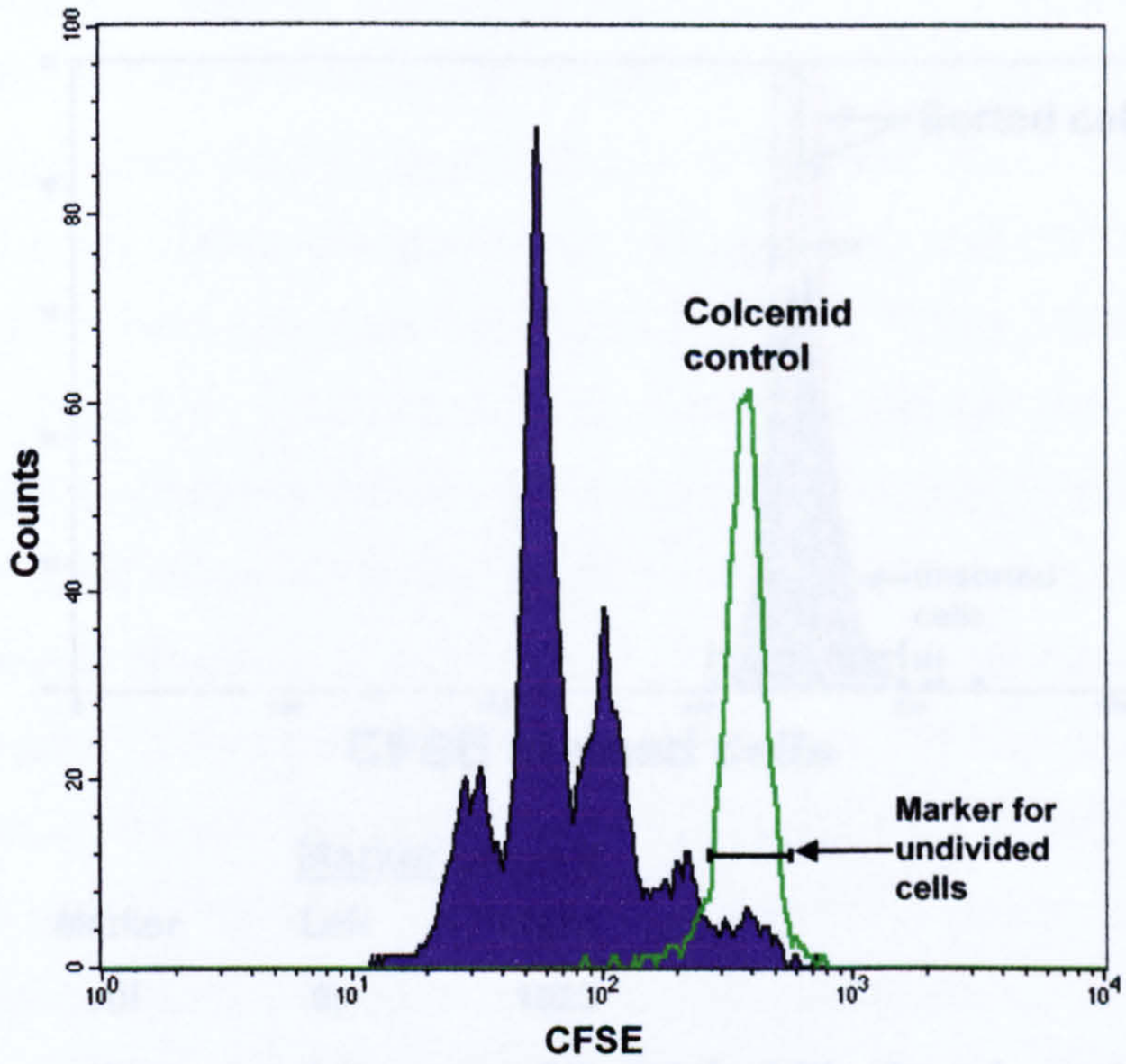

Figure 4-4 Histogram of cell division peaks and colcemid control.

An example of the peaks of cell division obtained after 3 days in culture, following CFSE staining and sort 1. The histogram is gated on the viable $CD34^+$ cells. The peak shown in green represents sorted cells incubated in the presence of 0.4µg/ml colcemid to prevent further cell division. The colcemid control allows accurate identification of the undivided cell population.

4.5 Sorting Strategy to Allow High Resolution Tracking of Cell Division

In order to gain the maximum amount of information from these experiments it was necessary to devise a method which would allow calculation of the numbers of cells in each division together with their stem cell status. As can be seen in figure 4.5 when cells were stained with CFSE a relatively broad spectrum of staining was observed and as detailed in section 4.3, further culture of these cells gave indistinguishable peaks of cell division. By reducing the width of the peak i.e. by sorting a homogenously CFSE-stained population of cells, the subsequent peaks of cell division were enhanced. To achieve this, two very narrow channels (19-22 channel widths) were sorted left and right, and kept separate throughout subsequent culture. The channel widths were set by the operator using the FACS sorter software. Figure 4.5 shows the resultant peaks when the sorted cells were re-analysed; the figures in the table represent the channel widths for each marker.

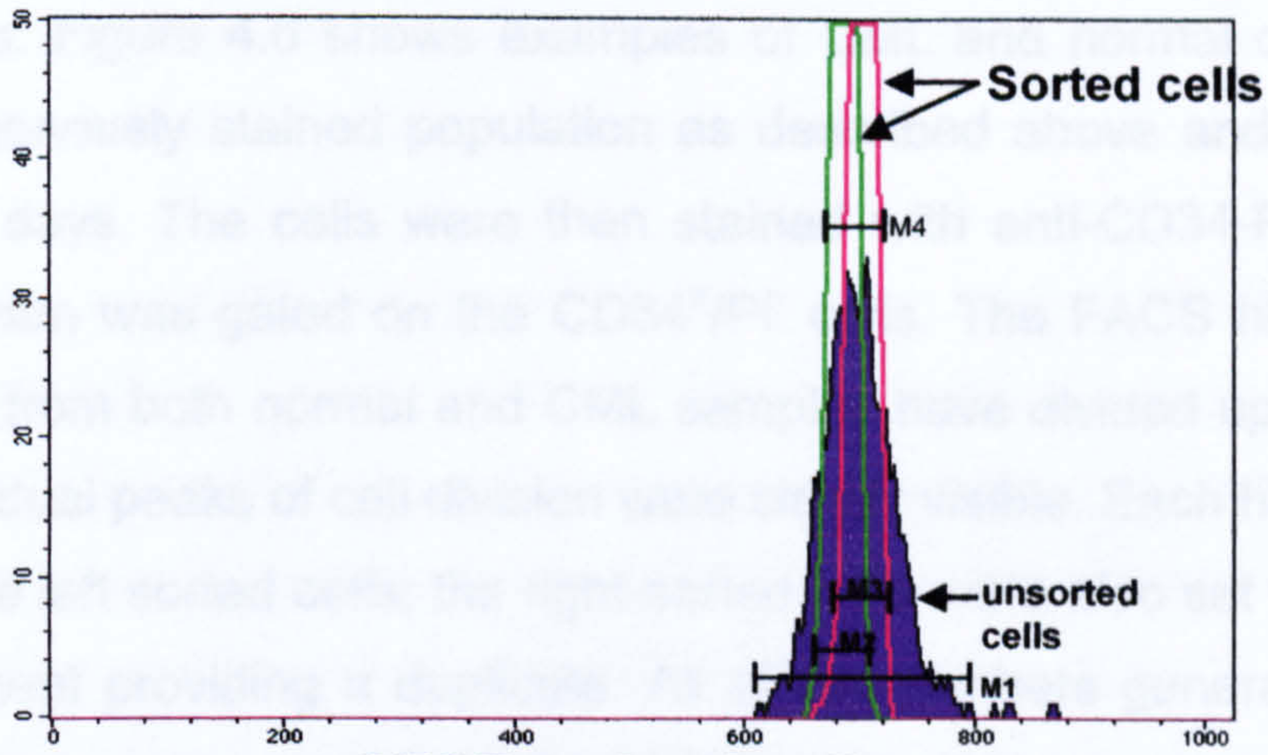

Marker bounds

Marker	Left	Right	
All	0,	1023	
M1	611,	797	total width of peak = 186 (channels)
M2	662,	710	width of L (sorted) = 48
M3	678,	727	width of R (sorted) = 49
M4	664,	729	total width of sorted = 65 (left + right)

Figure 4-5 Histogram showing analysis of sorted cells from first CFSE sort.

A histogram plot showing the widths of fluorescence peaks of unsorted and sorted cells as defined by the marker bounds. The unsorted cells are the solid blue peak and the left and right-sorted peaks are green and pink respectively. The marker bounds indicate the fluorescent channel limits in each peak.

The total width of the peak for unsorted cells was 186 channels, marker (M1). M2 (sorted left) and M3 (sorted right) were 48 and 49 channels respectively. Although the markers for sorting were set around 20 channels, in practice the resultant sorted channel widths were wider. This was due to the mechanics of sorting and the settings applied. The total width of the two sorted peaks (M4) was 65 channels, which is considerably less than the starting width of 186 channels. If the channel widths were set beyond the limits described, the resolution in the peaks of cell division was not observed. In terms of recovered cell numbers, the 2-sorted peaks amounted to approximately 40% of the available viable stem cells. To obtain enough sorted cells for further culture it was necessary to sort around 3-4x10^7 cells in total. Taking the cell viabilities into account the number of sorted cells recovered was 4.5-7.8x10^6 in total for both peaks.

Having successfully achieved the desired resolution in the peaks of cell division, this technology was utilised to investigate the proliferative potential of normal and CML G0 cells. Figure 4.6 shows examples of CML and normal cells first sorted into a homogenously stained population as described above and then placed in culture for 3 days. The cells were then stained with anti-CD34-PE and PI. The CFSE histogram was gated on the $CD34^+/PI^-$ cells. The FACS histograms show that the cells from both normal and CML samples have divided up to 5 times and that the individual peaks of cell division were clearly visible. Each histogram shown represents the left sorted cells; the right-sorted cells were also set up in culture for each experiment providing a duplicate. All of the numbers generated from these experiments were a mean of the left and right sorts. M1 represents the undivided cells as established with the colcemid control cells, and M2-M6 the peaks of cell division. The small numbers of cells to the right of the undivided cells in the normal example were probably doublets, however without access to doublet discriminator software it was not possible to confirm this.

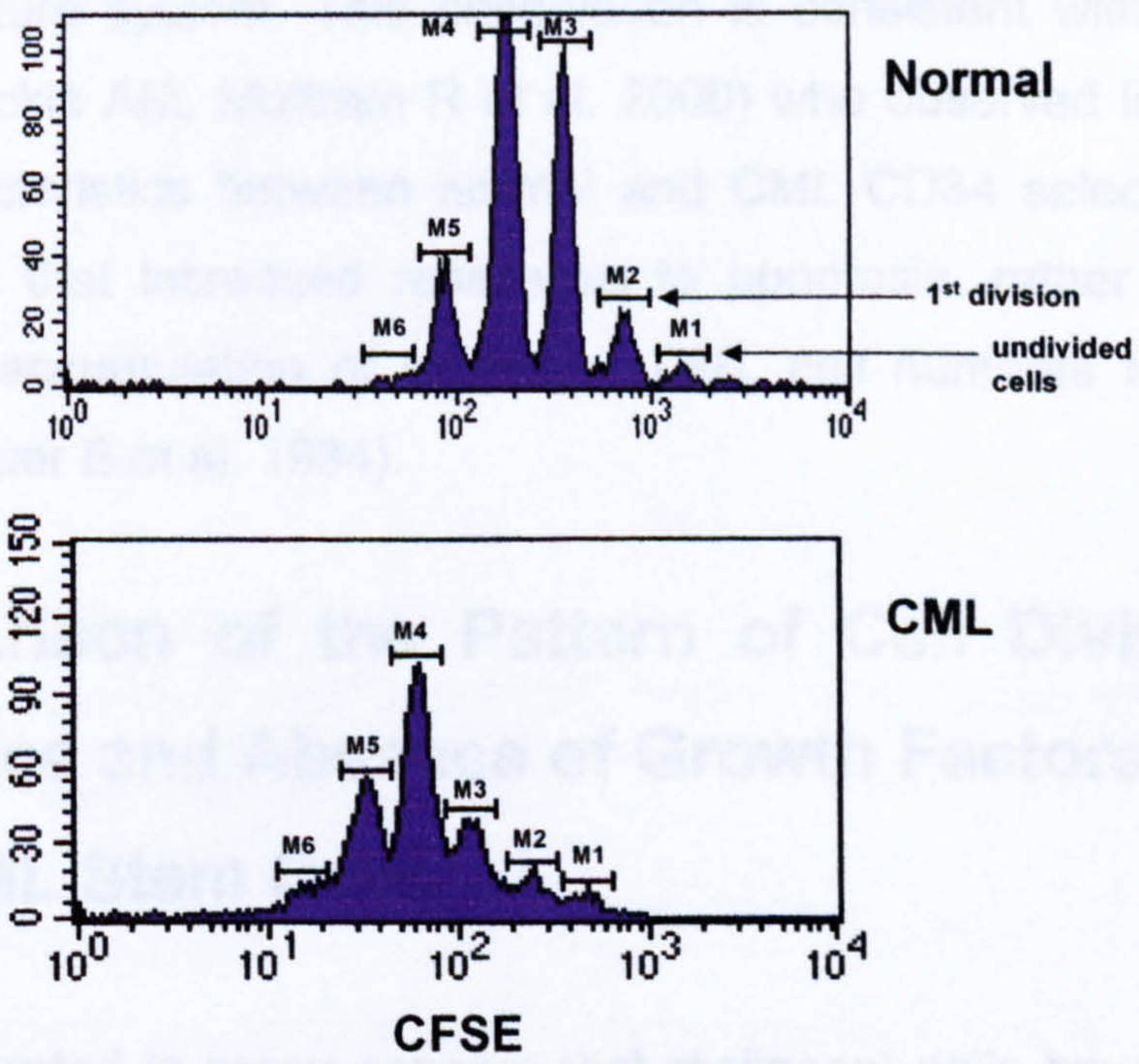

Figure 4-6 CFSE histograms showing resolution of peaks of cell division for normal and CML cells.

Histogram plots showing the peaks of cell division obtained following sort 1 and 3 days in culture with growth factors for a normal and CML sample. The histograms are gated on the PI^-CD34^+ cells. The markers show the position of each peak including the undivided cells (M1) identified by the colcemid control.

The precise identification of the division history in a population of cultured cells provides data unavailable otherwise. If the number of cells used to establish the

culture is known, as well as the number of cells recovered at the end point, it is possible to calculate the proportion of input cells recovered in each peak of cell division. In combination with a stem cell marker such as CD34 it is also possible to gain information on the stem cell status in each division under different conditions.

For both normal and CML examples, shown in figure 4.6, a population of cells in M1 i.e. undivided, is clearly visible. This indicates there is a degree of heterogeneity in the starting population with some of the cells "primed" to go into division under appropriate stimuli. Also in both examples, there are cells that have undergone different numbers of divisions (M2-M5) suggesting that there may be cells responding differently to the growth factor conditions in the culture or to products secreted by other cells. For both normal and CML, most of the cells appear to be in M3, M4 and M5, which show the largest peaks. The cells in both cultures have divided up to 5 times suggesting a division time of around 12 hours. It is interesting that the number of cell divisions is similar for both normal and CML, indicating that the CML cells are not dividing at a greater rate than the normal ones in this culture system. This observation is consistent with the findings of Buckle et al (Buckle AM, Mottram R et al. 2000) who observed little difference in cell cycle characteristics between normal and CML CD34 selected cells. It has been suggested that increased resistance to apoptosis, rather than faster cell division, allows accumulation of excessive CML cell numbers in the circulation (Bedi A, Zehnbauer B et al. 1994).

4.6 Comparison of the Pattern of Cell Division in the Presence and Absence of Growth Factors for Normal and CML Stem Cells

It is well documented in many cancers that malignant cells have the capacity to proliferate in the absence of exogenous growth factors (Rodeck U, et al. 1993). The development of a method for tracking cell division in stem cells allowed comparison of the properties of normal and CML cells in vitro. CD34 selected cells, from both normal and CML samples, were recovered from frozen, stained with 1μm CFSE and incubated overnight in the presence or absence of a 5 growth factor cocktail containing IL-3, IL-6, G-CSF, hSCF and Flt3-L as described in the methods. The following day the cells were stained with anti-CD34-PE and PI before sorting into two narrow channels as described above. Cells were then

incubated, again in the presence or absence growth factors, for a further 3 days. 1-5x10^4 cells from each of the sorted populations were incubated in the presence of 0.4µg/ml colcemid as described. After the 3day culture period, the cells were stained with anti-CD34-PE and PI and sorted (sort 2) into divided and undivided populations. Figure 4.7 shows normal cells (as in fig 4.6) in the presence and absence of added growth factors.

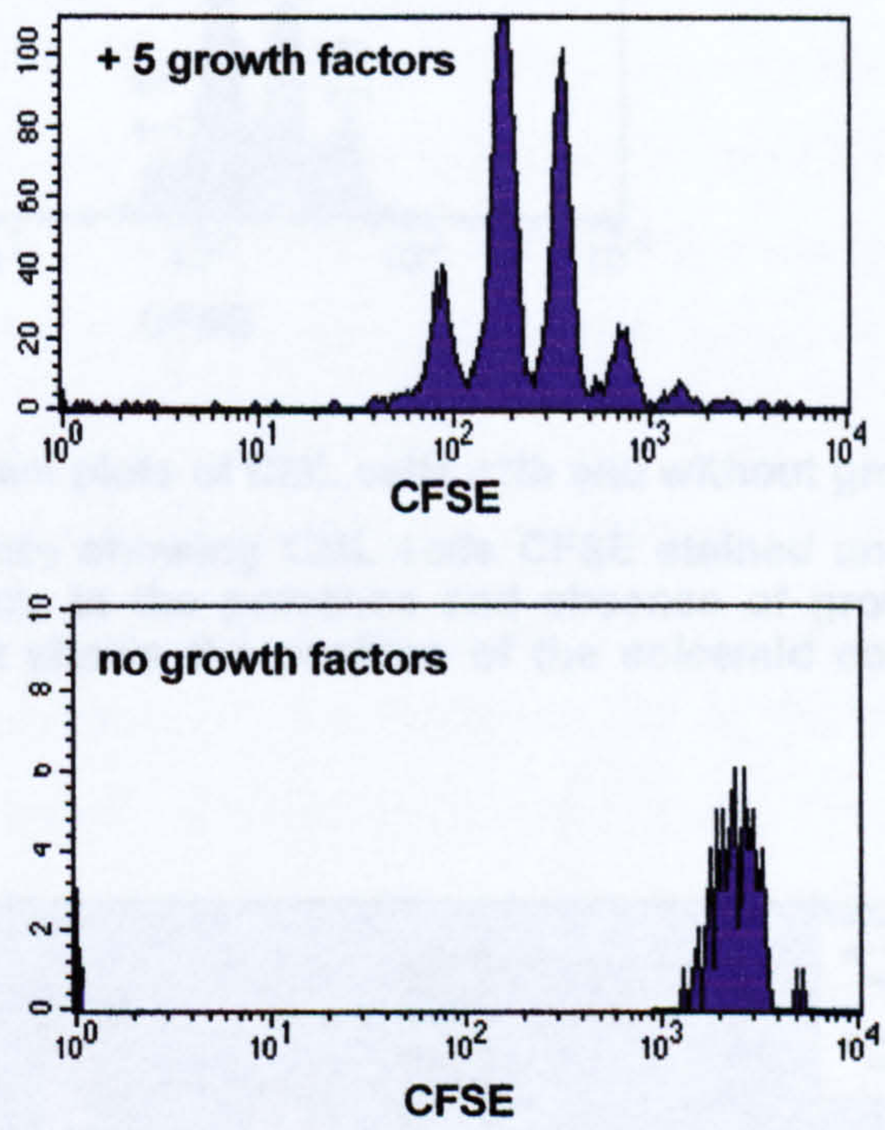

Figure 4-7 CFSE histogram plots of normal cells with and without growth factors.

Histogram plots of normal CFSE stained, sorted cells, following 3 days in culture in the presence or absence of growth factors. The histograms are gated on the PI^-CD34^+ cells.

The histogram, which is gated on the viable stem cells, shows that in the presence of growth factors, normal stem cells were able to undergo up to 5 divisions in the 3-day time period. However, in the absence of growth factors, normal cells were unable to divide and only a small undivided peak, representing the remaining viable stem cells was observed.

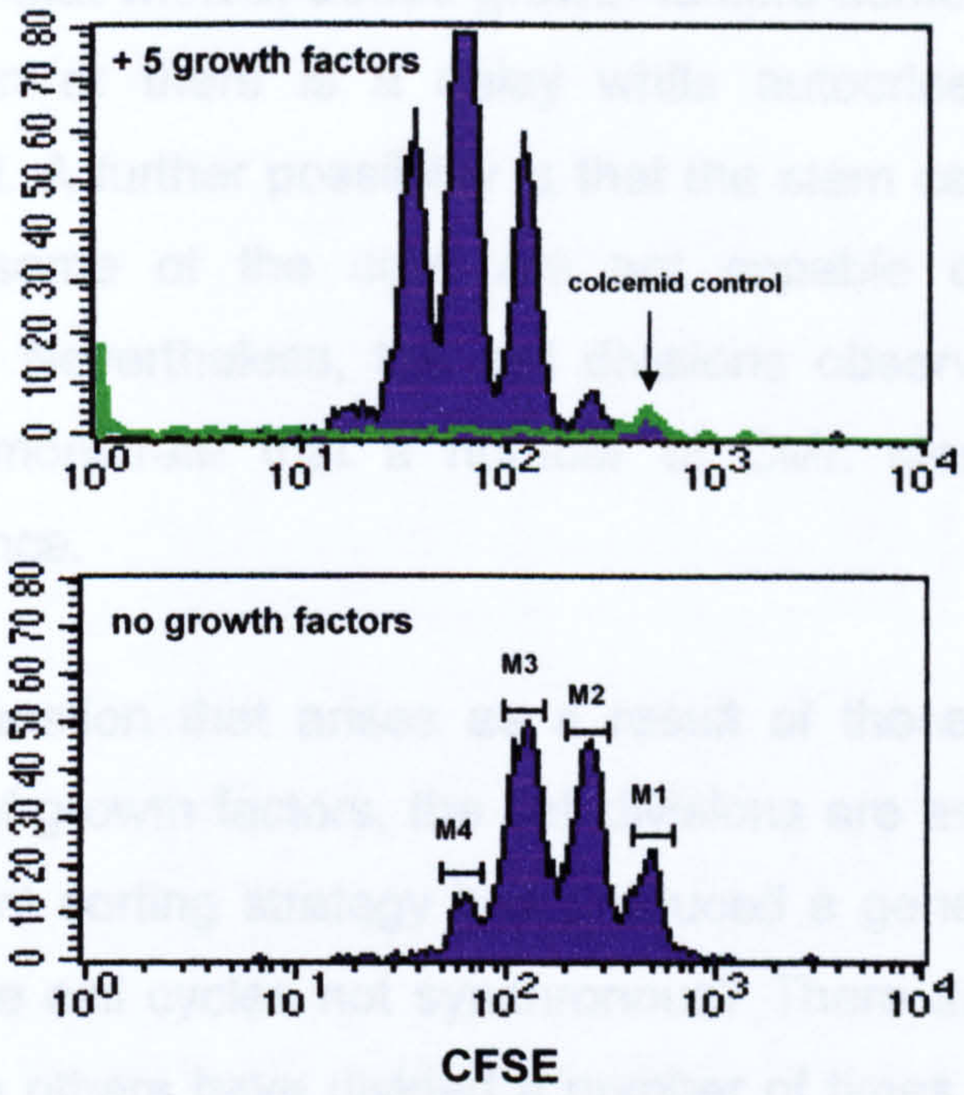

Figure 4-8 CFSE histogram plots of CML cells with and without growth factors.

Histogram plots showing CML cells CFSE stained and sorted followed by 3 days in culture in the presence and absence of growth factors. The green overlaid peak shows the position of the colcemid control i.e. the undivided cells.

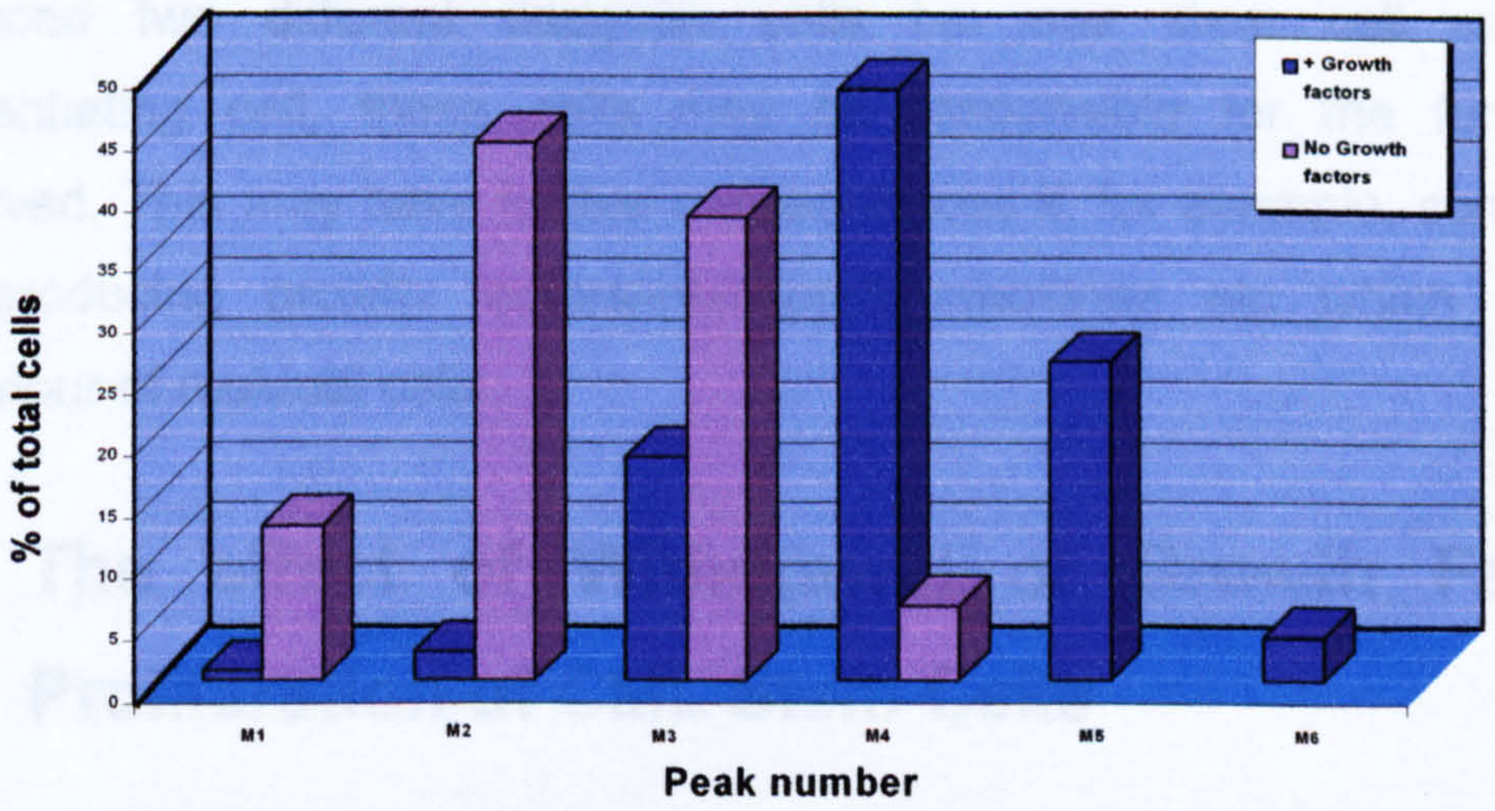

Figure 4-9 Graph of the percentage of cells in each peak for CML cells with and without growth factor

Graphic representation of the percentage of CML cells in each peak in the presence and absence of growth factors, as shown in figure 4.8.

In the CML example shown in figure 4.8, the stem cells have divided a comparable number of times in the presence of growth factors as the normal cells, and with similar kinetics. In contrast, in the absence of growth factors, the CML cells have been able to divide up to 3 times as shown by the markers M2-M4, demonstrating growth factor independence. However, the percentage of cells in M1 is higher in the absence than in the presence of growth factors as shown in figure 4.9,

suggesting that without added growth factors some of the cells either fail to enter cell division or there is a delay while autocrine growth factor production is established. A further possibility is that the stem cell population is heterogeneous and that some of the cells are not capable of growth factor independent expansion. Nevertheless, the cell divisions observed in the absence of growth factors demonstrate that a number of CML stem cells exhibit growth factor independence.

Another question that arises as a result of these observations, is why, in the presence of growth factors, the cell divisions are asynchronous. In other words, if the stringent sorting strategy has produced a generally homogenous population, why are the cell cycles not synchronous? There are cells that have divided only once, while others have divided a number of times. Apart from the possibility that the cell population exhibits a significant degree of heterogeneity, another explanation may be that as the cells divide they respond to growth factor stimuli in a variety of ways. The implication being, that the population is becoming more heterogeneous with every division. For instance, all of the cells in M2 must have come from M1 so if some of the cells have gone through one division which has produced two different daughter cells i.e. one stem cell copy and one differentiating cell, these cells may be responsible for the further divisions observed. This may have further consequences if, for example, some of the cells are producing growth factors/inhibitors/chemokines etc which influence the behaviour of residual cells.

4.7 The effect of Withdrawal of Growth Factors on Proliferation of CML Stem Cells

The ability of CML stem cells to proliferate in the absence of exogenous growth factors could have implications for disease progression. If cells are able to thrive outwith the stem cell niche, and proliferate autonomously, then the capacity for maintenance of disease is escalated. In an effort to gain some understanding of the CML cells capability for proliferation, the culture period was extended to 12 days. It was possible that prior to culture in conditions of growth factor starvation, the cells had gained mitotic signals from previous in vivo stimuli. By culturing cells for a longer time period and monitoring the behaviour of cells that had arisen

within the culture, a clearer picture of the extended proliferative capacity of the cells could be ascertained.

	Fold amplification (mean)
+GF	
Day 3	18.2 ± 7
Day 6	107 ± 41
Day 12	233 ± 47
-GF	
Day 3	7.6 ± 4
Day 6	6 ± 4
Day 12	32 ± 19

Table 4-2 Table of mean fold amplification for CML cells with and without growth factors.

The table shows the mean fold amplification of CML cells cultured in the presence and absence of growth factors over a period of 12 days. The fold amplification was calculated as the total viable cell output proportionate to the input cell number. The figures represent the mean of 5 CML samples ± SEM.

While the CML stem cells were able to divide up to 4 times in the absence of growth factors in the 3 day time period, there was a reduction in the overall recovery of viable cells. It remained a possibility that the assay, at 3 days, was selecting cells able to proliferate without growth factor stimulation, but unable to sustain the culture beyond this time period. To address these issues the cells were cultured for 12 days, with viability and cell recovery assessed on days 3, 6, and 12, in the presence and absence of growth factors. Table 4.2 shows that in the presence of growth factors the mean total viable cell number increased by 18.2-, 107-, and 233-fold on days 3, 6, and 12 respectively ($p=0.06$ between days 3 and 6, $p=0.05$ between days 6 and 12). In the absence of supplementary growth factors the mean total viable cell number increased by 7.6-, 6-, and 32-fold on days 3, 6, and 12. The figures in this table represent the mean of 5 CML samples ± SEM based on an input number of $5x10^4$ cells per assay in 1ml medium. The figures did not achieve statistical significance in the absence of growth factors; $p=0.2$ between days 3 and 6, and $p=0.16$ between days 6 and 12, however there was considerable variation between patient samples, which is a consistent feature of CML. The slight fall in fold amplification on day 6 could be due to the death of cells that although Ph^+ may not be fully growth factor independent. There may be a lag period as the cells adjust to growth factor starvation either by producing autocrine growth factors or by circumventing the processes that require exogenous stimuli. By day 12 the fold amplification had increased to 32, demonstrating that growth factor independence is a typical characteristic of CML

stem cells and is in accordance with other published results (Pierce A, Spooncer E et al. 2002) (Witte O N 2001).

4.8 Expression of CD34 in CML Cells in the Presence and Absence of Growth Factors

Having observed significant differences in the proliferation of stem cells from CML patients in the presence and absence of growth factors, the level of CD34 expression was examined in these cultures. Clearly the stem cell status may well impact on their ability to maintain disease and is an important consideration for possible eradication of CML.

A detectable difference in CD34 expression was observed in the presence and absence of growth factors for the CML samples. Figure 4.10 illustrates, in this representative example, in the absence of growth factors, cells that divided up to 4 times retained high levels of CD34 expression, compared to cells undergoing division in the presence of growth factors. The difference in CD34 expression between the two sets of conditions was highly significant by division 3 (p=.009).

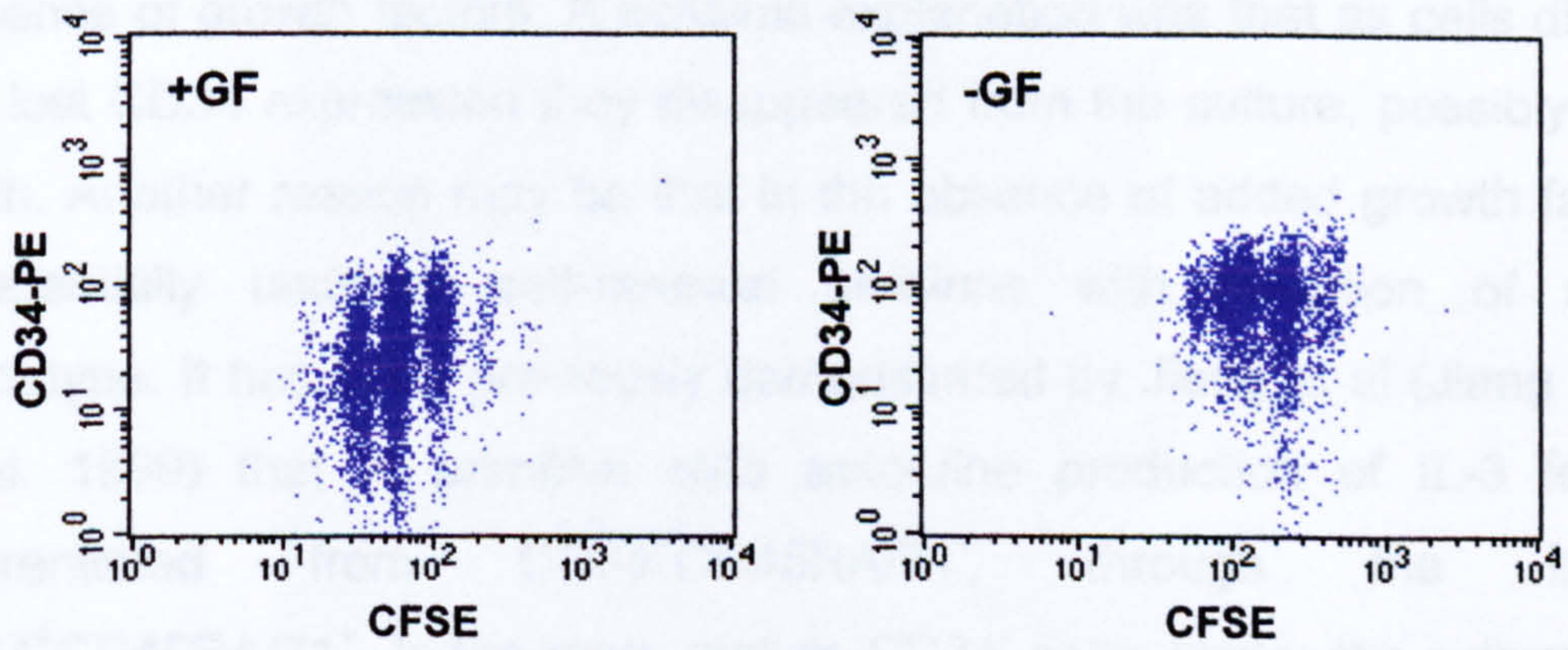

Figure 4-10 FACS plots of CFSE versus CD34 expression for CML cells with and without growth factors.

The plots are gated on the viable cells following 3 days in culture in the presence and absence of growth factors, after the first CFSE sort to enhance resolution of the peaks of cell division. The cells were stained with anti-CD34PE and PI and analysed by FACS.

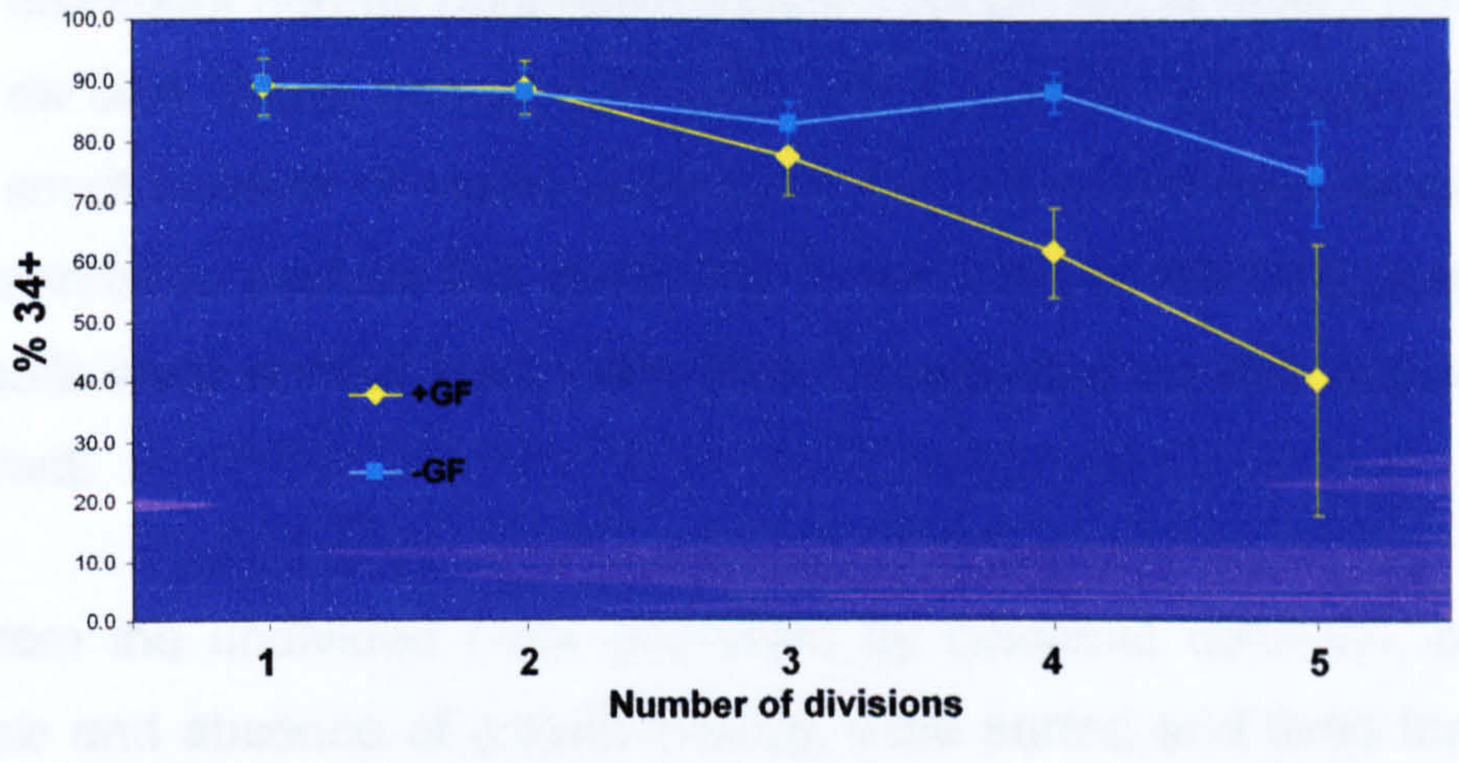

Figure 4-11. Graph of CD34$^+$ percentage versus peaks of cell division in the presence and absence of growth factors.

The graph shows the percentage of CML viable CD34$^+$ cells as a function of cell division. The cells were cultured for 3 days in the presence and absence of growth factors following the first CFSE sort, before being stained with anti-CD34PE and PI and assessed by FACS.

The graph in figure 4.11 shows the percentage of cells that remained CD34$^+$ for divisions 0-4, for CML cells cultured in the presence and in the absence of added growth factors. In the presence of growth factors the percentage of CD34$^+$ cells has fallen from 90 to 42%, whereas in the absence of growth factors the CD34$^+$ percentage was 75 after the same 4 divisions. This shows that the proportion of cells that retained CD34 expression was greater in the absence, than in the presence of growth factors. A possible explanation was that as cells differentiated and lost CD34 expression they disappeared from the culture, possibly due to cell death. Another reason may be that in the absence of added growth factors, cells preferentially undergo self-renewal divisions with retention of a primitive phenotype. It has been previously demonstrated by Jiang et al (Jiang X, Lopez A et al. 1999) that in primitive cells autocrine production of IL-3 fell as cells differentiated from CD34$^+$CD45RA/71$^-$, through the intermediate CD34$^+$CD45RA/71$^+$, to the more mature CD34$^-$ cells. Under the culture conditions described here, survival may perhaps depend on the retention of a primitive phenotype and possibly on autocrine production of growth factors.

4.9 Demonstration of Leukaemic Status in the Undivided cells

It was important to establish that the cells that survived in the undivided fraction were in fact leukaemic cells. It was a possibility that these cells could have been a

deeply quiescent normal population (known to co-exist in CML) that had failed to go into division. When normal cells were cultured in the absence of growth factors a very small number of viable stem cells was observed (see section 4.6) and it was essential to exclude this possibility in the case of the CML samples, since if these cells were normal stem cells, they represented no risk to the well being of the patient.

Cells from the undivided peak (identified by colcemid controls), cultured in the presence and absence of growth factors, were sorted and fixed for FISH. Figure 4.12 shows a representative example of the cells stained with the D-FISH probe for BCR-ABL and ABL-BCR. The detection of double signal i.e. recombinant genes established the presence of leukaemic cells, which were greater than 95% of the total sorted cells. The FISH picture is the D-FISH probe, which labels BCR, and ABL, red and green respectively. Two yellow fusion signals are observed on BCR-ABL and ABL-BCR. The double fusion signal reduces the chances of a false positive often observed when the chromosomes are in particularly close proximity. A positive is recorded only when two fusion signals are detected with both a red and green signal.

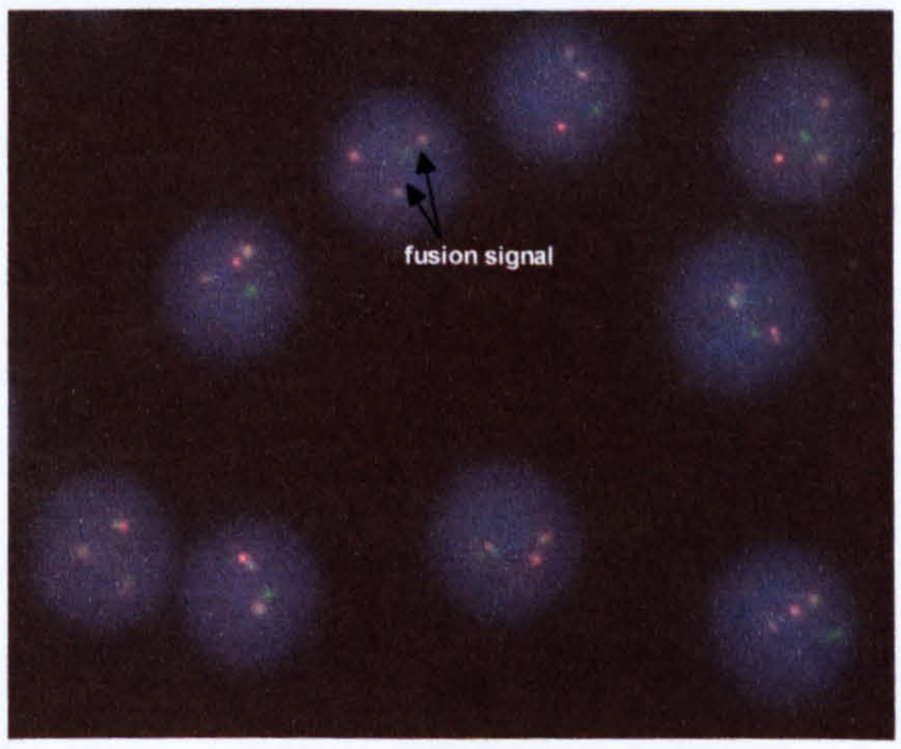

Figure 4-12 FISH analysis of undivided cells.

The cells have been cultured in the absence of growth factors for 3 days, before being sorted into divided and undivided populations and fixed for FISH.

4.10 Discussion

In conclusion, these experiments have confirmed that CML stem cells are clearly different from normal stem cells in their response to withdrawal of growth factors in this culture system. The ability of CML stem cells to divide in the absence of

exogenous growth factors is a feature of malignant cells that is not observed for normal cells. Although all of the CML samples had FISH performed prior to commencement of the experiments, it still remained a possibility that a very small number of normal stem cells were present in the CML population. The demonstration that normal stem cells were unable to divide in the absence of growth factors indicated that any cell division in growth factor deficient media was due to CML cell proliferation. It was possible that undivided cells in the CML population contained some normal cells, however sorting the undivided population and performing FISH confirmed that these cells were almost completely Ph^+ within the limits of detection. Therefore, proliferation in the absence of growth factors could be used as an indication of leukaemic cell division as opposed to normal cell division, not observed under these conditions.

Chapter 5 Results 3 – The Effect of STI571 on the Pattern of Cell Division in Normal and CML Stem Cells

5.1 Introduction

The molecular event that gives rise to the disease of chronic myeloid leukaemia is a reciprocal translocation between chromosomes 9 and 22 (Rowley JD 1973). The resultant product is a shortened chromosome 22, known as the Philadelphia chromosome, which in turn gives rise to the BCR-ABL oncogene (Shtivelman E, Lifshitz B et al. 1985). The fusion gene product is a p210 oncoprotein containing a constitutively activated tyrosine kinase (TK) that is responsible for the CML phenotype (Ben-Neriah Y, Daley GQ et al. 1986) (Lugo TG, Pendergast AM et al. 1990). The TK activity of normal c-ABL is tightly regulated and shuttles between the nucleus and cytoplasm, whereas BCR-ABL is exclusively cytoplasmic. It is the deregulated TK activity of bcr-abl, together with the cytoplasmic location, that are considered to be the defining elements in the CML phenotype (Lugo TG, Pendergast AM et al. 1990). The bcr-abl TK phosphorylates a number of cellular proteins, that in turn impact on a myriad of downstream targets involved in many cellular processes, including cell growth, stromal interaction and apoptosis (Salgia R, Li JL et al. 1997; Deininger M, Vieira S et al. 2000) (Gordon MY, Dowding CR et al. 1987). With a defined molecular target, it was feasible to design specific inhibitors of the bcr-abl TK activity, potentially abrogating its downstream effects with minimal consequence for normal cells.

As a result of synthesis and screening of a large number of small molecule TK inhibitors, Signal Transduction Inhibitor 571 (STI571) was identified as a potential therapeutic agent for CML (Buchdunger E, Zimmermann J et al. 1996). From results of clinical trials, STI was very effective in chronic phase, reducing white cell numbers to within normal limits in a few weeks. With relatively few side effects for the patient, STI was well tolerated with none of the debilitating toxicity observed with other forms of chemotherapy, largely due to its selectivity for leukaemic cells (Druker BJ, Tamura S et al. 1996). On treatment with STI, 97% of patients achieved a complete haematological response and 75% achieved a complete cytogenetic response (Kantarjian H, Sawyers C et al. 2002). However, the results

in blast crisis were less encouraging, with only transient haematological responses observed, and few molecular responses recorded (Hughes T, Kaeda J et al. 2002). There are now documented cases of relapse in patients who achieved a complete cytogenetic response on STI, which indicates that the disease progressed even in the presence of the drug (Sawyers CL, Hochhaus A et al. 2002). Using very sensitive Q-PCR it has been observed that patients achieving remissions with STI still have detectable BCR-ABL transcripts and that few patients have been negative on treatment (Hughes T, Kaeda J et al. 2002). These observations lead to the premise that a small population of cells was able to survive exposure to the drug and could possibly contribute to relapse at a later date. It was proposed that one source of surviving leukaemic cells could be the quiescent population, identified in previous experiments in chapter 4. The aim of the next set of experiments was to determine the effect of STI on the pattern of cell division in CML stem cells and to assess which cells, if any, survived exposure to the drug.

5.2 Effect of Different Concentrations of STI571 on the Growth of CML Cells in Culture

The objective was to determine the response of a number of CML samples to differing concentrations of STI. Since the clinically effective and achievable dose of STI in the initial trials was 1μM (Buchdunger E, Zimmermann J et al. 1996; Druker BJ, Tamura S et al. 1996; Peng B, Hayes M et al. 2004), this was the starting concentration used in these experiments. CD34 enriched stem cells from 5 CML patient samples were recovered from cryopreservation and cultured in the presence and absence of a 5 growth factor cocktail as described in the methods. The no growth factor arm was included as a selection for leukaemic cell proliferation, as normal cells were unable to proliferate under these conditions (as shown in chapter 4).

All of the samples were from patients at diagnosis and before clinical intervention, and all were >95% BCR-ABL positive by FISH. STI was added on day 0 at concentrations of 0, 1, 5 and 10μM. On days 3, 6 and 12 triplicate wells for each concentration were harvested, counted and assessed for viability by trypan blue exclusion. Figure 5.1 shows graphs of viable cell numbers on days 3, 6 and 12 in the presence and absence of growth factors, with increasing concentrations of

STI. In the presence of growth factors (figure 5.1(A)), the mean total viable cell number continued to increase over the 12 day period in the absence of STI. However, in the presence of 1, 5, and 10μM STI the total viable cell number was consistently lower than the control. In the absence of growth factors (figure 5.1(B)), or STI in parallel cultures, the total viable cell number was lower than in the presence of growth factors, but still showed an increase over time. The addition of STI at concentrations of 1-10μM reduced the viable cell number to a greater extent when no exogenous growth factors were present. In these cultures, the decrease in cell proliferation as a result of growth factor starvation and cell kill by STI were indistinguishable but the cumulative effect was a reduction in viable cell recovery.

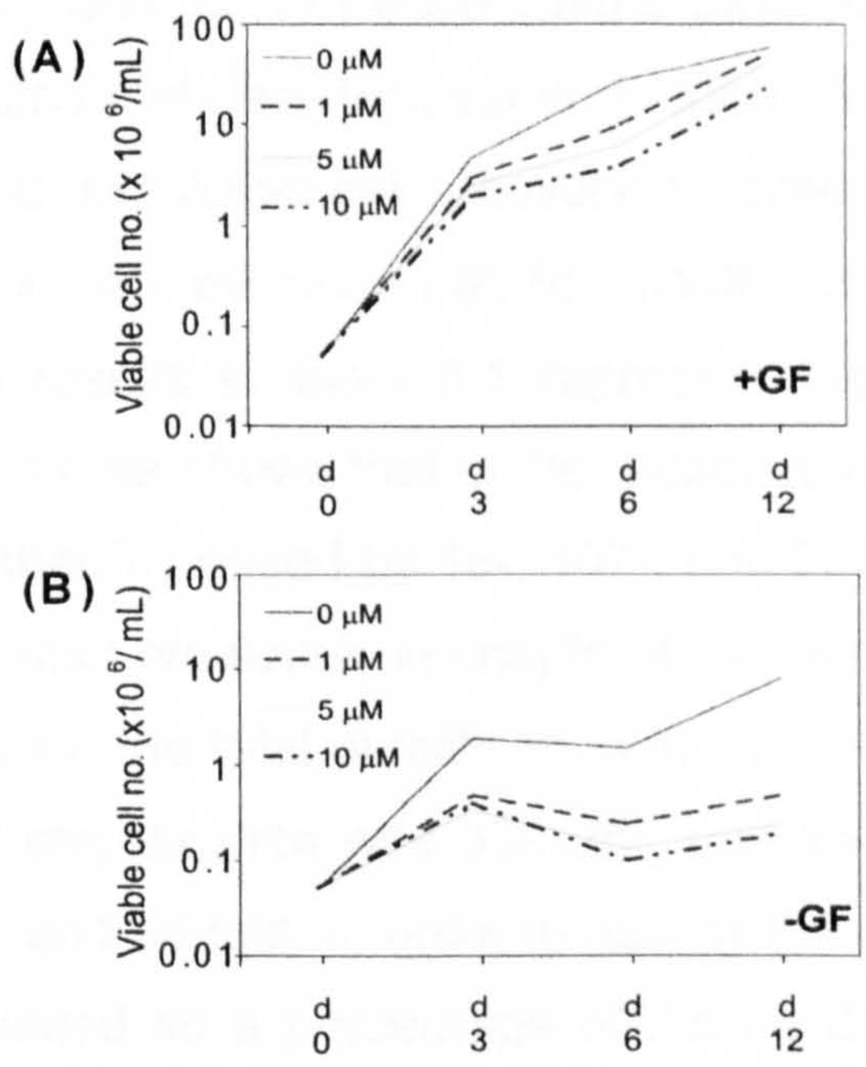

Figure 5-1 Graphs of viable cell number with concentration of STI over time.

The cells were cultured in the presence and absence of growth factors, with differing concentrations of STI. $5x10^4$ cells in 1ml of media were used to establish the cultures and the viable cell number assessed by typan blue exclusion on days 3, 6, and 12 as described in the text.

	0 µM STI571	1 µM STI571		5 µM STI571		10 µM STI571	
	Fold amplification (mean)	Fold amplification (mean)	% Recovery (mean)	Fold amplification (mean)	% Recovery (mean)	Fold amplification (mean)	% Recovery (mean)
+GF							
Day 3	18 ± 7	11 ± 4	62	7 ± 3	39	10 ± 6	55
Day 6	107 ± 40	38 ± 17	36	25 ± 12	23	15 ± 5	14
Day 12	233 ± 54	204 ± 74	87	172 ± 68	74	95 ± 43	41
-GF							
Day 3	7.6 ± 4	1.8 ± 0.6	24	1.4 ± 0.7	18	1.6 ± 1	21
Day 6	6 ± 4	1 ± 0.3	17	0.6 ± 0.3	10	0.4 ± 0.2	7
Day 12	32 ± 19	2 ± 1.4	6	1 ± 0.6	3	0.8 ± 0.3	2.5

Table 5-1 Table of fold amplification and viable cell recovery ±GF and ± STI. The figures are the mean of 5 CML samples ±SEM.

Table 5.1 shows the fold amplification for the same cultures ±STI and ±growth factors on days 3, 6, and 12. For each culture $5x10^4$ cells were added to 1ml of media in 24 well plates and each well set up in triplicate. On days 3, 6, and 12 the wells were harvested and viable cell recovery assessed by trypan blue exclusion. The fold amplification was calculated as the viable cell output proportional to the input number. The results in table 5.1 represent the mean of 5 CML patient samples ± SEM. The data shows that in the presence of growth factors, the mean total viable cell number increased by 18-, 107-, and 233-fold on days 3, 6, and 12 respectively (as detailed previously in chapter 4, section 4.7). The addition of 1, 5, and 10µM STI reduced the total amplification to 11-, 7-, and 10-fold by day 3. By day 6 the total cell amplification was 38-, 25-, and 15-fold and by day 12 it had reached 204-, 172-, and 95-fold. In order to assess the effect of STI, the viable cell recovery was calculated as a percentage of the no drug control. The maximum effect of STI was observed on day 6 when the overall recovery of viable cells was reduced to 36%, 23%, and 14% of control for 1, 5, and 10µM STI respectively. However, by day 12 the viable cell recoveries had improved to 87% and 74% of the control for 1 and 5µM STI. (p=0.048). For 10µM STI, although the viable cell recovery had improved from 14 to 41% this did not achieve statistical significance.

In the absence of growth factors and STI the mean total viable cell number increased by 7.6-, 6-, and 32-fold on days 3, 6, and 12 respectively (as detailed previously in chapter 4 section 4.7). In the presence of 1, 5, and 10µM STI the fold amplification of viable cells was reduced to 1.8-, 1.4-, and 1.6-fold by day 3, to 1-, 0.6-, and 0.4-fold by day 6, and to 2-, 1-, and 0.8-fold on day 12. The maximum

effect of STI was observed on day 12 when the overall viable cell recoveries were 6%, 3%, and 2.5% for 1, 5, and 10μM STI respectively.

In the presence of growth factors the mean viable cell recovery decreased between days 3 and 6 in the presence of 1, 5, and 10μM STI but increased between days 6 and 12 suggesting that a subset of Ph^+ cells were insensitive to STI at greater than clinically achievable concentrations. Figure 5.2 shows graphic representations of the recoveries of viable cells for each STI concentration ±growth factors. As stated above, the recovery of viable cells in the presence of growth factors and STI at each concentration showed a decline on day 6 and an increase between days 6 and 12. In the absence of growth factors, although the fold amplification increased between days 6 and 12 for each concentration, as shown in table 5.1, the recovery of viable cells continued to decrease over this time period. The data generated in these experiments suggested that a small population of cells were able to survive exposure to STI, at 10μM. It was proposed that the CFSE assay described in the previous chapter could be used to identify which cells were able tolerate exposure to the drug and would generate further information on the stem cell status.

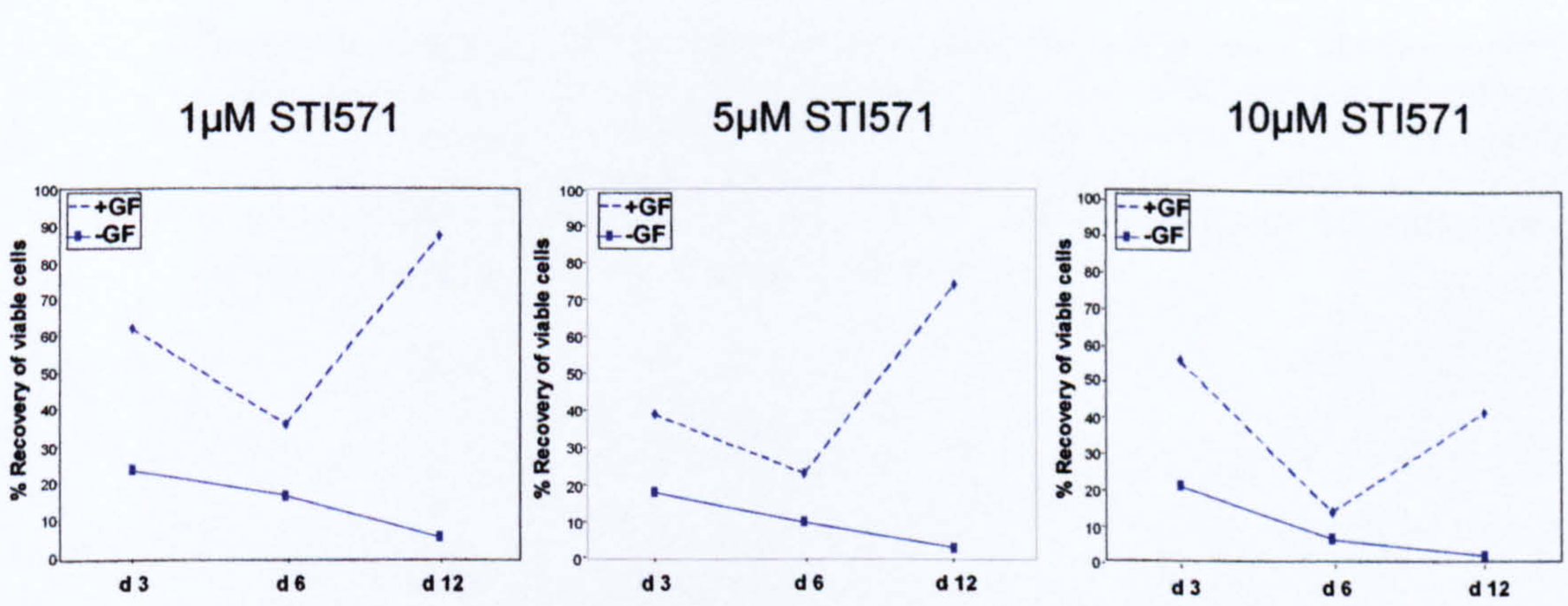

Figure 5-2 Graphs of cell recovery ±growth factors and ±STI.

The cells were cultured for 12 days as described in the text. The viable cell number was assessed on days 3, 6, and 12 by trypan blue exclusion. The viable cell recovery was calculated as a proportion of the input cell number ($5x10^4$) in 1ml of media ±GF. The results are the mean of 5 CML samples.

5.3 The Effect of STI571 on the Pattern of Cell Division in Normal and CML Stem Cells

As demonstrated in the previous chapters, quiescent stem cells could be identified in all CML samples; it was consequently hypothesised that these cells may be the

ones that survive exposure to STI. Figure 5.3 shows a schematic outline of the experimental strategy used here, and illustrates that following the first sort to enhance resolution of the peaks of cell division (detailed in chapter 4, section 4.5), the sorted cells were incubated in serum free medium with or without a 5 growth factor cocktail for a further 3 days. Although previous experiments had shown that normal cells failed to proliferate in the absence of growth factors, the introduction of STI into the culture may have influenced this; therefore control cells were treated in the same way as experimental ones. The cells were incubated in the presence or absence of 10μM STI, cultured for 3 days and further sorted into divided and undivided fractions. As 10μM had been the most effective concentration of STI in reducing the recovery of viable cells this was the concentration used for the rest of the experiments, although this was not clinically achievable. The three-day time point was chosen, as the effect of STI could be observed within this time frame. Figure 5.4 illustrates the sorting and gating strategy used for these experiments. For both sorts the cells were first gated on the viable (PI^-) population and on the $CD34^+$ population, before setting the markers for sorting.

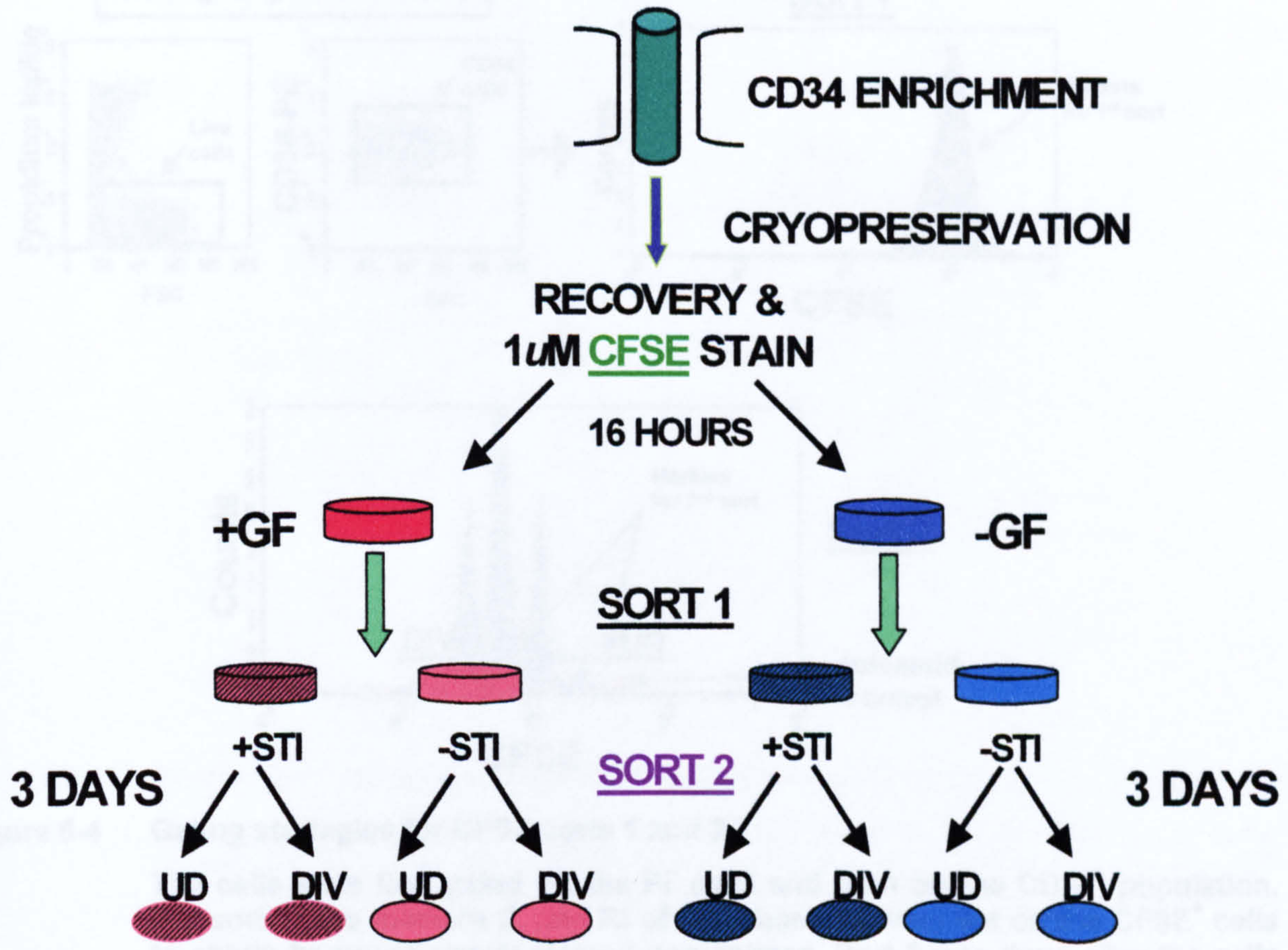

Figure 5-3 Schematic outline of the CFSE sorting and experimental strategy.

Following recovery from cryopreservation, the cells were stained with 1μM CFSE and cultured overnight ± growth factors. The cells were then sorted (sort 1) to obtain homogeneously stained $CFSE^{+}$ populations before being cultured for 3 days ± GF and ± STI. After 3 days the cells were further sorted (sort 2) into undivided (UD) and divided (DIV) cell populations identified by the colcemid control cells as described previously.

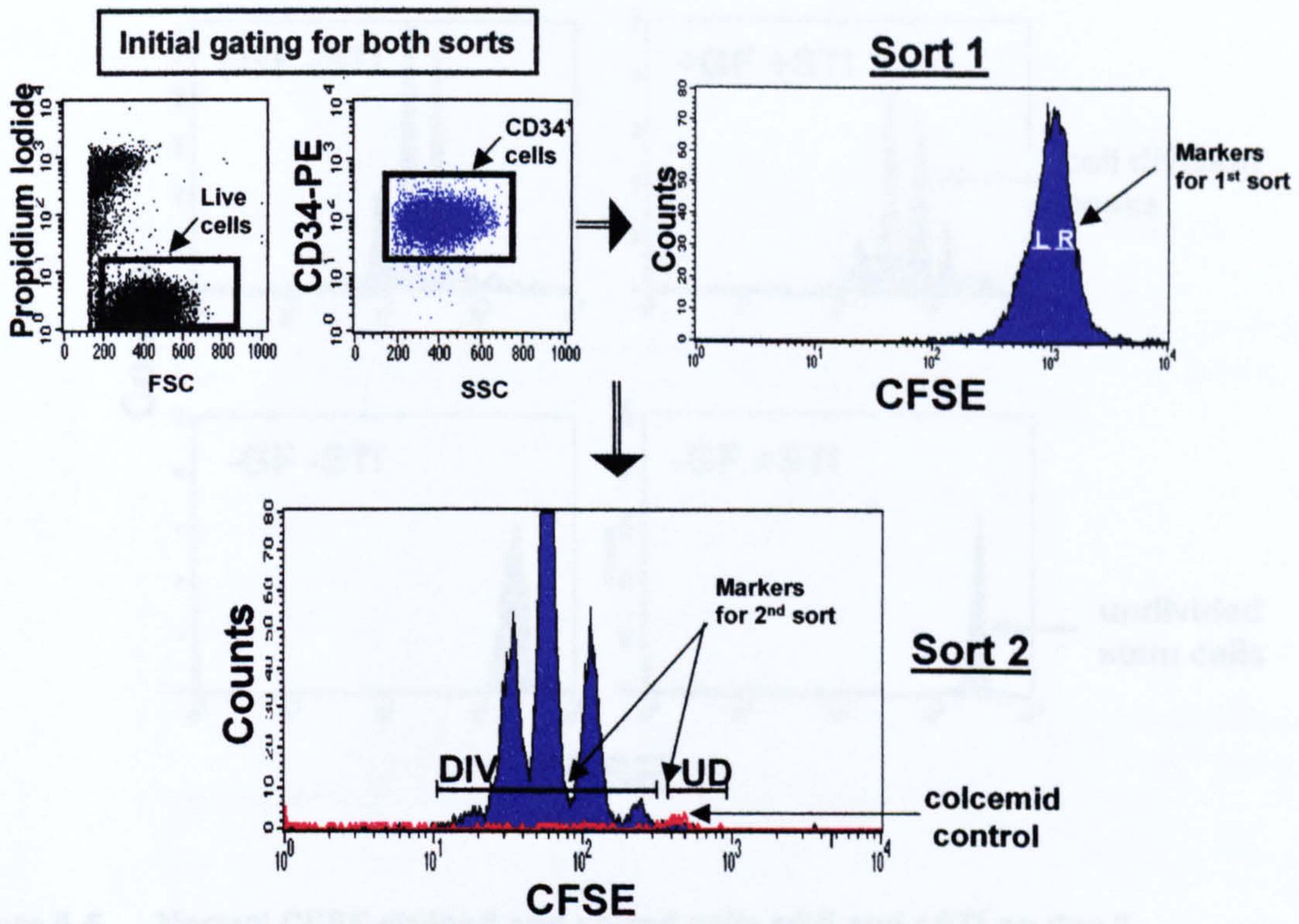

Figure 5-4 Gating strategies for CFSE sorts 1 and 2.

The cells were first gated on the PI^- cells and then on the $CD34^+$ population. For sort 1, two markers (L and R) of ~20 channels were set on the $CFSE^+$ cells to obtain homogeneously stained populations. Sort 2 was done after the cells had been in culture for a further 3 days. The colcemid control identifies the position of the undivided cells, and allows the markers to be set for sort 2.

Figure 5.5 shows normal cells in the presence and absence of 10μM STI, and ±growth factors. The histograms are gated on the viable (PI^-) and $CD34^+$ cells; therefore the peaks of cell division represent the viable, $CD34^+$ cells in each culture. As previously shown in chapter 4 section 4.6, in the presence of exogenous growth factors, stem cells have undergone up to 5 divisions with a small, undivided peak observed. The addition of STI did not affect the cell cycle kinetics or the recovery of viable stem cells. The cells were able to undergo a similar number of divisions in the presence of STI as in the absence. This was not surprising, as STI had previously been shown to have little effect on the proliferation of normal stem cells at this concentration. It has however, been documented that at concentrations of >10μM STI, inhibition of proliferation in normal cells is observed, possibly due to the inhibition of other tyrosine kinases (Deininger MW, Goldman JM et al. 1997).

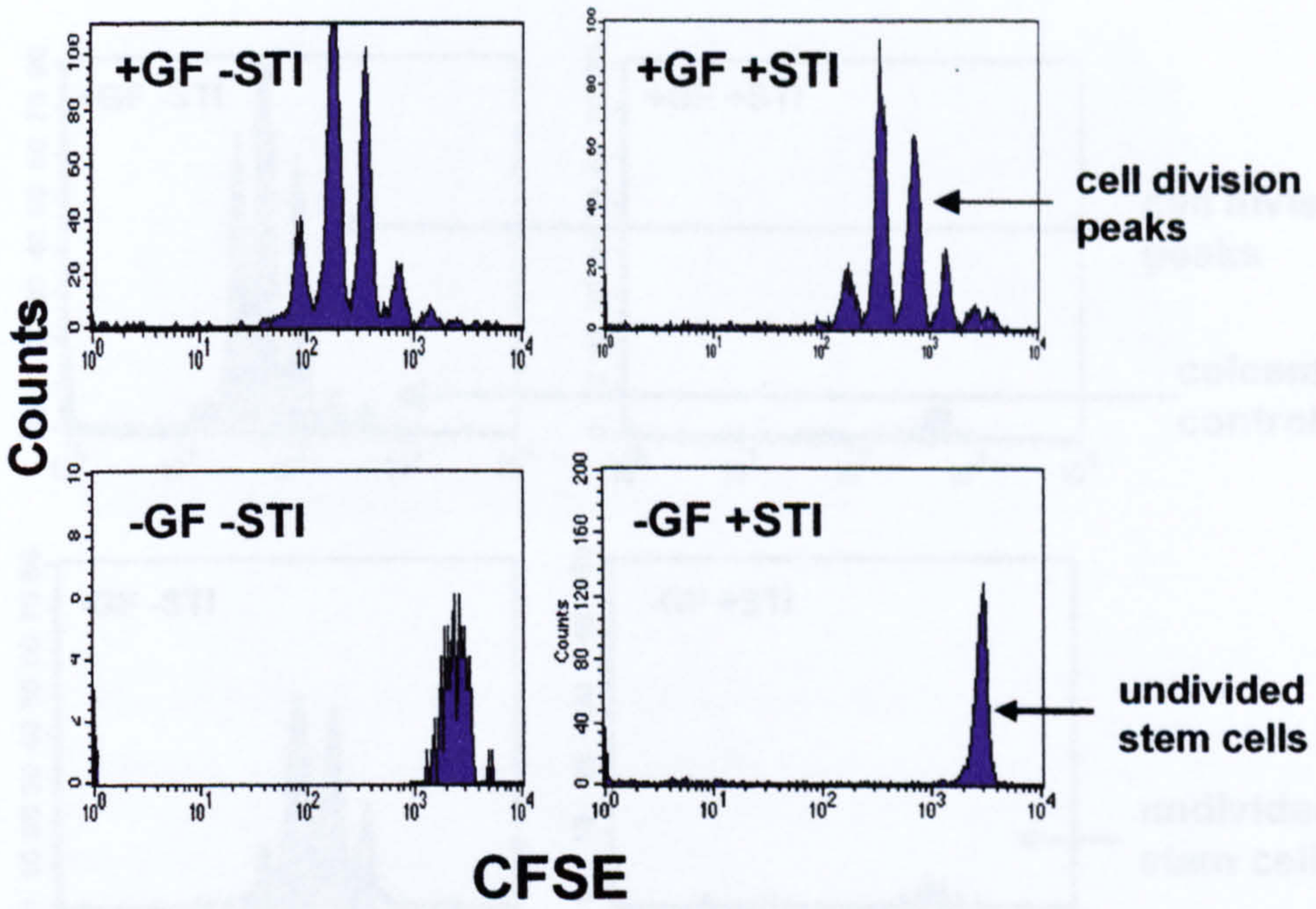

Figure 5-5 Normal CFSE stained and sorted cells ±GF and ±STI on day 3.

The plots were gated on the PI^-, $CD34^+$ population. Normal cells were unaffected by the addition of STI to the culture with GF. In the absence of GF there were no cell divisions and only a small number of undivided cells remained viable

In contrast to the normal example for CML 1 shown in figure 5.6, the addition of STI to the culture eliminated all of the dividing cells both in the presence and absence of growth factors. In both instances, a small, undivided peak was observed representing viable stem cells that had survived exposure to the drug.

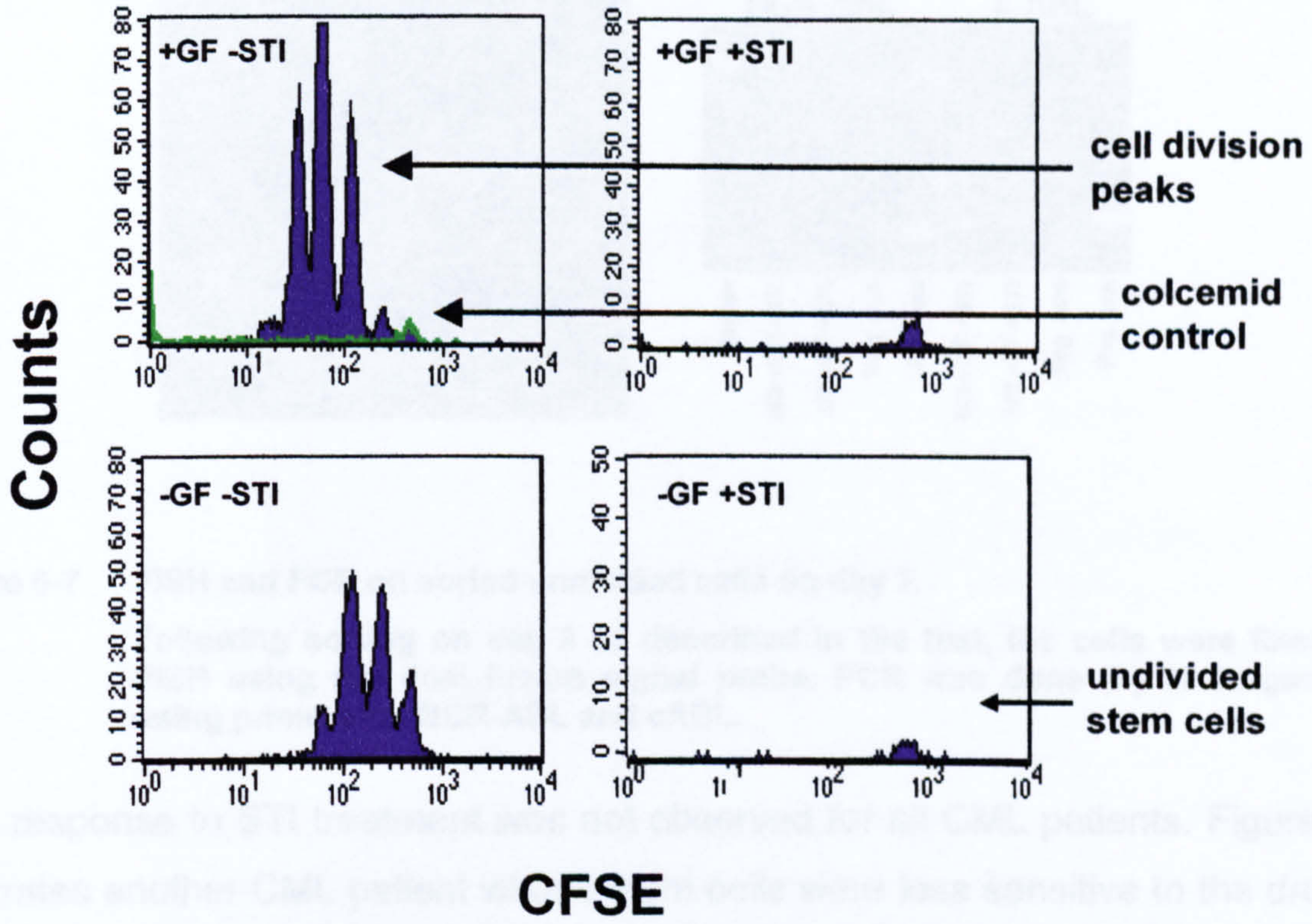

Figure 5-6 CML 1 CFSE stained and sorted cells ±GF and ±STI on day 3.

All plots were gated on the PI^-, $CD34^+$ population. STI has killed all of the dividing cells both in the presence and absence of growth factors. A small, undivided peak is observed ±GF following drug treatment.

The CML undivided cells were sorted and processed for FISH and RT-PCR. Representative examples are shown in figure 5.7, which demonstrated that these cells were part of the leukaemic clone. The FISH picture shows the dual fusion signal, which gives two yellow signals when BCR-ABL and ABL-BCR are detected. The red and green signals are the single BCR and ABL genes. The PCR picture illustrates the presence of BCR-ABL transcripts in the sorted undivided cells from cultures ± growth factors following treatment with STI. It was important to exclude the possibility that these cells were a very small number of normal cells that had been unaffected by STI exposure. The previous observation that CML cells exhibit growth factor independence (chapter 4) is also evident in this example, which shows 4 peaks of cell division in the absence of added growth factors.

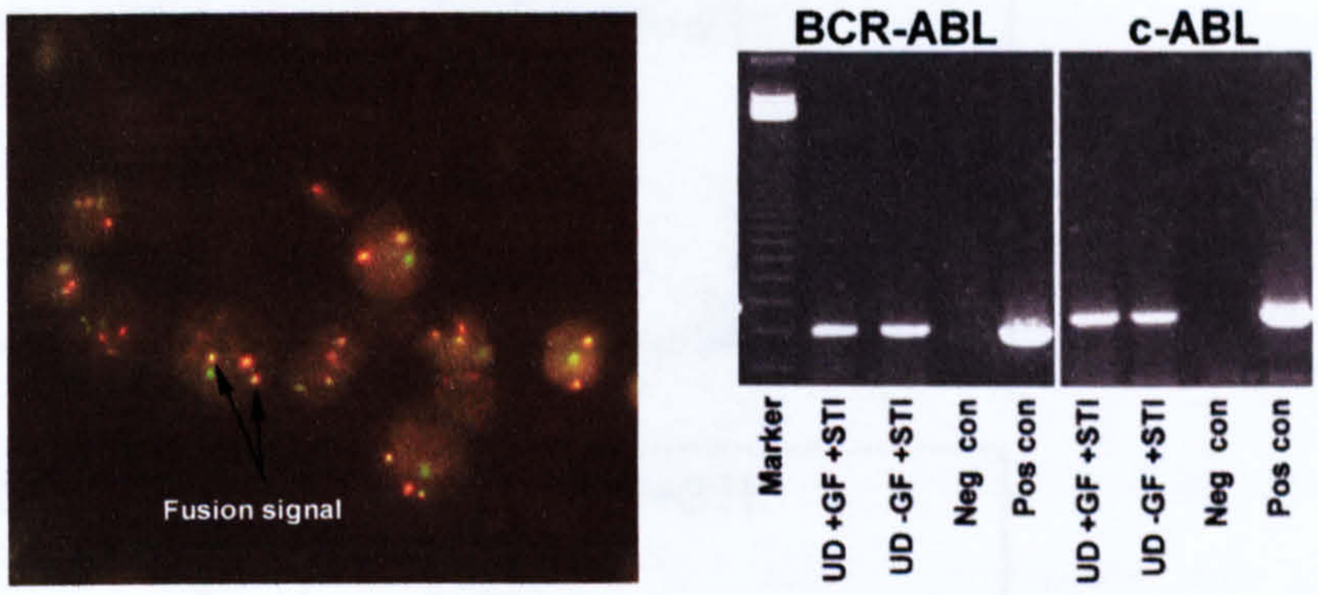

Figure 5-7 FISH and PCR on sorted undivided cells on day 3.

Following sorting on day 3 as described in the text, the cells were fixed for FISH using the dual fusion signal probe. PCR was done (by H Jorgensen) using primers for BCR-ABL and cABL.

This response to STI treatment was not observed for all CML patients. Figure 5.8 illustrates another CML patient whose stem cells were less sensitive to the drug in this assay. In the presence of growth factors and 10μM STI, a number of cells have been able to undergo up to 4 divisions. In conditions of growth factor starvation, and 10μM STI, some of the cells have still been able to undergo 1 division. The relative difference between the divisions ± growth factors may be attributable to the decline in cell proliferation at this early time point; as observed when the cells were cultured for 12 days in the absence of growth factors, detailed in the previous chapter. (Chapter 4, section 4.7). The differences in patient responses to STI exposure seen here may reflect a range of sensitivities to the drug, analogous to observations of in vivo responses.

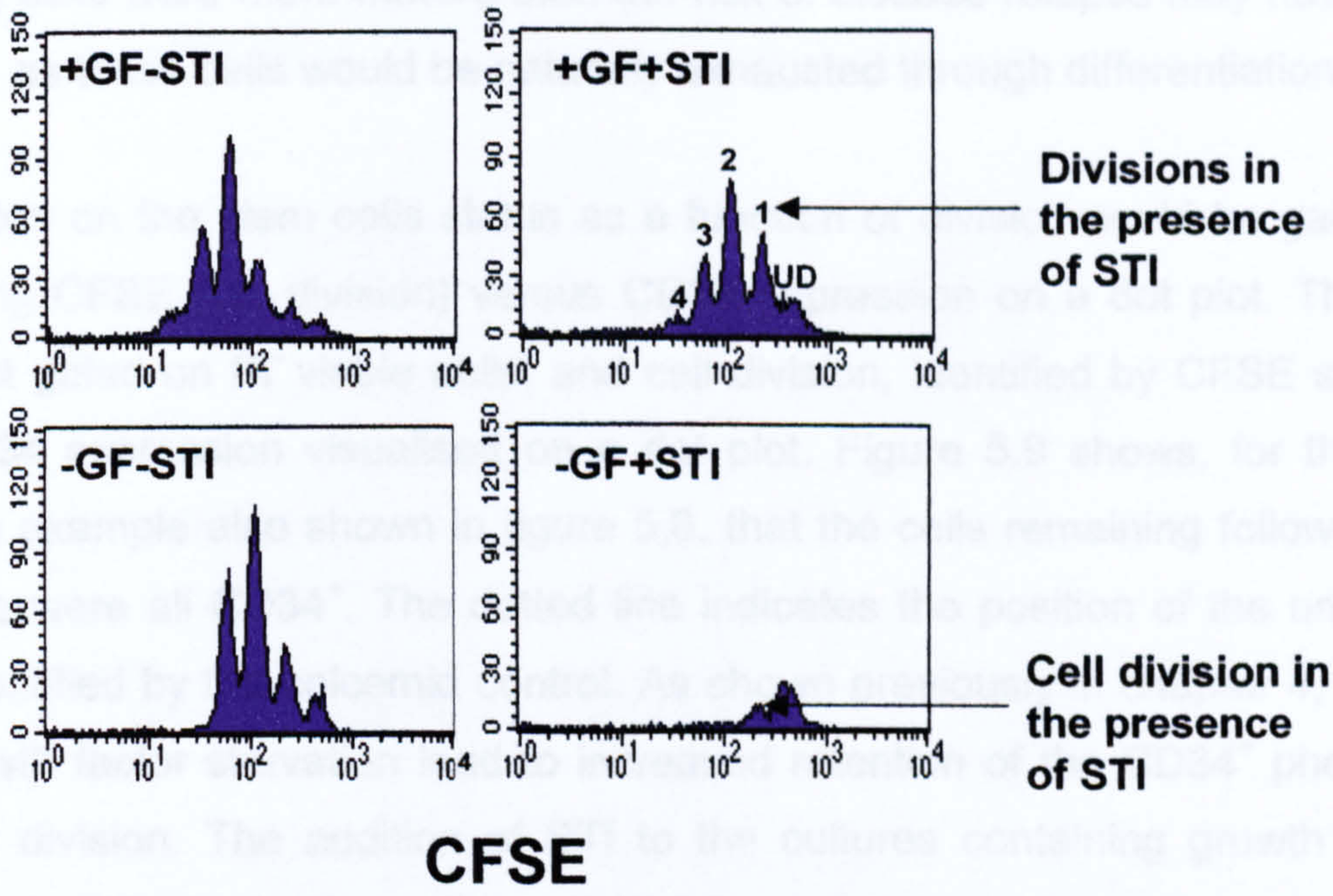

Figure 5-8 CML 2 CFSE stained and sorted cells ±GF and ±STI.

The histograms were gated on the PI^-, $CD34^+$ cells. The peaks of cell division with GF and STI are indicated showing that the cells have been able to divide up to 4 times in the presence of 10μM STI. In the absence of GF with STI, some cells have been able to undergo 1 cell division.

Although STI is targeted to BCR-ABL^+ cells, published reports have suggested that inherent resistance occurs, possibly due to over-expression of BCR-ABL or to mutations in the ATP binding site on the tyrosine kinase. In all patient samples used in this study, a quiescent population was identified following STI exposure (n=5), and in all cases these cells were $CD34^+$ and BCR-ABL^+ by FISH. The CD34 status of the cultures was recorded routinely and this allowed access to data on the expression of this stem cell marker under a range of conditions. As CML is a stem cell disease with the capability for production of excessive cell numbers, the expression of a stem cell marker could serve as an indication of the replicative potential of the malignant cells.

5.4 The Effect of STI Exposure on the Expression of CD34 in CML

It was important to illustrate what happened to the stem cell status in the treated cultures. For example STI may have induced differentiation including loss of CD34 and have exerted its effects in this way. It was also important to assess the proliferation potential of any cells, which survived exposure to the drug. If the

surviving cells were more mature then the risk of disease relapse may have been reduced, as these cells would be naturally exhausted through differentiation.

Information on the stem cells status as a function of division could be gained by visualising CFSE (i.e. division) versus CD34 expression on a dot plot. The cells were first gated on PI^- viable cells, and cell division, identified by CFSE staining, with CD34 expression visualised on a dot plot. Figure 5.9 shows, for this STI-sensitive example also shown in figure 5.6, that the cells remaining following STI exposure were all $CD34^+$. The dotted line indicates the position of the undivided cells, identified by the colcemid control. As shown previously in chapter 4, section 4.8, growth factor starvation lead to increased retention of the $CD34^+$ phenotype with cell division. The addition of STI to the cultures containing growth factors eliminated all of the dividing cells and all of the remaining viable cells were $CD34^+$. In the second less sensitive example, shown in figure 5.10, where STI has not eliminated the dividing cells, the expression of CD34 remained high. This would suggest that the most primitive cells show increased resistance to the effects of the drug. Given that more primitive stem cells have the capacity for greater expansion, this could potentially lead to disease relapse.

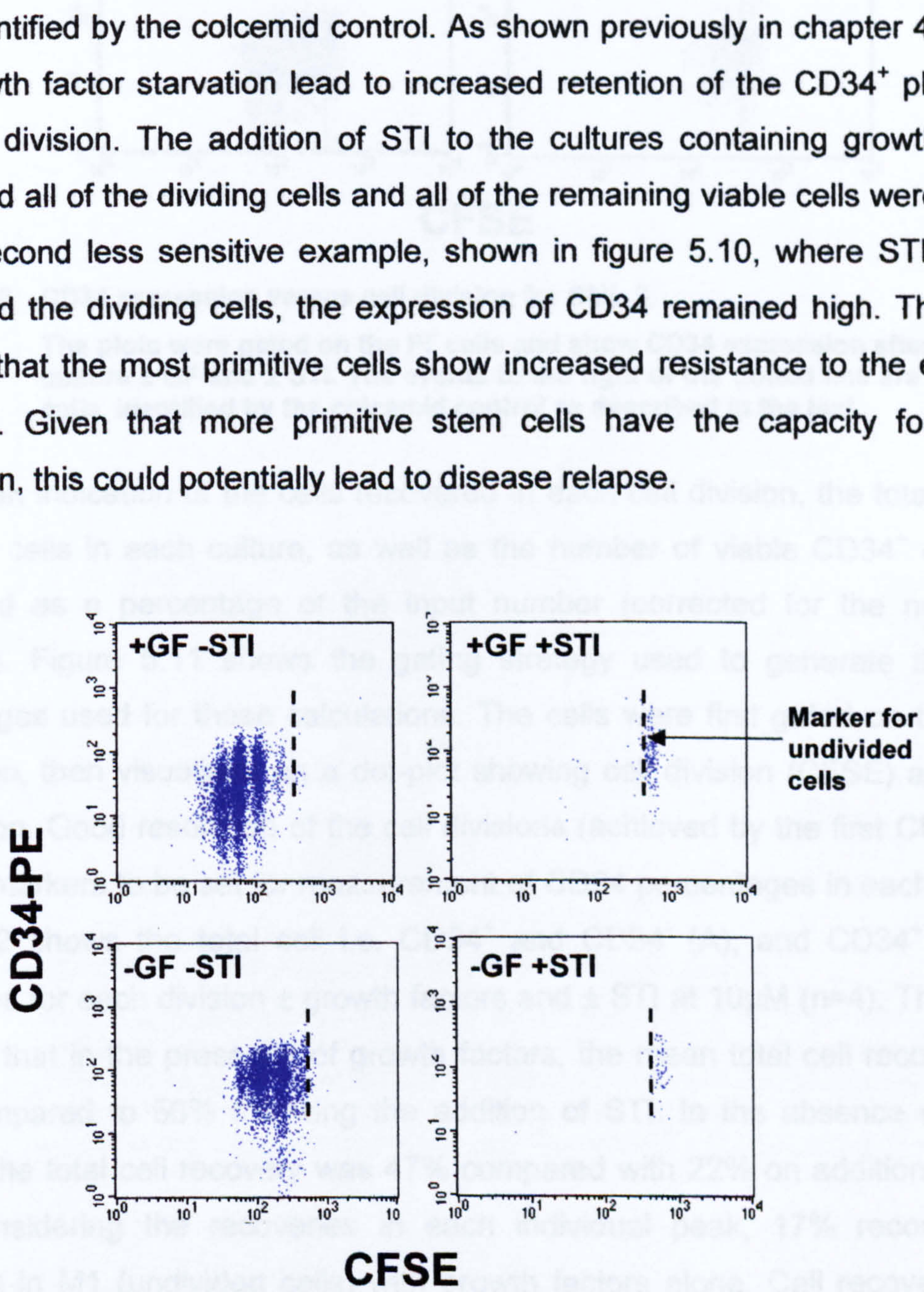

Figure 5-9 CD34 expression with cell division.

The plots are gated on the PI^- cells and show cell divisions (CFSE) versus CD34 expression. This is the same sample shown in figure 5.6 (CML 1). The dotted line represents the position of the undivided cells.

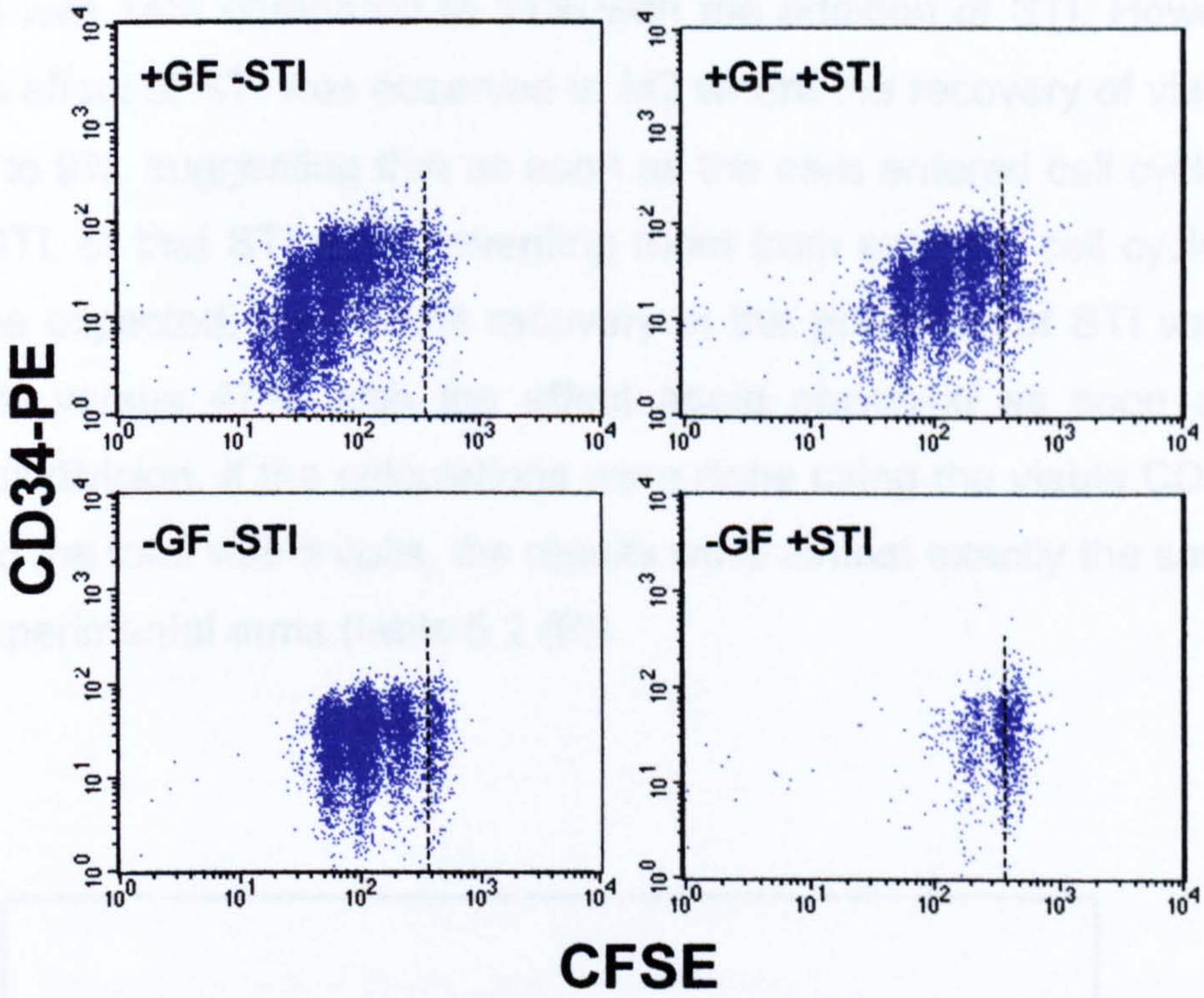

Figure 5-10 CD34 expression versus cell division for CML 2.

The plots were gated on the PI^- cells and show CD34 expression after 3 days in culture ± GF and ± STI. The events to the right of the dotted line are undivided cells, identified by the colcemid control as described in the text.

To give an indication of the cells recovered in each cell division, the total number of viable cells in each culture, as well as the number of viable $CD34^+$ cells was calculated as a percentage of the input number (corrected for the number of divisions). Figure 5.11 shows the gating strategy used to generate the CD34 percentages used for these calculations. The cells were first gated on the viable population, then visualised on a dot-plot showing cell division (CFSE) and CD34 expression. Good resolution of the cell divisions (achieved by the first CFSE sort) allowed markers to be set for measurement of CD34 percentages in each division. Table 5.2 shows the total cell i.e. $CD34^+$ and $CD34^-$ (A), and $CD34^+$ only (B) recoveries for each division ± growth factors and ± STI at 10μM (n=4). The figures illustrate that in the presence of growth factors, the mean total cell recovery was 91% compared to 56% following the addition of STI. In the absence of growth factors, the total cell recovery was 47% compared with 22% on addition of 10μM STI. Considering the recoveries in each individual peak, 17% recovery was observed in M1 (undivided cells) with growth factors alone. Cell recovery in the presence of STI was 16%, which was not significantly different. It would appear that STI did not affect the recovery of viable cells until division 3, where the recovery decreased from 28% with growth factors alone to 1.6% with the addition of STI. In the absence of growth factors, the percentage of cells in the undivided

peak (M1) was 14% compared to 11% with the addition of STI. However, in this culture the effect of STI was observed in M2 where the recovery of viable cells fell from 21% to 9%, suggesting that as soon as the cells entered cell cycle they were killed by STI, or that STI was preventing them from entering cell cycle. As would perhaps be expected, the overall recovery in the presence of STI was markedly lower, 22% versus 47%, with the effect again observed as soon as the cells entered cell division. If the calculations were done using the viable $CD34^+$ cells as opposed to the total viable cells, the results were almost exactly the same for each of the 4 experimental arms (table 5.2 (B))

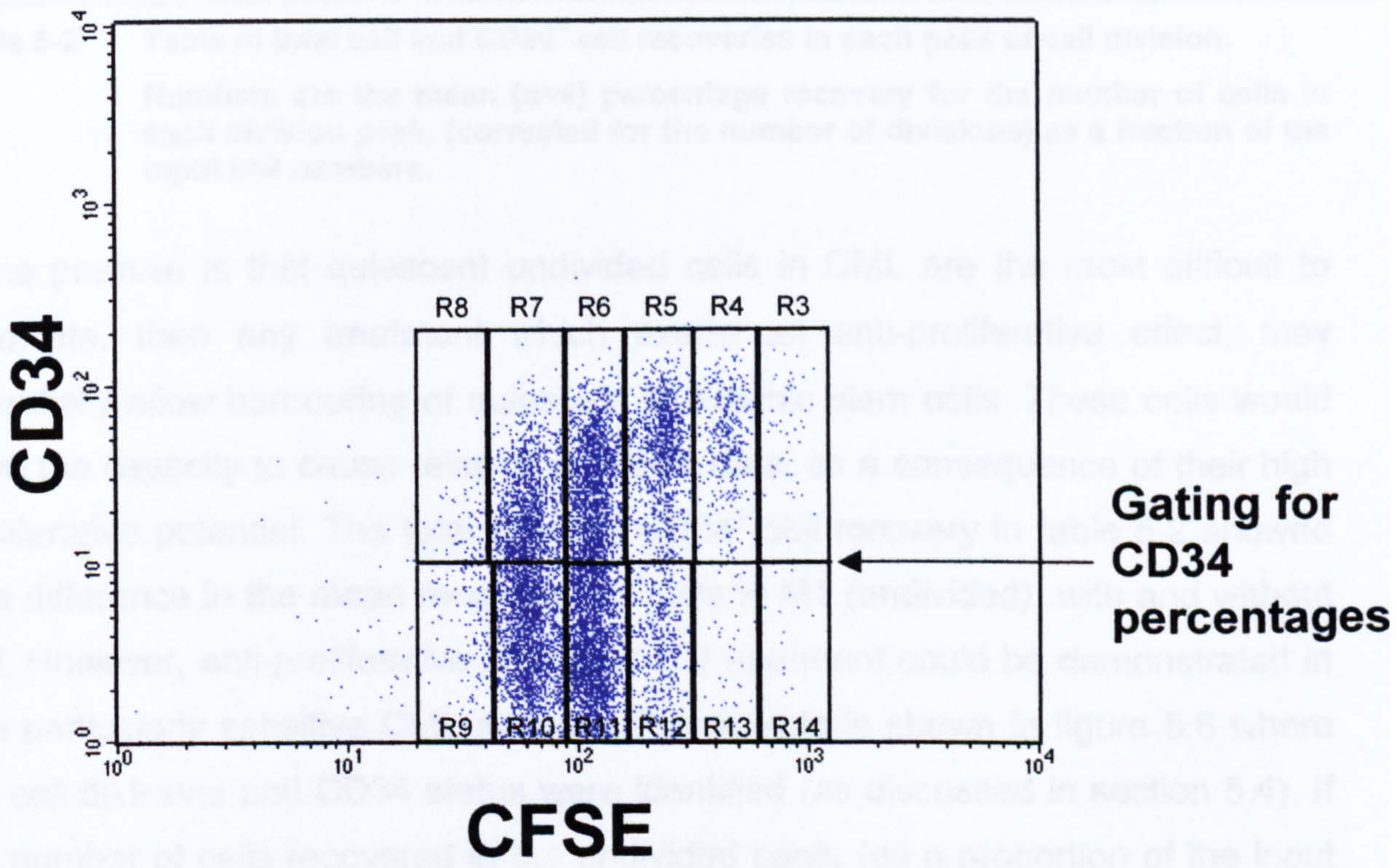

Figure 5-11 FACS plot of cell division (CFSE) with CD34 expression.

The cells were cultured for 3 days in the presence of GF, after initial sorting of CFSE stained cells as described in the text. Cells were then stained with anti-CD34-PE and gates set for each division to calculate the percentage of $CD34^+$ and $CD34^-$ cells in each division. This plot was gated on the PI^- population. R3 and R14 represent the undivided cells identified by the colcemid control.

(A) Total cell recovery

Conditions	Recovery in M1 (mean %)	Recovery in M2 (mean %)	Recovery in M3 (mean %)	Recovery in M4 (mean %)	Recovery in M5 (mean %)	Total recovery (mean %)
+GF	17	13	26	28	6	91
+GF + STI	16	15	23	1.6	0.9	56
-GF	14	21	10	1.4	-	47
-GF+STI	11	9	2	0.2	-	22

(B) Recovery of $CD34^+$ cells

Conditions	Recovery in M1 (mean %)	Recovery in M2 (mean %)	Recovery in M3 (mean %)	Recovery in M4 (mean %)	Recovery in M5 (mean %)	Total recovery (mean %)
+GF	11	13	28	28	6	85
+GF + STI	15	16	23	1.6	0.9	55
-GF	13	25	11	1.4	-	51
-GF+STI	11	10	2	0.2	-	24

Table 5-2 Table of total cell and $CD34^+$ cell recoveries in each peak of cell division.

Numbers are the mean (n=4) percentage recovery for the number of cells in each division peak, (corrected for the number of divisions) as a fraction of the input cell numbers.

If the premise is that quiescent undivided cells in CML are the most difficult to eradicate, then any treatment which exerts an anti-proliferative effect, may potentially allow harbouring of quiescent leukaemic stem cells. These cells would have the capacity to cause relapse at a later date, as a consequence of their high proliferative potential. The total cell and $CD34^+$ cell recovery in table 5.2 showed little difference in the mean recoveries of cells in M1 (undivided), with and without STI. However, anti-proliferative effects of STI treatment could be demonstrated in one particularly sensitive CML sample. This sample is shown in figure 5.6 where the cell divisions and CD34 status were identified (as discussed in section 5.4). If the number of cells recovered in the undivided peak, (as a proportion of the input number) was calculated, with growth factors alone, the recovery in M1 was 3.2% ± 0.4% and in the presence of STI was 15.6% ± 1.4% (p=0.014). This demonstrated that STI was exerting an anti-proliferative effect, as the cells had backed up in the undivided peak, i.e. the recovery of undivided cells had increased in the presence of the drug. It remained a possibility that the cells identified in the undivided peak were early apoptotic cells, however due to limitations in this assay it was not possible to confirm this. Further work by our group (not shown in this thesis), has established that the undivided cells, which survive STI exposure, have the capacity to proliferate upon removal of the drug and therefore retain the potential to cause disease relapse (Jorgensen HG, Allan EK et al. 2005).

Holtz et al (Holtz MS, Slovak ML et al. 2002) have demonstrated that STI selectively inhibits the proliferation of primitive CML progenitors and more recently Bhatia et al (Bhatia R, Holtz M et al. 2003) have shown that malignant progenitors persist in patients treated with STI. Studies within our group have shown that the anti-proliferative effect of STI can be enhanced or reduced by the introduction of other drugs in combination with STI in vitro (Jorgensen HG, Allan EK et al. 2005). Holtz et al have also demonstrated that haemopoietic progenitor cells persist in CML patients treated with STI who are in complete cytogenetic remission, and confirmed that BCR-ABL mRNA levels in the progenitor cells were higher than in the more mature MNC (Holtz MS, Forman SJ et al. 2005). However, it is still too early to assess whether these cells can ultimately contribute to relapse in patients treated with STI therapy.

5.5 Summary

In summary, the experiments presented in this chapter were aimed at assessing the sensitivity of a number of CML patient stem cells to differing doses of STI. These results established a range of sensitivities to the drug with one particular example, which was very susceptible. Having established test doses and a time frame for the protocol, further work investigated the pattern of cell division in the presence of the drug, together with the effects on the stem cell status. It was confirmed that some cells from every patient sample survived exposure to the drug at greater than clinically achievable doses. It was also established that these cells were part of the leukaemic clone by FISH, and expressed the stem cell marker CD34. It was further determined that the surviving cells were the undivided, quiescent cells and that STI exerted anti-proliferative activity (shown in one example) by causing the number of undivided cells to increase in the presence of the drug. Taken together it would seem likely that STI is not going to cure CML as a single therapy. However, in combination with other agents aimed at inducing quiescent cells into cycle, or by increasing their susceptibility to other agents, a more effective treatment may be feasible. In an effort to identify potential therapeutic targets, an investigation of the gene expression profile of normal and CML quiescent cells compared to cycling cells was undertaken, and the following chapter describes the preliminary analysis.

Chapter 6 Results 4 – A Comparison of the Gene Expression Profile of Normal and CML Quiescent and Dividing Stem Cells.

6.1 Introduction

Advances in the treatment of chronic myeloid leukaemic saw the first molecularly targeted therapy for a human cancer reach the clinic. STI571 (STI) was rationally designed to inhibit the constitutively active tyrosine kinase of the BCR-ABL oncoprotein. This in turn, is responsible for BCR-ABL-induced transformation in primitive haemopoietic stem cells typical of CML disease. Initial clinical trials with STI showed remarkable results particularly in chronic phase, with almost all patients achieving a haematologic response and many achieving major or complete cytogenetic responses. However, molecular remissions were rare and detectable levels of BCR-ABL transcripts were noted in patients achieving a complete cytogenetic response, with cases of disease relapse whilst on therapy documented. It was clear that some cells were resistant to the effects of STI and able to repopulate the haemopoietic system post-treatment.

The results presented in the previous chapter identified a quiescent population of primitive stem cells that survived exposure to STI at concentrations in excess of those used clinically. Other reports have also documented progenitor cells that remain viable in vitro and in vivo following exposure to STI (Holtz MS, Slovak ML et al. 2002; Hughes TP, Kaeda J et al. 2003). In an effort to characterise the quiescent cells compared to cycling cells in both normal and CML, a microarray approach was used. Gene expression profiling had been used successfully in other studies of leukaemia, identifying a previously unrecognised class of mixed lineage leukaemia (MLL) (Armstrong SA, Staunton JE et al. 2002). It was anticipated that a microarray approach would yield important information not only concerning leukaemic cells, but also regarding normal haemopoietic stem cell biology. It was hoped that differences in the expression profiles would yield targets valuable for CML therapy alone, or perhaps in combination with other known cytotoxic agents. Quiescent cells were identified and sorted using the protocols described in chapter 3, then processed for RNA. The RNA was converted to

biotinylated cRNA, applied to Affymetrix U133A gene chips and the results analysed by two different methods.

6.2 Sorting to Isolate Quiescent and Cycling Stem Cell Fractions

It was of critical importance that the cell populations used for microarray studies were subject to consistent conditions, as any deviation in the protocol may have induced changes in gene expression related to procedure. The Hoechst (HST) and Pyronin (Py) sorting strategy (as described in chapter 3, section 3.1.3) was used to generate quiescent cells in G0 and cycling cells in G1/S/G2/M from previously CD34 selected samples A representative CML sample is shown in figure 6.1. The plots illustrate the cells were first gated on the PI^- viable cells and then on the $CD34^+$ population. The gates on the HST/Py plot are set for sorting G0 ($HST^{lo}Py^{lo}$) and cycling cells in G1/S/G2/M. This protocol was previously verified for sorting of cell cycle phases in chapter 3 section 3.14.

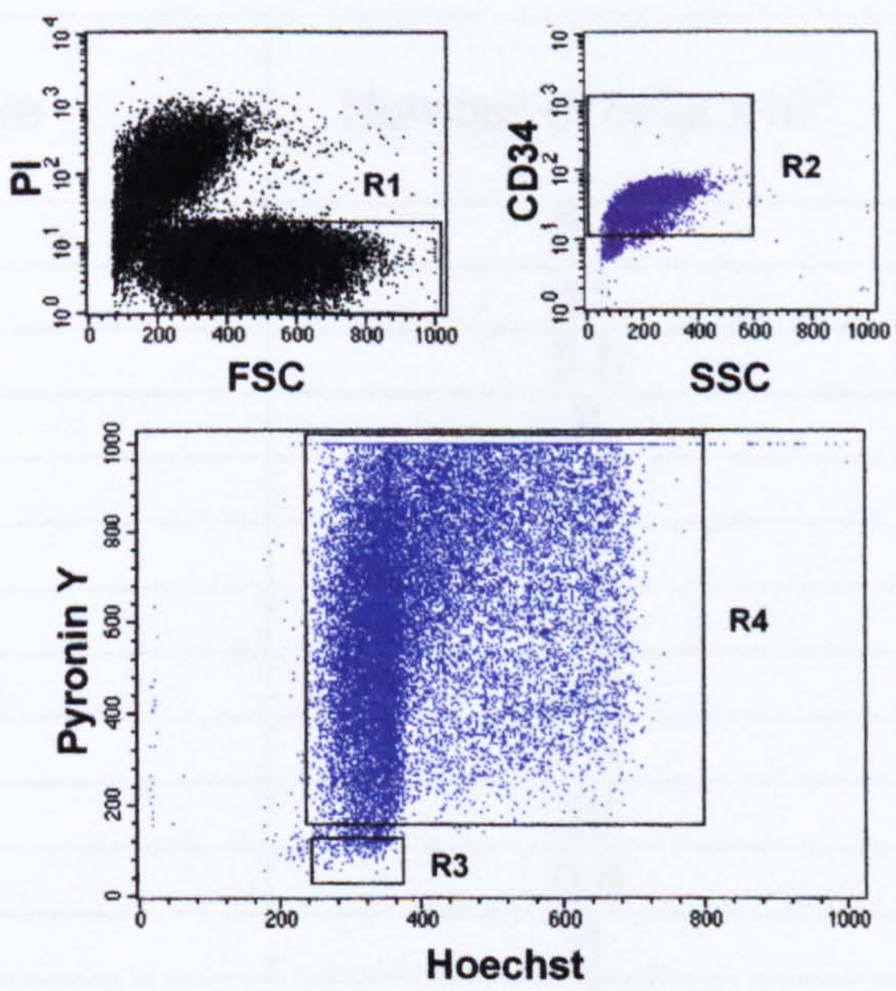

Figure 6-1 Sorting gates for isolation of G0 and dividing cells.

The cells were incubated overnight in growth factor medium to enable recovery from cryopreservation. The following day the cells were stained with PI, anti-CD34FITC, HST and Py. The sorting gates were set firstly on the viable PI^- cells (R1), then on the $CD34^+$ cells (R2). Further gates were set on the G0 (R3) and dividing cells (R4).

To maintain consistency (essential for arrays), all of the samples were positively selected using the Isolex method described in section 3.2.1 of chapter 3. In total 5 CML samples and 3 normal samples were sorted and processed for RNA as described in materials and methods section 2.3.4.12. Unfortunately, one of the normal G0 samples failed to produce enough RNA for the microarray experiment, which meant that the normal G0 set had only 2 samples; the corresponding normal divided cell sample was included.

6.3 Generation of RNA for Application to Arrays

The total number of sorted cells together with the amount of RNA obtained form each sample is shown in table 6.1. The cell numbers were from the sorter counts and in an effort to conserve cells no further counting was done. As shown in the table, the amount of RNA obtained varied considerably from 0.07µg to 45µg and did not appear to correlate well with starting cell number although this could be due in part, to the reduced accuracy of the sorter counts. The level of the least amount of RNA necessitated that an amplification protocol be employed in order to generate data on every sample.

Sample	Number of cells $x10^6$	Total amount of RNA µg
CML 1 G0	0.4	0.07
CML 1 Div	11	17
CML 2 G0	0.5	0.16
CML 2 DIV	8	45
CML 3 G0	0.4	0.38
CML 3 DIV	11	37
CML 4 G0	0.05	0.07
CML 4 DIV	0.5	0.80
CML 5 G0	0.4	0.09
CML 5 DIV	10	10.2
NORM 1 G0	0.8	0.34
NORM 1 DIV	6	15
NORM 2 G0	1	0.84
NORM 2 DIV	10	3.3
NORM 3 DIV	8	14

Table 6-1 Table of sorted cell numbers and total RNA .

Normal and CML cells were sorted to produce quiescent G0 and cycling S/G2/M cell populations. The cells were immediately placed into Trizol and stored at –80^{0}C. When all of the samples had been sorted, RNA was extracted in a single batch. The concentrations of RNA were measured at the microarray facility using the Nanodrop machine.

It was crucial that all of the samples were treated similarly, to enable comparison of the expression profiles. Although the samples were sorted on different days, the RNA processing was done in a single batch using the same reagents. The RNA samples were then handed over to the Sir Henry Wellcome Functional Genomics (SHWFG) facility at the University of Glasgow, where the remaining procedures were carried out. These included; measurement and quality assessment of RNA, generation of cDNA, amplification of RNA, labelling of cRNA, application to Affymetrix gene chips U133A, generation of results and analysis of data. Analysis included normalization of the data, production of gene lists and clustering analysis. Additional analysis of the data was done by myself using the GeneSpring®(Silicon Genetics) program.

The Affymetrix microarray methodology was chosen as the internal controls and reproducibility were robust and the system had been used in numerous previous studies. This study used the HU-133A GeneChip which contains 22,000 probes representing 12,600 well substantiated genes. The sequences were selected from GenBank®, dbEST, and RefSeq and sequence clusters created from UniGene database (build 133, April 2001) and refined by comparison with other public databases. It was decided at this early stage that only validated gene sequences would be used which incorporated a limited number of expressed sequence tags (EST), most of which are contained in the HU-133B chip. Affymetrix GeneChips contain reference standards for both gene expression and target intensity, which enable scaling and normalization of the data. Sets of genes known to be expressed in a diverse range of human tissues are included on the chip. This technology allows data from different experiments to be compared quantitatively.

6.4 Production of Gene Lists

Normalization of the data and generation of gene lists was done by the SHWFG facility at the University of Glasgow where the microarray experiments were carried out. Normalization was done using the robust multichip average (RMA), a published, validated method of normalization specific to Affymetrix GeneChip technology (Irizarry RA, Hobbs B et al. 2003).

Lists of differentially expressed genes for the desired comparisons were produced using Rank Products (RP); a recently published method which sorts all genes according to their expression changes and provides statistical confidence levels

which are particularly applicable to small and noisy data sets (Breitling R, Armengaud P et al. 2004). A more sophisticated level of analysis was done using an innovative method for identification of functional gene classes known as Iterative Group Analysis (iGA). This method generates a biological summary of the physiological processes altered in a particular experiment and provides powerful statistical confidence measures (Breitling R, Amtmann A et al. 2004). These results will be discussed in detail later.

6.5 Analysis of Data Using GeneSpring®

Conducted by myself, the gene lists imported into the GeneSpring (Silicon Genetics) program were normalized data produced by SHWFG using RP as detailed above.

The results were generated on the basis of defined comparisons. The sample groups of most interest were: 1. CML G0 versus CML dividing, 2. Normal G0 versus Normal dividing, 3. CML G0 versus Normal G0, 4. CML dividing versus Normal dividing. Lists of genes were collated and ranked in order of fold change with an indication of false discovery rate (FDR) i.e. a conservative estimate of the expected percentage of false positives. For practical purposes an arbitrary cut-off of 5% was used, in the initial assessment of the data. As this was a relatively small sample group the FDR was quite high for many of the genes in the comparisons.

Comparisons	Regulated	Number of Genes
CML G0 Vs CML DIV	UP	1088
CML G0 Vs CML DIV	DOWN	614
Norm G0 Vs Norm DIV	UP	448
Norm G0 Vs Norm DIV	DOWN	1676
CML G0 Vs Norm G0	UP	1793
CML G0 Vs Norm G0	DOWN	208
CML DIV Vs Norm DIV	UP	743
CML DIV Vs Norm DIV	DOWN	139

Table 6-2 Table of the number of genes changed for each comparison .

The results represented in the table are the numbers of genes changed either up or down, as identified by RP analysis, for each comparison.

Table 6.2 shows the number of consistently differentiated genes up- and down-regulated for each comparison. This illustrates that hundreds of genes were changed between the groups, which were accompanied by large differences in fold change and FDR. In addition, the lists were not clustered into functional

groups, which made identification of the most relevant genes more difficult. As with all global expression arrays the analysis yields very large amounts of data and to facilitate identification of the most significant genes, clustering analysis is required.

The data was subsequently re-analysed using the GeneSpring® program. Normalized raw data from Affymetrix gene chips was imported into the program, which allowed the data to be manipulated such that genes could be grouped according to fold change. Analysis of the data using scatter plots generated groups of genes with >3, >4 and >5 fold changes. Table 6.3 shows the number of genes changed either increased or decreased, for each comparison.

Comparison	>3-Fold	>4-Fold	>5-Fold
CML G0 Vs CML DIV	37	21	10
Norm G0 Vs Norm DIV	188	92	47
CML G0 Vs Norm G0	168	85	49
CML DIV Vs Norm DIV	49	27	8

Table 6-3 Table of the numbers of changed genes with fold change .

The genes changed and the level of fold change was generated by GeneSpring analysis of RP lists imported into the program.

The greatest number of genes changed >3-fold (188) was in the Normal G0 versus Normal dividing group and the least number >3-fold changed (37) was in the CML G0 versus CML dividing. There was a large number of genes >3-fold changed between CML G0 and Normal G0 (168) suggesting that the normal G0 cells were very different in their gene expression, from either their dividing counterparts or CML G0 cells. Figure 6.2 shows a mathematical model of the relative distance in terms of gene expression between the samples. The Euclidean distance diagram represents the data (>3-fold change) plotted on a relative scale. Euclidean distance is plotted using the formula: distance (x,y) = sqrt(SUM(xi – yi)2)½ (where the sum is over all points i), which calculates the geometric distance in the multidimensional space. It gives an indication of how close the groups are in terms of gene expression.

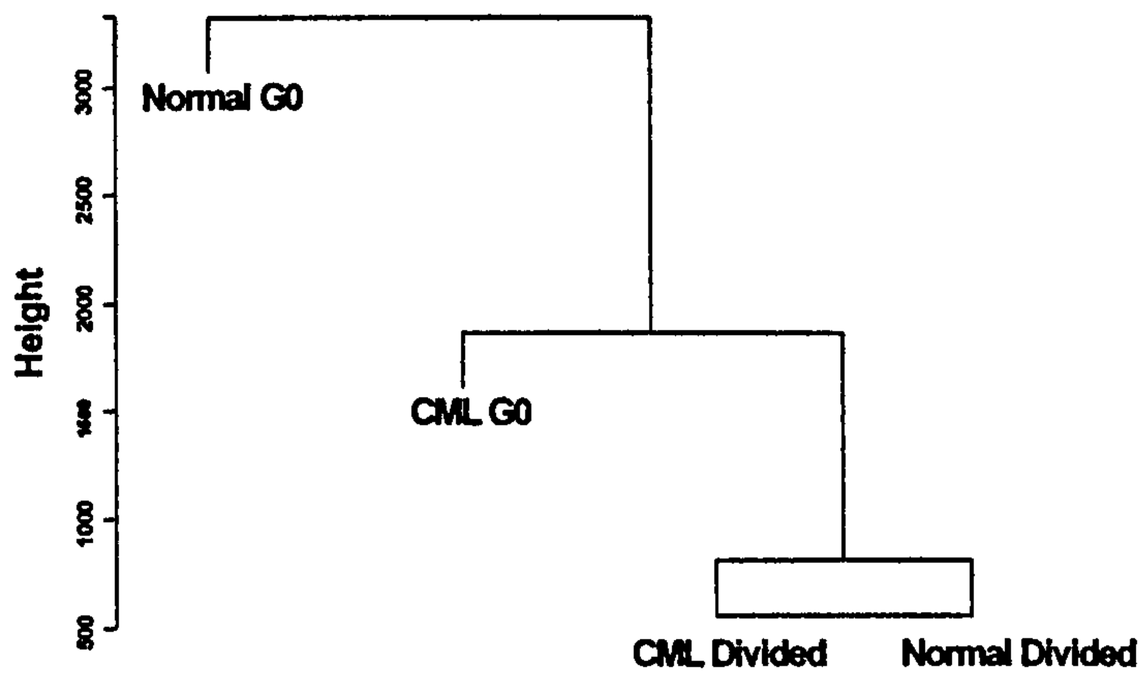

Figure 6-2 Euclidean distance diagram of gene differences >3-fold changed .

The model was created using the genes >3-fold changed, up or down, between the groups to give an indication of how close each group was in gene expression. The height scale is arbitrary and indicates the relative distance between the groups.

The diagram in figure 6.2 shows that CML and normal dividing cells are closest in gene expression and that normal G0 cells show the least homogeneity with the other sample groups, since they are separated by the greatest distance. The diagram also illustrates that CML G0 cells are closer in gene expression to normal and CML dividing cells than to Normal G0 cells.

6.6 Analysis of Gene Expression in Normal G0 Versus Normal Dividing Cells

One of the particular areas of interest in terms of gene expression was the difference between Normal G0 and Normal dividing cells. The gene expression of such specific populations of normal stem cells has not been previously investigated. It has been shown that most mobilised primitive stem cells are out of cycle i.e. in G0, and it was anticipated that this data set would shed some light on the gene expression profile of quiescent stem cells compared to cycling cells (Uchida N, He D et al. 1997).

Given that the cells were sorted on the basis of cell cycle position, the change in expression of cell cycle genes was examined. Table 6.4 shows a list of cell cycle genes and their fold change between Normal G0 and Normal dividing cells. The

list shows significant up-regulation of many cell cycle associated genes in dividing cells, which would be expected if the cells were accurately sorted into their cell cycle compartments. This was a further confirmation of the success of the sorting strategy using HST and Py for identification of cell cycle position. In addition, the dividing cells also showed up regulation of genes associated with transcription and translation, which would be anticipated in cells exhibiting greater cellular activity.

Gene	Fold up-regulation
CDC2	8
CDC20	6
CCNB2	5
CCN1	3.5
CDC25	3.5
MCM2	4
MCM5	3
CHEK1	4
CDC6	5
CDKN3	4

Table 6-4 Table of cell cycle genes up-regulated in normal cycling cells.

The table shows a selection of gene up-regulated in normal dividing versus quiescent cells. An indication of the fold change for each gene is also shown.

Curiously, the greatest fold change in Normal G0 versus Normal dividing cells was seen in a set of chemokine genes, specifically the ligands, not the receptors, which were between 5 and 10 fold up-regulated in the quiescent cells. The significance of this observation is not immediately obvious and no other published work on haematopoietic stem cells has suggested a role for these chemokines in maintenance of quiescence. These data will be discussed in more detail later.

6.7 Analysis of Gene Expression in CML G0 Versus CML Dividing Cells

As the analysis of cell cycle genes in normal cells had shown good differential expression between G0 and dividing cells it was anticipated that the same would hold true for the CML cells, since these had been sorted in the same way. However, similar differences in cell cycle associated gene expression were not observed in the CML samples. There appeared to be significant up-regulation of cell cycle genes in the CML sorted quiescent cells compared to normal G0, such that these more closely resembled dividing cells. One possible explanation may be that the sorted population of cells was heterogeneous and contained cycling cells

in the quiescent fraction. However, on the basis of the normal data, the sorting strategy would appear to be robust. Another potential explanation could be that the CML cells were more efficient in dye efflux by ABCG2 transporters, known to efflux Hoechst. This would place some cells in the G0 gate when in fact they were cycling cells. Increased expression of the ABCG2 transporter in stem cells has been identified in primitive haemopoietic cells, specifically in side population (SP) cells (Scharenberg CW, Harkey MA et al. 2002). ABCG2 is responsible for Hoechst efflux, which places the SP cells in a particular position on a FACS plot where dual fluorescence of Hoechst is analysed. However, the data generated in this microarray experiment does not show significant up regulation of ABCG2 in the CML G0 versus CML dividing cells or indeed between the CML and normal cells. If expression of ABC transporter genes in CML cells were a factor in determining their position on the Hoechst and Pyronin FACS plot, it would be expected to show some differential expression between CML and Normal cells. However, it was possible that the set level of 3 fold differential expression was too high to detect changes in ABCG2 transporter activity. The only way to exclude the possibility of the influence of ABCG2 would be to sort the cells using a different FACS staining strategy and examine the expression of cell cycle genes. The fact remains that quiescent CML stem cells behave differently from CML cycling cells as demonstrated in chapter 5, where these cells were shown to survive exposure to STI. Such distinct differences in cell behaviour would not be expected if the cell cycle position identified as G0 was an artefact of the staining and sorting strategy.

Although expression of cell cycle genes in the G0 CML cells has cast some doubt on the integrity of the sorting procedure, a similar up-regulation of the same group of chemokine genes observed in the Normal G0 cells was also observed for the CML G0 cells. This would suggest that these populations of cells share at least some similar characteristics. Figure 6.3 shows a Venn diagram of the comparisons of Normal G0 versus Normal dividing and CML G0 versus CML dividing cells.

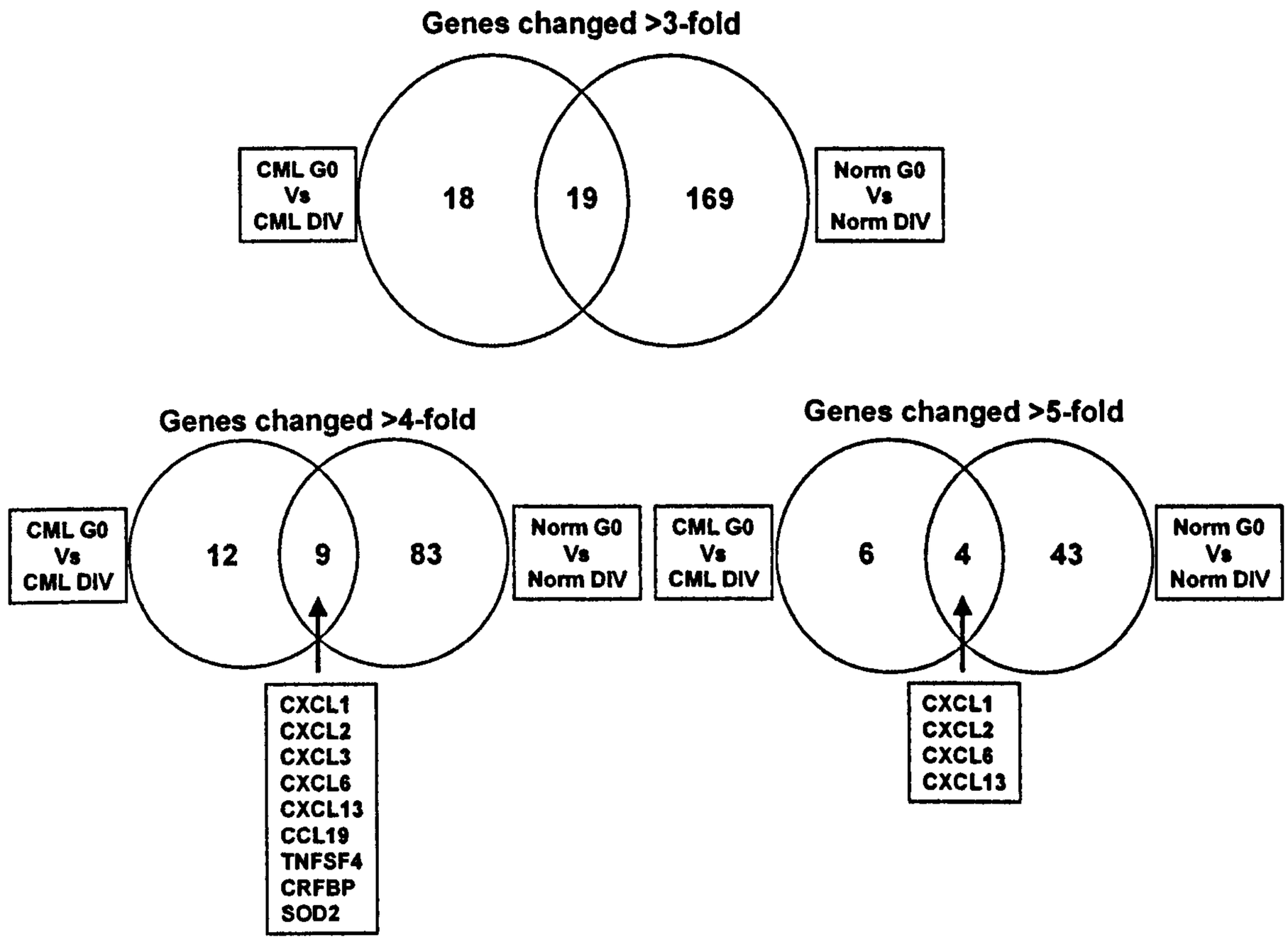

Figure 6-3 Venn diagrams of differential gene expression between all comparisons.

The Venn diagrams were created in GeneSpring by selecting all genes >3-, >4- and >5-fold, changed between the groups as illustrated. Genes common to both groups for >4-fold and >5-fold are shown in the boxes.

Figure 6.3 illustrates that of genes showing >3-fold change, 188 genes were differentially expressed in Normal G0 versus Normal dividing cells, 37 genes were expressed in CML G0 versus CML dividing and that 19 genes were commonly expressed in both Normal and CML G0 versus dividing cells. When the level of change is set at >4-fold, 9 genes were common to both groups. Significantly, 7 of the 9 genes encode chemokines. If a similar comparison is done with the fold change set at >5, as shown in figure 6.4, 47 genes were changed in Normal G0 versus dividing, 10 genes were changed in CML G0 versus dividing, and 4 genes were common to both comparisons. The 4 common genes, >5-fold up-regulated in the G0 cells were all chemokine genes, and this was a surprising finding. The particular chemokines identified have not been previously associated with stem cell quiescence. This may be an important observation, as the level of up regulation (5-10-fold) in quiescent cells, is significant compared to cycling cells. Also, although genes encoding the ligands were up regulated, there was no up-regulation of the corresponding receptors as shown in table 6.5, suggesting that this was not an autocrine mechanism. The involvement of these particular

chemokines in quiescent stem cells has not been documented and as such represents a novel observation, which merits further investigation.

Receptor	Present	Comments
CXCR1	+	↑ Norm vs CML
CXCR2	-	
CXCR3	+	
CXCR4	+	3-fold ↑ in Norm G0
CXCR5	-	
CCR1	-	
CCR2A	-	
CCR4	+	
CCR5	+	
CCR6	-	
CCR7	-	
CCR8	-	
CCR10	-	
CCRL1	+	↓Norm vs CML

Table 6-5 Table of gene expression of chemokine receptors.

The table shows the presence or not of signals on the arrays for chemokine receptor genes. The levels of expression between the groups were similar unless otherwise indicated.

6.8 Iterative group analysis (iGA) to Identify Functional Gene Classes for Each Comparison

Iterative group analysis (iGA) is based on the premise that combined expression change of some or all members of a functional group is physiologically relevant. iGA uses statistics to identify functional gene classes that are significantly changed in an experiment, and at the same time determines which of the class members are most likely to be differentially expressed. iGA does not depend on fixed lists of differentially changed genes but instead uses an iterative procedure to determine the optimal threshold for each functional class. By concentrating on gene groups rather than single genes it is feasible to establish statistical significance even in the absence of experimental replication, as the group members serve as internal replicates. This is a powerful tool that enhances the sensitivity of gene detection especially in small data sets such as this one. A further advantage of this technique for the analysis of microarray experiments is that it allows comparison of data from different platforms or analytical techniques (Breitling R, Amtmann A et al. 2004).

Using the iGA method, the data from these experiments was further analysed to identify clusters of significantly changed genes. The list of genes and their functional class assignments is contained in Appendix 1. These results also identify the greatest changes in gene expression as being between the Normal G0 cells and their dividing counterparts, with some 20 gene groups significantly changed. Interestingly, most of the changed groups in the dividing cell up-regulated cohort are related to cell cycle. The differential expression of cell cycle genes strongly suggests that the sorting strategy has indeed isolated quiescent, G0 cells from cycling ones.

Analysis of up-regulated genes in the Normal G0 samples shows significant expression of chemokine genes identifying not only the ones found in the GeneSpring analysis, but a further 5 genes in this functional class. In addition, the gene groups are ranked in order of significance with chemokine genes at the top of the list. This analysis corroborates the GeneSpring data, and increases the significance of this observation. The relevance of this finding will be studied in further experiments, as no previously published work has established a role for these chemokines in stem cell quiescence.

In the CML G0 versus cycling cells, the consistent up regulation of genes associated with initiation of cell cycle observed in the normal samples, was not detected in this clustering analysis. However, there was significant up regulation of genes associated with the mitotic phase of the cell cycle and of those associated with spindle formation and chromosome assembly. This suggests that there were considerable differences in gene expression between the two CML cell populations. However, it would appear that cells identified as quiescent CML cells are not truly quiescent in the same way as normal cells are. The G0 CML cells appear to have little differential expression of genes associated with early cell cycle events, but have increased expression of genes involved in the later mitotic phase. This would support the findings documented in chapter 3 of this thesis, which identified a significant increase in the proportion of cells in the S/G2/M phase of the cell cycle, for CML samples compared to normal. The CML G0 cells were clearly very different from normal G0 cells; however, the same up-regulation of chemokine genes was observed in the CML quiescent cells as in the normal ones, albeit at a slightly lower level. It is possible that the genes associated with expression of chemokines are a quiescent stem cell feature and the aberrant cell cycle gene expression is a consequence of malignancy.

6.9 Summary

In conclusion, the microarray study has confirmed that for normal cells, significant up-regulation of cell cycle genes was observed in sorted cycling compared to quiescent cells. For CML samples this differential cell cycle gene expression was not observed, suggesting that quiescent CML cells display altered expression of some cell cycle associated genes. Gene expression profiling also identified an unexpected cohort of chemokine genes 5-10-fold up-regulated in quiescent stem cells from both normal and CML samples.

Chapter 7 Discussion

7.1 Introduction

The aim of the work presented in this thesis was to isolate and characterise quiescent haemopoietic stem cells (HSC) from CML and normal patients. These isolated stem cell populations were used to determine if cell cycle position affected their sensitivity to a specifically targeted treatment, STI. These cell populations were further utilised in a microarray study in an effort to identify genotypic differences between quiescent and cycling stem cells, and between normal and CML stem cells.

7.2 Identification and Isolation of Stem Cells in Different Phases of the Cell Cycle

HSC comprise a very small proportion of the circulating progenitors, typically around 0.1% in normal individuals. Although there are no definitive markers for human stem cells, CD34 is the most commonly used. This sialomucin molecule is expressed on the surface of cells capable of rescuing a myeloablated host, and therefore possessing the capacity to generate every cell of the haemopoietic system. In practice, stem cell populations enriched by selection with this marker, have been used clinically for transplantation for a number of years. All samples in this study were enriched for $CD34^+$ cells by either positive or negative selection, prior to sorting by flow cytometry. The different CD34 selection methods generate subtly different populations of stem cells. Positive selection separates cells bearing the CD34 antigen from the whole population. Negative selection uses a cocktail of antibodies to a variety of lineage markers, which allows removal of these cells leaving the immature $CD34^+$ cells, which express no lineage markers. Generally the percentage of $CD34^+$ cells is lower for the negative selection. If $CD34^-Lin^-$ cells (possibly more immature than $CD34^+Lin^-$) are present in the population, they will be retained by a negative selection but lost in a positive selection. However, all of the FACS sorting experiments described in this thesis included gating on the $CD34^+$ population, which in effect excludes any $CD34^-Lin^-$ cells.

Stem cells are generally accepted to be predominantly quiescent and enter cell cycle relatively infrequently. It is proposed that this affords them protection from

potentially damaging influences, and reduces the incidence of genetic mutation associated with DNA replication. It is possible that quiescence is a factor in the maintenance of malignant stem cell disease and the experiments described in this thesis were aimed at addressing the importance of a quiescent phenotype in leukaemic survival following cytotoxic therapy, and the possible implications for disease persistence.

Previous work by Holyoake et al had demonstrated that a quiescent stem cell population existed in CP CML and that these cells could be isolated by FACS sorting (Holyoake T, Jiang X et al. 1999). Intracellular staining of DNA by Hoechst (HST) and RNA by Pyronin Y (Py) is the most commonly used method of isolating viable cells in different phases of the cell cycle. Most other dyes used in flow cytometry for discrimination of cell cycle phases (e.g. propidium iodide) are not able to distinguish the G0 and G1 phases. In addition, most stains require the cells to be fixed and therefore non viable. Furthermore, HST and Py can be combined with additional stains, as described below, which allow more specific cell populations to be isolated.

Using the HST and Py staining method, G0 and dividing populations were identified (shown in figure 3.6). In addition, setting gates around the viable (PI^-) $CD34^+$ cells allowed G0 and cycling stem cells to be sorted separately (figure 3.7). Success of the sorting strategy was confirmed by PCR analysis of the CML sorted cells showing the presence of PCNA (synthesised in S-phase) in the cycling cells, which was absent in the G0 and G1 cells. Interestingly, another cell cycle associated gene MCM5, which is synthesised when cells enter G1, was also observed in the G0 cells. However, other studies have documented aberrant expression of MCM5 in malignant cells of the oesophagus, which may be related to disruption in cell cycle control in cancer cells (Going JJ, Keith WN et al. 2002). Unfortunately, due to limitations in the availability of material, it was not possible to repeat the PCR confirmation experiments with a normal sample. These preliminary results showed we could successfully isolate viable, quiescent and cycling, stem cell populations.

One of the first observations following HST and Py staining, was that the proportion of cells in G0 was lower in the CML samples. There was also a significant difference in the proportion of cells in G1, 70.9% in normal compared to 50.6% in CML. The percentage of cells in G0 was consistently lower for CML

samples compared to normal, suggesting that there were fewer quiescent stem cells in CML. Given that all cells were stained following 24hrs in culture after recovery from cryopreservation, it would appear that the CML cells displayed an increased cell cycle activation, with fewer cells in G0/G1 than in the normal samples. Kramer et al have made similar observations for $CD34^+$ cells in both BM and PB from newly diagnosed CML patients. They noted the proportion of cycling progenitor cells was higher in CML PB and BM compared to matched samples from $BCR\text{-}ABL^-$ myeloproliferative disease, and concluded that $BCR\text{-}ABL^+$ $CD34^+$ cells display an increased cell cycle activation (Kramer A, Loffler H et al. 2001). Although the results presented here, and those of Kramer et al, indicate that a greater proportion of the CML cells are in the S/G2/M phase of the cell cycle, it does not imply that these cells are cycling more rapidly. Rather it suggests CML cells are more likely to enter cell division, but does not give information on the time taken to complete the cell cycle. Furthermore, data on the division history of CML and normal stem cells detailed in chapter 4, indicates that both populations undergo a similar number of divisions following 3 days in culture with growth factors, after the same initial 24 hours recovery from cyropreservation. Moreover, Buckle et al have also demonstrated that CML stem cells do not exhibit increased cell cycling compared to normal stem cells (Buckle AM, Mottram R et al. 2000) These observations suggest similar cell cycle kinetics for CML and normal $CD34^+$ stem cells, at least in vitro.

7.3 Comparison of Division History and Stem Cell Status in Normal and CML Cells

The experiments described in chapter 4 investigated some of the characteristics of CML stem cells compared to normal stem cells in vitro. Culturing cells in the absence of exogenous growth factors identified distinct differences between normal and CML stem cells. To gain some understanding of the behaviour of stem cells under varying conditions, a method of tracking cell division and stem cell status was devised. By staining cells with a permanent, non-toxic cytoplasmic dye (CFSE) and developing a sorting strategy to enhance the resolution of cell division peaks, it was possible to precisely track the pattern of cell division. In addition, it was possible to calculate with some accuracy, stem cell amplifications together with the proportions of cells recovered in each peak of division relative to the number of input cells. When sorted $CD34^+$ cells were cultured in the presence and

absence of a 5 growth factor cocktail containing IL-3, IL-6, SCF, GCSF and Flt3L, there were distinct differences between normal and CML cells. In the presence of growth factors, both normal and CML cells have undergone up to 5 divisions in 3 days. However, in the absence of growth factors, normal cells were unable to divide and only a very small proportion remained viable and undivided. It is possible that these cells represent a deeply quiescent population resistant to the detrimental effects of growth factor starvation, or that they are early apoptotic cells still able to exclude PI. Unfortunately, it was not possible using this FACS staining strategy to confirm either status.

In contrast, in the absence of growth factors, CML cells were able to divide up to 3 times, demonstrating their growth factor independence. This is in accordance with other published data, which was recently convincingly substantiated when $CD34^+$ normal cord blood (CB) cells infected with retrovirus encoding $p210^{BCR\text{-}ABL}$, displayed a growth factor independent phenotype (Chalandon Y, Jiang X et al. 2004). The mechanism of growth factor independence in CML cells is not clearly defined. It has previously been shown that in primitive CML cells growth factor autonomous proliferation was associated with autocrine production of IL-3 and GCSF (Jiang X, Lopez A et al. 1999). In other studies, we have further demonstrated that whereas quiescent CML $CD34^+$ cells have no detectable IL-3 transcripts, following culture in the absence of growth factors these cells spontaneously up regulate IL-3 expression as they enter cell cycle (Holyoake T, Jiang X et al. 2001). Further experiments by Jiang et al demonstrated the rapid acquisition of autocrine IL-3 production by BCR-ABL transduced primitive murine BM cells, which was associated with immediate growth factor independence (Jiang X, Ng E et al. 2002). Chalandon et al also found that in $p210^{BCR\text{-}ABL}$ retrovirally transduced cells, growth factor independent proliferation was associated with autocrine production, not only of IL-3, but also of GCSF and erythropoietin. This evidence strongly suggests that bcr-abl confers a growth factor independent phenotype in association with autocrine growth factor production. Furthermore, proliferation in the absence of growth factors can be considered selective for Ph^+ cells, as normal cells fail to divide under these conditions.

Experimental analysis of CD34 status together with cell division showed CML cells preferentially maintained expression of CD34 following growth factor withdrawal. In the presence of added growth factors the percentage of $CD34^+$ cells declined with division, however, in the absence of growth factors, the cells retained significant

levels of CD34 expression. This suggests that in the absence of exogenous growth factors, the cells that are able to survive and divide are the most primitive i.e. expressing the CD34 stem cell marker, and that they maintain this status with division.

Interestingly, both in the presence and absence of growth factors, a small number of undivided cells were observed in all CML samples, which displayed a high level of CD34 expression. It remained a possibility that these cells represented a small number of primitive normal cells, analogous to the in vivo population known to coexist alongside Ph^+ cells. Sorting divided and undivided populations allowed FISH analysis, which showed that all of the undivided cells were in fact BCR-ABL^+, confirming their leukaemic status. This data verified that, even when exposed to a potent growth factor cocktail, a number of CML stem cells remained undivided. This methodology does not allow assessment of cell cycle status, only division history. It is likely that the undivided cells were indeed quiescent, having failed to enter cell division after 3 days in the presence of growth factors, however it was not possible to confirm this using this experimental strategy.

7.4 The Effect of STI571 on Cell Division in Normal and CML Stem Cells

The central role of bcr-abl in leukaemic transformation presented an attractive target for drug therapy. A small molecule inhibitor, STI, was found to inhibit the constitutive tyrosine kinase activity of bcr-abl^+ cells both in vitro and in vivo. However, in vitro studies with STI had revealed that some Ph^+ cells were able to survive exposure to the drug (Deininger MW, Goldman JM et al. 1997). Clinical observations suggest that all BCR-ABL^+ cells are not eliminated by STI treatment, and the potential for relapse exists in the majority of treated patients. One of the mechanisms of resistance to STI is the development of mutations in the kinase domain of bcr-abl, which inhibit STI binding and can be detected prior to treatment. It is possible that this could explain the differences in sensitivities to STI documented in the work presented in chapter 5 of this thesis, however only mutation analysis could confirm this.

There are other proposed mechanisms to explain the resistance of CML cells to STI. For example, it has recently been reported that activity of the ABC

transporter, Pgp, can reduce intracellular concentrations of STI, leading to less effective inhibition of the tyrosine kinase activity (Illmer T, Schaich M et al. 2004). Mahon et al have also demonstrated that Pgp activity may be responsible for resistance to STI in cell lines, however it has not been conclusively established if overexpression of this transporter is a clinical feature of CML disease (Mahon FX, Belloc F et al. 2003). Conversely, others have shown that overexpression of Pgp, at least in BCR-ABL$^+$ cell lines, does not confer resistance to STI in vitro (Ferrao PT, Frost MJ et al. 2003).The evidence so far has not confirmed if drug efflux is a significant factor in STI resistance.

Gene amplification and overexpression of BCR-ABL have also been described in STI resistant cells, and it is generally accepted that reactivation of the bcr-abl tyrosine kinase is required to induce a malignant phenotype. However these mechanisms remain controversial in the clinical setting. Although gene amplification has been described in some patients, whether this results in increased bcr-abl protein has not been established (Gorre ME, Mohammed M et al. 2001).

It was possible that a quiescent phenotype could allow stem cells to escape the effects of cytotoxic therapy. In an effort to identify which CML cells (if any) could survive exposure to STI, the previous experimental strategy to identify division history and stem cell status was utilised. CML and normal CD34$^+$ cells were stained with CFSE and cultured in the presence or absence of STI, with a relatively short time frame (3days) to exclude the possibility of outgrowth of resistant mutant clones. Cultures of CML cells in the absence of growth factors were included in an effort to focus on leukaemic cell proliferation without the potential contribution of normal cells, unable to divide under these conditions.

Preliminary experiments were aimed at establishing a test concentration of STI in excess of clinical doses, to determine if any CML cells were able to survive at greater than clinically achievable doses. Pharmacokinetic studies demonstrated that at the prescribed dose of 300mg/day, a peak plasma concentration of 1μM was achieved in the patient. 10μM STI was selected for all subsequent studies as this represented 10x the clinically achievable dose at the time of the experiments. More recently, in vivo doses have been escalated to 600-800mg/day, giving peak plasma concentrations of 5-7μM (Peng B, Hayes M et al. 2004).

The experiments described in chapter 5 demonstrated that some CML stem cells could survive when cultured in the presence of 10μM STI, which had little effect on normal stem cell proliferation in this system. Effects of higher concentrations of STI (>10μM) on normal cells have been observed, possibly due to inhibition of c-kit or other tyrosine kinases. Holtz et al have documented that whereas some effect of STI on normal CFC is observed at 5μM, it does not affect more primitive LTC-IC (Holtz MS, Slovak ML et al. 2002). It is worth mentioning that many of the early investigations into the effectiveness of STI as an agent that inhibited the proliferation of Ph^+ cells examined its effects on very heterogeneous cell populations or in cell lines. Work in this thesis focused specifically on the stem cell fraction, and the importance of this defined population will become evident as this discussion develops.

Tracking the pattern of cell division by staining and sorting stem cell populations +/- STI revealed that in all CML samples, a population of undivided cells was able to survive exposure to STI at greater than clinically achievable doses. It was also evident that a range of sensitivities to STI existed among CML patients. In a particularly sensitive example all of the dividing cells, +/- growth factors were killed by STI. In less sensitive patients a number of cells were able to divide +/-growth factors and also in the presence of 10μM STI. A possible explanation for this heterologous response of patient cells may be that some patients harbour a small number of cells with a mutation, which renders them insensitive to STI treatment. Such mutations in either the ATP binding pocket or in other parts of the protein that confer conformational changes have been documented in cases of resistance. There is now evidence that these mutations exist in a small number of cells even before treatment, and that elimination of the STI-sensitive cells reveals their presence (Roche-Lestienne C, Lai JL et al. 2003). More recent evidence suggests that kinase domain mutations exist in around 22% of STI-naive CML patients. However, their existence does not correlate directly with resistance to STI therapy. The authors concluded that additional factors were required to induce a fully resistant phenotype (Willis S, Lange T et al. 2005).

These data support the theory that innate or acquired resistance to STI is not the only explanation for disease persistence. Indeed, data presented in chapter 5 of this work offers an alternative explanation for the minimal residual disease observed in STI treated patients, namely, that it is the quiescent cells that are able to evade therapy. In support of this, it has recently been demonstrated that non-

proliferating $CD34^+$ $BCR\text{-}ABL^+$ cells are resistant to the effects of apoptosis inducing stimuli including STI, and that only dividing cells display sensitivity to the effects of these agents (Holtz MS, Forman SJ et al. 2005). If quiescent cells can re-enter cell cycle then the potential for relapse exists and represents a genuine clinical problem. It is still too early to assess whether the remissions due to STI therapy will be durable. Evidence from patients who had to stop the drug due to complications, suggests that relapse from disease reactivation is a distinct possibility.

Observations in the experiments described in this thesis may have implications in the therapeutic context. If quiescence or a non-dividing state allows cells to escape the effects of STI, then any treatment that induces quiescence has the potential to perpetuate disease. In the experiments described in chapter 5, analysis of the most STI-sensitive example revealed an increased recovery of cells in the undivided peak as a proportion of the input number, demonstrating that STI was exerting an anti-proliferative effect. A similar observation was made by Holtz et al. Using a similar FACS sorting strategy, they also found that exposure to 5μM STI increased the proportion (relative to the input number) of primitive undivided cells (Holtz MS, Slovak ML et al. 2002). In addition, they also observed that whereas increased proliferation was inhibited by STI, there was no concomitant effect in apoptosis, suggesting that STI was exerting a cytostatic and not a cytotoxic effect.

These data raise concerns in relation to the clinical effectiveness of STI treatment. If one of the effects of STI therapy is to reduce the number of committed progenitors but also to induce the quiescence of primitive leukaemic stem cells, then long-term patient survival may be jeopardised. It has already been documented that most patients who achieve a complete cytogenetic response also harbour detectable BCR-ABL transcripts, and that molecular remissions are rare (Hughes TP, Kaeda J et al. 2003).

In separate studies not included in this thesis, we have identified combinations of STI with other agents that reduce the quiescent fraction in vitro following treatment. Evaluation of the effects of treatment on the primitive $CD34^+$ $BCR\text{-}ABL^+$ population revealed that STI in combination with lonafarnib, a farnesyl transferase inhibitor, reduced the number of undivided cells and inhibited their ability to proliferate on removal of the drug, which was not observed for other drug

combinations (Jorgensen HG, Allan EK et al. 2005). If leukaemic stem cells are able to evade STI therapy when they are quiescent, then only combinations of agents that induce cell cycle and target CML stem cells in concert are likely to be effective. Although there is accumulating evidence to suggest primitive quiescent CML stem cells are the most resistant to STI treatment in vitro, it is impossible to say if disease persistence in vivo is due to the same cell population. Clearly, in vivo stem cells are subject to microenvironmental stimuli impossible to mimic in vitro.

7.5 Gene Expression Profiling of Quiescent Versus Cycling Normal and CML Cells

Comprehensive analysis of gene expression by cDNA microarrays has become an important tool for research in many areas. This technology produces a snapshot of the gene expression profile of a cell and provides information on the relative levels of gene expression between different cells. Microarrays have been used extensively in the search for distinctions between subsets of cells; indeed a recent Pubmed search on "microarray" yielded over 10,000 references, a testament to the universal appeal of this relatively new methodology. Analysis of microarray data has moved on from single gene differences to the generation of "molecular signatures" or groups of genes consistently changed between samples. However, the enormous data sets generated by these types of analyses has emphasised the importance of ever more defined cell populations in the generation of meaningful data. Recently, microarrays have been used successfully to identify consistent gene differences between populations of haemopoietic stem cells (Manfredini R, Zini R et al. 2005), and to identify genes associated with CML disease (Nowicki MO, Pawlowski P et al. 2003). The potential to identify both known and novel gene differences using microarrays, together with the ability to sort very specific cell populations (as described in chapter 3), was the rational for the experiments presented in chapter 6 of this thesis.

In an effort to gain insight into the properties of quiescent stem cells such as surface markers, receptors, and possible therapeutic targets, gene expression profiling was carried out using microarray technology. Utilising the HST and Py FACS sorting strategy developed in chapter 3, populations of viable, quiescent and cycling stem cells were isolated from normal and CML samples. Five CML

and three normal samples were sorted and processed for total RNA. Affymetrix GeneChip® U133A arrays were used and the processing carried out at the University of Glasgow. Affymetrix arrays were chosen, currently the gold standard in array technology, largely due to their stringent internal controls, which minimise the potential for false results. These data were analysed by two different methods, GeneSpring® and IGA (Iterative Group Analysis). The first level of analysis by GeneSpring generated lists of genes with fold change of >3-, >4- and >5-fold between comparative groups. Due to the large number of genes changed between samples in this study, a minimum arbitrary cut-off of 3-fold was used in the GeneSpring analysis. IGA is a recently published method of analysis generating gene groups and statistical significance of changed groups, and is particularly applicable to small data sets such as this (Breitling R, Amtmann A et al. 2004).

The largest number of genes changed in this study was between normal quiescent (G0) and cycling cells. Analysis showed that these populations exhibited significant differences in their expression profiles. One of the most interesting was the extent of cell cycle associated genes that were up-regulated in normal cycling cells compared to quiescent cells, e.g. MCM2, 4, 5, 6, and 7, CDC2, 6, 7, and 20, Cyclin A2 and E2, PCNA and CDC25. This expression profile verified the sorting strategy for the isolation of G0 and cycling cells. Interestingly, examination of the expression profile of CML G0 cells revealed that these cells were much closer in expression to both normal and CML cycling cells. Indeed a mathematical model (Euclidean distance) of the differences in gene expression of all genes (not just cell cycle genes) >3-fold changed, demonstrated that normal G0 cells exhibited the greatest differences in gene expression when compared to the other three groups.

Further analysis revealed that the differential gene expression in cell cycle genes observed for normal G0 versus cycling cells was different for CML, indicating that CML G0 cells were expressing many cell cycle associated genes, notwithstanding they appeared in the G0 sorting gate. It is possible that overexpression of the Hoechst efflux pump ABCG2 in CML cells could have placed them in the G0 gate. Initial analysis revealed a slight increase in expression of ABCG2 of 1.5-fold in the CML G0 cells compared with their cycling counterparts. However, this was associated with a false discovery rate of 11%, which suggests this finding was not universal for all samples, indicating it was unlikely to be a significant factor. In addition, ABCG2 did not appear as statistically significant in the IGA analysis.

These findings suggest that CML cells may not be quiescent in the same way that normal G0 cells are and that they already exhibit activation of a number of cell cycle genes. This could explain the results shown in chapter 3 which indicated greater cell cycle activation for CML cells in culture compared to normal cells. It may be that CML G0 cells, although they are not actively dividing, are 'primed' to go into division in a way that differs from normal stem cells.

IGA analysis of the genes up-regulated in the normal cycling versus G0 cells identified genes associated with DNA replication initiation as the most significantly changed gene group. In total, 20 gene groups were identified as significantly changed for these samples with mitosis, DNA replication and genes associated with early cell cycle events identified as the most important statistically. These data again increased confidence in the sorting methodology for isolation of cells in different phases of the cell cycle. Conversely, for the CML cycling versus G0 cells, the top changed group was genes associated with mitosis and spindle formation, later cell cycle events, than for the normal cells. These data confirm the observation in chapter 3, that in the CML samples, there were significantly more cells at the later S/G2/M phase of the cell cycle compared to normal cells, where most were in G1. IGA analysis of genes up-regulated in CML G0 versus normal G0 again identified cell cycle genes as significantly changed between these groups, indicating increased cell cycle activation in the CML G0 cells compared to normal G0. These results are in accordance with the work of other groups identifying greater cell cycle activation in CML cells (Kramer A, Loffler H et al. 2001; Kronenwett R, Butterweck U et al. 2005).

These observations suggest that strategies to induce CML quiescent cells into active cell cycle, thereby reducing resistance to drug therapy, may be relatively easy if they already exhibit activation of a number of cell cycle genes. This would result in more effective bcr-abl^{+} cell kill by STI. Anecdotal evidence that this may occur in vivo comes from studies of patients on STI therapy, who undergo concurrent stem cell mobilisation with GCSF to obtain stem cells for future autologous transplant. A recent study by Le Coutre's group has shown that following simultaneous GCSF mobilisation and STI treatment, one patient achieved a complete molecular remission, rare in patients treated with STI alone, and that most stem cell harvests were free of detectable BCR-ABL mRNA transcripts (Kreuzer KA, Kluhs C et al. 2004). Another recent study concluded that GCSF treatment increased the response to STI in 62% of patients. This also

included patients with a previous history of extended (median 22 months) STI treatment without a major cytogenetic response (CCR), notwithstanding the chances of patients achieving CCR after 12 months of therapy is extremely low. They concluded that the improved responses were due to reduced neutropenia, which allowed sustained STI treatment (Quintas-Cardama A, Kantarjian H et al. 2004). It would be difficult to reproduce these results in vitro if mobilisation from the BM is preceded by induction of cell cycle, before reverting to a quiescent state in the PB, as reported by Wright et al, and this is a factor in STI response (Wright DE, Cheshier SH et al. 2001).

Comparison of the significantly up-regulated genes in normal G0 versus cycling cells yielded a completely unexpected group of chemokine genes as the top changed group. The most significantly up-regulated chemokine genes in the quiescent cells included CXCL1, 2, 3, 6, 8, 10, 11, 13, and CCL19. Interestingly, although the ligands were up-regulated, the corresponding receptors were not. Many chemokines have been shown to play a role in both positive and negative regulation of haemopoiesis. However, cellular context and maturity almost certainly influence specific responses to individual and/or combinations of chemokines. In addition, it has been shown recently that the effects of the chemokine SDF-1 (secreted by BM cells) can selectively reverse the inhibitory effect of a range of myelosuppressive chemokines on haemopoietic progenitor cells (Broxmeyer HE, Cooper S et al. 2005). This may be one mechanism that allows differential responses in a context dependant manner and may represent a further level of proliferative control in stem cells.

To our knowledge, the significance of the up-regulation in chemokine genes identified in the microarray study in the maintenance of stem cell quiescence has not been reported and as such represents a novel finding. The differential expression observed in these samples could be a consequence of GCSF mobilisation prior to sample collection, and only a comparison with matched samples from resting BM would address this question. Other microarray studies that compared BM and MPB have not identified differences in expression of any of these chemokine genes. Either there are no differences in expression of these genes between BM and MPB, or the subsets we have sorted represent such a small proportion that their differential expression is lost in the milieu.

A possible explanation for these findings may be that quiescent cells produce these chemoattractant chemokines to recruit neutrophils, which in turn increase the local concentration of proteases and facilitate exit from the BM niche. Surprisingly, CML G0 cells also showed up-regulation of the same chemokine genes compared to their cycling counterparts, albeit at slightly lower levels than normal G0 cells. CML patients have not been exposed to GCSF, and it is interesting to speculate that perhaps this is one mechanism which allows the premature release of CML progenitors into the circulation, characteristic of CML disease. In support of this, expression of CXCR4, the receptor for SDF-1 expressed by stromal cells, was 2.9-fold lower in the quiescent CML cells than in normal G0 cells, suggesting that these cells display altered adhesive interactions, which again may promote their release into the circulation. In addition, Cashman et al documented that addition of SDF-1 to normal long-term BM cultures inhibited cell cycle entry of primitive quiescent CFC, and the addition of a CXCR4 antagonist prevented activated CFC from re-entering a quiescent state. Interestingly, this effect was not observed for CML CFC and could perhaps be explained by the lower levels of CXCR4 expression observed in this study for quiescent CML cells (Cashman J, Clark-Lewis I et al. 2002). A recent microarray study by Kronenwett et al compared $CD34^+$ cells from CML BM and PB to normal $CD34^+$ BM and GCSF mobilised PB. Although these populations are heterogeneous compared with the sorted populations we have used, they include the subsets we have separated and demonstrate certain similarities. For example, these researchers also identified enhanced cell cycle gene expression in the CML $CD34^+$ cells compared to normal $CD34^+$ cells. In addition they also identified lower expression of CXCR4 on CML CD34+ cells compared to normal (Kronenwett R, Butterweck U et al. 2005). These findings increase our confidence in the array data and further increase the significance of the novel gene expression profiles we have identified. To date there is no published data on such specifically isolated stem cell populations as those used in this study. Although sample numbers were small, sophisticated statistical methods allowed us to generate significant data sets, which also identified genes observed in other published gene lists.

One of the aims of this work was to identify possible CML targets that could be exploited in a therapeutic context. Although the analysis so far has not yielded specific gene differences that are immediately obvious as targets, the data analysis is not complete and will be subject to further investigation.

Conclusions and Future Aims

The data presented in this thesis has focused on isolation of specifically defined stem cell populations from normal and CML patients. Culture of CML stem cells has identified a population of quiescent cells resistant to a specific targeted therapy, analogous to an in vivo population known to evade this therapy. The development of FACS sorting strategies allowed separation of stem cell populations on the basis of their cell cycle position and enabled microarray analysis of these specific cell subsets. Aberrant cell cycle gene expression was identified in the CML G0 cells compared to normal cells. Importantly, a group of chemokine genes was identified as being up-regulated in quiescent cells from both normal and CML samples and signifies a novel finding which may be of major consequence in the understanding of haemopoietic stem cell biology.

The data generated by these experiments have both answered and raised a number of questions. It is clear that a quiescent phenotype, especially in malignant cells, confers certain survival advantages. It is also apparent that some therapies induce quiescence, exacerbating the problem of disease persistence. Microarray analysis has yielded a significant amount of data, which has yet to be fully analysed. The results presented in this thesis represent the first round of analysis and further work will almost certainly identify other genes of significant importance. The unexpected up-regulation of a cohort of chemokine genes in quiescent cells deserves further investigation. One of the first questions is whether this is a product of G-CSF mobilisation. This will be addressed by examining gene expression in sorted, quiescent BM stem cells, initially by real time PCR and possibly by microarrays. Independent validation of the genes identified by microarrays will be required and this will be done by real time PCR, to enable relative quantitation of gene expression. The limited amount of patient material obtained following the stringent sorting reduces the opportunities for further experimentation.

Some of these problems could be resolved by repeating the experiments in an animal model e.g. mouse. If microarray results for normal cells can be reproduced in the murine system it is anticipated that a considerable amount of data regarding normal stem cell biology would be obtained. Furthermore, these data could be used to identify possible targets in CML quiescent cells, which could be exploited

to increase the effectiveness of cytotoxic therapies. We anticipate experiments essential to verify biological function will be performed. For the chemokines identified, ELISA or protein analysis would confirm their presence in cultures of quiescent versus cycling cells. Once again the problem of limited patient material restricts the options for further experimentation, which could also be resolved by using an animal model. There is no doubt that studies which elucidate stem cell properties contribute appreciably to our understanding of malignant stem cell disease.

Bibliography

Abkowitz JL Catlin SN, et al. (2002). "Evidence that the number of hematopoietic stem cells per animal is conserved in mammals." Blood. **100**(7): 2665-7.

Ahuja HG, Jat PS, et al. (1991). "Abnormalities of the retinoblastoma gene in the pathogenesis of acute leukemia." Blood **78**: 3259-3268.

Akashi K, Traver D, et al. (2000). "A clonogenic common myeloid progenitor that gives rise to all myeloid lineages." Nature. **404**(6774): 193-7.

Allman D, Sambandam A, et al. (2003). "Thymopoiesis independent of common lymphoid progenitors." Nat Immunol. **(2)**: 168-74.

Amos TAS, Lewis JL, et al. (1995). "Apoptosis in chronic myeloid leukaemia: normal responses by progenitor cells to growth factor deprivation, X-irradiation and glucocorticoids." Br.J.Haematol. **91**: 387-393.

Amsellem S, Pflumio F, et al. (2003). "Ex vivo expansion of human hematopoietic stem cells by direct delivery of the HOXB4 homeoprotein." Nat Med. **9**(11): 1423-7.

Arai F, Hirao A, et al. (2004). "Tie2/angiopoietin-1 signalling regulates hematopoietic stem cell quiescence in the bone marrow niche." Cell. **118**(2): 149-61.

Armstrong SA, Staunton JE, et al. (2002). "MLL translocations specify a distinct gene expression profile that distinguishes a unique leukemia." Nat Genet. **30**(1): 41-7.

Barczak A, Rodriguez MW, et al. (2003). "Spotted long oligonucleotide arrays for human gene expression analysis." Genome Res. **13**(7): 1775-85.

Bartram CR, De Klein A, et al. (1983). "Translocation of c-*abl* oncogene correlates with the presence of a Philadelphia chromosome in chronic myelocytic leukaemia." Nature **306**: 277-280.

Baugh LR, Hill AA, et al. (2001). "Quantitative analysis of mRNA amplification by in vitro transcription." Nucleic Acids Res. **29**(5): E29.

Bedi A,. Zehnbauer B, et al. (1994)."Inhibition of apoptosis by BCR-ABL in chronic myeloid leukemia". Blood. **83:** 2038-2044.

Ben-Neriah Y, Daley GQ, et al. (1986). "The chronic myelogenous leukemia-specific P210 protein is the product of the bcr/abl hybrid gene." Science **233**: 212-214.

Bennett JH. (1858). "Case of hypertrophy of the spleen and liver, in which death took place from suppuration of the blood." Edinb.Med.Surg.J. **64**: 413-423.

Bhardwaj G, Murdoch B, et al. (2001). "Sonic hedgehog induces the proliferation of primitive human hematopoietic cells via BMP regulation." Nat Immunol. **2**(2): 172-80.

Bhatia M, Bonnet D, et al. (1997). "Identification of a novel CD34 negative population of primitive human hematopoietic cells capable of repopulating NOD/SCID mice". Blood. **1:** 258a.

Bhatia M, Bonnet D, et al. (1998). "A newly discovered class of human hematopoietic cells with SCID-repopulating activity." Nature Med. 4(9): 1038-1045.

Bhatia M, Bonnet D, et al. (1999). "Bone Morphogenic Proteins Regulate the Developmental Program of Human Hematopoietic Stem Cells." J. Exp. Med. **189**(7): 1139-1148.

Bhatia R, Munthe HA, et al. (2000). "Chronic myelogenous leukemia primitive hematopoietic progenitors demonstrate increased sensitivity to growth factor-induced proliferation and maturation." Exp Hematol **28**(12): 1401-12.

Bhatia R, Williams AD, et al. (2002). "Contact with fibronectin enhances preservation of normal but not chronic myelogenous leukemia primitive hematopoietic progenitors." Exp Hematol. **30**(4): 324-32.

Bhatia R, Holtz M, et al. (2003)."Persistence of malignant hematopoietic progenitors in chronic myelogenous leukemia patients in complete cytogenetic remission following imatinib mesylate treatment". Blood. **101:** 4701-4707.

Bhatia R and Verfaillie CM. (1998). "Inhibition of BCR-ABL expression with antisense oligodeoxynucleotides restores beta1 integrin-mediated adhesion and proliferation inhibition in chronic myelogenous leukemia hematopoietic progenitors." Blood **91**(9): 3414-22.

Bonnet D, Bhatia M, et al. (1999). "Cytokine treatment or accessory cells are required to initiate engraftment of purified primitive human hematopoietic cells transplanted at limiting doses into NOD/SCID mice." Bone Marrow Transplant. **3**: 203-9.

Bose, S, Deininger M, et al. (1998). "The presence of typical and atypical BCR-ABL fusion genes in leukocytes of normal individuals: biologic significance and implications for the assessment of minimal residual disease." Blood.

Bradford GB, Williams B, et al. (1997). "Quiescence, cycling, and turnover in the primitive hematopoietic stem cell compartment." Exp.Hematol. **25**: 445-453.

Breitling R, Amtmann A, et al. (2004). "Iterative Group Analysis (iGA): a simple tool to enhance sensitivity and facilitate interpretation of microarray experiments." BMC Bioinformatics **5**(1): 34.

Breitling R, Armengaud P, et al. (2004). "Rank products: a simple, yet powerful, new method to detect differentially regulated genes in replicated microarray experiments." FEBS Lett. **573**(1-3): 83-92.

Broxmeyer HE, Orschell CM, et al. (2005). "Rapid mobilization of murine and human hematopoietic stem and progenitor cells with AMD3100, a CXCR4 antagonist." J Exp Med. **201**(8): 1307-18.

Brummendorf TH, Rufer N, et al. (2001). "Limited telomere shortening in hematopoietic stem cells after transplantation." Ann N Y Acad Sci **938:** 1-7.

Brun AC, Bjornsson JM, et al. (2004). "Hoxb4-deficient mice undergo normal hematopoietic development but exhibit a mild proliferation defect in hematopoietic stem cells." Blood **103**(11): 4126-33.

Buchdunger E, Zimmermann J, et al. (1996). "Inhibition of the Abl protein-tyrosine kinase in vitro and in vivo by a 2-phenylaminopyrimidine derivative." Cancer Res **56**(1): 100-104.

Buckle AM, Mottram R, et al. (2000). "The effect of Bcr-Abl protein tyrosine kinase on maturation and proliferation of primitive haematopoietic cells". Mol Med. **10.:** 892-902.

Calvi LM, Adams GB, et al. (2003). "Osteoblastic cells regulate the haematopoietic stem cell niche." Nature. **425**(6960): 841-6.

Cheng T, Rodrigues N, et al. (2000). "Hematopoietic stem cell quiescence maintained by p21cip1/waf1." Science **287**(5459): 1804-8.

Cheshier SH, Morrison SJ, et al. (1999). "In vivo proliferation and cell cycle kinetics of long-term self-renewing hematopoietic stem cells." Proc Nat Acad Sci U S A. **96**(6): 3120-5.

Chu S, Xu H, et al. (2005). "Detection of BCR-ABL kinase mutations in CD34+ cells from chronic myelogenous leukemia patients in complete cytogenetic remission on imatinib mesylate treatment." Blood **105**(5): 2093-8.

Civin CI, Strauss LC, et al. (1984). "Antigenic analysis of hematopoiesis. III. A hematopoietic progenitor cell surface antigen defined by a monoclonal antibody raised against KG-1a cells." J.Immunol. **133**: 157-165.

Civin CI, Strauss LC, et al. (1990)."Positive stem cell selection - basic science". Bone Marrow Purging and Processing. S. Gross, A. P. Gee and D. A. Worthington-White. New York, Wiley-Liss: 387-402.

Clarkson B, Strife A, et al. (2003). "Chronic myelogenous leukemia as a paradigm of early cancer and possible curative strategies." Leukemia. **17**(7): 211-62.

Clarkson B and Strife A. (1993). "Linkage of proliferative and maturational abnormalities in chronic myelogenous leukemia and relevance to treatment." Leukemia **7**(11): 1683-1721.

Collett MS and Erikson RL. (1978). "Protein kinase activity associated with the avian sarcoma virus src gene product." Proc Natl Acad Sci U S A. **75**(4): 2021-4.

Corbin AS, Buchdunger E, et al. (2002). " Analysis of the structural basis of specificity of inhibition of the Abl kinase by STI571." J Biol Chem. **277**(35): 32214-9.

Coulombel L, Kalousek DK, et al. (1983). "Long-term marrow culture reveals chromosomally normal hematopoietic progenitor cells in patients with Philadelphia

chromosome-positive chronic myelogenous leukemia." N.Engl.J.Med. **308**: 1493-1498.

Craddock CF, Nakamoto B, et al. (1997). "Antibodies to VLA4 integrin mobilize long-term repopulating cells and augment cytokine-induced mobilization in primates and mice." Blood **90**(12): 4779-88.

Craigie D. (1858). "Case of disease of the spleen, in which death took place in consequence of the presence of purulent matter in the blood." Edinb.Med.Surg.J. **64**: 400-413.

Daga A, Podesta M, et al. (2000). "The retroviral transduction of HOXC4 into human CD34(+) cells induces an in vitro expansion of clonogenic and early progenitors." Exp Hematol. **28**(5): 569-74.

Daley GQ, Van Etten RA, et al. (1990). "Induction of chronic myelogenous leukemia in mice by the $P210^{bcr/abl}$ gene of the Philadelphia chromosome." Science **247**: 824-830.

Danet GH, Luongo JL, et al. (2002). "C1qRp defines a new human stem cell population with hematopoietic and hepatic potential." Proc Natl Acad Sci U S A. **99**(16): 10441-5.

Dao MA, Arevalo J, et al. (2003). "Reversibility of CD34 expression on human hematopoietic stem cells that retain the capacity for secondary reconstitution." Blood **101**(1): 112-8.

de Braekeleer M. (1987). "Variant Philadelphia translocations in chronic myeloid leukemia." Cytogenet.Cell Genet. **44**: 215-222.

Deininger M, Vieira S, et al. (2000). "BCR-ABL tyrosine kinase activity regulates the expression of multiple genes implicated in the pathogenesis of chronic myeloid leukaemia." Cancer Res **60**: 2049-2055.

Deininger MWN, Goldman JM, et al. (1997). "The tyrosine kinase inhibitor CGP57148B selectively inhibits the growth of BCR-ABL-positive cells." Blood **90**: 3691-3698.

Dexter TM, Allen TD, et al. (1977). "Conditions controlling the proliferation of haemopoietic stem cells in vitro." J.Cell Physiol. **91**: 335-344.

Dimri GP, Martinez JL, et al. (2002). "The Bmi-1 oncogene induces telomerase activity and immortalizes human mammary epithelial cells." Cancer Res **62**(16): 4736-45.

Donahue RE, Kirby MR, et al. (1996). "Peripheral blood $CD34^+$ cells differ from bone marrow $CD34^+$ cells in Thy-1 expression and cell cycle status in nonhuman primates mobilized or not mobilized with granulocyte colony-stimulating factor and/or stem cell factor." Blood **87**: 1644-1653.

Dooley DC, Oppenlander BK, et al. (2004). "Analysis of primitive CD34- and CD34+ hematopoietic cells from adults: gain and loss of CD34 antigen by undifferentiated cells are closely linked to proliferative status in culture." Stem Cells **22**(4): 556-69.

Down JD and Ploemacher RE. (1993). "Transient and permanent engraftment potential of murine hematopoietic stem cell subsets: differential effects of host conditioning with gamma radiation and cytotoxic drugs." Exp Hematol. **21**(7): 913-21.

Druker BJ, Tamura S, et al. (1996). "Effects of a selective inhibitor of the Abl tyrosine kinase on the growth of Bcr-Abl positive cells." Nat Med **2**: 561-566.

Duncan AW, Rattis FM, et al. (2005). "Integration of Notch and Wnt signalling in hematopoietic stem cell maintenance." Nat Immunol. **6**(3): 314-22.

Durand RE and Olive PL. (1982). "Cytotoxicity, mutagenicity and DNA damage by Hoechst 33342." The Journal of Histochemistry and Cytochemistry. **30**(2): 111-6.

Durig J, Rosenthal C, et al. (2000)."Biological effects of stroma-derived factor-1 alpha on normal and CML CD34+ haemopoietic cells". Leukemia. **14:** 1652-60.

Eaves CJ and Eaves AC. (1987)."Cell culture studies in CML". Bailliere's Clinical Haematology. K. Hinton. London, Bailliere Tindall/W.B. Saunders: 931-961.

Evsikov AV and Solter D. (2003). "Comment on " 'Stemness': transcriptional profiling of embryonic and adult stem cells" and "a stem cell molecular signature"." Science **302**(5644): 393.

Farley TJ, Ahmed T, et al. (1997). "Optimization of CD34+ cell selection using immunomagnetic beads: implications for use in cryopreserved peripheral blood stem cell collections." J Hematother **6**(1): 53-60.

Feinstein E, Cimino G, et al. (1991). " p53 in chronic myelogenous leukemia in acute phase." Proc Natl Acad Sci U S A. **88**(14): 6293-7.

Ferrao PT, Frost MJ, et al. (2003). "Overexpression of P-glycoprotein in K562 cells does not confer resistance to the growth inhibitory effects of imatinib (STI571) in vitro." Blood **102**(13): 4499-503.

Fialkow PJ, Jacobson RJ, et al. (1977). "Chronic myelocytic leukemia: Clonal origin in a stem cell common to the granulocyte, erythrocyte, platelet and monocyte/macrophage." Am.J.Med. **63**: 125-130.

Gallacher L, Murdoch B, et al. (2000). "Isolation and characterization of human CD34(-)Lin(-) and CD34(+)Lin(-) hematopoietic stem cells using cell surface markers AC133 and CD7." Blood **95**(9): 2813-20.

Goga A, McLaughlin J, et al. (1995). "Alternative signals to RAS for hematopoietic transformation by the *BCR-ABL* oncogene." Cell **82**: 981-988.

Going JJ, Keith WN, et al. (2002). "Aberrant expression of minichromosome maintenance proteins 2 and 5, and Ki-67 in dysplastic squamous oesophageal epithelium and Barrett's mucosa." Gut. **50**(3): 373-7.

Golub TR, Slonim DK, et al. (1999). "Molecular Classification of Cancer: Class Discovery and Class Prediction by Gene Expression Monitoring." Science **286**(5439): 531-537.

Goodell MA, Brose K, et al. (1996). "Isolation and functional properties of murine hematopoietic stem cells that are replicating in vivo." J.Exp.Med. **183**: 1797-1806.

Goodell MA, Rosenzweig M, et al. (1997). "Dye efflux studies suggest that hematopoietic stem cells expressing low or undetectable levels of CD34 antigen exist in multiple species." Nature Med. **3**: 1337-1345.

Gordon MY, Lewis JL, et al. (2002). "Of mice and men...and elephants." Blood **100**(13): 4679-80.

Gordon MY, Dowding CR, et al. (1987). "Altered adhesive interactions with marrow stroma of haematopoietic progenitor cells in chronic myeloid leukaemia." Nature **328**: 342-344.

Gorre ME, Mohammed M, et al. (2001). "Clinical resistance to STI-571 cancer therapy caused by BCR-ABL gene mutation or amplification." Science. **293**(5531): 876-80.

Gothot A, Pyatt R, et al. (1997). "Functional heterogeneity of human $CD34^+$ cells isolated in subcompartments of the G_0/G_1 phase of the cell cycle." Blood **90**: 4384-4393.

Graham SM, Jorgensen HG, et al. (2002). "Primitive, quiescent, Philadelphia-positive stem cells from patients with chronic myeloid leukemia are insensitive to STI571 in vitro." Blood **99**(1): 319-325.

Groffen J, Stephenson JR, et al. (1984). "Philadelphia chromosomal breakpoints are clustered within a limited region, bcr, on chromosome 22." Cell **36**: 93-99.

Gunsilius E, Duba HC, et al. (2000). "Evidence from a leukaemia model for maintenance of vascular endothelium by bone-marrow-derived endothelial cells." Lancet **355**(9216): 1688-91.

Hao QL, Zhu J, et al. (2001). "Identification of a novel, human multilymphoid progenitor in cord blood." Blood. **97**(12): 3683-90.

Harrison DE and Astle CM. (1982). "Loss of stem cell repopulating ability upon transplantation. Effects of donor age, cell number, and transplantation procedure." J Exp Med **156**(6): 1767-79.

Harrison DE and Zhong RK. (1992). "The same exhaustible multilineage precursor produces both myeloid and lymphoid cells as early as 3-4 weeks after marrow transplantation." Proc Natl Acad Sci U S A. **89**(21): 10134-8.

Heisterkamp N, Jenster G, et al. (1991). "Human bcr-abl gene has a lethal effect on embryogenesis." Transgenic Res **1**(1): 45-53.

Heisterkamp N, Jenster G, et al. (1990). "Acute leukemia in *bcr/abl* transgenic mice." Nature **344**: 251-253.

Hess DA, Meyerrose TE, et al. (2004). "Functional characterization of highly purified human hematopoietic repopulating cells isolated according to aldehyde dehydrogenase activity." Blood. **104**(6): 1648-55.

Hidalgo A, Weiss LA, et al. (2002). "Functional selectin ligands mediating human CD34(+) cell interactions with bone marrow endothelium are enhanced postnatally." J Clin Invest. **110**(4): 559-69.

Hogan CJ, Shpall EJ, et al. (2002). "Differential long-term and multilineage engraftment potential from subfractions of human CD34+ cord blood cells transplanted into NOD/SCID mice." Proc Natl Acad Sci U S A. **99**(1): 413-8.

Holtz MS, Forman SJ, et al. (2005). "Nonproliferating CML CD34(+) progenitors are resistant to apoptosis induced by a wide range of proapoptotic stimuli." Leukemia **19]**(6): 1034-41.

Holtz MS, Slovak M.L, et al. (2002). "Imatinib mesylate (STI571) inhibits growth of primitive malignant progenitors in chronic myelogenous leukemia through reversal of abnormally increased proliferation." Blood **99**(10): 3792-3800.

Holyoake T, Jiang X, et al. (1999). "Isolation of a highly quiescent subpopulation of primitive leukemic cells in chronic myeloid leukemia." Blood **94**(6): 2056-2064.

Hoover RR, Gerlach MJ, et al. (2001). "Cooperative and redundant effects of STAT5 and Ras signalling in BCR/ABL transformed hematopoietic cells." Oncogene **20**(41): 5826-35.

Horita M, Andreu E.J, et al. (2000). "Blockade of the BCR-ABL kinase activity induces apoptosis of chronic myelogenous leukaemia cells by suppressing signal transducer and activator of transcription 5-dependent expression of BCL-xL." J Exp Med **191**(6): 977-984.

Hrabe de Angelis M, McIntyre J 2nd, et al. (1997). "Maintenance of somite borders in mice requires the Delta homologue Dll1." Nature. **386**(6626): 717-21.

Huettner CS, Zhang P, et al. (2000). "Reversibility of acute B-cell leukaemia induced by BCR-ABL1." Nature Gen. **24**: 57-60.

Hughes T, Kaeda J, et al. (2002)."Molecular Responses to Imatinib (STI571) or Interferon + Ara-C as Initial Therapy for CML; Results in the IRIS Study". Blood. **100:** Abstract.

Hughes TP, Kaeda J, et al. (2003). "Frequency of major molecular responses to imatinib or interferon alfa plus cytarabine in newly diagnosed chronic myeloid leukemia." N Engl J Med. **349**(15): 1423-32.

Hunter T and Sefton BM. (1980). "Transforming gene product of Rous sarcoma virus phosphorylates tyrosine." Proc Natl Acad Sci U S A. **77**(3): 1311-5.

Ikeda S, Kishida S, et al. (1998). "Axin, a negative regulator of the Wnt signalling pathway, forms a complex with GSK-3beta and beta-catenin and promotes GSK-3beta-dependent phosphorylation of beta-catenin." EMBO J. **17**(5): 1371-84.

Ilaria RL Jr and Van Etten R. (1996). "P210 and P190(BCR/ABL) induce the tyrosine phosphorylation and DNA binding activity of multiple specific STAT family members." J Biol Chem **271**(49): 31704-10.

Illmer T, Schaich M, et al. (2004). "P-glycoprotein-mediated drug efflux is a resistance mechanism of chronic myelogenous leukemia cells to treatment with imatinib mesylate." Leukemia. **18**(3): 401-8.

Irizarry RA, Hobbs B, et al. (2003). "Exploration, normalization, and summaries of high density oligonucleotide array probe level data." Biostatistics **4**(2): 249-64.

Ivanova NB, Dimos JT, et al. (2002). "A stem cell molecular signature." Science **298**(5593): 601-4.

Iwama A, Oguro H, et al. (2004). "Enhanced self-renewal of hematopoietic stem cells mediated by the polycomb gene product Bmi-1." Immunity **21**(6): 843-51.

Jennings BA and Mills KI. (1998). "c-myc locus amplification and the acquisition of trisomy 8 in the evolution of chronic myeloid leukaemia." Leuk Res **22**(10): 899-903.

Jiang R, Lan Y, et al. (1998). "Defects in limb, craniofacial, and thymic development in Jagged2 mutant mice." Genes Dev **12**(7): 1046-57.

Jiang X, Lopez A, et al. (1999). "Autocrine production and action of IL-3 and granulocyte colony-stimulating factor in chronic myeloid leukaemia." Proceedings of the National Academy of Sciences, USA **96**(22): 12804-12809.

Jiang Y, Prosper F, et al. (2000). "Opposing effects of engagement of integrins and stimulation of cytokine receptors on cell cycle progression of normal human hematopoietic progenitors." Blood. **95**(3): 846-54.

Jiang Y, Zhao RC, et al. (2000). "Abnormal integrin-mediated regulation of chronic myelogenous leukemia CD34+ cell proliferation: BCR/ABL up-regulates the cyclin-dependent kinase inhibitor, p27Kip, which is relocated to the cell cytoplasm and incapable of regulating cdk2 activity." Proc Natl Acad Sci U S A. **97**(19): 10538-43.

Jo DY, Rafii S, et al. (2000). "Chemotaxis of primitive hematopoietic cells in response to stromal cell-derived factor-1." J Clin Invest. **105**(1): 101-11.

Jorgensen HG, Allan EK, et al. (2005). "Lonafarnib reduces the resistance of primitive quiescent CML cells to imatinib mesylate in vitro." Leukemia May 12:1-8 [Epub ahead of print].

Kamel-Reid S and Dick JE. (1988). "Engraftment of immune-deficient mice with human hematopoietic stem cells". Science. **242**(4886): 1706-9.

Kantarjian H, Sawyers C, et al. (2002). "Hematologic and cytogenetic responses to imatinib mesylate in chronic myelogenous leukemia." N Engl J Med, Erratum in: N Engl J Med 2002 Jun 13;346(24):1923. **346:** 645-52.

Kantarjian HM, O'Brien S, et al. (2003). "Imatinib mesylate therapy improves survival in patients with newly diagnosed Philadelphia chromosome-positive chronic myelogenous leukemia in the chronic phase: comparison with historic data." Cancer. **98**(12): 2636-42.

Kikuta T, Shimazaki C, et al. (2000). "Mobilization of hematopoietic primitive and committed progenitor cells into blood in mice by anti-vascular adhesion molecule-1

antibody alone or in combination with granulocyte colony-stimulating factor." Exp Hematol. **28**(3): 311-317.

King HC and Sinha AA. (2001). "Gene expression profile analysis by DNA microarrays: promise and pitfalls." JAMA. **286**(18): 2280-8.

Kishida S, Yamamoto H, et al. (1998). "Axin, a negative regulator of the wnt signalling pathway, directly interacts with adenomatous polyposis coli and regulates the stabilization of beta-catenin." J Biol Chem **273**(18): 10823-6.

Kondo M, Scherer DC, et al. (2000). "Cell-fate conversion of lymphoid-committed progenitors by instructive actions of cytokines." Nature. **407**((6802): 383-6.

Kondo M, Weissman IL, et al. (1997). "Identification of clonogenic common lymphoid progenitors in mouse bone marrow." Cell. **91**(5): 661-72.

Konopka JB, Watanabe SM, et al. (1985). "Cell lines and clinical isolates derived from Ph1-positive chronic myelogenous leukemia patients express c-abl proteins with a common structural alteration." Proc.Natl.Acad.Sci.USA **82**: 1810.

Konopka JB, Watanabe SM, et al. (1984). "An alteration of the human c-abl protein in K562 leukemia cells unmasks associated tyrosine kinase activity." Cell **37**: 1035-1042.

Koschmieder S, Gottgens B, et al. (2005). " Inducible chronic phase of myeloid leukemia with expansion of hematopoietic stem cells in a transgenic model of BCR-ABL leukemogenesis." Blood. **105**(1): 324-34.

Kramer A, Loffler H, et al. (2001). "Proliferating status of peripheral blood progenitor cells from patients with BCR/ABL-positive chronic myelogenous leukemia." Leukemia. **15:** 62-8.

Krause DS, Kapadia SU, et al. (1997). "Regulation of CD34 expression in differentiating M1 cells." Exp Hematol **25**(10): 1051-61.

Kronenwett R, Butterweck U et al (2005). "Distinct molecular phenotype of malignant CD34+ hematopoietic stem and progenitor cells in chronic myeloid leukaemia. Oncogene **24**(34): 5313-5324.

Ladd AC, Pyatt R, et al. (1997). "Orderly process of sequential cytokine stimulation is required for activation and maximal proliferation of primitive human bone marrow $CD34^+$ hematopoietic progenitor cell residing in G_o." Blood **90**: 658-668.

Laneuville P. (1995). "Abl tyrosine protein kinase." Semin Immunol **7**: 255-266.

Latt SA. (1974)."Detection of DNA synthesis in interphase nuclei by fluorescence microscopy. "J.Cell Biology. **62:** 546.

Le Coutre P, Mologni L, et al. (1999). "In vivo eradication of human BCR/ABL-positive leukemia cells with an ABL kinase inhibitor." J Natl Cancer Inst **91**: 163-168.

Le Coutre P, Tassi E, et al. (2000). "Induction of resistance to the Abelson inhibitor STI571 in human leukemic cells through gene amplification." Blood **95**(5): 1758-66.

Lessard J and Sauvageau G. (2003). "Bmi-1 determines the proliferative capacity of normal and leukaemic stem cells." Nature. **423**(6937): 255-60.

Levesque JP, Hendy J, et al. (2003). "Disruption of the CXCR4/CXCL12 chemotactic interaction during hematopoietic stem cell mobilization induced by GCSF or cyclophosphamide." J Clin Invest **111**(2): 187-96.

Li X, Dancausse H, et al. (2003)."Labeling Schwann cells with CFSE-an in vitro and in vivo study." J Neurosci Methods. **125::** 83-91.

Ling X, Ma G, et al. (2003). "Bcr and Abl interaction: oncogenic activation of c-Abl by sequestering Bcr." Cancer Res **63**(2): 298-303.

Loewe H and Urbanietz J. (1974)."Basisch substitutierte 2.6-bis-benzimidazol-derivate, eine neue chemotherapeutisch active korperklasse." Arzneimforsch. **24:** 478.

Loontiens FG, Regenfuss P, et al. (1990)."Binding characteristics of Hoechst 33258 with calf thymus DNA, poly [d(A-T)], and d(CCGGAATTCCGG): multiple stoichiometries and determination of tight binding with a wide spectrum of site affinities." Biochemistry. **29:** 9029-39.

Lozzio CB and Lozzio BB. (1975). "Human chronic myelogenous leukemia cell-line with positive Philadelphia chromosome." Blood **45**(3): 321-34.

Lugo TG, Pendergast AM, et al. (1990). "Tyrosine kinase activity and transformation potency of *bcr-abl* oncogene products." Science **247**: 1079-1082.

Lyons AB and Parish CR. (1994). "Determination of lymphocyte division by flow cytometry." J.Immunol.Methods **171**: 131-137.

Ma Q, Jones D, et al. (1999). "The chemokine receptor CXCR4 is required for the retention of B lineage and granulocytic precursors within the bone marrow microenvironment." Immunity **4**: 463-71.

Ma Q, Jones D, et al. (1998). " Impaired B-lymphopoiesis, myelopoiesis, and derailed cerebellar neuron migration in CXCR4- and SDF-1-deficient mice." Proc Natl Acad Sci U S A. **95**(16): 9448-53.

Mahmud N, Devine SM, et al. (2001). "The relative quiescence of hematopoietic stem cells in nonhuman primates." Blood **97**(10): 3061-8.

Mahon FX, Belloc F, et al. (2003). "MDR1 gene overexpression confers resistance to imatinib mesylate in leukemia cell line models." Blood. **101**(6): :2368-73.

McWhirter JR and Wang JY. (1993). "An actin-binding function contributes to transformation by the Bcr-Abl oncoprotein of Philadelphia chromosome-positive human leukemias." EMBO J **12**: 1533-1546.

Melo J. (1996). "The diversity of Bcr-Abl fusion proteins and their relationship to leukaemia phenotype." Blood **88**: 2375-2384.

Melo JV and Deininger MW. (2004). "Biology of chronic myelogenous leukemia--signalling pathways of initiation and transformation." Hematol Oncol Clin North Am **18**(3): 545-68.

Melo JV, Gordon D.E, et al. (1993). "The ABL-BCR fusion gene is expressed in chronic myeloid leukemia." Blood **81**: 158-165.

Meydan N, Grunberger T, et al. (1996). " Inhibition of acute lymphoblastic leukaemia by a Jak-2 inhibitor." Nature. **379**(6566): 645-8.

Montecino-Rodriguez E, Leathers H, et al. (2001). "Bipotential B-macrophage progenitors are present in adult bone marrow." Nat Immunol. **1**: 83-8.

Morrison SJ and Weissman IL. (1994). "The long-term repopulating subset of hematopoietic stem cells is deterministic and isolatable by phenotype." Immunity **1**(8): 661-73.

Morrison SJ, Wandycz AM, et al. (1997). "Identification of a lineage of multipotent hematopoietic progenitors." Development. **124**(10): 1929-39.

Morrison SJ, Prowse KR, et al. (1996). "Telomerase activity in hematopoietic cells is associated with self-renewal potential." Immunity **5**: 207-216.

Morrison SJ and Weissman IL. (1994). "The long-term repopulating subset of hematopoietic stem cells is deterministic and isolatable by phenotype." Immunity **1**: 661-673.

Nagar B, Bornmann WG, et al. (2002). "Crystal structures of the kinase domain of c-Abl in complex with the small molecule inhibitors PD173955 and imatinib (STI-571)." Cancer Res. **62**(15): 4236-43.

Nagasawa T, Hirota S, et al. (1996). "Defects of B-cell lymphopoiesis and bone-marrow myelopoiesis in mice lacking the CXC chemokine PBSF/SDF-1." Nature. **382**(6592): 635-8.

Neves H, Ramos C, et al. (1999). "The nuclear topography of ABL, BCR, PML, and RARalpha genes: evidence for gene proximity in specific phases of the cell cycle and stages of hematopoietic differentiation." Blood **93**(4): 1197-207.

Nilsson SK, Johnston HM, et al. (2001). "Spatial localization of transplanted hemopoietic stem cells: inferences for the localization of stem cell niches." Blood. **97**(8): 2293-9.

Nowell PC and Hungerford DA. (1960). "A minute chromosome in human chronic granulocytic leukemia." Science **132**: 1497-1501.

Okuno Y, Huettner CS, et al. (2002). "Distal elements are critical for human CD34 expression in vivo." Blood. **100**(13): 4420-6.

Okuno Y, Iwasaki H, et al. (2002). "Differential regulation of the human and murine CD34 genes in hematopoietic stem cells." Proc Natl Acad Sci U S A. **99**(9): 6246-51.

Orlando V. (2003). "Polycomb, epigenomes, and control of cell identity." Cell. **112**(5): 599-606.

Osawa M, Hanada K, et al. (1996). "Long-term lymphohematopoietic reconstitution by a single CD34-low/negative hematopoietic stem cell." Science **273**: 242-245.

Pang L, Reddy PV, et al. (2003). "Studies on BrdU labeling of hematopoietic cells: stem cells and cell lines." J Cell Physiol **197**(2): 251-60.

Park IK, Qian D, et al. (2003). "Bmi-1 is required for maintenance of adult self-renewing haematopoietic stem cells." Nature **423**(6937): 302-5.

Patel OV, Suchyta SP, et al. (2005). "Validation and application of a high fidelity mRNA linear amplification procedure for profiling gene expression." Vet Immunol Immunopathol **105**(3-4): 331-42.

Pear WS, Miller JP, et al. (1998). "Efficient and rapid induction of a chronic myelogenous leukaemia-like myeloproliferative disease in mice receiving aP210 bcr/abl-transduced bone marrow." Blood **92**: 3780-3792.

Peled A, Hardan I, et al. (2002)."Immature leukemic CD34+CXCR4+ cells from CML patients have lower integrin-dependent migration and adhesion in response to the chemokine SDF-1." Stem Cells. **20:** 259-66.

Peled A, Petit I, et al. (1999). "Dependence of human stem cell engraftment and repopulation of NOD/SCID mice on CXCR4." Science **283**(5403): 845-8.

Pendergast AM, Gishizky ML, et al. (1993). "SH1 domain autophosphorylation of P210 BCR/ABL is required for transformation but not growth factor independence." Mol.Cell.Biol. **13**: 1728-1736.

Peng B, Hayes M, et al. (2004)."Pharmacokinetics and pharmacodynamics of imatinib in a phase I trial with chronic myeloid leukemia patients. "J Clin Oncol. **22:** 935-42.

Peters DG, Hoover RR, et al. (2001). "Activity of the farnesyl protein transferase inhibitor SCH66336 against BCR/ABL-induced murine leukaemia and primary cells from patients with chronic myeloid leukaemia." Blood **97**: 1404-1412.

Petit I, Szyper-Kravitz M, et al. (2002). "G-CSF induces stem cell mobilization by decreasing bone marrow SDF-1 and up-regulating CXCR4." Nat Immunol. **3**(7): 687-94 Erratum in: Nat Immunol 2002 Aug;3(8):787.

Phillips RL, Ernst RE, et al. (2000). "The Genetic Program of Hematopoietic Stem Cells." Science **288**(5471): 1635-1640.

Pierce A, Spooncer E, et al. (2002). "BCR-ABL alters the proliferation and differentiation response of multipotent hematopoietic cells to stem cell factor." Oncogene. **21:**((19)): 3068-75.

Ploemacher RE and Brons NHC. (1988). "Isolation of hemopoietic stem cell subsets from murine bone marrow: II. Evidence for an early precursor of day-12 CFU-S and cells associated with radioprotective ability." Exp.Hematol. **16**: 27-32.

Ploemacher RE, Van Der Sluijs JP, et al. (1989). "An in vitro limiting-dilution assay of long-term repopulating hematopoietic stem cells in the mouse." Blood **74**: 2755-2763.

Pluk H, Dorey K, et al. (2002). "Autoinhibition of c-Abl." Cell. **108**(2): 247-59.

Ponchio L, Conneally E, et al. (1995). "Quantitation of the quiescent fraction of long-term culture-initiating cells (LTC-IC) in normal human blood and marrow and the kinetics of their growth factor-stimulated entry into S-phase in vitro." Blood **86**: 3314-3321.

Ponchio L and Eaves C.J. (1995)."Very primitive hematopoietic cells (LTC-IC) in normal adult human blood and marrow show differences in the regulation of their cycling state." Blood. **1:** 493a.

Pui JC, Allman D, et al. (1999). "Notch1 expression in early lymphopoiesis influences B versus T lineage determination." Immunity. **11**(3): 299-308.

Puil NL, Liu J, et al. (1994). "Bcr-Abl oncoproteins bind directly to activators of the ras signalling pathway." EMBO J. **13**: 764-773.

Ramalho-Santos M, Yoon S, et al. (2002). " "Stemness": transcriptional profiling of embryonic and adult stem cells." Science. **298**(5593): 597-600.

Reichert A, Heisterkamp N, et al. (2001). "Treatment of Bcr/Abl-positive acute lymphoblastic leukemia in P190 transgenic mice with the farnesyl transferase inhibitor SCH66336." Blood. **97**(5): 1399-403.

Reya T. (2003). "Regulation of hematopoietic stem cell self-renewal." Recent Prog Horm Res **58**: 283-95.

Reya T, Duncan AW, et al. (2003). "A role for Wnt signalling in self-renewal of haematopoietic stem cells." Nature. **423**(6938): 409-14.

Richmond LJ, Alcorn MJ, et al. (2002)."CML leukapheresis products can be enriched for CD34+ cells and simultaneously depleted of CD15+ cells using a simple Ab cocktail. "Cytotherapy. **4:** 407-13.

Rodeck U. (1993). "Growth factor independence and growth regulatory pathways in human melanoma development." Cancer Metastasis Rev. **(3-4):**(Sep;12): 219-26.

Rolink AG, Nutt SL, et al. (1999). "Long-term in vivo reconstitution of T-cell development by Pax5-deficient B-cell progenitors." Nature **401**(6753): 603-6.

Rosenberg N, Baltimore D, et al. (1975). "In vitro transformation of lymphoid cells by Abelson murine leukemia virus." Proc Natl Acad Sci U S A. **75**(5): 1932-6.

Rowley JD. (1973). "A new consistent chromosomal abnormality in chronic myelogenous leukaemia identified by quinacrine fluorescence and Giemsa staining." Nature **243**: 290-293.

Rozman C, Urbano-Ispizua A, et al. (1995). "Analysis of the clinical relevance of the breakpoint location within M-BCR and the type of chimeric mRNA in chronic myelogenous leukemia." Leukemia. **9**(6): 1104-7.

Saeland S, Duvert V, et al. (1992). "Distribution of surface-membrane molecules on bone marrow and cord blood CD34$^+$ hematopoietic cells." Exp.Hematol. **20**: 24-33.

Salgia R, Li JL, et al. (1997). "BCR/ABL induces multiple abnormalities of cytoskeletal function." J Clin Invest **100**: 46-57.

Sato T, Laver JH, et al. (1999). "Reversible expression of CD34 by murine hematopoietic stem cells." Blood **94**(8): 2548-2554.

Sauvageau G, Thorsteinsdottir U, et al. (1995). "Overexpression of HOXB4 in hematopoietic cells causes the selective expansion of more primitive populations *in vitro* and *in vivo*." Genes Dev. **9**: 1753-1765.

Sawyers CL. (1999). "Chronic Myeloid Leukemia." N Eng J Med **340**(17): 1330-1340.

Sawyers CL, Hochhaus A, et al. (2002)."Imatinib induces hematologic and cytogenetic responses in patients with chronic myelogenous leukemia in myeloid blast crisis: results of a phase II study." Blood. **99:** 3530-9.

Scharenberg CW, Harkey MA, et al. (2002)."The ABCG2 transporter is an efficient Hoechst 33342 efflux pump and is preferentially expressed by immature human hematopoietic progenitors." Blood. **99:** 507-512.

Scher CD and Siegler R. (1975). "Direct transformation of 3T3 cells by Abelson murine leukemia virus." Nature **253**: 729-731.

Schwartzberg PL, Stall AM, et al. (1991). "Mice homozygous for the abl^{m1} mutation show poor viability and depletion of selective B and T cell populations." Cell **65**: 1165-1175.

Senechal K, Halpern J, et al. (1996). "The CRKL adaptor protein transforms fibroblasts and functions in transformation by the BCR-ABL oncogene." J Biol Chem **271**(38): 23255-61.

Sensebe L, Deschaseaux M, et al. (1997). "The broad spectrum of cytokine gene expression by myeloid cells from the human marrow microenvironment." Stem Cells **15**(2): 133-43.

Shah NP, Nicoll JM, et al. (2002). "Multiple BCR-ABL kinase domain mutations confer polyclonal resistance to the tyrosine kinase inhibitor imatinib (STI571) in chronic phase and blast crisis chronic myeloid leukemia." Cancer Cells **2**(2): 117-25.

Shapiro HM. (1981). "Flow Cytometric Estimation of DNA and RNA content in intact cells stained with Hoechst 33342 and Pyronin Y." Cytometry **2**: 143-150.

Shtivelman E, Lifshitz B, et al. (1985). "Fused transcript of abl and bcr genes in chronic myelogenous leukaemia." Nature **315**: 550-554.

Sill H, Goldman JM, et al. (1995). "Homozygous deletions of the p16 tumor-suppressor gene are associated with lymphoid transformation of chronic myeloid leukemia." Blood **85**(8): 2013-6.

Silver RT, Woolf SH, et al. (1999). "An evidence-based analysis of the effect of busulfan, hydroxyurea, interferon, and allogeneic bone marrow transplantation in treating the chronic phase of chronic myeloid leukemia: developed for the American Society of Hematology." Blood **94**(5): 1517-36.

Skorski T, Bellacosa A, et al. (1997). "Transformation of hematopoietic cells by BCR/ABL requires activation of a PI-3k/Akt-dependent pathway." EMBO J **16**: 6151-6161.

Spangrude GJ, Heimfeld S, et al. (1988). "Purification and characterization of mouse hematopoietic stem cells." Science **241**: 58-62.

Spiers ASD. (1977). "The clinical features of chronic granulocytic leukaemia." Clin.Haematol. **6**: 77-95.

Steidl U, Kronenwett R, et al. (2002). "Gene expression profiling identifies significant differences between the molecular phenotypes of bone marrow-derived and circulating human CD34+ hematopoietic stem cells." Blood **99**(6): 2037-2044.

Storms RW, Trujillo AP, et al. (1999). "Isolation of primitive human hematopoietic progenitors on the basis of aldehyde dehydrogenase activity." Proc Natl Acad Sci U S A. **96**(16): 9118-23.

Szilvassy SJ, Humphries RK, et al. (1990). "Quantitative assay for totipotent reconstituting hematopoietic stem cells by a competitive repopulation strategy." Proc.Natl.Acad.Sci.USA **87**: 8736-8740.

Taagepera S, McDonald D, et al. (1998). "Nuclear-cytoplasmic shuttling of C-ABL tyrosine kinase." Proc Natl Acad Sci U S A. **95**(13): 7457-62.

Taylor E. (1965). "The mechanism of colchicine inhibition of mitosis. 1. The kinetics of inhibition and the binding of H3-colchicine." J Cell Biol SUPPL:145-60.

Thijsen S, Schuurhuis G, et al. (1999). "Chronic myeloid leukemia from basics to bedside." Leukemia **13**(11): 1646-74.

Thomas J, Wang L, et al. (2004). "Active transport of imatinib into and out of cells: implications for drug resistance." Blood **104**(12): 3739-45.

Till JE and McCulloch E.A. (1961). "A direct measurement of the radiation sensitivity of normal mouse bone marrow cells." Radiat.Res. **14**: 213-222.

Tipping AJ, Mahon FX, et al. (2001). "Restoration of sensitivity to STI571 in STI571-resistant chronic myeloid leukemia cells." Blood. **98**(13): 3864-7.

Traxler P, Bold G, et al. (2001). "Tyrosine kinase inhibitors: from rational design to clinical trials." Med Res Rev. **21**(6): :499-512.

Traycoff CM, Halstead B, et al. (1998). "Chronic myelogenous leukaemia $CD34^+$ cells exit G_0/G_1 phases of cell cycle more rapidly than normal marrow $CD34^+$ cells." Br.J.Haematol. **102**: 759-767.

Uchida N, He D, et al. (1997). "The Unexpected G0/G1 Cell Cycle Status of Mobilized Hematopoietic Stem Cells From Peripheral Blood." Blood **89**(2): 465-472.

Udomsakdi C, Eaves CJ, et al. (1992). "Rapid decline of chronic myeloid leukemic cells in long-term culture due to a defect at the leukemic stem cell level." Proc.Natl.Acad.Sci.USA **89**: 6192-6196.

Van Etten RA. (1999). "Cycling, stressed-out and nervous: cellular functions of c-Abl." Trends Cell Biol. **9**: 179-186.

Varnum-Finney B, Brashem-Stein C, et al. (2003). "Combined effects of Notch signalling and cytokines induce a multiple log increase in precursors with lymphoid and myeloid reconstituting ability." Blood **101**(5): 1784-9.

Varnum-Finney B, Xu L, et al. (2000). "Pluripotent, cytokine-dependent, hematopoietic stem cells are immortalized by constitutive Notch1 signalling." Nat Med. **6**(11): 1278-81.

Vassilopoulos G, Wang PR, et al. (2003). "Transplanted bone marrow regenerates liver by cell fusion." Nature **422**(6934): 901-4.

Verfaillie CM, McCarthy JB, et al. (1992). "Mechanisms underlying abnormal trafficking of malignant progenitors in chronic myelogenous leukemia." J.Clin.Invest. **90**: 1232-1241.

Vigneri P and Wang JY. (2001). "Induction of apoptosis in chronic myelogenous leukemia cells through nuclear entrapment of BCR-ABL tyrosine kinase." Nat Med **7**(2): 228-34.

Virchow R. (1845). "Weisses blut." Froriep's.Notizen. **36**: 151-156.

Voncken JW, van Schaick H, et al. (1995). "Increased neutrophil respiratory burst in bcr-null mutants." Cell **80**(5): 719-28.

Voss J, Posern G, et al. (2000). "The leukaemic oncoproteins Bcr-Abl and Tel-Abl (ETV6/Abl) have altered substrate preferences and activate similar intracellular signalling pathways." Oncogene **19**(13): 1684-90.

Wagers AJ and Weissman IL. (2004). "Plasticity of adult stem cells." Cell **116**(5): 639-48.

Wagers AJ, Sherwood RI, et al. (2002). "Little evidence for developmental plasticity of adult hematopoietic stem cells." Science **297**(5590): 2256-9.

Wen ST, Jackson PK, et al. (1996). "The cytostatic function of c-Abl is controlled by multiple nuclear localization signals and requires the p53 and Rb tumor suppressor gene products." EMBO J **15**(7): 1583-95.

Witte O. (2001). "The role of Bcr-Abl in chronic myeloid leukemia and stem cell biology." Semin Hematol. **38(3 Suppl 8)**: 3-8.

Witte ON, Goff S, et al. (1980). "A transformation-defective mutant of Abelson murine leukemia virus lacks protein kinase activity." Proc Natl Acad Sci U S A. **77**(8): 4993-7.

Witte ON, Rosenberg N, et al. (1979). "Preparation of syngeneic tumor regressor serum reactive with the unique determinants of the Abelson murine leukemia virus-encoded P120 protein at the cell surface." J Virol **31**(3): 776-84.

Witte ON, Rosenberg NE, et al. (1979). "A normal cell protein cross-reactive to the major Abelson murine leukaemia virus gene product." Nature. **281**(5730): 396-8.

Wright DE, Cheshier SH, et al. (2001). "Cyclophosphamide/granulocyte colony-stimulating factor causes selective mobilization of bone marrow hematopoietic stem cells into the blood after M phase of the cell cycle." Blood **97**(8): 2278-85.

Xue Y, Gao X, et al. (1999). "Embryonic lethality and vascular defects in mice lacking the Notch ligand Jagged1." Hum Mol Genet **8**(5): 723-30.

Yaish P, Gazit A, et al. (1988). "Blocking of EGF-dependent cell proliferation by EGF receptor kinase inhibitors." Science **242**(4880): 933-5.

Yin AH, Miraglia S, et al. (1997). "AC133, a Novel Marker for Human Hematopoietic Stem and Progenitor Cells." Blood **90**(12): 5002-5012.

Yuan Y, Shen H, et al. (2004). "In vivo self-renewing divisions of haematopoietic stem cells are increased in the absence of the early G1-phase inhibitor, p18INK4C." Nat Cell Biol **6**(5): 436-42.

Zanjani ED, Almeida-Porada G, et al. (2003). "Reversible expression of CD34 by adult human bone marrow long-term engrafting hematopoietic stem cells." Exp Hematol **31**(5): 406-12.

Zanjani ED, Flake AW, et al. (1999). "Homing of human cells in the fetal sheep model: modulation by antibodies activating or inhibiting very late activation antigen-4-dependent function." Blood **94**(4): 2515-22.

Zanjani ED, Flake AW, et al. (1994). "Long-term repopulating ability of xenogeneic transplanted human fetal liver hematopoietic stem cells in sheep." J.Clin.Invest. **93**: 1051-1055.

Zhang J, Niu C, et al. (2003). "Identification of the haematopoietic stem cell niche and control of the niche size." Nature. **425**(6960): 836-41.

Zhang, X and Ren R. (1998). "BCR-ABL efficiently induces a myeloproliferative disease and production of excess interleukin-3 and granulocyte-macrophage colony-stimulating factor in mice: a novel model for chronic myelogenous leukemia." Blood **92**(10): 3829-3840.

Zhao R, Fan E, et al. (1999). "Introduction of BCR/ABL in normal CD34+ cells recreates the phenotype characteristics of CML." Blood **94**: 388A(abstr).

Ziegler BL, Valtieri M, et al. (1999). " KDR receptor: a key marker defining hematopoietic stem cells." Science **285**(5433): 1553-8.

Appendix 1

Experiment report

Software

This refers to software that actually runs the whole analysis automatically. In particular it:

- • Generates a directory structure for a project and its experiments
- • Manages the security of the project
- • Performs *RMA* low-level analysis
- • Performs *RP* identification of differentially expressed genes for a number of between-group comparisons
- • Functionally annotates the list of *RP*-identified top genes
- • Performs *iGA* to find differentially expressed functional classes of genes (written by Rainer Breitling).
- • Presents the *RP* and *iGA* results in form of web pages and/or downloadable tab-delimited text files suitable for reading in Excel.

The software has been written and implemented by Pawel Herzyk in the Autumn 2003 – Spring 2004.

Project

Project refers to data that belongs to a particular researcher or a group of researchers. Each PI (principal investigator) can only have one project that can be divided into many experiments. Each project has associated:

- • **Name** - this is usually constructed from the PI's name e.g. `john_dav` would be a name of a project owned by John Davis.
- • **Class** - this could be `Microarray` or `Proteomics`
- • **Type** - e.g. `Affymetrix` or `Spotted` depending on the type of microarrays used

Experiment

Each project can be divided into experiments. Each experiment contains data from a number of replicated (or not) samples corresponding to different conditions.

Array

This refers to an identifiable type of array e.g. `U133` is the Affymetrix human array HG-U133.

Chip

Some Affymetrix arrays may consist of several subarrays. E.g. HG-U133 array is in fact represented by two arrays HG-U133A and HG-U133B. In this case we say that the array has two chips A and B. If the array has only one chip it is denoted as N (for none).

Normalisation
This really is a shorthand for low-level analysis. In case of Affymetrix data this consists of

- Background correction
- Multichip normalisation on the probe level
- Summary of the log-normalised probe level data into a probe-set level data

By default we use Robust Multichip Average (RMA) method implemented in module Affy in the Bioconductor microarray analysis software.

Differential Expression
A method of identification of differentially expressed genes between two groups of replicated samples. We use the RankProducts method(RP) developed in University of Glasgow.

Differentialy expressed gene classes
A method for identification of functional gene classes that are differentially expressed in a given comparison. We use the Iterative Group Analysis method developed in the University of Glasgow.

Baseline
For every comparison between two groups of replicated samples we select one of the groups as a reference (baseline). This is usually done upon suggestion from a researcher who owns the data.

Treatment
This refers to the group of replicated samples that has not been selected as baseline. The software analyses the expression of a treatment group with respect to the baseline.

Direction
This refers to the direction of the differential expression of the treatment with respect to the baseline:

- *Positive* - means a list of genes with significantly higher expression in the treatment group than in the baseline group
- *Negative* - means a list of genes with significantly lower expression in the treatment group than in the baseline group

RPhtml
Results of RP in html format

RPtext
Results of RP in tab-delimited text format

iGAcla
Results of iGA in **Classic** mode (html format). Look at paragraph **Mode** in section **iGA report** for more explanations.

iGArep
Results of iGA in **Representative** mode (html format). Look at paragraph **Mode** in section **iGA report** for more explanations.

RP report

Comparison
This refers to a comparison between two groups of replicated samples. E.g.: *Samples: A,B,C vs Samples: D,E,F* means that samples A,B,C correspond to the *treatment* group and D,E,F correspond to the *baseline* group.
Probe-set ID
The Affymetrix probe-set identificator
RPscore
This is a measure of differential expression calculated by the RP method. For every gene this is calculated as a geometric mean of fold-change ranks over the number of all possible between-chip comparisons contributing to a given between-group comparison.
FDR
This is a conservative estimate of False Discovery Rate. If you cut the differentially expressed gene-list at the particular position associated with a particular FDR then it shows the expected percentage of false positives.
FCrma
Before FunAlyse version 1.4.1 this is a mean fold-change over all possible between-chip comparisons contributing to a given between-group comparison.
From FunAlyse version 1.4.1 onwards this is calculated as an antilog of a mean log-fold-change over all possible between-chip comparisons contributing to a given between-group comparison.
In both cases if you have two groups of three Affymetrix chips the FCrma is calculated over all nine comparisons.
FCnom
It has been demonstrated in the experiment where selected genes were spiked-in at known concentrations on the HG-U95A chip that the fold-changes calculated after RMA low-level analysis are significantly lower than the nominal fold-changes calculated from the spiked-in gene concentrations. The relation between these two fold-changes was calculated by a fitting procedure:
log2(rma FC) = 0.61 x log2(nominal FC)
Consequently, the FCnom corresponds to the mean nominal fold-change obtained from the rma fold-changes using the above equation over all possible between-chip comparisons contributing to a given between-group comparison. Please, treat it with caution as it is not known how universal the above equation is. Consult Figure 6 in the original paper Cope et al. 2003 (PubMed abstract).
Gene annotation database
This is a database that contains functional annotation of your genes. Every gene in the reported list of differentially expressed genes has a hyperlink to it. Currently, we use the following databases:

- Human, Mouse and Rat - SOURCE database
- *Arabidopsis* - MIPS and TAIR databases
- *Drosophila* - FlyBase
- Yeast - SGD database

Gene symbol
Common gene symbol used by biologists.
Gene ID
Publicly used gene identificator.
Title
Short functional annotation of a gene. This is very brief, you shouldn't rely on it too much.

iGA report

Mode
The iGA module in the FunAlyse software can work in two modes: **Classic** - all probe-sets on the chip are taking part in the iGA calculations. **Representative** - only one probe-set per gene is selected. This is to remove a bias towards a particular groups in case more then one probe-set represent a gene contributing to this group. A probe set producing the best **RPscore** in a given comparison (calculated seperately for positive and negative expression) is selected as a *representative* for that gene. The non-redundant set of genes is defined differently for different organisms. For Human, Mouse and Rat they are defined using *Unigene IDs*, for Arabidopsis and Yeast they are defined on the base of *gene IDs* whilst for Drosophila it is based on *gene symbols*.
Number of probe-sets on the chip
A number of Affymetrix probe-sets on a given chip. In the **Classic** mode some probe-sets may refer to the same gene.
Number of annotated probe-sets
A number of probe-sets on a given chip that have functional annotation in the current Affymetrix annotation file that has been used for functional group construction.
Number of groups
A total number of functionally annotated gene-groups. They are pre-constructed independently of the microarray experiment. Usually we use GeneOntology (GO) annotations present in the Affymetrix annotation file but you may advise us to use other annotation sources.
Number of singletons
A number of functionally annotated gene-groups that contain a single gene. These are not particularly useful for iGA.
Significance threshold
A threshold for **P-value changed**. P-values lower than the threshold are considered statistically significant. (see also *P-value changed*)
File Name
A name of the input file that contains full list of genes sorted by RankProducts score **RPscore** that is our measure of gene differential expression.
Annotations
This is a name of the Affymetrix functional annotation file used for the functional group construction.
Top changed groups

A list of significantly differentially expressed gene-groups.

Group Members

Number of probe-sets that belong to a particular group.

Changed Members

Number of **group members** that have actually contributed to achieving a given **P-value changed** for this group.

P-value changed

This tells you what is a probability of a random event that 'that many' of **changed members** out of 'that many' **group members** has been found 'that high' on the RP list of 'that many' sorted genes. This is calculated from the hyper-geometric distribution. Consult Figure 1 in the original paper

P-value

Going down from the top of the RP list, for every encountered subset of a particular gene group we calculate the p-value that tells you how probable a random event is that such subset was found 'that high' on the RP list. This is calculated from the hyper-geometric distribution. In this context **P-value changed** is a smallest p-value over all the above subsets. Consult Figure 1 in the original paper

Percent changed

This is simply *changed members* over *group members* times 100.

Rank

This is rank of a particular gene in the list of differentially expressed genes. This list was created from the RP list by exclusion of genes that are not assigned to the functional gene-groups.

iGA report on the differentially expressed functional gene classes: *up-regulated CML G0 vs Normal G0*

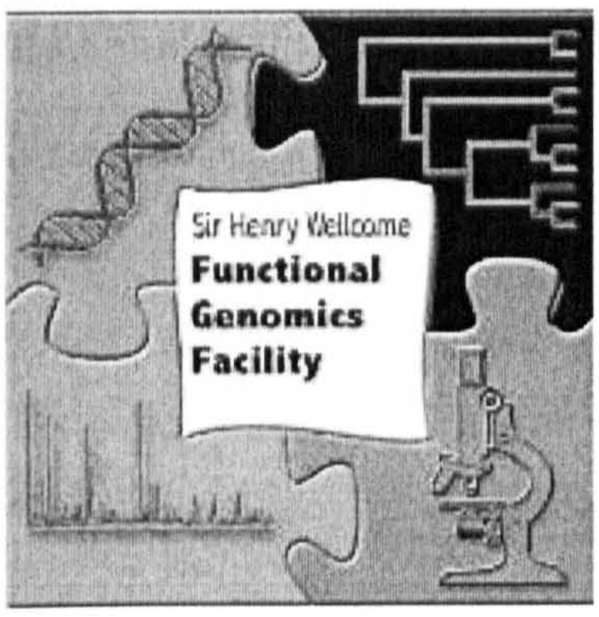

General Information	
Mode	Representative
Number of genes on chip	12698
Number of annotated genes	9533
Number of groups	3991
Number of singletons	1649
Significance threshold	2.5e-04
File name	**↑CML G0 Vs N G0**

Top Changed Groups	Group Members	Changed Members	P-Value Changed	Percent Changed
5833 - hemoglobin complex	9	3	5.7e-10	33.33
15671 - oxygen transport	9	3	5.7e-10	33.33
5344 - oxygen transporter activity	11	3	1.1e-09	27.27
7067 - mitosis	74	9	7.7e-09	12.16
5819 - spindle	11	4	1.5e-06	36.36
79 - regulation of cyclin dependent protein kinase activity	34	5	3.0e-06	14.71
6260 - DNA replication	76	7	9.8e-06	9.21
9440 - cyanate catabolism	2	2	4.4e-05	100.00
4792 - thiosulfate sulfurtransferase activity	2	2	4.4e-05	100.00
5638 - lamin filament	2	2	2.3e-04	100.00
9113 - purine base biosynthesis	4	4	2.4e-04	100.00

Changed group breakdown:

Group	P-value	Probe-set ID	Rank	Gene ID	Gene Symbol	Title
5833 - hemoglobin complex	9.4e-04	209116_x_at	1	M25079	HBB	hemoglobin, beta
	7.9e-07	213515_x_at	2	AI133353	HBG1	hemoglobin, gamma A
show the whole group	5.7e-10	206834_at	3	NM_000519	HBD	hemoglobin, delta

15671 - oxygen transport	9.4e-04	209116_x_at	1	M25079	HBB	hemoglobin, beta
	7.9e-07	213515_x_at	2	AI133353	HBG1	hemoglobin, gamma A
show the whole group	5.7e-10	206834_at	3	NM_000519	HBD	hemoglobin, delta
5344 - oxygen transporter activity	1.2e-03	209116_x_at	1	M25079	HBB	hemoglobin, beta
	1.2e-06	213515_x_at	2	AI133353	HBG1	hemoglobin, gamma A
show the whole group	1.1e-09	206834_at	3	NM_000519	HBD	hemoglobin, delta
7067 - mitosis	8.9e-02	202870_s_at	12	NM_001255	CDC20	CDC20 cell division cycle 20 homolog (S. cerevisiae)
	1.0e-02	202705_at	20	NM_004701	CCNB2	cyclin B2
	1.3e-03	203213_at	28	AL524035	CDC2	cell division cycle 2, G1 to S and G2 to M
	2.0e-04	219306_at	38	NM_020242	KNSL7	kinesin-like 7
	3.6e-05	204240_s_at	49	NM_006444	SMC2L1	SMC2 structural maintenance of chromosomes 2-like 1 (yeast)
	2.7e-06	203968_s_at	52	NM_001254	CDC6	CDC6 cell division cycle 6 homolog (S. cerevisiae)
	1.9e-07	204695_at	55	AI343459	CDC25A	cell division cycle 25A
	1.1e-08	218662_s_at	57	NM_022346	HCAP-G	chromosome condensation protein G
show the whole group	7.7e-09	209642_at	78	AF043294	BUB1	BUB1 budding uninhibited by benzimidazoles 1 homolog (yeast)
5819 - spindle	1.4e-02	202870_s_at	12	NM_001255	CDC20	CDC20 cell division cycle 20 homolog (S. cerevisiae)
	5.5e-04	207828_s_at	31	NM_005196	CENPF	centromere protein F, 350/400ka (mitosin)
	3.6e-05	204444_at	59	NM_004523	KIF11	kinesin family member 11
show the whole group	1.5e-06	217879_at	81	AL566824	CDC27	cell division cycle 27
79 - regulation of cyclin dependent protein kinase activity	1.0e-01	209714_s_at	30	AF213033	CDKN3	cyclin-dependent kinase inhibitor 3 (CDK2-associated dual specificity phosphatase)
	6.4e-03	218723_s_at	34	NM_014059	RGC32	response gene to complement 32
	8.1e-	203968_s_at	52	NM_001254	CDC6	CDC6 cell division cycle 6

	04					homolog (S. cerevisiae)
	4.0e-05	204695_at	55	AI343459	CDC25A	cell division cycle 25A
show the whole group	3.0e-06	205394_at	65	NM_001274	CHEK1	CHK1 checkpoint homolog (S. pombe)
6260 - DNA replication	3.2e-02	209773_s_at	4	BC001886	RRM2	ribonucleotide reductase M2 polypeptide
	6.4e-02	203968_s_at	52	NM_001254	CDC6	CDC6 cell division cycle 6 homolog (S. cerevisiae)
	1.0e-02	201755_at	56	NM_006739	MCM5	MCM5 minichromosome maintenance deficient 5, cell division cycle 46 (S. cerevisiae)
	2.5e-03	205909_at	72	NM_002692	POLE2	polymerase (DNA directed), epsilon 2 (p59 subunit)
	6.3e-04	204127_at	87	BC000149	RFC3	replication factor C (activator 1) 3, 38kDa
	8.7e-05	204767_s_at	92	BC000323	FEN1	flap structure-specific endonuclease 1
show the whole group	9.8e-06	204126_s_at	95	NM_003504	CDC45L	CDC45 cell division cycle 45-like (S. cerevisiae)
9440 - cyanate catabolism	2.7e-03	209605_at	13	D87292	TST	thiosulfate sulfurtransferase (rhodanese)
	4.4e-05	203524_s_at	64	NM_021126	MPST	mercaptopyruvate sulfurtransferase
4792 - thiosulfate sulfurtransferase activity	2.7e-03	209605_at	13	D87292	TST	thiosulfate sulfurtransferase (rhodanese)
	4.4e-05	203524_s_at	64	NM_021126	MPST	mercaptopyruvate sulfurtransferase
5638 - lamin filament	3.8e-03	203411_s_at	18	NM_005572	LMNA	lamin A/C
	2.3e-04	203276_at	109	NM_005573	LMNB1	lamin B1
9113 - purine base biosynthesis	7.8e-02	201014_s_at	191	NM_006452	PAICS	phosphoribosylaminoimidazole carboxylase, phosphoribosylaminoimidazole succinocarboxamide synthetase
	7.7e-03	214431_at	347	NM_003875	GMPS	guanine monphosphate synthetase
	7.3e-04	212378_at	492	NM_000819	GART	phosphoribosylglycinamide formyltransferase, phosphoribosylglycinamide synthetase, phosphoribosylaminoimidazole synthetase
	2.4e-04	209433_s_at	705	AI457120	PPAT	phosphoribosyl pyrophosphate amidotransferase

iGA report on the differentially expressed functional gene classes: *up-regulated Normal G0 vs CML G0*

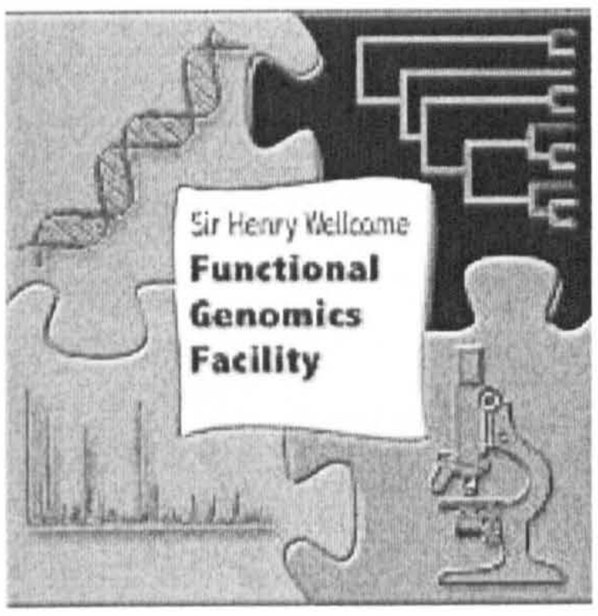

General Information	
Mode	Representative
Number of genes on chip	12698
Number of annotated genes	9530
Number of groups	3988
Number of singletons	1644
Significance threshold	2.5e-04
File name	**↑N G0 vs CML G0**

Top Changed Groups	Group Members	Changed Members	P-Value Changed	Percent Changed
19884 - antigen presentation, exogenous antigen	13	5	7.1e-12	38.46
19886 - antigen processing, exogenous antigen via MHC class II	14	5	1.6e-11	35.71
45012 - MHC class II receptor activity	14	5	1.6e-11	35.71
8009 - chemokine activity	40	7	8.9e-08	17.50
6935 - chemotaxis	86	7	1.8e-05	8.14
9596 - detection of pest, pathogen or parasite	4	2	7.4e-05	50.00

Changed group breakdown:

Group	P-value	Probe-set ID	Rank	Gene ID	Gene Symbol	Title
19884 - antigen presentation, exogenous antigen	1.4e-03	209480_at	1	M16276	HLA-DQB1	major histocompatibility complex, class II, DQ beta 1
	5.2e-06	212671_s_at	3	BG397856	HLA-DQA1	major histocompatibility complex, class II, DQ alpha 1
	7.9e-09	213831_at	4	X00452	HLA-DQA2 /// HLA-DQA1	major histocompatibility complex, class II, DQ alpha 2 ///

						major histocompatibility complex, class II, DQ alpha 1
	2.4e-11	209728_at	5	BC005312	HLA-DRB4	major histocompatibility complex, class II, DR beta 4
show the whole group	7.1e-12	213537_at	7	AI128225	HLA-DPA1	major histocompatibility complex, class II, DP alpha 1
19886 - antigen processing, exogenous antigen via MHC class II	1.5e-03	209480_at	1	M16276	HLA-DQB1	major histocompatibility complex, class II, DQ beta 1
	6.0e-06	212671_s_at	3	BG397856	HLA-DQA1	major histocompatibility complex, class II, DQ alpha 1
	1.0e-08	213831_at	4	X00452	HLA-DQA2 /// HLA-DQA1	major histocompatibility complex, class II, DQ alpha 2 /// major histocompatibility complex, class II, DQ alpha 1
	3.5e-11	209728_at	5	BC005312	HLA-DRB4	major histocompatibility complex, class II, DR beta 4
show the whole group	1.6e-11	213537_at	7	AI128225	HLA-DPA1	major histocompatibility complex, class II, DP alpha 1
45012 - MHC class II receptor activity	1.5e-03	209480_at	1	M16276	HLA-DQB1	major histocompatibility complex, class II, DQ beta 1
	6.0e-06	212671_s_at	3	BG397856	HLA-DQA1	major histocompatibility complex, class II, DQ alpha 1
	1.0e-08	213831_at	4	X00452	HLA-DQA2 /// HLA-DQA1	major histocompatibility complex, class II, DQ alpha 2 /// major histocompatibility complex, class II

						DQ alpha 1
	3.5e-11	209728_at	5	BC005312	HLA-DRB4	major histocompatibility complex, class II, DR beta 4
show the whole group	1.6e-11	213537_at	7	AI128225	HLA-DPA1	major histocompatibility complex, class II, DP alpha 1
8009 - chemokine activity	9.2e-02	210163_at	23	AF030514	CXCL11	chemokine (C-X-C motif) ligand 11
	1.5e-02	204533_at	45	NM_001565	CXCL10	chemokine (C-X-C motif) ligand 10
	9.8e-04	209774_x_at	47	M57731	CXCL2	chemokine (C-X-C motif) ligand 2
	1.4e-04	205242_at	64	NM_006419	CXCL13	chemokine (C-X-C motif) ligand 13 (B-cell chemoattractant)
	1.2e-05	206336_at	73	NM_002993	CXCL6	chemokine (C-X-C motif) ligand 6 (granulocyte chemotactic protein 2)
	1.9e-06	204470_at	91	NM_001511	CXCL1	chemokine (C-X-C motif) ligand 1 (melanoma growth stimulating activity, alpha)
show the whole group	8.9e-08	207850_at	92	NM_002090	CXCL3	chemokine (C-X-C motif) ligand 3
6935 - chemotaxis	1.9e-01	210163_at	23	AF030514	CXCL11	chemokine (C-X-C motif) ligand 11
	6.2e-02	204533_at	45	NM_001565	CXCL10	chemokine (C-X-C motif) ligand 10
	8.6e-03	209774_x_at	47	M57731	CXCL2	chemokine (C-X-C motif) ligand 2
	2.6e-03	205242_at	64	NM_006419	CXCL13	chemokine (C-X-C motif) ligand 13 (B-cell chemoattractant)
	4.9e-04	206336_at	73	NM_002993	CXCL6	chemokine (C-X-C motif) ligand 6 (granulocyte chemotactic protein 2)
	1.6e-04	204470_at	91	NM_001511	CXCL1	chemokine (C-X-C motif) ligand 1 (melanoma growth stimulating activity

						alpha)
show the whole group	1.8e-05	207850_at	92	NM_002090	CXCL3	chemokine (C-X-C motif) ligand 3
9596 - detection of pest, pathogen or parasite	1.4e-02	203932_at	33	NM_002118	HLA-DMB	major histocompatibility complex, class II, DM beta
show the whole group	7.4e-05	217478_s_at	34	X76775	HLA-DMA	major histocompatibility complex, class II, DM alpha

iGA report on the differentially expressed functional gene classes: *up-regulated CML Divided vs Normal Divided*

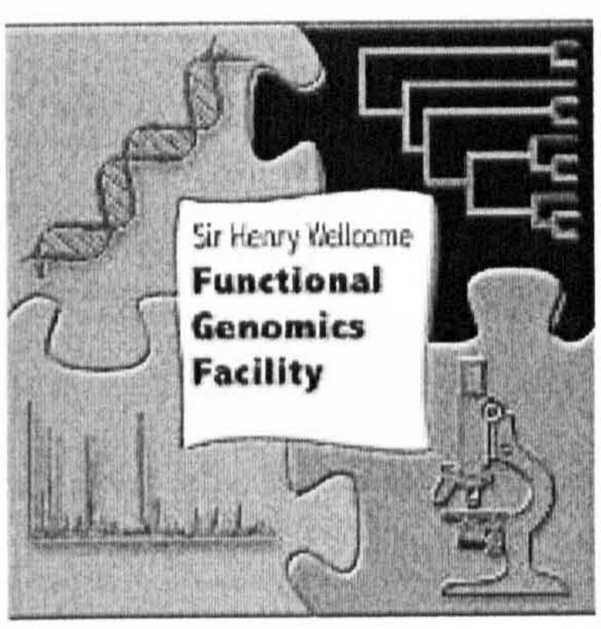

General Information	
Mode	Representative
Number of genes on chip	12698
Number of annotated genes	9532
Number of groups	3990
Number of singletons	1648
Significance threshold	2.5e-04
File name	**↑CML DIV vs N DIV**

Top Changed Groups	Group Members	Changed Members	P-Value Changed	Percent Changed
5819 - spindle	11	4	2.0e-06	36.36
6265 - DNA topological change	7	2	1.4e-04	28.57

Changed group breakdown:

Group	P-value	Probe-set ID	Rank	Gene ID	Gene Symbol	Title
5819 - spindle	4.0e-02	207828_s_at	35	NM_005196	CENPF	centromere protein F, 350/400ka (mitosin)
	1.2e-03	204444_at	46	NM_004523	KIF11	kinesin family member 11
	3.8e-05	217878_s_at	60	AI203880	CDC27	cell division cycle 27
show the whole group	2.0e-06	202870_s_at	87	NM_001255	CDC20	CDC20 cell division cycle 20 homolog (S. cerevisiae)
6265 - DNA topological change	1.3e-02	201292_at	18	AL561834	TOP2A	topoisomerase (DNA) II alpha 170kDa
show the whole group	1.4e-04	208900_s_at	25	AW025108	TOP1	topoisomerase (DNA) I

iGA report on the differentially expressed functional gene classes: *up-regulated Normal Divided vs CML Divided*

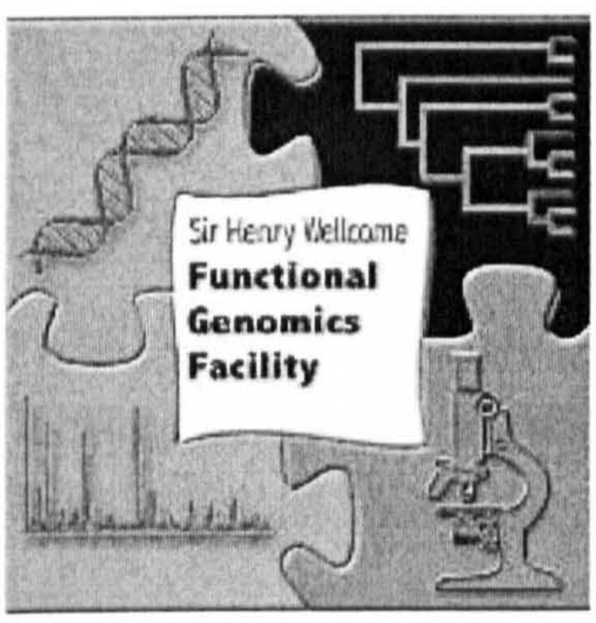

General Information	
Mode	Representative
Number of genes on chip	12698
Number of annotated genes	9532
Number of groups	3988
Number of singletons	1646
Significance threshold	2.5e-04
File name	**↑N DIV vs CML DIV**

Top Changed Groups	Group Members	Changed Members	P-Value Changed	Percent Changed
19884 - antigen presentation, exogenous antigen	13	7	2.0e-12	53.85
19886 - antigen processing, exogenous antigen via MHC class II	14	6	2.9e-11	42.86
45012 - MHC class II receptor activity	14	6	2.9e-11	42.86
8009 - chemokine activity	40	8	5.7e-09	20.00
6935 - chemotaxis	86	8	2.6e-06	9.30
9596 - detection of pest, pathogen or parasite	4	2	1.9e-04	50.00

Changed group breakdown:

Group	P-value	Probe-set ID	Rank	Gene ID	Gene Symbol	Title
19884 - antigen presentation, exogenous antigen	1.4e-03	213831_at	1	X00452	HLA-DQA2 /// HLA-DQA1	major histocompatibility complex, class II, DQ alpha 2 /// major histocompatibility complex, class II, DQ alpha 1
	1.7e-06	209480_at	2	M16276	HLA-DQB1	major histocompatibility complex, class II, DQ beta 1
	7.9e-09	212671_s_at	4	BG397856	HLA-DQA1	major histocompatibility complex, class II, DQ alpha 1

	6.3e-09	209728_at	18	BC005312	HLA-DRB4	major histocompatibility complex, class II, DR beta 4
	1.8e-10	211991_s_at	28	M27487	HLA-DPA1	major histocompatibility complex, class II, DP alpha 1
	1.2e-11	208894_at	31	M60334	HLA-DRA	major histocompatibility complex, class II, DR alpha
show the whole group	2.0e-12	201137_s_at	50	NM_002121	HLA-DPB1	major histocompatibility complex, class II, DP beta 1
19886 - antigen processing, exogenous antigen via MHC class II	1.5e-03	213831_at	1	X00452	HLA-DQA2 /// HLA-DQA1	major histocompatibility complex, class II, DQ alpha 2 /// major histocompatibility complex, class II, DQ alpha 1
	2.0e-06	209480_at	2	M16276	HLA-DQB1	major histocompatibility complex, class II, DQ beta 1
	1.0e-08	212671_s_at	4	BG397856	HLA-DQA1	major histocompatibility complex, class II, DQ alpha 1
	8.8e-09	209728_at	18	BC005312	HLA-DRB4	major histocompatibility complex, class II, DR beta 4
	3.1e-10	211991_s_at	28	M27487	HLA-DPA1	major histocompatibility complex, class II, DP alpha 1
show the whole group	2.9e-11	208894_at	31	M60334	HLA-DRA	major histocompatibility complex, class II, DR alpha
45012 - MHC class II receptor activity	1.5e-03	213831_at	1	X00452	HLA-DQA2 /// HLA-DQA1	major histocompatibility complex, class II, DQ alpha 2 /// major histocompatibility complex, class II, DQ alpha 1
	2.0e-06	209480_at	2	M16276	HLA-	major

					DQB1	histocompatibility complex, class II, DQ beta 1
	1.0e-08	212671_s_at	4	BG397856	HLA-DQA1	major histocompatibility complex, class II, DQ alpha 1
	8.8e-09	209728_at	18	BC005312	HLA-DRB4	major histocompatibility complex, class II, DR beta 4
	3.1e-10	211991_s_at	28	M27487	HLA-DPA1	major histocompatibility complex, class II, DP alpha 1
show the whole group	2.9e-11	208894_at	31	M60334	HLA-DRA	major histocompatibility complex, class II, DR alpha
8009 - chemokine activity	4.5e-02	204533_at	11	NM_001565	CXCL10	chemokine (C-X-C motif) ligand 10
	2.8e-03	210163_at	19	AF030514	CXCL11	chemokine (C-X-C motif) ligand 11
	4.1e-04	202859_x_at	35	NM_000584	IL8	interleukin 8
	4.5e-05	204470_at	48	NM_001511	CXCL1	chemokine (C-X-C motif) ligand 1 (melanoma growth stimulating activity, alpha)
	3.6e-06	207850_at	57	NM_002090	CXCL3	chemokine (C-X-C motif) ligand 3
	3.1e-07	209774_x_at	67	M57731	CXCL2	chemokine (C-X-C motif) ligand 2
	4.4e-08	206336_at	83	NM_002993	CXCL6	chemokine (C-X-C motif) ligand 6 (granulocyte chemotactic protein 2)
show the whole group	5.7e-09	210072_at	98	U88321	CCL19	chemokine (C-C motif) ligand 19
6935 - chemotaxis	9.5e-02	204533_at	11	NM_001565	CXCL10	chemokine (C-X-C motif) ligand 10
	1.2e-02	210163_at	19	AF030514	CXCL11	chemokine (C-X-C motif) ligand 11
	3.8e-03	202859_x_at	35	NM_000584	IL8	interleukin 8
	8.9e-04	204470_at	48	NM_001511	CXCL1	chemokine (C-X-C motif) ligand 1 (melanoma growth stimulating activity

						alpha)
	1.5e-04	207850_at	57	NM_002090	CXCL3	chemokine (C-X-C motif) ligand 3
	2.9e-05	209774_x_at	67	M57731	CXCL2	chemokine (C-X-C motif) ligand 2
	9.1e-06	206336_at	83	NM_002993	CXCL6	chemokine (C-X-C motif) ligand 6 (granulocyte chemotactic protein 2)
show the whole group	2.6e-06	210072_at	98	U88321	CCL19	chemokine (C-C motif) ligand 19
9596 - detection of pest, pathogen or parasite	2.2e-02	203932_at	52	NM_002118	HLA-DMB	major histocompatibility complex, class II, DM beta
show the whole group	1.9e-04	217478_s_at	54	X76775	HLA-DMA	major histocompatibility complex, class II, DM alpha

iGA report on the differentially expressed functional gene classes: *up-regulated Normal Divided vs Normal G0*

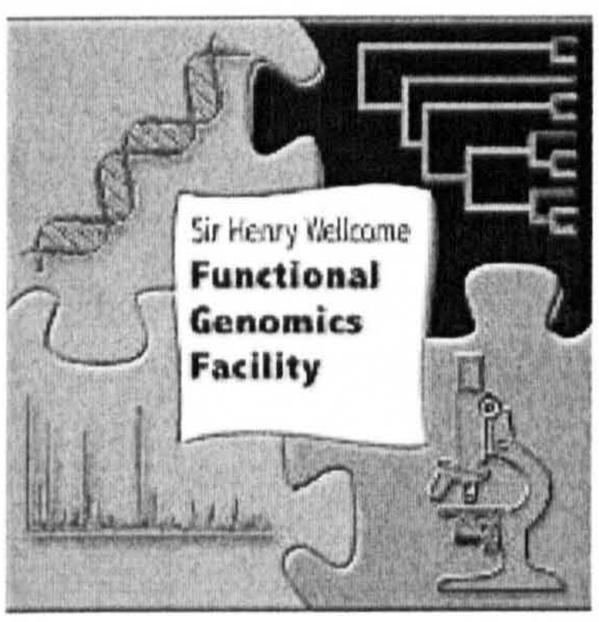

General Information	
Mode	Representative
Number of genes on chip	12698
Number of annotated genes	9532
Number of groups	3990
Number of singletons	1648
Significance threshold	2.5e-04
File name	**↑N DIV vs N G0**

Top Changed Groups	Group Members	Changed Members	P-Value Changed	Percent Changed
6270 - DNA replication initiation	17	7	1.4e-10	41.18
7067 - mitosis	74	11	1.5e-10	14.86
6260 - DNA replication	76	11	1.7e-10	14.47
8094 - DNA-dependent ATPase activity	13	6	6.3e-10	46.15
79 - regulation of cyclin dependent protein kinase activity	34	6	1.4e-07	17.65
6281 - DNA repair	96	9	6.0e-07	9.38
5660 - delta-DNA polymerase cofactor complex	3	3	8.7e-07	100.00
3684 - damaged DNA binding	35	6	1.2e-06	17.14
5833 - hemoglobin complex	9	3	2.1e-06	33.33
15671 - oxygen transport	9	3	2.1e-06	33.33
5344 - oxygen transporter activity	11	3	4.1e-06	27.27
4748 - ribonucleoside-diphosphate reductase activity	2	2	1.1e-05	100.00
7089 - traversing start control point of mitotic cell cycle	6	3	1.5e-05	50.00
76 - DNA replication checkpoint	4	2	2.3e-05	50.00
776 - kinetochore	14	3	2.6e-05	21.43
5876 - spindle microtubule	4	2	4.0e-05	50.00
8156 - negative regulation of DNA replication	4	2	4.6e-05	50.00

6189 - 'de novo' IMP biosynthesis	3	3	1.8e-04	100.00	
9113 - purine base biosynthesis	4	4	2.2e-04	100.00	
5762 - mitochondrial large ribosomal subunit	4	4	2.2e-04	100.00	
166 - nucleotide binding	91	6	2.4e-04	6.59	

Changed group breakdown:

Group	P-value	Probe-set ID	Rank	Gene ID	Gene Symbol	Title
6270 - DNA replication initiation	3.3e-02	204126_s_at	19	NM_003504	CDC45L	CDC45 cell division cycle 45-like (S. cerevisiae)
	2.6e-03	202107_s_at	43	NM_004526	MCM2	MCM2 minichromosome maintenance deficient 2, mitotin (S. cerevisiae)
	7.3e-05	222037_at	47	AI859865	MCM4	MCM4 minichromosome maintenance deficient 4 (S. cerevisiae)
	1.4e-06	201930_at	49	NM_005915	MCM6	MCM6 minichromosome maintenance deficient 6 (MIS5 homolog, S. pombe) (S. cerevisiae)
	5.3e-08	216237_s_at	61	AA807529	MCM5	MCM5 minichromosome maintenance deficient 5, cell division cycle 46 (S. cerevisiae)
	4.2e-09	210983_s_at	83	AF279900	MCM7	MCM7 minichromosome maintenance deficient 7 (S. cerevisiae)
show the whole group	1.4e-10	204510_at	88	NM_003503	CDC7	CDC7 cell division cycle 7 (S. cerevisiae)
7067 - mitosis	3.1e-02	203213_at	4	AL524035	CDC2	cell division cycle 2, G1 to S and G2 to M
	1.2e-03	202870_s_at	7	NM_001255	CDC20	CDC20 cell division cycle 20 homolog (S. cerevisiae)
	7.1e-05	203968_s_at	11	NM_001254	CDC6	CDC6 cell division cycle 6 homolog (S. cerevisiae)
	4.3e-06	202705_at	15	NM_004701	CCNB2	cyclin B2
	3.0e-06	219306_at	30	NM_020242	KNSL7	kinesin-like 7
	1.7e-07	209642_at	33	AF043294	BUB1	BUB1 budding uninhibited by benzimidazoles 1 homolog (yeast)
	1.1e-08	203362_s_at	37	NM_002358	MAD2L1	MAD2 mitotic arrest deficient-like 1 (yeast)
	6.0e-10	203418_at	39	NM_001237	CCNA2	cyclin A2

	1.9e-10	203755_at	41	NM_001211	BUB1B	BUB1 budding uninhibited by benzimidazoles 1 homolog beta (yeast)
	1.6e-10	204695_at	42	AI343459	CDC25A	cell division cycle 25A
show the whole group	1.5e-10	218662_s_at	45	NM_022346	HCAP-G	chromosome condensation protein G
6260 - DNA replication	8.0e-03	209773_s_at	1	BC001886	RRM2	ribonucleotide reductase M2 polypeptide
	3.3e-03	203968_s_at	11	NM_001254	CDC6	CDC6 cell division cycle 6 homolog (S. cerevisiae)
	4.3e-04	204126_s_at	19	NM_003504	CDC45L	CDC45 cell division cycle 45-like (S. cerevisiae)
	2.0e-05	204127_at	21	BC000149	RFC3	replication factor C (activator 1) 3, 38kDa
	6.7e-07	221521_s_at	22	BC003186	Pfs2	DNA replication complex GINS protein PSF2
	6.9e-08	208955_at	28	AB049113	DUT	dUTP pyrophosphatase
	3.6e-09	204768_s_at	31	NM_004111	FEN1	flap structure-specific endonuclease 1
	2.2e-10	201477_s_at	32	NM_001033	RRM1	ribonucleotide reductase M1 polypeptide
	1.8e-10	202107_s_at	43	NM_004526	MCM2	MCM2 minichromosome maintenance deficient 2, mitotin (S. cerevisiae)
	1.7e-10	205909_at	46	NM_002692	POLE2	polymerase (DNA directed), epsilon 2 (p59 subunit)
show the whole group	1.7e-10	222037_at	47	AI859865	MCM4	MCM4 minichromosome maintenance deficient 4 (S. cerevisiae)
8094 - DNA-dependent ATPase activity	5.7e-02	202107_s_at	43	NM_004526	MCM2	MCM2 minichromosome maintenance deficient 2, mitotin (S. cerevisiae)
	1.8e-03	222037_at	47	AI859865	MCM4	MCM4 minichromosome maintenance deficient 4 (S. cerevisiae)
	3.5e-05	201930_at	49	NM_005915	MCM6	MCM6 minichromosome maintenance deficient 6 (MIS5 homolog, S. pombe) (S. cerevisiae)
	1.0e-06	216237_s_at	61	AA807529	MCM5	MCM5 minichromosome maintenance deficient 5, cell division cycle 46 (S. cerevisiae)
	3.0e-08	209849_s_at	74	AF029669	RAD51C	RAD51 homolog C (S. cerevisiae)
show the whole group	6.3e-10	210983_s_at	83	AF279900	MCM7	MCM7 minichromosome maintenance deficient 7 (S. cerevisiae)

79 - regulation of cyclin dependent protein kinase activity	3.9e-02	203968_s_at	11	NM_001254	CDC6	CDC6 cell division cycle 6 homolog (S. cerevisiae)
	3.0e-03	205394_at	23	NM_001274	CHEK1	CHK1 checkpoint homolog (S. pombe)
	1.0e-04	209714_s_at	26	AF213033	CDKN3	cyclin-dependent kinase inhibitor 3 (CDK2-associated dual specificity phosphatase)
	1.0e-05	203418_at	39	NM_001237	CCNA2	cyclin A2
	3.3e-07	204695_at	42	AI343459	CDC25A	cell division cycle 25A
show the whole group	1.4e-07	205034_at	70	NM_004702	CCNE2	cyclin E2
6281 - DNA repair	3.7e-01	205909_at	46	NM_002692	POLE2	polymerase (DNA directed), epsilon 2 (p59 subunit)
	1.5e-01	201202_at	69	NM_002592	PCNA	proliferating cell nuclear antigen
	3.8e-02	209849_s_at	74	AF029669	RAD51C	RAD51 homolog C (S. cerevisiae)
	8.9e-03	205733_at	81	NM_000057	BLM	Bloom syndrome
	1.5e-03	205024_s_at	84	NM_002875	RAD51	RAD51 homolog (RecA homolog, E. coli) (S. cerevisiae)
	3.2e-04	203209_at	92	BC001866	RFC5	replication factor C (activator 1) 5, 36.5kDa
	4.8e-05	209507_at	96	BC005264	RPA3	replication protein A3, 14kDa
	5.5e-06	203564_at	97	NM_004629	FANCG	Fanconi anemia, complementation group G
show the whole group	6.0e-07	204766_s_at	99	NM_002452	NUDT1	nudix (nucleoside diphosphate linked moiety X)-type motif 1
5660 - delta-DNA polymerase cofactor complex	6.6e-03	204127_at	21	BC000149	RFC3	replication factor C (activator 1) 3, 38kDa
	1.5e-04	201202_at	69	NM_002592	PCNA	proliferating cell nuclear antigen
	8.7e-07	203209_at	92	BC001866	RFC5	replication factor C (activator 1) 5, 36.5kDa
3684 - damaged DNA binding	1.1e-01	204768_s_at	31	NM_004111	FEN1	flap structure-specific endonuclease 1
	1.9e-02	209421_at	58	U04045	MSH2	mutS homolog 2, colon cancer, nonpolyposis type 1 (E. coli)

	2.5e-03	209849_s_at	74	AF029669	RAD51C	RAD51 homolog C (S. cerevisiae)
	1.7e-04	204531_s_at	77	NM_007295	BRCA1	breast cancer 1, early onset
	1.2e-05	205024_s_at	84	NM_002875	RAD51	RAD51 homolog (RecA homolog, E. coli) (S. cerevisiae)
show the whole group	1.2e-06	203564_at	97	NM_004629	FANCG	Fanconi anemia, complementation group G
5833 - hemoglobin complex	2.8e-03	206834_at	3	NM_000519	HBD	hemoglobin, delta
	6.1e-05	213515_x_at	13	AI133353	HBG1	hemoglobin, gamma A
show the whole group	2.1e-06	209116_x_at	29	M25079	HBB	hemoglobin, beta
15671 - oxygen transport	2.8e-03	206834_at	3	NM_000519	HBD	hemoglobin, delta
	6.1e-05	213515_x_at	13	AI133353	HBG1	hemoglobin, gamma A
show the whole group	2.1e-06	209116_x_at	29	M25079	HBB	hemoglobin, beta
5344 - oxygen transporter activity	3.5e-03	206834_at	3	NM_000519	HBD	hemoglobin, delta
	9.4e-05	213515_x_at	13	AI133353	HBG1	hemoglobin, gamma A
show the whole group	4.1e-06	209116_x_at	29	M25079	HBB	hemoglobin, beta
4748 - ribonucleoside-diphosphate reductase activity	2.1e-04	209773_s_at	1	BC001886	RRM2	ribonucleotide reductase M2 polypeptide
	1.1e-05	201477_s_at	32	NM_001033	RRM1	ribonucleotide reductase M1 polypeptide
7089 - traversing start control point of mitotic cell cycle	2.5e-03	203213_at	4	AL524035	CDC2	cell division cycle 2, G1 to S and G2 to M
	1.8e-05	203968_s_at	11	NM_001254	CDC6	CDC6 cell division cycle 6 homolog (S. cerevisiae)
show the whole group	1.5e-05	204510_at	88	NM_003503	CDC7	CDC7 cell division cycle 7 (S. cerevisiae)
76 - DNA replication checkpoint	4.6e-03	203968_s_at	11	NM_001254	CDC6	CDC6 cell division cycle 6 homolog (S. cerevisiae)
show the whole group	2.3e-05	204126_s_at	19	NM_003504	CDC45L	CDC45 cell division cycle 45-like (S. cerevisiae)

776 - kinetochore	4.7e-02	209642_at	33	AF043294	BUB1	BUB1 budding uninhibited by benzimidazoles 1 homolog (yeast)
	1.3e-03	203362_s_at	37	NM_002358	MAD2L1	MAD2 mitotic arrest deficient-like 1 (yeast)
show the whole group	2.6e-05	203755_at	41	NM_001211	BUB1B	BUB1 budding uninhibited by benzimidazoles 1 homolog beta (yeast)
5876 - spindle microtubule	5.9e-03	218009_s_at	14	NM_003981	PRC1	protein regulator of cytokinesis 1
show the whole group	4.0e-05	202095_s_at	25	NM_001168	BIRC5	baculoviral IAP repeat-containing 5 (survivin)
8156 - negative regulation of DNA replication	4.6e-03	203968_s_at	11	NM_001254	CDC6	CDC6 cell division cycle 6 homolog (S. cerevisiae)
show the whole group	4.6e-05	218350_s_at	27	NM_015895	GMNN	geminin, DNA replication inhibitor
6189 - 'de novo' IMP biosynthesis	3.3e-02	201014_s_at	107	NM_006452	PAICS	phosphoribosylaminoimidazole carboxylase, phosphoribosylaminoimidazole succinocarboxamide synthetase
	6.0e-04	212378_at	117	NM_000819	GART	phosphoribosylglycinamide formyltransferase, phosphoribosylglycinamide synthetase, phosphoribosylaminoimidazole synthetase
	1.8e-04	213302_at	251	AL044326	PFAS	phosphoribosylformylglycinamidine synthase (FGAR amidotransferase)
9113 - purine base biosynthesis	4.4e-02	201014_s_at	107	NM_006452	PAICS	phosphoribosylaminoimidazole carboxylase, phosphoribosylaminoimidazole succinocarboxamide synthetase
	1.1e-03	212378_at	117	NM_000819	GART	phosphoribosylglycinamide formyltransferase, phosphoribosylglycinamide synthetase, phosphoribosylaminoimidazole synthetase
	2.3e-04	214431_at	176	NM_003875	GMPS	guanine monphosphate synthetase
	2.2e-04	209434_s_at	461	U00238	PPAT	phosphoribosyl pyrophosphate amidotransferase
5762 - mitochondrial large ribosomal subunit	4.1e-02	218049_s_at	98	NM_014078	MRPL13	mitochondrial ribosomal protein L13
	1.5e-03	203931_s_at	144	NM_002949	MRPL12	mitochondrial ribosomal protein L12

	2.4e-04	208787_at	196	BC003375	MRPL3	mitochondrial ribosomal protein L3
	2.2e-04	213897_s_at	493	AI832239	MRPL23	mitochondrial ribosomal protein L23
166 - nucleotide binding	1.0e-01	203968_s_at	11	NM_001254	CDC6	CDC6 cell division cycle 6 homolog (S. cerevisiae)
	1.1e-02	204033_at	17	NM_004237	TRIP13	thyroid hormone receptor interactor 13
	9.9e-04	204127_at	21	BC000149	RFC3	replication factor C (activator 1) 3, 38kDa
	1.0e-03	222037_at	47	AI859865	MCM4	MCM4 minichromosome maintenance deficient 4 (S. cerevisiae)
	1.1e-03	210983_s_at	83	AF279900	MCM7	MCM7 minichromosome maintenance deficient 7 (S. cerevisiae)
show the whole group	2.4e-04	203209_at	92	BC001866	RFC5	replication factor C (activator 1) 5, 36.5kDa

iGA report on the differentially expressed functional gene classes: *up-regulated Normal G0 vs Normal Divided*

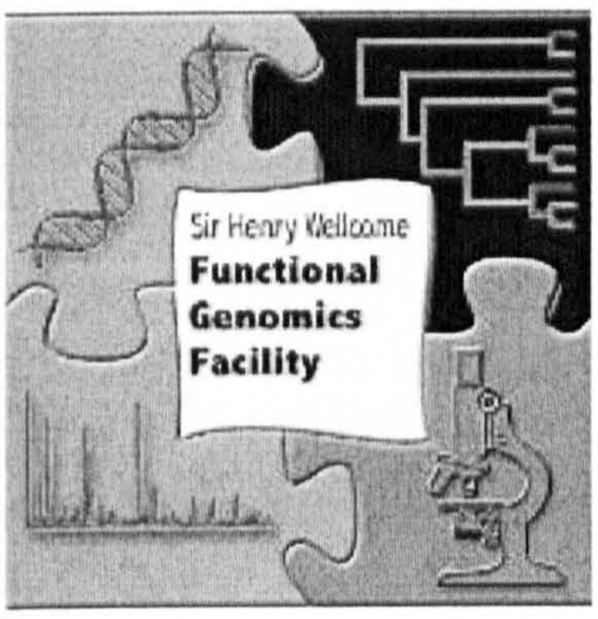

General Information	
Mode	Representative
Number of genes on chip	12698
Number of annotated genes	9529
Number of groups	3990
Number of singletons	1646
Significance threshold	2.5e-04
File name	**↑N G0 vs N D**

Top Changed Groups	Group Members	Changed Members	P-Value Changed	Percent Changed
8009 - chemokine activity	40	9	2.4e-10	22.50
6935 - chemotaxis	86	10	8.7e-09	11.63
7001 - chromosome organization and biogenesis (sensu Eukaryota)	54	7	5.5e-08	12.96
786 - nucleosome	42	5	2.8e-07	11.90
6334 - nucleosome assembly	47	5	5.0e-07	10.64
5694 - chromosome	37	4	7.3e-06	10.81
6928 - cell motility	99	7	5.9e-05	7.07
8219 - cell death	16	3	1.2e-04	18.75
9596 - detection of pest, pathogen or parasite	4	4	2.4e-04	100.00
16126 - sterol biosynthesis	3	3	2.4e-04	100.00

Changed group breakdown:

Group	P-value	Probe-set ID	Rank	Gene ID	Gene Symbol	Title
8009 - chemokine activity	1.7e-02	210163_at	4	AF030514	CXCL11	chemokine (C-X-C motif) ligand 11
	7.6e-04	209774_x_at	10	M57731	CXCL2	chemokine (C-X-C motif) ligand 2
	1.1e-04	204533_at	23	NM_001565	CXCL10	chemokine (C-X-C motif) ligand 10
	3.2e-06	205242_at	25	NM_006419	CXCL13	chemokine (C-X-C motif) ligand 13 (B-

						cell chemoattractant)
	4.0e-07	207850_at	37	NM_002090	CXCL3	chemokine (C-X-C motif) ligand 3
	1.7e-08	206336_at	42	NM_002993	CXCL6	chemokine (C-X-C motif) ligand 6 (granulocyte chemotactic protein 2)
	2.7e-09	204470_at	56	NM_001511	CXCL1	chemokine (C-X-C motif) ligand 1 (melanoma growth stimulating activity, alpha)
	1.4e-09	202859_x_at	82	NM_000584	IL8	interleukin 8
show the whole group	2.4e-10	210072_at	88	U88321	CCL19	chemokine (C-C motif) ligand 19
6935 - chemotaxis	3.6e-02	210163_at	4	AF030514	CXCL11	chemokine (C-X-C motif) ligand 11
	3.5e-03	209774_x_at	10	M57731	CXCL2	chemokine (C-X-C motif) ligand 2
	1.1e-03	204533_at	23	NM_001565	CXCL10	chemokine (C-X-C motif) ligand 10
	6.8e-05	205242_at	25	NM_006419	CXCL13	chemokine (C-X-C motif) ligand 13 (B-cell chemoattractant)
	1.8e-05	207850_at	37	NM_002090	CXCL3	chemokine (C-X-C motif) ligand 3
	1.8e-06	206336_at	42	NM_002993	CXCL6	chemokine (C-X-C motif) ligand 6 (granulocyte chemotactic protein 2)
	6.2e-07	204470_at	56	NM_001511	CXCL1	chemokine (C-X-C motif) ligand 1 (melanoma growth stimulating activity, alpha)
	6.6e-07	202859_x_at	82	NM_000584	IL8	interleukin 8
	8.3e-08	210072_at	88	U88321	CCL19	chemokine (C-C motif) ligand 19
show the whole group	8.7e-09	214435_x_at	92	NM_005402	RALA	v-ral simian leukemia viral oncogene homolog A (ras related)
7001 - chromosome organization and	1.1e-02	215071_s_at	2	AL353759	HIST1H2AC	histone 1, H2ac

biogenesis (sensu Eukaryota)						
	9.4e-05	202708_s_at	3	NM_003528	HIST2H2BE	histone 2, H2be
	6.0e-05	209806_at	14	BC000893	HIST1H2BK	histone 1, H2bk
	9.0e-06	214290_s_at	24	AI313324	HIST2H2AA	histone 2, H2aa
	1.0e-06	208886_at	33	BC000145	H1F0	H1 histone family, member 0
	4.7e-07	208859_s_at	53	AI650257	ATRX	alpha thalassemia/mental retardation syndrome X-linked (RAD54 homolog, S. cerevisiae)
show the whole group	5.5e-08	209911_x_at	63	BC002842	HIST1H2BD	histone 1, H2bd
786 - nucleosome	8.8e-03	215071_s_at	2	AL353759	HIST1H2AC	histone 1, H2ac
	5.7e-05	202708_s_at	3	NM_003528	HIST2H2BE	histone 2, H2be
	2.8e-05	209806_at	14	BC000893	HIST1H2BK	histone 1, H2bk
	3.3e-06	214290_s_at	24	AI313324	HIST2H2AA	histone 2, H2aa
show the whole group	2.8e-07	208886_at	33	BC000145	H1F0	H1 histone family, member 0
6334 - nucleosome assembly	9.8e-03	215071_s_at	2	AL353759	HIST1H2AC	histone 1, H2ac
	7.1e-05	202708_s_at	3	NM_003528	HIST2H2BE	histone 2, H2be
	3.9e-05	209806_at	14	BC000893	HIST1H2BK	histone 1, H2bk
	5.1e-06	214290_s_at	24	AI313324	HIST2H2AA	histone 2, H2aa
show the whole group	5.0e-07	208886_at	33	BC000145	H1F0	H1 histone family, member 0
5694 - chromosome	7.8e-03	215071_s_at	2	AL353759	HIST1H2AC	histone 1, H2ac
	4.4e-05	202708_s_at	3	NM_003528	HIST2H2BE	histone 2, H2be
	1.0e-04	214290_s_at	24	AI313324	HIST2H2AA	histone 2, H2aa
show the whole group	7.3e-06	208886_at	33	BC000145	H1F0	H1 histone family, member 0
6928 - cell motility	2.1e-01	204533_at	23	NM_001565	CXCL10	chemokine (C-X-C motif) ligand 10
	3.6e-02	204748_at	29	NM_000963	PTGS2	prostaglandin-endoperoxide synthase 2 (prostaglandin G/H synthase and cyclooxygenase)
	1.3e-02	209108_at	47	AF053453	TM4SF6	transmembrane 4 superfamily

						member 6
	1.6e-03	203476_at	49	NM_006670	TPBG	trophoblast glycoprotein
	1.3e-03	205844_at	78	NM_004666	VNN1	vanin 1
	2.0e-04	202859_x_at	82	NM_000584	IL8	interleukin 8
show the whole group	5.9e-05	201005_at	96	NM_001769	CD9	CD9 antigen (p24)
8219 - cell death	1.0e-02	201324_at	6	NM_001423	EMP1	epithelial membrane protein 1
	2.3e-03	202073_at	43	AV757675	OPTN	optineurin
show the whole group	1.2e-04	200602_at	59	NM_000484	APP	amyloid beta (A4) precursor protein (protease nexin-II, Alzheimer disease)
9596 - detection of pest, pathogen or parasite	1.8e-01	205101_at	463	NM_000246	MHC2TA	MHC class II transactivator
	1.4e-02	217478_s_at	472	X76775	HLA-DMA	major histocompatibility complex, class II, DM alpha
	8.5e-04	203932_at	525	NM_002118	HLA-DMB	major histocompatibility complex, class II, DM beta
	2.4e-04	210514_x_at	695	AF226990	HLA-G	HLA-G histocompatibility antigen, class I, G
16126 - sterol biosynthesis	4.6e-02	213577_at	150	AA639705	SQLE	squalene epoxidase
	2.6e-03	209146_at	273	AV704962	SC4MOL	sterol-C4-methyl oxidase-like
	2.4e-04	211423_s_at	415	D85181	SC5DL	sterol-C5-desaturase (ERG3 delta-5-desaturase homolog, fungal)-like

	7.4e-06	203418_at	17	NM_001237	CCNA2	cyclin A2
	5.8e-07	210997_at	22	M77227	HGF	hepatocyte growth factor (hepapoietin A; scatter factor)
	7.4e-08	202870_s_at	29	NM_001255	CDC20	CDC20 cell division cycle 20 homolog (S. cerevisiae)
	3.8e-09	218663_at	32	NM_022346	HCAP-G	chromosome condensation protein G
	7.3e-10	219306_at	40	NM_020242	KNSL7	kinesin-like 7
	1.8e-10	209083_at	43	U34690	CORO1A	coronin, actin binding protein, 1A
show the whole group	1.5e-10	202240_at	44	NM_005030	PLK1	polo-like kinase 1 (Drosophila)
5819 - spindle	2.6e-02	204444_at	23	NM_004523	KIF11	kinesin family member 11
	4.8e-04	202870_s_at	29	NM_001255	CDC20	CDC20 cell division cycle 20 homolog (S. cerevisiae)
	2.0e-05	204709_s_at	49	NM_004856	KIF23	kinesin family member 23
	3.0e-07	208079_s_at	54	NM_003158	STK6	serine/threonine kinase 6
show the whole group	5.7e-09	210052_s_at	65	AF098158	TPX2	TPX2, microtubule-associated protein homolog (Xenopus laevis)
5871 - kinesin complex	2.2e-02	204444_at	23	NM_004523	KIF11	kinesin family member 11
	9.1e-04	204709_s_at	49	NM_004856	KIF23	kinesin family member 23
show the whole group	2.8e-05	209408_at	68	U63743	KIF2C	kinesin family member 2C
775 - chromosome, pericentric region	8.5e-03	204162_at	9	NM_006101	KNTC2	kinetochore associated 2
	4.3e-05	204962_s_at	11	NM_001809	CENPA	centromere protein A, 17kDa
show the whole group	2.8e-05	209408_at	68	U63743	KIF2C	kinesin family member 2C
3777 - microtubule	6.3e-02	204444_at	23	NM_004523	KIF11	kinesin family member 11

iGA report on the differentially expressed functional gene classes: *up-regulated CML Divided vs CML G0*

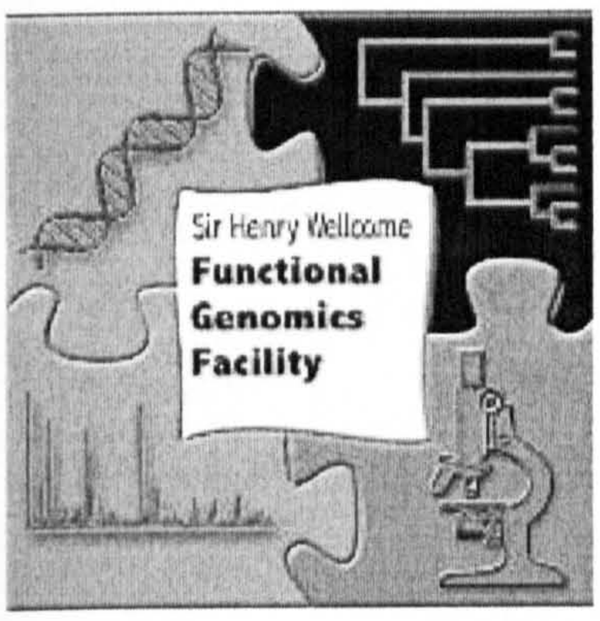

General Information	
Mode	Representative
Number of genes on chip	12698
Number of annotated genes	9531
Number of groups	3990
Number of singletons	1648
Significance threshold	2.5e-04
File name	**↑CML G0 vs CML DIV**

Top Changed Groups	Group Members	Changed Members	P-Value Changed	Percent Changed
7067 - mitosis	74	10	1.5e-10	13.51
5819 - spindle	11	5	5.7e-09	45.45
5871 - kinesin complex	9	3	2.8e-05	33.33
775 - chromosome, pericentric region	9	3	2.8e-05	33.33
3777 - microtubule motor activity	27	4	5.4e-05	14.81
4869 - cysteine protease inhibitor activity	16	3	6.4e-05	18.75
278 - mitotic cell cycle	3	2	7.1e-05	66.67
776 - kinetochore	14	3	1.1e-04	21.43
5876 - spindle microtubule	4	3	2.1e-04	75.00
22 - mitotic spindle elongation	2	2	2.2e-04	100.00

Changed group breakdown:

Group	P-value	Probe-set ID	Rank	Gene ID	Gene Symbol	Title
7067 - mitosis	5.3e-02	203213_at	7	AL524035	CDC2	cell division cycle 2, G1 to S and G2 to M
	2.1e-03	204162_at	9	NM_006101	KNTC2	kinetochore associated 2
	5.2e-05	202954_at	10	NM_007019	UBE2C	ubiquitin-conjugating enzyme E2C

motor activity						
	8.4e-03	204709_s_at	49	NM_004856	KIF23	kinesin family member 23
	9.0e-04	209408_at	68	U63743	KIF2C	kinesin family member 2C
show the whole group	5.4e-05	218355_at	75	NM_012310	KIF4A	kinesin family member 4A
4869 - cysteine protease inhibitor activity	5.0e-03	204971_at	3	NM_005213	CSTA	cystatin A (stefin A)
	2.5e-03	210140_at	45	AF031824	CST7	cystatin F (leukocystatin)
show the whole group	6.4e-05	202095_s_at	48	NM_001168	BIRC5	baculoviral IAP repeat-containing 5 (survivin)
278 - mitotic cell cycle	1.0e-02	218663_at	32	NM_022346	HCAP-G	chromosome condensation protein G
show the whole group	7.1e-05	212949_at	47	D38553	BRRN1	barren homolog (Drosophila)
776 - kinetochore	7.1e-02	209642_at	50	AF043294	BUB1	BUB1 budding uninhibited by benzimidazoles 1 homolog (yeast)
	3.6e-03	203362_s_at	62	NM_002358	MAD2L1	MAD2 mitotic arrest deficient-like 1 (yeast)
show the whole group	1.1e-04	203755_at	66	NM_001211	BUB1B	BUB1 budding uninhibited by benzimidazoles 1 homolog beta (yeast)
5876 - spindle microtubule	2.0e-02	202095_s_at	48	NM_001168	BIRC5	baculoviral IAP repeat-containing 5 (survivin)
	3.6e-04	218355_at	75	NM_012310	KIF4A	kinesin family member 4A
show the whole group	2.1e-04	218009_s_at	104	NM_003981	PRC1	protein regulator of cytokinesis 1
22 - mitotic spindle elongation	1.0e-02	204709_s_at	49	NM_004856	KIF23	kinesin family member 23
	2.2e-04	218009_s_at	104	NM_003981	PRC1	protein regulator of cytokinesis 1

iGA report on the differentially expressed functional gene classes: *up-regulated CML G0 vs CML Divided*

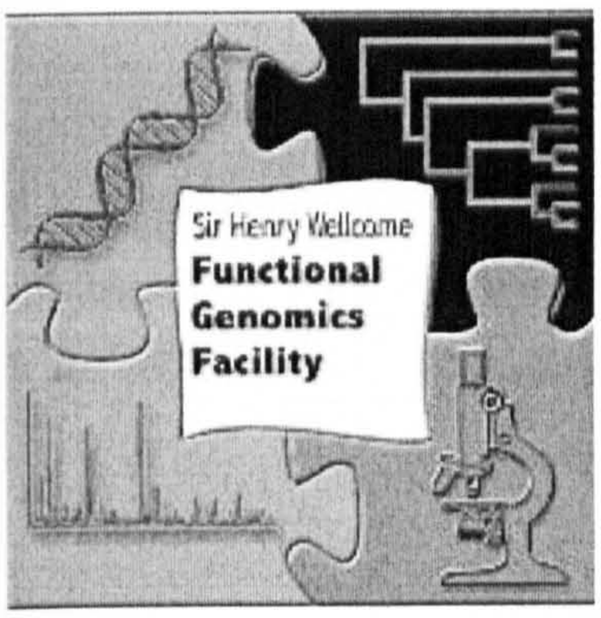

General Information	
Mode	Representative
Number of genes on chip	12698
Number of annotated genes	9532
Number of groups	3991
Number of singletons	1649
Significance threshold	2.5e-04
File name	**↑CML G0 vs CML DIV**

Top Changed Groups	Group Members	Changed Members	P-Value Changed	Percent Changed
8009 - chemokine activity	40	7	4.0e-11	17.50
6935 - chemotaxis	86	9	2.0e-08	10.47
5833 - hemoglobin complex	9	3	5.7e-05	33.33
47115 - trans-1,2-dihydrobenzene-1,2-diol dehydrogenase activity	3	2	1.3e-04	66.67
15125 - bile acid transporter activity	3	2	1.3e-04	66.67

Changed group breakdown:

Group	P-value	Probe-set ID	Rank	Gene ID	Gene Symbol	Title
8009 - chemokine activity	1.7e-02	210163_at	4	AF030514	CXCL11	chemokine (C-X-C motif) ligand 11
	2.5e-04	204533_at	6	NM_001565	CXCL10	chemokine (C-X-C motif) ligand 10
	2.4e-06	202859_x_at	7	NM_000584	IL8	interleukin 8
	1.3e-07	207850_at	12	NM_002090	CXCL3	chemokine (C-X-C motif) ligand 3
	2.9e-09	204470_at	15	NM_001511	CXCL1	chemokine (C-X-C motif) ligand 1 (melanoma growth stimulating activity, alpha)
	8.7e-11	205114_s_at	18	NM_002983	MGC12815	chemokine (C-C

						motif) ligand 3-like, centromeric
show the whole group	4.0e-11	209774_x_at	24	M57731	CXCL2	chemokine (C-X-C motif) ligand 2
6935 - chemotaxis	3.6e-02	210163_at	4	AF030514	CXCL11	chemokine (C-X-C motif) ligand 11
	1.2e-03	204533_at	6	NM_001565	CXCL10	chemokine (C-X-C motif) ligand 10
	2.4e-05	202859_x_at	7	NM_000584	IL8	interleukin 8
	2.9e-06	207850_at	12	NM_002090	CXCL3	chemokine (C-X-C motif) ligand 3
	1.5e-07	204470_at	15	NM_001511	CXCL1	chemokine (C-X-C motif) ligand 1 (melanoma growth stimulating activity, alpha)
	5.4e-08	209774_x_at	24	M57731	CXCL2	chemokine (C-X-C motif) ligand 2
	1.3e-07	206336_at	45	NM_002993	CXCL6	chemokine (C-X-C motif) ligand 6 (granulocyte chemotactic protein 2)
	3.7e-08	214974_x_at	57	AK026546	CXCL5	chemokine (C-X-C motif) ligand 5
show the whole group	2.0e-08	205242_at	75	NM_006419	CXCL13	chemokine (C-X-C motif) ligand 13 (B-cell chemoattractant)
5833 - hemoglobin complex	2.8e-02	209116_x_at	30	M25079	HBB	hemoglobin, beta
	2.7e-03	204419_x_at	85	NM_000184	HBG1	hemoglobin, gamma A
show the whole group	5.7e-05	219672_at	86	NM_016633	ERAF	erythroid associated factor
47115 - trans-1,2-dihydrobenzene-1,2-diol dehydrogenase activity	1.2e-02	204151_x_at	37	NM_001353	AKR1C1	aldo-keto reductase family 1, member C1 (dihydrodiol dehydrogenase 1; 20-alpha (3-alpha)-hydroxysteroid dehydrogenase)
show the whole group	1.3e-04	216594_x_at	64	S68290	AKR1C1 /// AKR1C2	aldo-keto reductase family

						1, member C1 (dihydrodiol dehydrogenase 1; 20-alpha (3-alpha)-hydroxysteroid dehydrogenase) /// aldo-keto reductase family 1, member C2 (dihydrodiol dehydrogenase 2; bile acid binding protein; 3-alpha hydroxysteroid dehydrogenase, type III)
15125 - bile acid transporter activity	1.2e-02	204151_x_at	37	NM_001353	AKR1C1	aldo-keto reductase family 1, member C1 (dihydrodiol dehydrogenase 1; 20-alpha (3-alpha)-hydroxysteroid dehydrogenase)
show the whole group	1.3e-04	216594_x_at	64	S68290	AKR1C1 /// AKR1C2	aldo-keto reductase family 1, member C1 (dihydrodiol dehydrogenase 1; 20-alpha (3-alpha)-hydroxysteroid dehydrogenase) /// aldo-keto reductase family 1, member C2 (dihydrodiol dehydrogenase 2; bile acid binding protein; 3-alpha hydroxysteroid dehydrogenase, type III)